BOOK OF ABSTRACTS NSSY 2024

Here we present the Abstract Book of fifth edition international edition of Nanoscience Summer School Yachay,(NSSY2024), held from the 19th of May until the 25th of May 2024 at Puerto Ayora, Galapagos Islands, Ecuador.

The NSSY2024 had plenary sessions from the most eminent scientist, invited talks from leading researchers in the field, and contributed talks chosen from the best-submitted abstracts.

We will also feature a two-day poster session

In this international edition of NSSY2024, there was the participation of 90 delegates between speakers,keynotes, professor, researches and students. Talks from latest work indifferent topics of nanoscience and nanotechnology, theoretical and experimental works and the ir applications.

Dr. Gema González
Dean School Physical Sciences and Nanotechnology, Yachay Tech University NSSY2024 Conference Chair
Chair Editor In Chief Acta Microscopica

NANOSCIENCE SUMMER SCHOOL 2024 @ YACHAY TECH INTERNATIONAL FIFTH EDITION

May 19th to 25th,2024

SCHOOL OF PHYSICAL SCIENCES AND NANOTECHNOLOGY

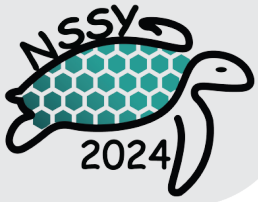

San Miguel de Urcuquí,
Hacienda San José s/n y Proyecto Yachay
Telephone:+593 62999500

Organizers
Gema González (Chair)
Charlotte Berrezueta (Co-chair)
Melany Aguilar Ramirez
Alexis Garzón
León Ocaña
Norman Wray

Local Team and Student Staff
Daniela Arellano
María Fernanda Bósquez
Evelyn Cifuentes
Bryan Pinargote
Cristina Rubio
María Belén Silva
Andrés Vera Ochoa

Scientific Advisory Board
Eric Anglaret
Paola Ayala (Co-chair)
Carla Bittencourt
Sofie Cambré
Silvia Giordani
Gema González
Shigeo Maruyama
Vincent Meunier (Co-chair)
Duncan Mowbray
Stephanie Reich
Humberto Terrones

Acta Microscopica Vol. 34, Supp. 2, 2025
Abstract Book NSSY 2024 - Galapagos 19-25 May, 2024

Monday

Tuesday

Wednesday

Thursday

Friday

Monday

Poster Session

Wednesday

Poster Session

Acta Microscopica Vol. 34, Supp. 2, 2025
Abstract Book NSSY 2024 - Galapagos 19-25 May, 2024

Conference

Monday

Acta Microscopica Vol. 34, Supp. 2, 2025
Abstract Book NSSY 2024 - Galapagos 19-25 May, 2024

The Importance of phonons in 2-D materials

Humberto Terrones[1]
[1] *Rensselaer Polytechnic Institute*
terroh@rpi.edu

Abstract

In this tutorial first I will review the most important concepts related to phonons in general and then, I will show their relevance in the characterization of 2-D materials such as graphene, transition metal dichalcogenides (TMDS) and hexagonal boron nitride hBN. The main points for obtaining a suitable phonon dispersion using density Functional Theory (DFT) will be explained. Moreover, I will explain the relationship of phonon dispersion with the Raman spectrum and the symmetry of the structure. Finally, experimental, and theoretical results will be compared.

References

[1] Terrones, H. Del Corro, E. Feng, S. Poumirol, J.M., Rhodes, D., Smirnov, D., Pradhan, N.R., Lin, Z., Nguyen, M.A.T., Elías, A.L., Mallouk, T.E.,Balicas, L., Pimenta, M.A., Terrones, M., "New First Order Raman-active Modes in Few Layered Transition Metal Dichalcogenides", Scientific Reports, Vol. 4, 4215, doi:10.1038/srep04215 (2014).

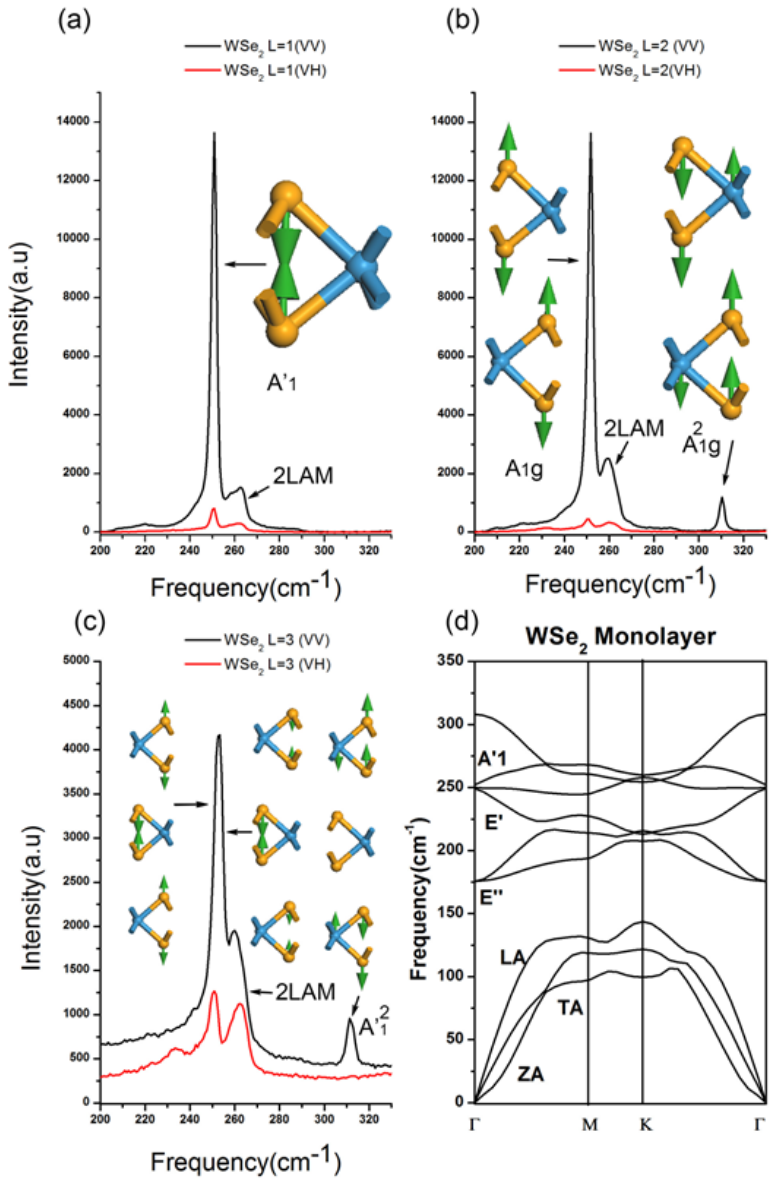

Figure 1: **Experimental Raman spectra of WSe2 taken with a 514 nm laser under conventional geometry (VV) and cross polarization (VH). (a) Monolayer (L=1). (b) Bilayer (L=2). (c) Trilayer (L=3). Insets show models of the out of plane vibrational modes present in each case. (d) Calculated DFPT phonon dispersion of the WSe2 monolayer.**

Acta Microscopica Vol. 34, Supp. 2, 2025
Abstract Book NSSY 2024 - Galapagos 19-25 May, 2024

A Theoretical Model for Magnetism in Gold Nanoparticles and its Connection to Spin-Dependent Catalysis in Mesoporous Materials.

Vladimiro Mujica[1]

[1] *Arizona State University, School of Molecular Sciences, 551 E University Dr, Tempe, AZ 85281, U.S.A.*

vmujica@asu.edu

Abstract

Magnetism is a size-dependent property in materials. An extreme case is gold, which is a diamagnetic metal but, in contrast, coated gold nanoparticles can become ferromagnetic depending on the chemical nature of the adsorbate. In a different direction, it has been experimentally observed that chiral molecules adsorbed on gold nanocavities can influence the catalytic properties of mesoporous TiO2 (1), a phenomenon that is related to the Chiral-Induced Spin Selectivity (CISS) effect.

In this contribution we will give an introduction to the physics of nanomagnetism in gold, and show how it is related to the onset of spin-polarized singlet states whose properties depend on the nature of the adsorbate species in coated gold nanoparticles. We will also show how the underlying mechanism for the enhanced catalytic activity for water oxidation observed in TiO2 is also connected to the appearance of spin-polarized singlet states.

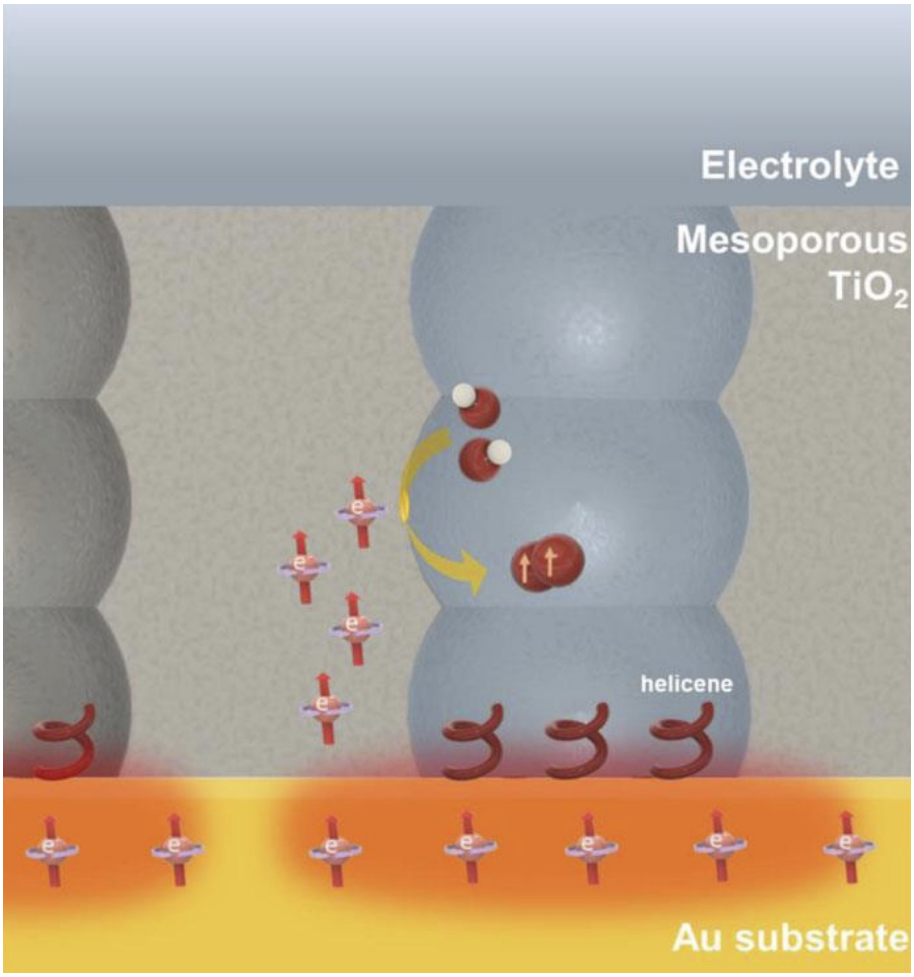

Figure 1: **Illustration of the CISS effect on the helicene-modified mesoporous TiO2 on the Au substrate. The chiral molecules could polarize the spin of electrons traveling through the gold (red areas) and turn the TiO2 into a spin-polarized state, which can then favor the formation of triplet O2 over H2O2 production.**

References

[1] Priscila Vensaus, Yunchang Liang, Nicolas Zigon, Narcis Avarvari, Vladimiro Mujica, Galo J. A. A. Soler-Illia, Magalí Lingenfelder; Hybrid mesoporous electrodes evidence CISS effect on water oxidation. J. Chem. Phys. 21 March 2024; 160 (11): 111103. https://doi.org/10.1063/5.0199339

Polymer matrix composites: The effect of hybrid nanofillers in their mechanical, thermal and viscoelastic behavior

Jennifer Tejedor[1], **Víctor H. Guerrero**[1]
[1] *Department of Materials, Escuela Politécnica Nacional, Quito 170525, Ecuador*
victor.guerrero@epn.edu.ec

Abstract

The development of polymer composites has attracted the attention of industries worldwide during the last few decades, due to the increasing demand of advanced materials used in different applications including coatings, packaging, automotive and aerospace components, semiconductors and civil structures. Epoxy resin is one of the preferred polymers to use as a matrix for many of these applications, due to its high strength, chemical stability, low shrinkage during curing, good adhesion, low price and easy processing. However, its inherent brittleness, high flammability and low impact resistance are drawbacks that have limited its applicability and encouraged its modification to improve its mechanical, thermal and physical properties. Composite engineering techniques based on the adequate selection and combination of particulate fillers, including hybridation and nanoscaling, can be used to tailor a wide range of properties [1]. This research aims to evaluate the effects of incorporating silica nanoparticles (SiO2-NP) and halloysite nanotubes (NTH) on the mechanical, thermal and viscoelastic properties of epoxy composites. The composites were prepared by casting, using for this purpose a diglycidyl ether bisphenol-A epoxy resin (DGEBA) and a diethylenetriamine (DETA) curing agent, both provided by Hexion Inc. with the commercial names of EPON 828 and EPIKURE 3223, respectively. The SiO2-NP were synthesized by a thermal method and acid pretreatment using rice husk as a natural precursor [2], while the NTH (30 - 70 nm) were obtained from Sigma Aldrich. The SiO2-NP and NTH were incorporated to the epoxy matrix to obtain filler percentages between 1.25 and 7.5 wt.%. A series of specimens were fabricated and subjected to bending tests according to ASTM D790-17, thermogravimetric, differential scanning calorimetry, and thermo-mechanical analyses, as well as dynamic mechanical analysis. The results showed that adding the inorganic fillers led to an increase in flexural modulus. In particular, the SiO2-NP composite with a filler percentage of 7.5 wt.% showed a 28.9% increase in flexural modulus. However, adding the inorganic particles slightly decreased the flexural strength. On the other hand, the addition of SiO2 and NTH fillers led to an increase in thermal stability at high degradation temperatures. According to the thermograms showed in Figure 1, at a temperature of around 400°C,

the loss of 80% of the initial mass of the unmodified epoxy resin occurs. Whereas, the hybrid composites filled with 3.5 wt.% SiO2-NP/NTH can withstand a higher degradation temperature of 637°C before losing 80% weight. Additionally, after the addition of the inorganic particles, there was a slight decrease in the coefficient of thermal expansion by up to 4%, indicating a higher dimensional stability of the composites. Finally, the influence of particle incorporation on the viscoelastic properties was evaluated. The results showed that adding the particles, either individually or in combination, increased the storage moduli (E'). In particular, E' increased 13% and 9% at 30°C when using a filler percentage of 7.5 wt.% SiO2-NP and NTH, respectively. Similarly, there was a 5.4% increase in E' for a 5:1.25 wt.% combination of NTH:SiO2-NP. Despite the increase in E' when using the combination of fillers, the moduli of the hybrid composites are lower than those achieved by the individual fillers. This behavior may indicate a higher interaction between the fillers than an interfacial interaction between the fillers and the matrix, resulting in interparticle agglomeration [3]. Similarly, the individual SiO2-NP and NTH composites presented the highest reductions of 24.8 and 22.7% for tan(delta), compared to the hybrid composites, suggesting a highly uniform distribution of the filler in single particle composites. Summarizing, the incorporation of the nanofillers, either individually or in combination, improved the mechanical, thermal, and viscoelastic properties of the epoxy matrix selected. This opens the possibility of using this type of particulate materials to improve other thermoset matrices without affecting their processability, strength, modulus and glass transition temperature.

References

[1] Guerrero V.H. et al. J. Mater. Sci. (2002) 37 (19) pp. 4127-4136.

[2] Tejedor J. et al. J. Phys. Conf. Ser. (2022) 2238 (1) 012005.

[3] Kashfipour M.A. et al. Adv. Compos. Hybrid Mater. (2018) 1 pp. 415–439.

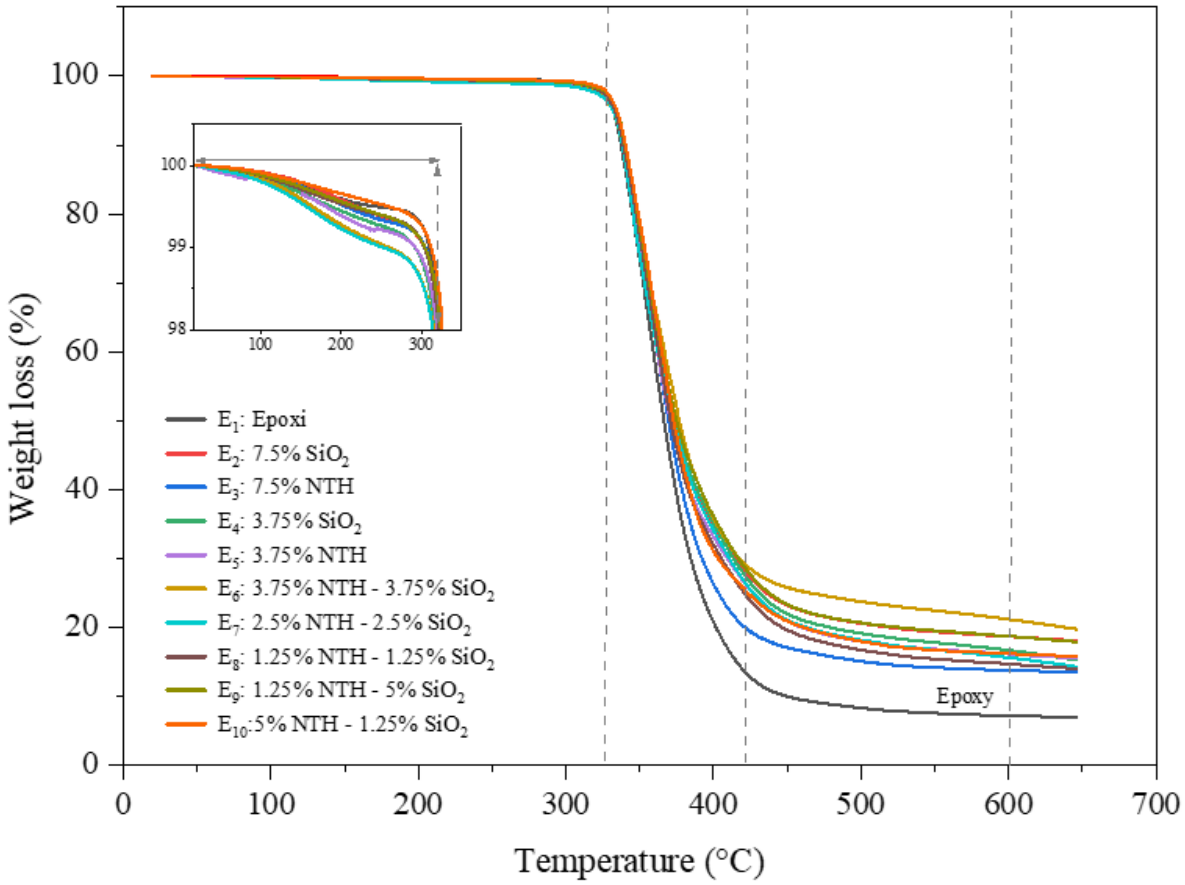

Figure 1: **Thermograms for SiO2-NP and NTH filled epoxy composites.**

Advancing Silicon Solar Cells: Enhancing Efficiency Through Heterojunction Integration with Inorganic Semitransparent Thin Film Technology

Benjamin Andrés Pusay Villarroel[1], Rosa Estefania Almache Hernandez[1], Pablo Rafael Ortega Villasclaras[2], Joaquim Puigdollers González[2].

[1] *School of Physical Sciences and Nanotechnology, Yachay Tech University, Urcuqui 100119, Ecuador*

[2] *Electronic Engineering Department, Universitat Politècnica de Catalunya, Jordi Girona 1 – 3, 08034, Barcelona, Spain*

bpusay@yachaytech.edu.ec

Abstract

Silicon is the predominant material in the photovoltaic industry, and one of the keys to reducing the cost of solar energy is to increase the efficiency of solar modules through processes that integrate into the current industry and make use of abundant materials on the planet. One strategy to achieve this is to simplify the manufacturing process of solar cells and adopt new techniques, such as multi-junction solar cells, to improve their electrical performance. Silicon is an abundant, stable material with advanced development, allowing it to have a broad industrial capacity to produce photovoltaic modules [1].

Thanks to its 1.1 eV band gap, silicon stands out as the optimal choice for the bottom cell in multi-junction or tandem solar cells. Harnessing this advanced and resilient technology is crucial to producing more efficient solar cells through the incorporation of emerging technologies featuring abundant and non-toxic materials. By doing so, we can enhance efficiency, trim production costs, and ultimately render solar energy more accessible and cost-effective on a global scale.

This research unveils a strategy to boost the efficiency of silicon solar cells by integrating a multi-junction solar cell as a substrate, giving rise to a tandem solar cell. The proposal involves employing robust methods to establish selective contacts on silicon, ensuring its readiness for the thermal and chemical processes essential for the development of inorganic solar cells, such as kesterites or CGS. This approach envisions the realization of a resilient, highly efficient, and sustainable multi-junction solar cell over the long term.

Proposed here are processes and strategies aimed at establishing semi-transparent selective contacts in solar cells with inorganic absorbers, such as kesterites or CGS, with the goal of creating a compatible substrate for tandem-type solar cells. In the context of the ETL, an alternative to the traditional CdS in inorganic solar cells is suggested, involving the use of i:ZnO/AZO buffer layers. These layers undergo treat

ments with polymers (PEI) to enhance their characteristics. In terms of the HTL, a back-contact layer has been developed as a substitute for metallic Mo layers, acting as an interface with V2Ox-based TCO. The implementation of this layer has yielded a semi-transparent device with promising features. These advancements hold the potential to significantly impact the efficiency and profitability of tandem solar cells with inorganic absorbers, potentially catalyzing the enhancement of semi-transparent inorganic solar cells [2].

In conclusion, we present a proposed manufacturing process for tandem solar cells utilizing emerging inorganic solar cells, such as CZTS and CGS, as the upper solar cell. The exploration of strategies aims to create a monolithic two-terminal (2T) device while maintaining the physical and electrical characteristics of each component throughout the process, incorporating both chemical and thermal procedures. These meticulous strategies play a pivotal role in achieving efficient and enduring devices. The implementation of these advanced techniques is expected to propel research and development in tandem solar cells based on abundant and sustainable materials, thereby significantly contributing to the widespread adoption of solar energy as a clean and renewable power source [3].

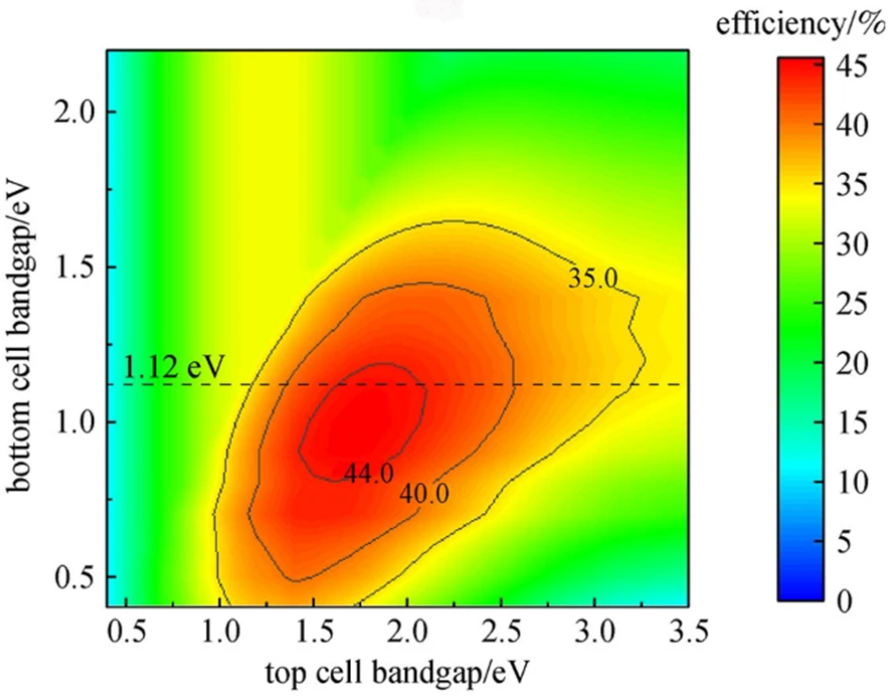

Figure 1: **Absorbers BandGap potential for the development of high-performance and low-cost Si-based tandem solar**

References

[1] ¨Lu, S., et al. Possible top cells for next-generation Si-based tandem solar cells. Front. Optoelectron. 13, 246–255 (2020). https://doi.org/10.1007/s12200-020-1050-y

[2] Ignacio Becerril-Romero, et al, Transition-Metal Oxides for Kesterite Solar Cells Developed on Transparent Substrates, ACS Appl. Mater. Interfaces 2020, 12, 30, 33656–33669

[3] Jeong, A.R., et al,. Electrical analysis of c-Si/CGSe monolithic tandem solar cells by using a cell-selective light absorption scheme. Sci Rep 7, 15723 (2017). https://doi.org/10.1038/s41598-017-15998-y

Acta Microscopica Vol. 34, Supp. 2, 2025
Abstract Book NSSY 2024 - Galapagos 19-25 May, 2024

Functional Materials Using the Segregated Network Approach

Alan Dalton[1]
[1] *University of Sussex*
a.b.dalton@sussex.ac.uk

Abstract

Segregated nanomaterial networks, obtained through drying of colloidal co-dispersions of nanoparticle filler and matrix particles, are a promising route to functional materials with low loadings of filler. The loading level at which a system-scale interconnected nanomaterial network is formed is known as the percolation threshold, and may be manipulated through choice of the matrix particles as well as the filler particles. Lowering the loading required to achieve a functional composite structure is critical to maximising the benefit of filler addition while avoiding any detrimental impacts on the properties of the matrix material.

In this talk I will describe various strategies to use the segregated network approach to fabricate materials with a range of functional properties from high performance notch filters to wholly recyclable RFID antennas.

I will highlight a specific example where we observe new unusual behaviour in such systems. Explosive percolation is an experimentally-elusive phenomenon where network connectivity coincides with onset of an additional modification of the system; materials with correlated localisation of percolating particles and emergent conductive paths can realise sharp transitions and high conductivities characteristic of the explosively-grown network. This leads to conductivities exceeding those of dense-packed networks of the pristine filler particles, illustrating the potential of explosive percolation by design to realise low-loading composites with dramatically-enhanced electrical transport properties.

Acta Microscopica Vol. 34, Supp. 2, 2025
Abstract Book NSSY 2024 - Galapagos 19-25 May, 2024

Development of vinyl polymeric composites and gels for biomedical and related applications

Antonio Díaz Barrios[1]

[1] *School of Chemical Science and Engineering, Yachay Tech University, Hacienda San José, 100650-Urcuqui, Ecuador*

adiaz@yachaytech.edu.ec

Abstract

On a global scale, polymers obtained by emulsion processes represent approximately 10% of total polymer production and more than 50% of these polymers are used directly in the form of aqueous dispersion. This type of polymers has the environmental advantage of replacing organic solvents with water in many industrial applications such as architectural paints and adhesives (1). In the medium and long term, the sustainability of materials manufacturing will be limited to having a low environmental impact. This limitation constitutes a driving force to promote innovation on new materials, this include hydro gels and polymeric composites made of water soluble polymer. Beside, of being water soluble materials, the purpose of developing these hybrid materials is to achieve the synergy between the intrinsic properties of this type of polymers and the materials they encapsulate or interact. This work shows early research of the author on vinyl acrylic polymer and nanosilver composites, with potential as antibacterial coating, and polymer gels for encapsulation and controlled release of drugs and bactericidal substances. Special emphasis is made to present more recent research work on the development of potential luminescent coatings based on selected composites of hydroxyapatite and barium titanate with vinyl acrylic polymer. Also, the development of luminescent solutions made of lineal and cross-linked vinyl caprolactam gels and on carbon quantum dots obtained from avocado seeds is presented. The experimental protocols include the synthesis of the polymer, hydro gels and composites above mentioned and their exhaustive characterization by IRFT, Raman, XPS and Photoluminescence spectroscopies, Thermogravimetric (TGA) analysis, dynamic light scattering, and TEM microscopy. As conclusions, the homo polymer vinyl caprolactam and their corresponding cross-linked hydrogels with poly ethylene glycol di acrylate (VCL-PEGDA), the carbon dots, and the corresponding nanocomposites were successfully synthesized, as demonstrated by the characterization techniques above mentioned. It is concluded that the vinyl acrylic polymer is acting as a very suitable matrix to hold and maintain the luminescent properties of hydroxyapatite and barium titanate nanoparticles. On the other side, in the direction of obtaining

environmental friendly materials, it is worth mentioning the use of biocompatible vinyl caprolactam hydro gels to substantially enhance the already good luminescent properties of organic carbon quantum dots obtained from carbon avocado seeds, as can be seen in Fig. 1.

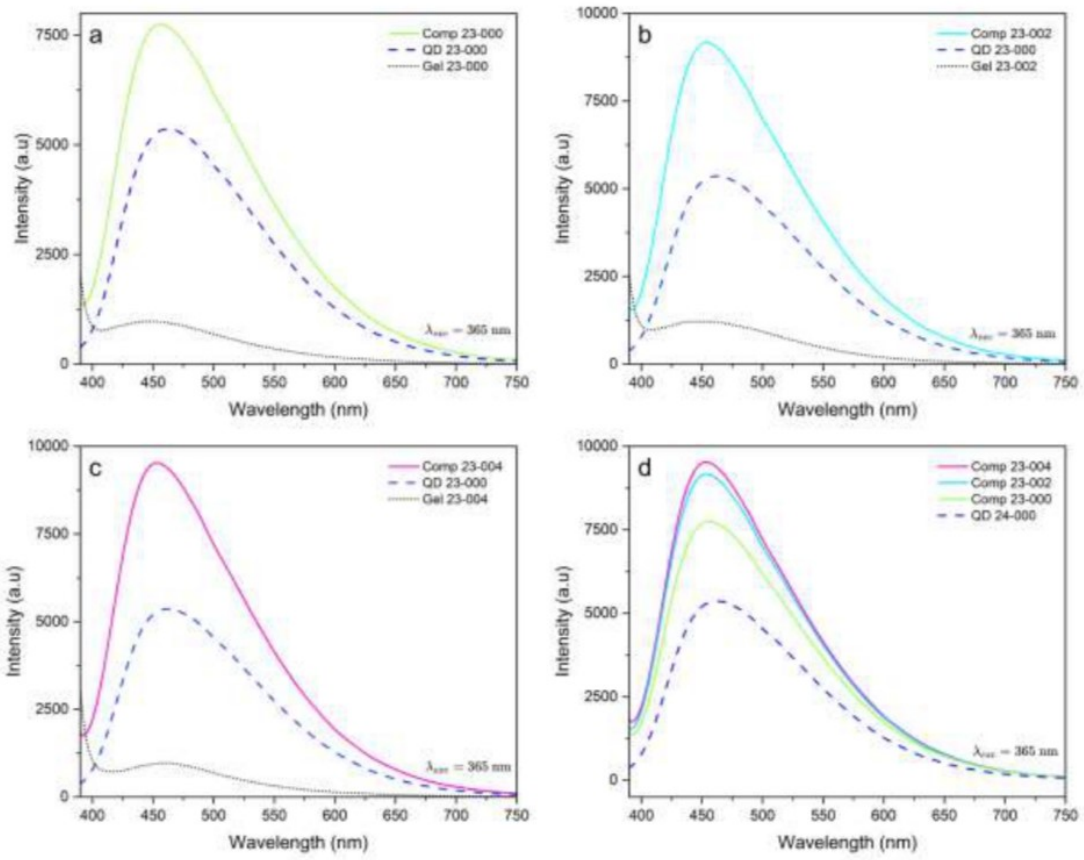

Figure 1: **Enhancement of luminescence of avocado quantum dots by encapsulation with VCL-PEGGD gels**

References

[1] M. J. Barandiaran, J. C. de la Cal, J. M. Asua: Emulsion Polymerization. Polymer Reaction Engineering, Chapter 6. J.M. Asua Editor., Blackwell, 2007

Acta Microscopica Vol. 34, Supp. 2, 2025
Abstract Book NSSY 2024 - Galapagos 19-25 May, 2024

Synthesis and characterization of nitrogen-doped carbon nanotubes using a mixture of alcohols and nitrogen precursors

Francisco Javier Sánchez Blanco[1], Julio C. Chacón-Torres[2], Florentino López Urías[1], Emilio Munoz Sandoval[1*]

[1] *Advanced Materials Department Potosino Institute of Scientific Research and Technology, A.C (IPICyT) San Luis Potosí, México.*

[2] *Advanced fuNcTiOnal Nanomaterials (ANTON), Yachay Tech University (UITEY), Hacienda San Jose S/N, Urcuquí, Ecuador*

francisco.sanchez@ipicyt.edu.mx

Abstract

In the production of carbon nanotubes, various synthesis methods and precursors have been studied. In the case of the catalytic chemical vapor deposition method, different precursors have been explored to control their efficiency and degree of graphitization. For example, the effect of the carbon-to-oxygen ratio on the degree of graphitization in the fabrication of Carbon Nanotubes (CNTs) using alcohols has been reported [1]. Ethanol is known for its high efficiency in CNT fabrication at low temperatures (700°C) [2], and isopropanol has been employed in the manufacturing of semiconductor CNTs [3]. In this study, carbon nanostructures were synthesized through catalytic chemical vapor deposition, utilizing methanol, ethanol, and isopropanol as carbon precursor solutions, and Fe2O3 (hematite) as the catalytic precursor. The effect of nitrogen on the morphology and quality of the fabricated carbon structures was also investigated. For this aspect, mixtures of methanol, ethanol, and isopropanol with acetonitrile, benzylamine, and pyridine were used as carbon and nitrogen precursors. The samples were characterized using Raman spectroscopy, X-ray diffraction (XRD), scanning electron microscopy (SEM), thermogravimetric analysis (TGA), X-ray photoelectron spectroscopy (XPS), atomic force microscopy (AFM), and cyclic voltammetry (CV). Raman spectroscopy revealed that carbon samples fabricated with ethanol or isopropanol exhibited high graphitization, with an intensity ratio between the D-band and G-band of ID/IG 0.24, as corroborated by XPS spectra. On the other hand, samples fabricated with methanol showed an I2D/IG value of 0.95, indicating the presence of few-layered graphitic material. XRD results presented signals of iron and graphite material in all cases. Scanning electron microscopy images displayed different structures depending on the carbon precursor and carbon-nitrogen combination. Thermogravimetric analysis indicated that the sample with the highest thermal stability in an oxygen environment was the one fabricated with the mixture of isopropanol

and benzylamine and Cyclic voltammetry analysis revealed interesting properties.

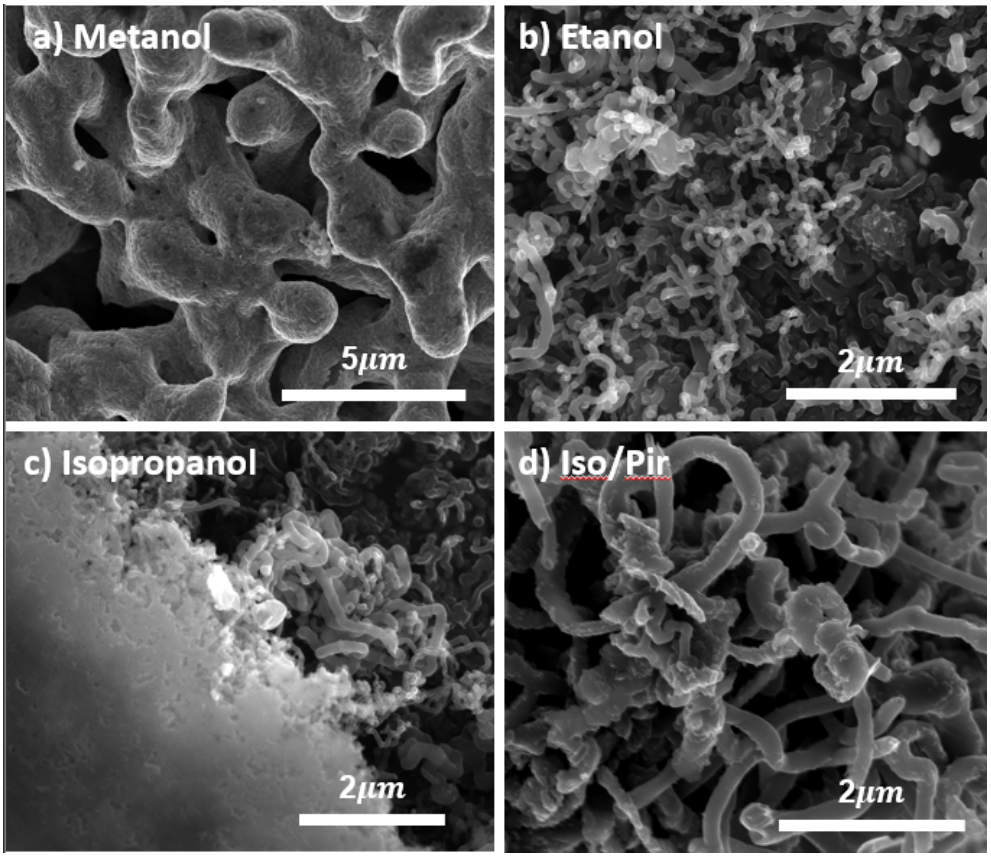

Figure 1: **Scanning electron micrographs of carbon nanostructures produced using (a) methanol, (b) ethanol, (c) isopropanol and (d) a mixture of isopropanol and Pyridine as a precursor solution**

References

[1] A. Grüneis, M.H. Rümmeli, C. Kramberger, A. Barreiro, T. Pichler, R. Pfeiffer, H. Kuzmany, T. Gemming, B. Büchner, High quality double wall carbon nanotubes with a defined diameter distribution by chemical vapor deposition from alcohol, Carbon N Y. 44 (2006) 3177–3182. https://doi.org/10.1016/j.carbon.2006.07.003

[2] H.J. Basheer, C. Pachot, U. Lafont, X. Devaux, N. Bahlawane, Low-Temperature Thermal CVD of Superblack Carbon Nanotube Coatings, Advanced Materials Interfaces. 4 (2017) 1–9. https://doi.org/10.1002/admi.201700238.

[3] J. Parker, C. Beasley, A. Lin, H.Y. Chen, H. S. P. Wong, Increasing the semiconducting fraction in ensembles of single-walled carbon nanotubes, Carbon 50 (2012) 5093-5098. DOI:10.1016/j.carbon.2012.06.049.

In situ Raman applied to the stability of boron-doped diamond electrodes

Laís Gimenes Vernasqui[1], Evaldo José Corat[1], Neidenêi Gomes Ferreira[1]

[1] *Instituto Nacional de Pesquisas Espaciais - Laboratório Associado de Sensores.*

laisvernasqui@gmail.com

Abstract

Boron-doped diamond (BDD) electrodes are widely regarded as ideal for applications in the electro-oxidation of pollutants due to their chemical stability, electrical conductivity, and wide potential window. Synthesizing this material on 3D substrates enhances its surface area, further improving its suitability for such applications. Physical, morphological, and electrochemical characterization techniques are commonly employed to understand these materials/composites. However, morphological/structural and electrochemical characterizations, when analyzed separately, may not always predict the material/composite behavior during real applications. This can hinder the development of new materials and widen the gap between research and commercial applications. Recent advancements in electrochemical analysis have led to increased utilization of in situ/operando techniques and, among these techniques, Raman spectroscopy stands out as a particularly promising method for in situ analysis due to its non-destructive nature and high sensitivity. However, there is limited literature applying this technique to BDD studies. In this context, this study presents stability analyses using two novel 3D boron-doped diamond electrodes (micro and ultrananocrystalline), with Raman spectra obtained during electrochemical analyses. The films were produced via a two-step growth process to ensure complete coverage of the substrate surface, resulting in a 3D sample. Film morphologies were thoroughly examined using FEG-SEM images at various sample planes and depths on both sides at different stages of film growth. Results from morphological and electrochemical characterizations indicate the film quality and that both developed materials are suitable for the proposed applications. In situ Raman measurements demonstrate their stability across the studied potential range. Additionally, the development of a new electrochemical cell obtained via 3D printing, suitable for use with porous or 3D electrodes, is highlighted.

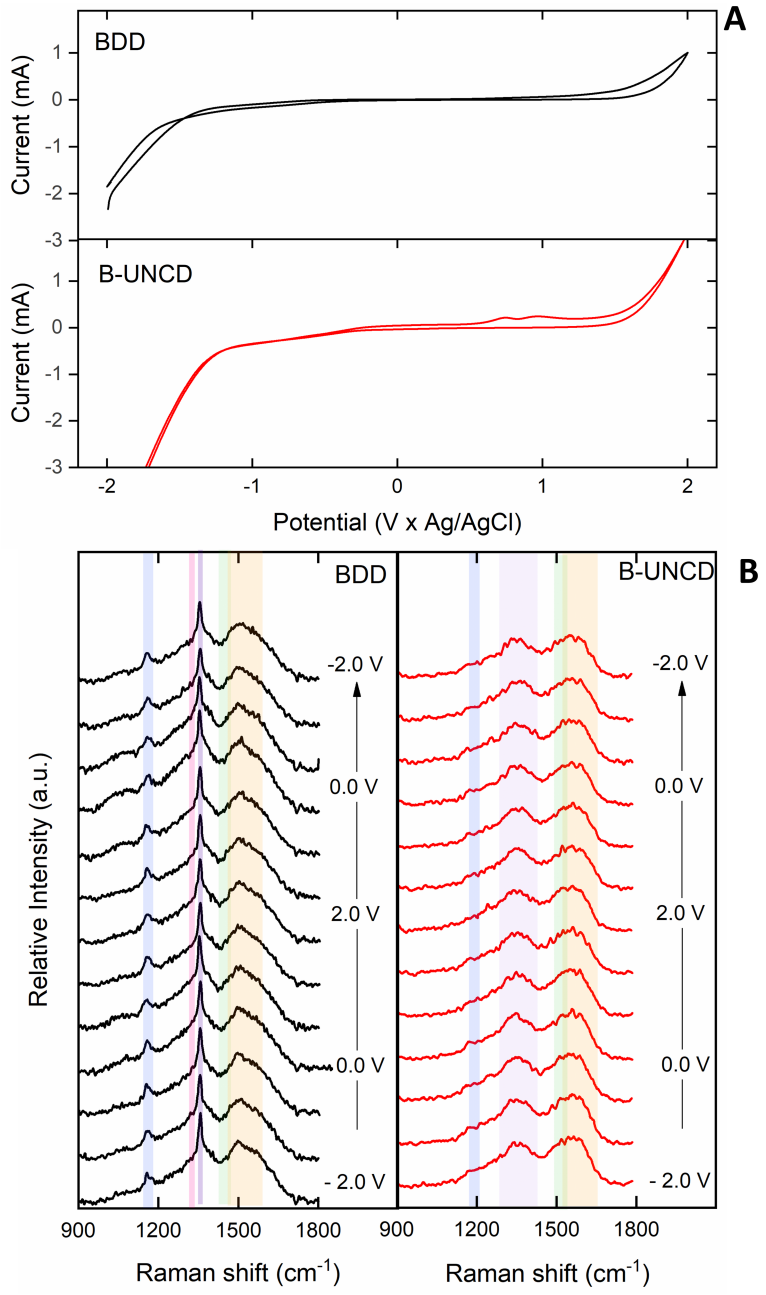

Figure 1: **A) CV obtained for BDD and B-UNCD samples (0.1 M.L-1 Na2SO4) and B) Raman spectra for both samples obtained during the electrochemical measurement.**

Modification of the electrical and optical properties of pectin films through thiourea-grafting and incorporation of silver nanoparticles

Araceli Granja Alvear[1], Sebastián Ojeda[1], Silvana Chiriboga[1], Juan Pablo Saucedo[1], Floralba López[1], Lola de Lima[1], Luis Borrero[2], Jesús González[2]

[1] *CATS Research Group, School of Chemical Sciences & Engineering, Yachay Tech University, 100119-Urcuquí, Ecuador*

[2] *Pontificia Universidad Católica del Ecuador, Facultad de Ciencias Exactas y Naturales, Escuela de Ciencias Físicas y Matemática, Laboratorio de Optica Aplicada, Quito 17-01-2184, Ecuador*

agranja@ist17dejulio.edu.ec

Abstract

In recent years, the interest of researchers in improving the mechanical, thermal, electrical and magnetic properties of polymeric materials has experienced a notable increase. In these modification studies, several options are explored, such as the addition of cross-linking agents or the incorporation of compounds to confer specific properties(A, Hiremath et al. Cogent Engineering (2021), (8) (1-23). These advances are closely linked to the development of nanotechnology, which has revealed the possibility of fusing the advantages of the outstanding properties of nanoparticles with polymeric matrices, giving rise to the formation of polymeric nanocomposites that can be used in multiple applications ranging from medicine such as drug delivery or as antimicrobial agents or more technological applications such as electrocatalysis (Granja A. et.al Mat. Res.(5) (2022))(Dolinska J. et al. ACS Omega (9) (2020)) . In this work, pectin-based thin films were synthesized and modified by thiourea grafting, followed by enrichment with silver nanoparticles, to modify the electrical properties of the pectin films. The silver nanoparticles were prepared by a chemical synthesis method in which the size and morphology of the naoparticles is controlled through the use of stabilizing agents, capping agents and reducing agents. The pectin films were prepared with a 1% solution and grafted with a thiourea solution plus epichlorohydrin and subsequently loaded with nanoparticles. The nanoparticles were analyzed by UV Vis and by SEM where sizes from 20 nm to approximately 120 nm were found. Subsequently, the electrical properties of the films were systematically evaluated using electrical impedance spectroscopy (EIS) to evaluate the conductivities. Additionally, the bandgap energy for the films was calculated using Tauc plots based on diffuse reflectance measurements. The findings indicate a notable improvement in the ionic conductivity of pectin-based films, attributed to the modification of the biopolymer graft polymerization process. Furthermore, the incorporation of silver nanoparticles is advantageous to improve the

ionic conductivity of the resulting nanocomposite. At the same time, both the graft polymerization process and the incorporation of silver nanoparticles contribute to an increase in the bandgap energy, as demonstrated by the findings from diffuse reflectance measurements. On the other hand, the optical properties of pristine and modified pectin films were evaluated by fluorescence spectroscopy, highlighting the remarkable photoluminescent properties exhibited by these films. These characteristics could be used in various applications such as photocatalysis, as well as the manufacture of photodiodes, given their ability to store and release light energy efficiently(Dolinska J. et al. ACS Omega (9) (2020))

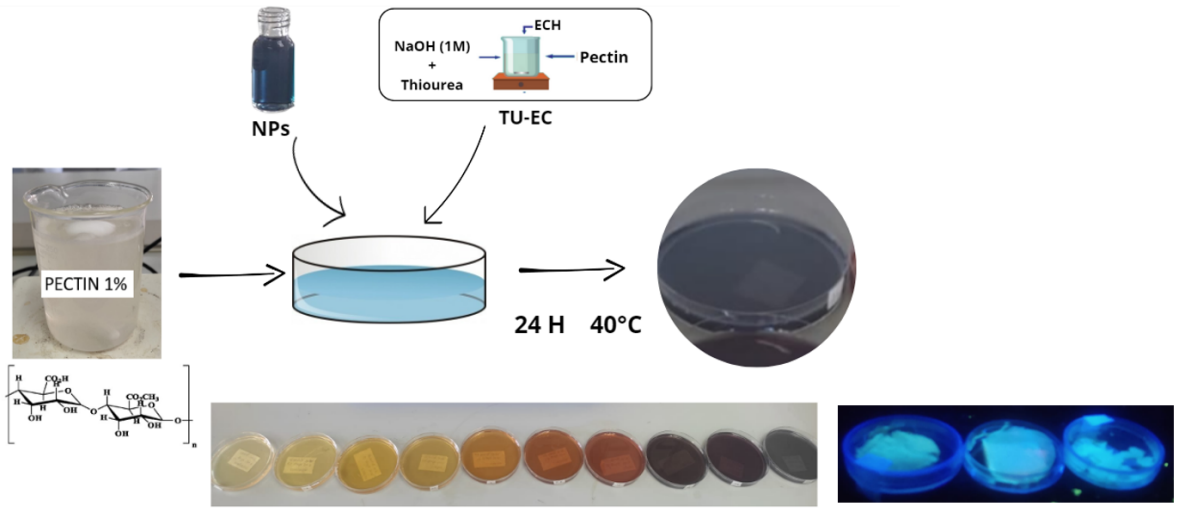

Figure 1: **Figure 1. Schematic representation of preparation of photoluminescent thiourea-grafted pectin films with silver nanostructures embedded.**

References

[1] A, Hiremath et al "Nanoparticles filled polymer nanocomposites: a technological review" Cogent Engineering (2021), 8: 1991229, pp 1-23 https://doi.org/10.1080/23311916.2021.1991229

[2] Granja LA. Polyvinyl Alcohol Films Loaded with Silver Nanostructures with Different Sizes and Shapes with Tunable Plasmonic and Electric Properties. A Spectroscopic Study. Materials Research. 2022;25:e20210574. DOI: 10.1590/1980-5373-MR-2021-0574.

[3] Dolinska J. Noble Metal Nanoparticles in Pectin Matrix. Preparation, Film Formation, Property Analysis, and Application in Electrocatalysis ACS Omega 2020, 5, 37, 23909–23918 9, 2020 DOI: 10.1021/acsomega.0c03167.

Tuesday

Tutorial: Optical Spectroscopy of Filled Carbon Nanotubes

Sofie Cambré[1]

[1] *NANOrOPT, Physics Department, University of Antwerp, Belgium*

sofie.cambre@uantwerpen.be

Abstract

Single-walled carbon nanotubes (SWCNTs) exhibit unique, remarkably diverse electronic and optical properties that depend critically on their exact chiral structure and are extremely sensitive to the local environment of the SWCNT. For this reason, optical spectroscopy is one of the most valuable methods to identify the different chiral species in a particular sample and at the same time probe their interactions with their local environment. In this tutorial, I will provide an overview of how optical spectroscopy can be used to assess the filling of SWCNTs with various species. I will start with the simple case of filling with water molecules [1-4], to then discuss filling with solvents with varying dielectric constant [5] towards filling of functional molecules that can create new properties such as energy transfer and specific one-dimensional alignment.[6-8] Finally I will discuss the synthesis of novel nanostructures in the interior of SWCNTs and how they can again be studied by optical spectroscopy.[9-10] Different optical techniques will be discussed, in particular absorption, wavelength-dependent resonant Raman scattering, fluorescence-excitation, transient absorption and nonlinear optical spectroscopy.

References

[1] S. Cambré et al, Phys. Rev. Lett. 104, 207401 (2010)

[2] S. Cambré et al Angew. Chem. 50, 2764 (2011)

[3] S. Cambré et al, ACS Nano 6, 2649 (2012)

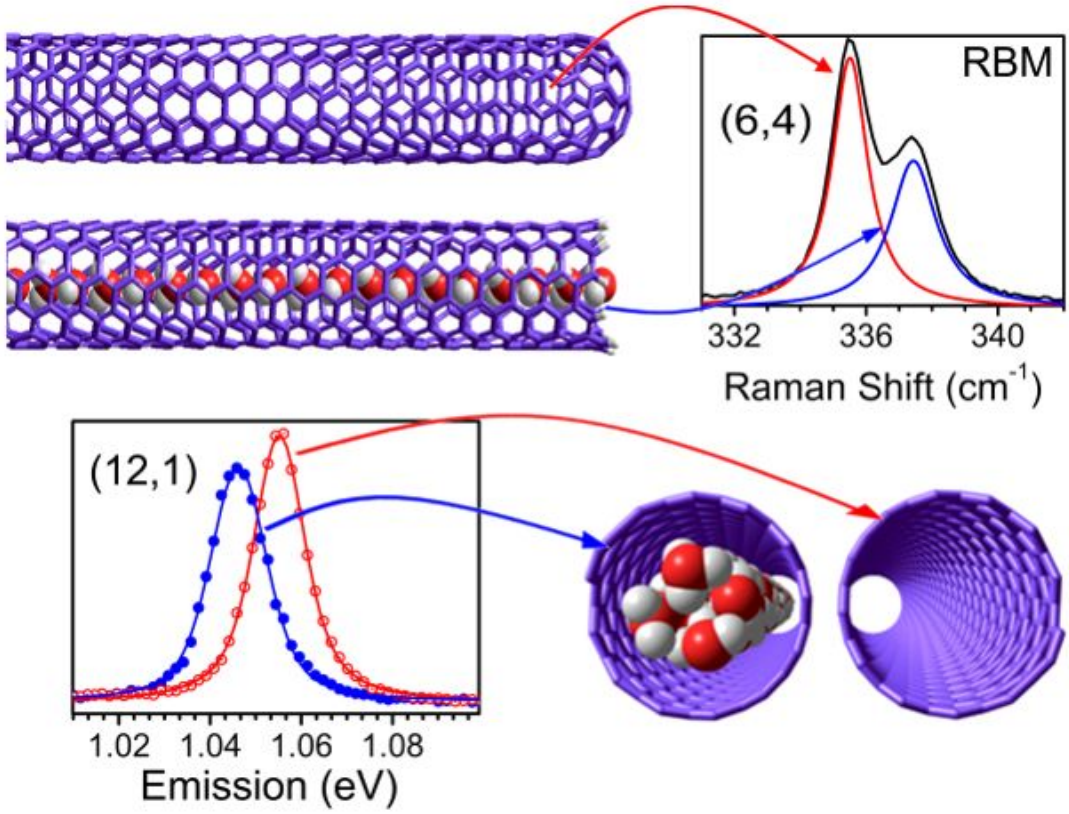

Figure 1: **Example of Raman and emission spectroscopy of empty and water-filled carbon nanotubes**

Dye molecules inside single-wall carbon nanotubes

Salomé Forel[1,2], Han Li[3], Stein van Bezouw[1], Jochen campo[1], Wim Wenseleers[1], Benjamin S. Flavel[3], Sofie Cambré[1]

[1] *Nanostructured and Organic Optical and Electronic Materials, University of Antwerp, Belgium.*

[2] *Laboratoire des Multimatériaux et Interfaces, CNRS/Université Claude Bernard Lyon 1, France*

[3] *Institute of Nanotechnology, Karlsruhe Institute of Technology, Karlsruhe 76021, Germany.*

salome.forel@univ-lyon1.fr

Abstract

The diverse chiral structures of single-walled carbon nanotubes (SWCNTs) offer a wide range of electronic and optical properties, making them highly promising for applications such as solar energy harvesting and high-performance (opto-)electronic devices. Beyond their intrinsic characteristics, SWCNTs possess a hollow core that can be filled with dyes [1] creating one-dimensional hybrids that integrate the unique properties of both the nanotube and the dyes. In this study [2], we present a novel approach involving thorough chirality sorting [3] and dye filling, resulting in the isolation of nearly single-chirality squaraine-filled SWCNTs, as illustrated in the photoluminescence-excitation (PLE) map depicted in Figure 1. Each combination of dye and SWCNT chirality exhibits distinct absorption wavelengths of the encapsulated dyes, influenced by the varying dye stacking driven by the diameter of the surrounding SWCNT. The diameter-dependent dye absorption, coupled with subsequent energy transfer, is experimentally elucidated through meticulous measurement and fitting of fluorescence-excitation maps for different chirality-sorted dye-filled SWCNT samples. This study establishes the SWCNT diameter as a critical factor for tuning the optical properties of these hybrids, providing new insights for potential applications in optoelectronics. Furthermore, a comparative analysis with molecular models sheds light on the diverse stacking configurations of dyes within the hollow space of SWCNTs with different diameters.

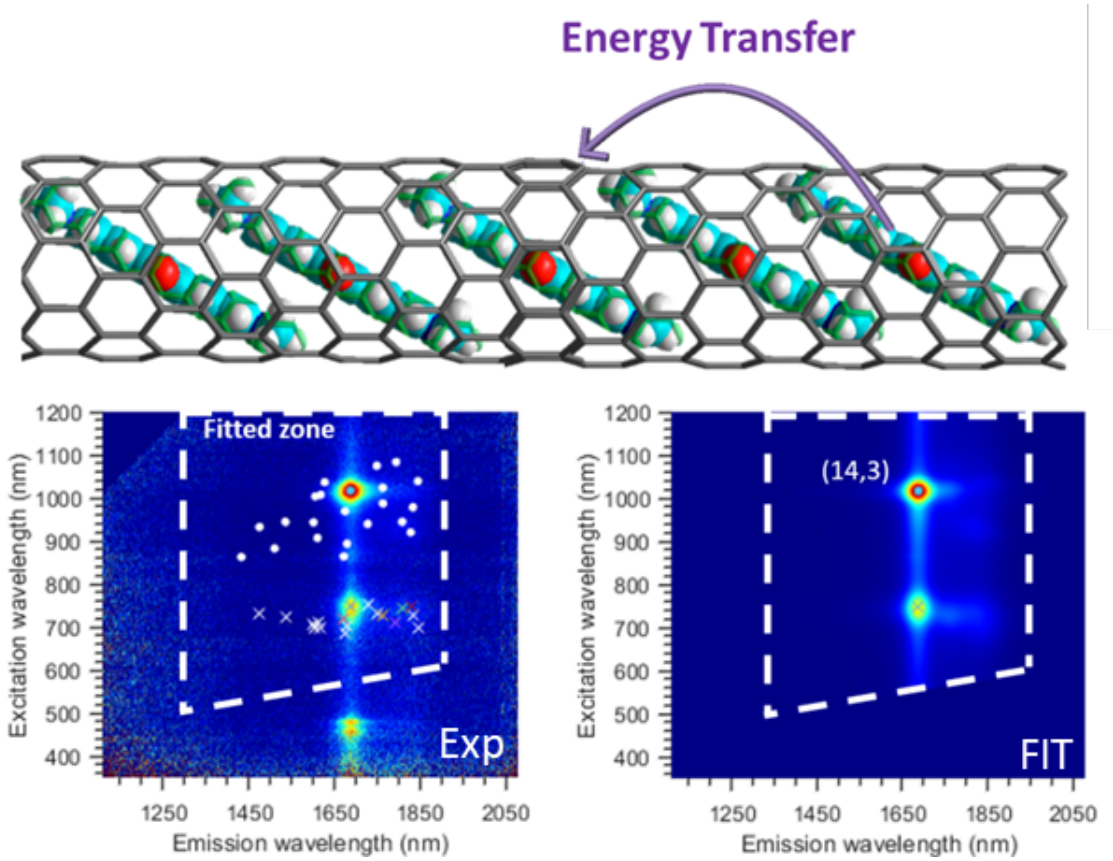

Figure 1: **Schematic view of the new hybrids (bottom) Example of a PLE map and the corresponding fit for one of the 15 samples. (left) experimental PLE maps, the white dots represent all the chiralities that have been fitted and the crosses represent the energy transfer. (right) Fitted PLE map, the most abundant chirality is labelled.**

References

[1] S. Cambré et al., Nature Nanotechnology 2015, 10 (3), 248–252 [2] S. Forel et al. Nanoscale, 2022, 14, 8385 [3] L. Han et al., ACS Nano 2020, 14 (1), 948–963.

Acta Microscopica Vol. 34, Supp. 2, 2025
Abstract Book NSSY 2024 - Galapagos 19-25 May, 2024

Unveiling degradation mechanisms of enhanced Polymers through advanced spectroscopy in extreme environments.

C Reinoso[1], E Iribarra[2], A Díaz-Barrios[3]

[1] *School of Physical Sciences and Nanotechnology, Yachay Tech University, 100119, Urcuquı, Ecuador.*

[2] *Escuela Politécnica Nacional, E11-253, Quito, Ecuador.*

[3] *Yachay Tech University, School of Chemical Sciences and Engineering, Urcuquí, 100119, Ecuador.*

creinoso@yachaytech.edu.ec

Abstract

Polymer materials have revolutionized various facets of human existence, providing indispensable contributions to modern life. New modification has been accomplished to give to them new mechanical, optic and electrical properties by incorporation of two dimensional carbon structures [Wu et all, 2023]. However, the widespread application of these traditional and enhanced polymers has brought about significant challenges, particularly in terms of disposal and waste management, casting a shadow over many mitigation efforts [Athulya et all, 2023]. In response to this environmental concern, our study delves into the intricacies of polymer degradation, employing cutting-edge physical methods of analysis, with a primary focus on X-ray Photoelectron Spectroscopy (XPS), complemented by Raman and FTIR studies. High Power UV light exposure, Electron gun irradiation, and synergistic techniques to accelerate the degradation process has been used in this work. Through the integration of these advanced spectroscopic tools, we aim to construct comprehensive libraries of degraded polymers, enabling thorough comparative analyses against those subjected to natural environmental exposure. Our investigation spans diverse environmental settings, encompassing seas, oceans, shores, rivers, and lagoons. The goal is to identify and correlate degradation patterns based on varying exposure durations, shedding light on how different environmental conditions influence polymer deterioration. Particularly, we meticulously scrutinize changes in functional groups at the C1s core level, utilizing XPS to discern alterations in the chemical structure [Kovac et all, 2011]. Two film polymers were fabricated freshly and exposed to 60 W High Power Ultraviolet Light generated by Helium gas plasma for 30 min and 60 min, respectively. The XPS analysis of these samples exhibits changes, especially at the Carbon main feature high resolution, where the emergence of C=O bonding and the noticeable loss of C-C bonding serve as crucial indicators. Part of these findings are presented in Figure 1, illustrating Polyethylene and Polyamine analysis. This systematic approach not only enhances our understanding of degradation mechanisms but also facilitates the

development of a comprehensive comprehension of how diverse environmental conditions impact the lifespan and stability of polymers. One noteworthy aspect of our research involves the deployment of polymer films in the Antarctic Ocean during the austral summer of 2024. This strategic placement takes advantage of the region's high UV light exposure, providing an ideal environment to study accelerated polymer degradation. The initial results of this pioneering endeavor are anticipated to be unveiled at the upcoming NSSY conference in May 2024, offering a glimpse into the unique challenges and opportunities presented by extreme environmental conditions. The study aims to provide critical insights into the effects of high UV exposure on polymer degradation, contributing valuable data to the broader understanding of polymer behavior in various environmental contexts. By unraveling the intricacies of polymer degradation through sophisticated spectroscopic techniques, our research not only contributes to the scientific community's knowledge base but also addresses pressing environmental concerns associated with polymer usage. The outcomes of this study are poised to advance our ability to manage and mitigate the environmental repercussions linked to the extensive utilization of polymers and its modified versions in everyday life. Ultimately, our findings may pave the way for the development of more sustainable and environmentally friendly traditional and enhanced polymer materials, ushering in a new era of responsible material usage.

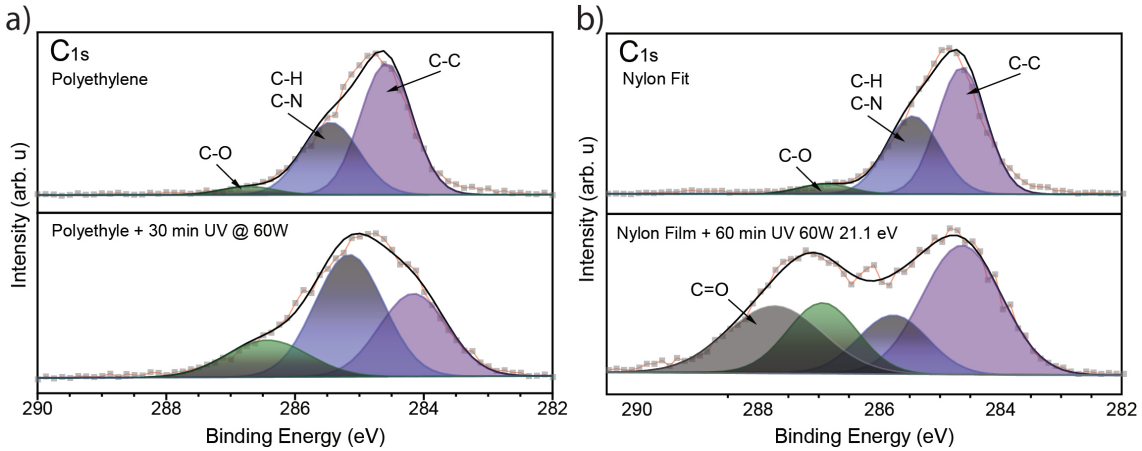

Figure 1: **XPS C1s spectra of a) Polyethylene film before and after being exposed to 30 min 60 Watts UV light. b) Polyamine film before and after being exposed to 60 min 60 Watts UV light.**

References

[1] Wu, Z., Zhao, Y., Yang, K., Guan, J., Wang, S., Gu, Y., ... & Ritchie, R. O. (2023). Enhancing the Mechanical Performance of Fiber-Reinforced Polymer Composites Using Carbon Nanotubes as an Effective Nano-Phase Reinforcement. Advanced Materials Interfaces, 10(3), 2201935.

[2] Athulya, P. A., & Chandrasekaran, N. (2023). Interactions of natural colloids with microplastics in aquatic environment and its impact on FTIR characterization of polyethylene and polystyrene microplastics. Journal of Molecular Liquids, 369, 120950.

[3] Kovac, J. (2011). Surface characterization of polymers by XPS and SIMS techniques. Mater. Technol, 45(3), 191-197.

Acta Microscopica Vol. 34, Supp. 2, 2025
Abstract Book NSSY 2024 - Galapagos 19-25 May, 2024

Fully atomic layer-deposited transparent electron selective carrier layer for Cd-free thin-film solar cells

Rosa Estefanía Almache[1], Benjamin Pusay[1], Pablo Ortega[2], Joaquim Puigdollers[2]

[1] *School of Physical Sciences and Nanotechnology, Yachay Tech University, Urcuqui 100119, Ecuador*

[2] *Electronic Engineering Department, Universitat Politècnica de Catalunya, Jordi Girona 1 – 3, 08034, Barcelona, Spain*

ralmache@yachaytech.edu.ec

Abstract

Thin film solar cells are a promising alternative for photovoltaic devices due to their composition of abundant elements, ease of production at low temperatures, and excellent optical absorption properties [1]. Additionally, these materials allow a tunable bandgap energy, which makes them an attractive candidate either as a top or bottom solar cell in tandem technologies combined with transparent selective contacts [2]. However, conventional thin film devices use a toxic cadmium sulfide CdS layer as electron selective contact (ETL), resulting in difficult-to-dispose chemical waste. This work explores the use of transition metal oxides (TMOs) as alternative electron transport layers to replace conventional and toxic CdS-based contacts in thin-film devices . Specifically, a conductive transparent stack of ZnO and aluminum doped zinc oxide ZnO:Al (AZO) films are deposited using atomic layer deposition technique (ALD), with the potential inclusion of a polyethylenimine (PEI) interlayer as dipole to enhance the overall electrical contact performance. Fabricated CZTSe thin film solar cells exhibit remarkable photocurrent density values of 35 mAcm-2, open-circuit voltage around 260 mV, and efficiencies up to 3.5% using front illumination (AM1.5G 1 kWm-2 solar spectrum, T = 25 ºC). The optical characteristics and elemental composition of the layers are also analyzed.

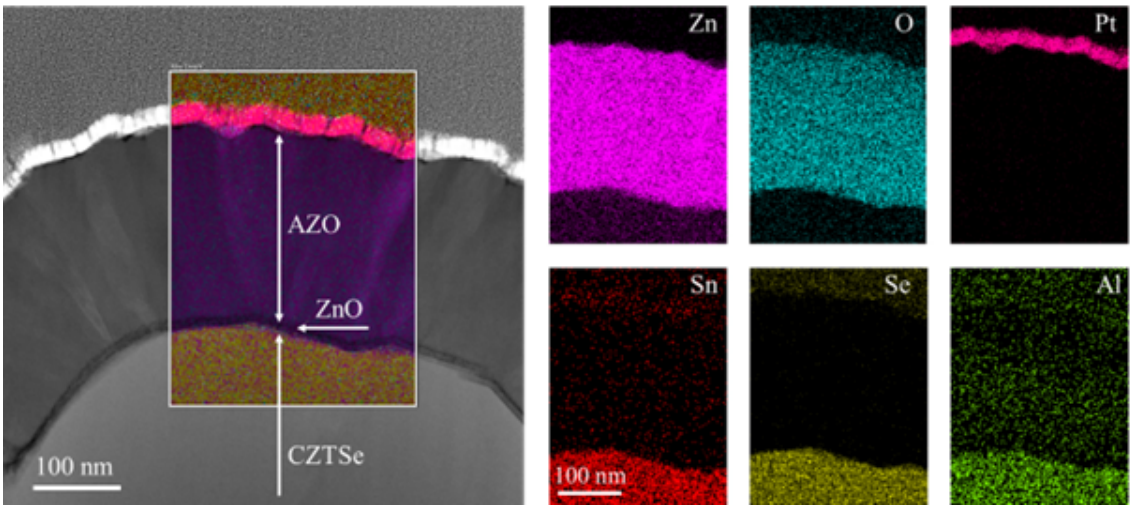

Figure 1: **STEM Image of a cross-section view of the ETL stack and EDS mapping images.**

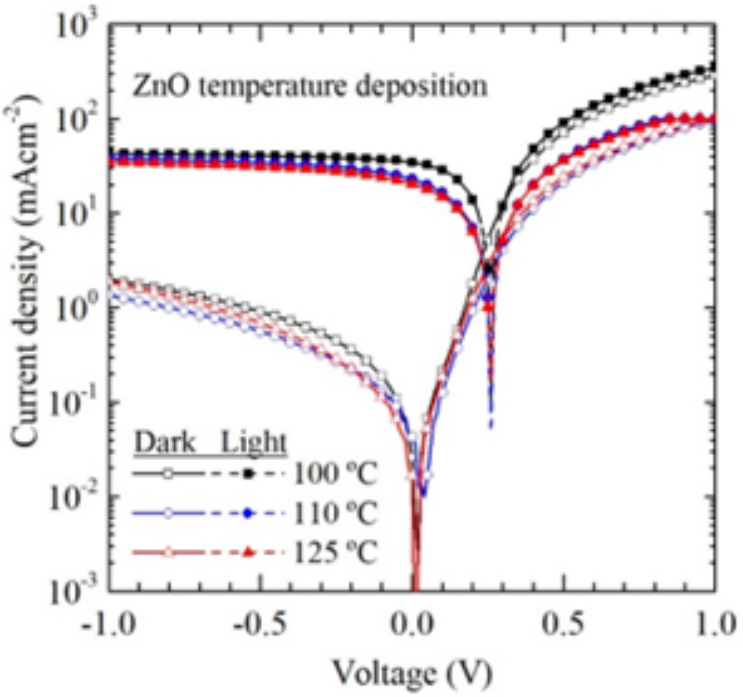

Figure 2: **Dark and light J-V characteristics for the best solar cells with the ZnO layer deposited at different ALD temperatures, 100 ºC, 110 ºC and 125 ºC.**

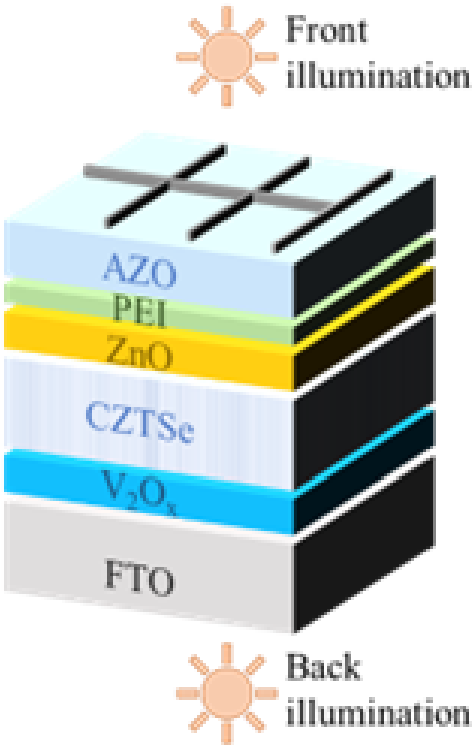

Figure 3: **Sketch of the CZTSe solar cell fabricated with ZnO/PEI as ETL**

References

[1] N. L. Muttumthala and A. Yadav, "A concise overview of thin film photovoltaics," Mater Today Proc, 2022, doi: https://doi.org/10.1016/j.matpr.2022.04.862.

[2] S. and P. M. and J. L.-K. Z. and S. E. Tiwari Kunal J. and Giraldo, "Recent Advances in the Kesterite-Based Thin Film Solar Cell Technology: Role of Ge," in Recent Advances in Thin Film Photovoltaics, N. B. Singh Udai P. and Chaure, Ed., Singapore: Springer Nature Singapore, 2022, pp. 41–66. doi: 10.1007/978-981-19-3724-8_3.

Mixed-Dimensional Nanostructures by van der Waals Epitaxy

Yarden Danieli[1], Noya-Ruth Itzhak[1], Olga Brontvein[2], Katya Rechav[2], Lothar Houben[2], Ifat Kaplan-Ashiri[2], Iddo Pinkas[2], Hagai Cohen[2], Irit Goldian[2], Sidney Cohen[2] and **Ernesto Joselevich**[1]

[1] *Department of Molecular Chemistry and Materials Science, Weizmann Institute of Science, Rehovot 76100, Israel*

[2] *Chemical Research Support Unit, Weizmann Institute of Science, Rehovot 76100, Israel*

ernesto.joselevich@weizmann.ac.il

Abstract

Mixed-dimensional heterostructures with unusual optoelectronic properties are created by placing two materials of different dimensionalities together, but often without control of their interface at the atomic level. Nanoribbons and nanofins combine in themselves the 2D character of their atomically thin constituents with the 1D character that arises from their elongated structure. They can have unique optoelectronic properties too, but are difficult to produce with well-defined edges and to assemble into ordered arrays for integration into devices. Our group has developed a series of epitaxial approaches for the guided growth of 1D nanostructures like nanotubes and nanowires with exquisite control of their orientation on surfaces. Here we extend this approach to create a variety of epitaxial mixed-dimensional nanostructures, including nanoribbons, nanofins and nanoplatelet-2D material heterostructures with a high degree of control at the atomic, nanoscopic and macroscopic levels, which enable their integration into devices. Under certain conditions, MoS_2 grows epitaxially on sapphire forming oriented hybrid nanoribbon-nanofin structures, which possess an advantageous geometry for fast and efficient photodetectors. $CsPbBr_3$ perovskite grows on $ReSe_2$ forming aligned rectangular nanoplates. Despite the highly symmetric cubic structure of the $CsPbBr_3$ perovskite, the nanoplatelets are elongated in one principal direction due to the broken symmetry of the $ReSe_2$ substrate. The $CsPbBr_3$ nanoplatelets on $ReSe_2$ have highly anisotropy tribological properties: They easily slide along their long axis, but are firmly locked along their short axis. Cross-sectional TEM shows that the $CsPbBr_3/ReSe_2$ interface is highly mismatched and incommensurate in the long axis direction, as typical of van der Waals epitaxy, but it is highly coherent with very low mismatch in the perpendicular direction. This explains the anisotropic growth and sliding of the $CsPbBr_3$ nanoplatelets on $ReSe_2$. The electronic and optoelectronic properties of the mixed-dimensional heterostructure are characterized by a series of methods. Our work underscores the potential and richness of van der Waals epitaxy for the creation of mixed-dimensional nanostructures and hetero-

structures with controlled shapes and orientations and their integration into devices.

Figure 1: **vdW epitaxy of CsPbBr3 on ReSe2**

Diatomites doped with nanoparticles for environmental remediation

Sarah Briceño[1], Melany Aguilar[1] and Gema Gonzalez[1]
[1] *YachayTech University*
sbricenio@yachaytech.edu.ec

Abstract

Diatomites, abundant and porous natural biomaterials, have gained attention for environmental remediation due to their high surface area and unique morphology (1). Incorporating plasmonic nanoparticles into diatomite matrices could be used for enhanced remediation applications. The synergistic effects between diatomites and nanoparticles, such as increased adsorption capacity, photocatalytic activity, and Surface-enhanced Raman scattering, are discussed (2). Various synthesis methods and characterization techniques are outlined to understand the structural and chemical modifications induced by nanoparticle doping (3). Applications in herbicide removal from water are highlighted. Furthermore, challenges and future perspectives in utilizing nanoparticle-doped diatomites for sustainable environmental remediation are addressed.

References

[1] Adrián León-Valencia, Sarah Briceño, Carlos Reinoso, Karla Vizuete, Alexis Debut, Manuel Caetano and Gema González. Photochemical Reduction of Silver Nanoparticles on Diatoms. Marine Drugs. (2023), 21(3), 185; https://doi.org/10.3390/md21030185

[2] M. Cristina Mina-Villarreal, Sarah Briceño, K. Vizuete, A. Debut and Gema González. Growth of multiwalled carbon nanotubes and carbon spheres on diatoms. Journal of Porous Materials, 30, 343–349 (2023). https://doi.org/10.1007/s10934-022-01345-8

[3] Sarah Briceño, E. A Chávez-Chico, G. González. Diatoms decorated with gold nanoparticles by In-situ and Ex-situ methods for in vitro gentamicin release. Materials Science and Engineering: C. 123, (2021), 112018. https://doi.org/10.1016/j.msec.2021.112018

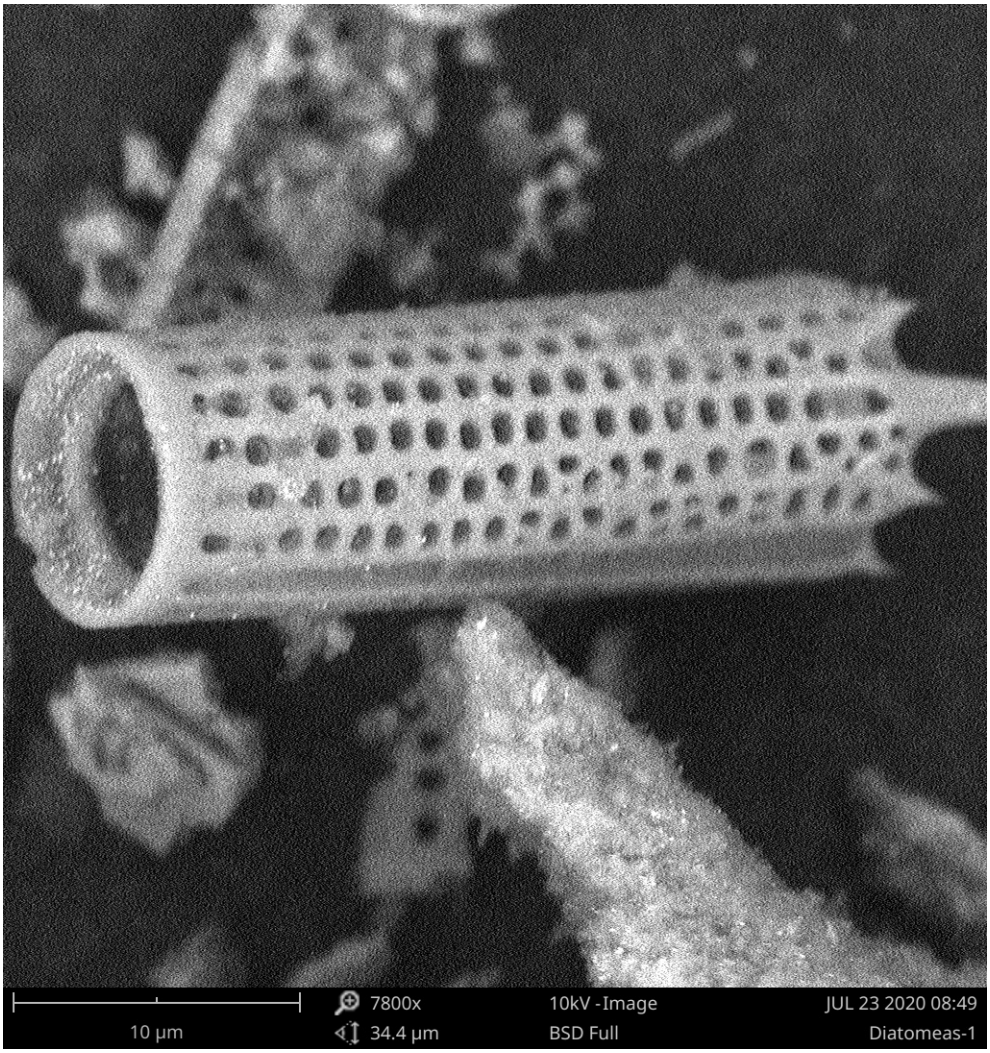

Figure 1: **Scanning electron micrograph of a diatomite coated with gold nanoparticles**

Acta Microscopica Vol. 34, Supp. 2, 2025
Abstract Book NSSY 2024 - Galapagos 19-25 May, 2024

Preparation and characterization of MoS2/rGO nanocomposites obtained by microwave-assisted synthesis and their photocatalytic evaluation for carbamazepine and ibuprofen removal.

Molina Mateo[1], Yolanda Angulo[1], Luis Cumbal[1]
[1] *University of the Armed Forces - ESPE. Center or Nanoscience and Nanotechnology*
mjmolina.m1@gmail.com

Abstract

Pharmaceuticals are emerging pollutants with potential adverse effects on the environment and organisms. Their presence in surface waters results from the ineffective removal of these pollutants by conventional wastewater treatment methods. In Ecuador, Carbamazepine (CBZ) and Ibuprofen (IBF) are emerging pollutants of interest due to their presence in surface water and the potential associated effects. CBZ's toxicological impact in accordance with Hai F. et al. Water. (2018) (10) (107) is linked to spina bifida and issues with the neurological development of the human embryo after intrauterine exposure. This is a significant concern, given the inability of drinking water treatment facilities to eliminate these substances. IBF's adverse effects in accordance with Ajibola A. et al. BECT (2021) (106) are more closely related to the drug's toxicity across different trophic levels and its capacity to alter the microbial composition of the human gut. Photocatalytic nanomaterials (NMs) present an alternative to mitigate the persistence of pharmaceuticals in wastewater.

This study aimed primarly to evaluate the photocatalytic activity of MoS2/rGO nanocomposite for the removal of CBZ and IBF. To achieve this, the synthesis of MoS2/rGO and its constituent NMs (GO and MoS2) was conducted. The synthesis of graphene oxide (GO) was performed by a modified Hummers and Offeman method, employing a 9B graphite rod as a cost-effective source of graphite. Meanwhile, the synthesis of MoS2 and MoS2/rGO was carried out using a relatively novel microwave-assisted synthesis method, particularly in the case of the MoS2/rGO synthesis.

The NMs underwent characterization using XRD, UV-vis, FT-IR, Raman, and electron microscopy techniques. Photocatalytic activity assessment was conducted by irradiating test solutions with a solar simulator, designed from a factorial experimental setup involving MoS2/rGO or MoS2 in combination with CBZ or IBF. The removal capacity was determined by measuring the remaining drug concentration in the test solutions using High Performance Liquid Chromatography (HPLC).

XRD and Raman characterizations of the NMs revealed successful synthesis of GO, MoS2 and MoS2/rGO. XRD analysis confirmed that the obtained diffraction patterns were consistent with the diffraction patterns aligned with literature-reported patterns, indicating a crystalline polytype mixture of 1T/2H for MoS2. Raman spectra exhibited characteristic peaks ($E^1{}_{2g}$ and A_{1g}) for MoS2 in the MoS2 and MoS2/rGO synthesized, while GO and MoS2/rGO displayed D and G bands typical for GO and rGO, albeit with varying intensity. FT-IR analysis identified acidic functional groups on the surface of both MoS2 and MoS2/rGO.

Electron micrographs depicted few-layered morphology for GO, nanoflower morphology for MoS2, and irregular 3D morphology for MoS2/rGO. It was observed that solar irradiation led to a pH decrease in most test solutions. Additionally, drug removal was noted with both MoS2/rGO and MoS2, with no statistically significant differences between the two. Regarding pharmaceuticals, removal was pH independent for CBZ and pH dependent for IBF.

In conclusion, it is feasible to synthesize few-layered GO using a 9B graphite rod as a cost-effective graphite source, along with MoS2 and MoS2/rGO employing a microwave-assisted synthesis method. The synthesized MoS2 consisted of a mixture of 1T/2H polytypes with acidic functional groups on its surface and exhibited a nanoflower morphology. Additionally, MoS2/rGO displayed more acidic functional groups than MoS2 and showcased an irregular 3D morphology. Lastly, both MoS2 and MoS2/rGO demonstrated the capability to remove CBZ and IBF, with the pH playing a significant role in influencing their efficiency.

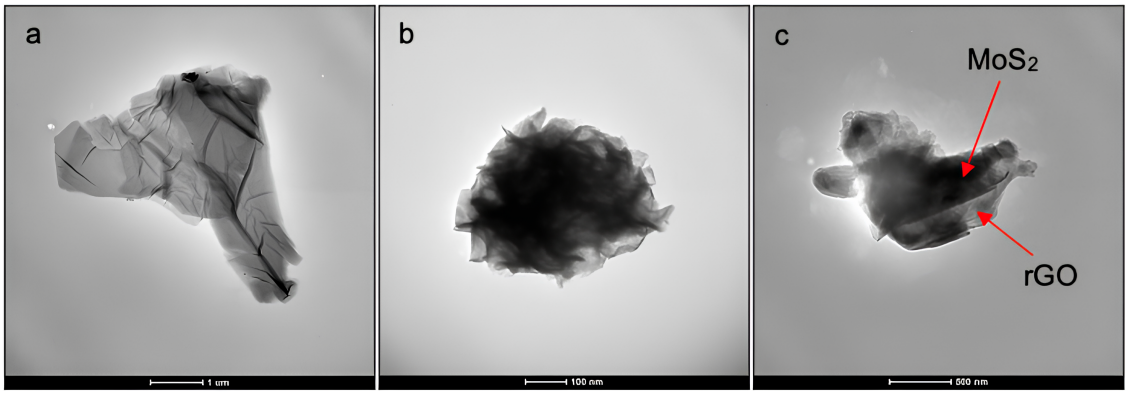

Figure 1: **a. TEM imagen of Graphene oxide showing a few-layered morphology, b. TEM image of MoS2 showing a nanoflower morphology c. TEM image of MoS2/rGO showing an irregular 3D morphology.**

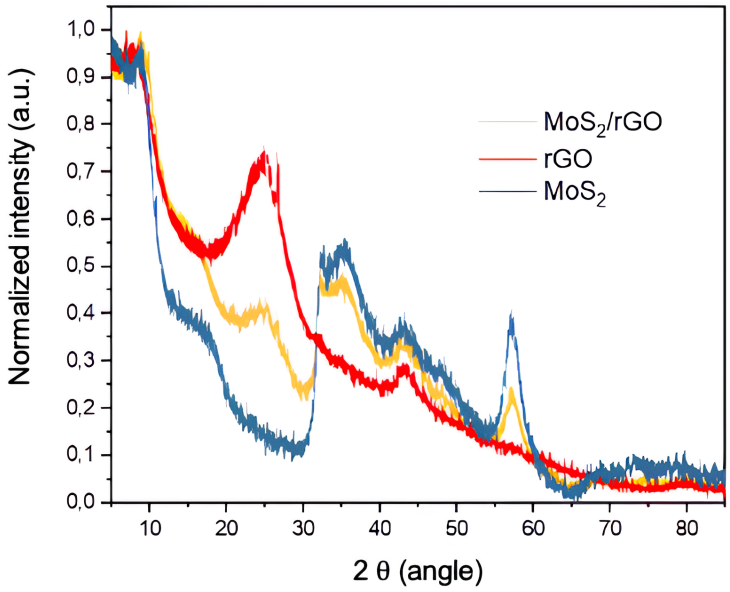

Figure 2: **XRD patterns of MoS2/rGO nanocomposite, MoS2, and reduced graphene oxide (rGO).**

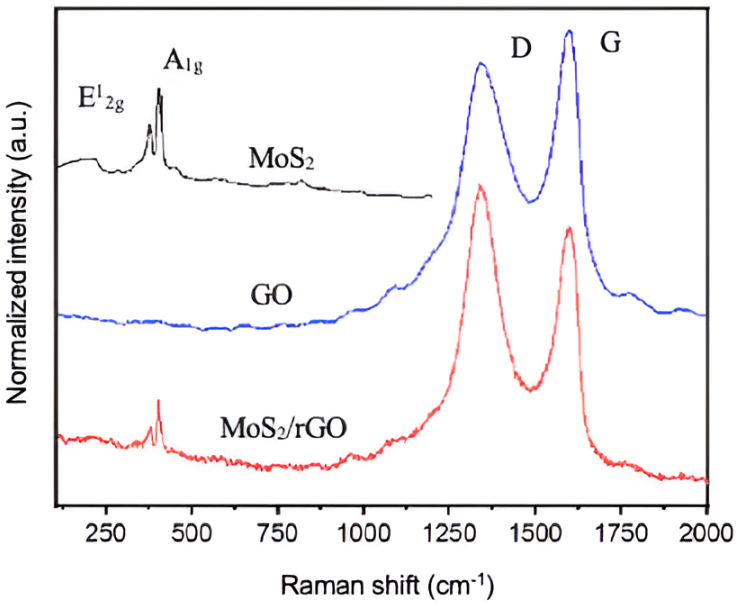

Figure 3: **Raman spectra of MoS2/rGO, MoS2, and graphene oxide (GO). The $E^1{}_{2g}$ and A_{1g} are the characteristic peaks of MoS2. The D and G bands are characteristic of GO.**

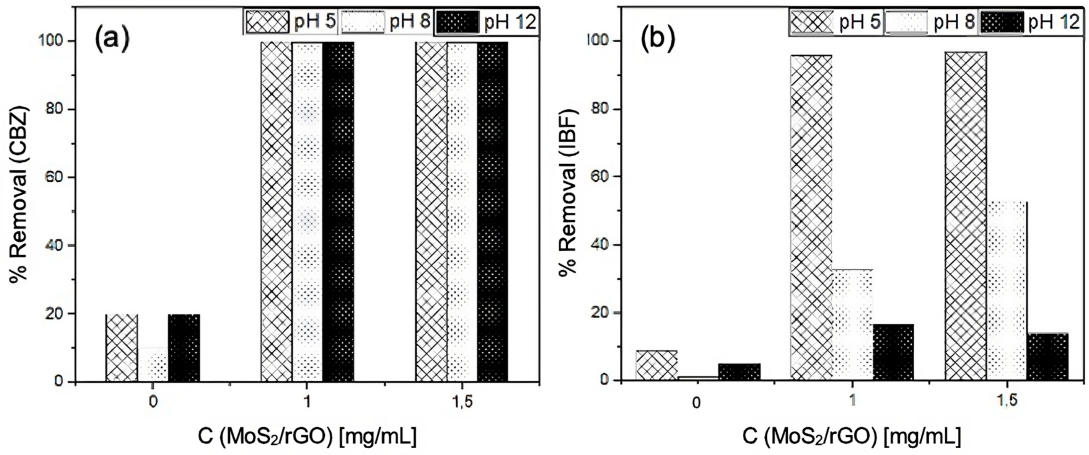

Figure 4: **(a) Percentage removal of carbamazepine (CBZ) between different concentrations of MoS2/rGO, (b) Percentage removal of ibuprofen (IBF) between different concentrations of MoS2/rGO.**

References

[1] Ajibola, A. S., Fawole, S. T., Ajibola, F. O., & Adewuyi, G. O. (2021). Diclofenac and Ibuprofen Determination in Sewage Sludge Using a QuEChERS Approach: Occurrence and Ecological Risk Assessment in Three Nigerian Wastewater Treatment Plants. Bulletin of Environmental Contamination and Toxicology, 106(4), 690–699. https://doi.org/10.1007/s00128-021-03139-1

[2] Hai, F. I., Yang, S., Asif, M. B., Sencadas, V., Shawkat, S., Sanderson-Smith, M., Gorman, J., Xu, Z. Q., & Yamamoto, K. (2018). Carbamazepine as a Possible Anthropogenic Marker in Water: Occurrences, Toxicological Effects, Regulations and Removal by Wastewater Treatment Technologies. Water (Switzerland), 10(2), 1–32. https://doi.org/10.3390/w10020107

Acta Microscopica Vol. 34, Supp. 2, 2025
Abstract Book NSSY 2024 - Galapagos 19-25 May, 2024

Exploring Polymer-Ionic Solution Interactions: An In-Depth Study Chitosan-Starch Matrix in ZnCl2-NH4Cl electrolytes for Zinc-Air Batteries

Sara L. Vaca[1], Vivian Morera Córdova[1], Lorena Álvarez Contreras[3], Juan P. Tafur[1,2]

[1] *Grupo de Investigación Aplicada en Materiales y Procesos (GIAMP), School of Chemical Sciences & Engineering, Yachay Tech University, San Miguel de Urcuquí, Hacienda San José s/n, Urcuquí 100115, Ecuador*

[2] *Departamento de Ingeniería Mecánica, Química y Diseño Industrial, Escuela Técnica Superior de Ingeniería y Diseño Industrial (ETSIDI), Universidad Politécnica de Madrid (UPM), Ronda de Valencia 3, 28012 Madrid, Spain*

[3] *Centro de Investigación en Materiales Avanzados S.C. (CIMAV), Miguel de Cervantes No. 120, Complejo Industrial Chihuahua, Chihuahua 31136, México*

*sara.vaca@yachaytech.edu.ec

Abstract

While Lithium-ion batteries dominate in portable device applications, the theoretical energy density provided by these batteries is only between 100 and 200 Wh kg-1, which is not adequate for industrial scale applications. Consequently, there's a pressing need to innovate and develop electrochemical storage devices that are not only sustainable and cost-effective but also boast a much higher energy density, [1]. Building on this perspective, the study conducted in [2] incorporates crucial data from a related investigation on chitosan-avocado seed starch hydrogels, offering a deeper understanding of the role of carbon content in hydrogel performance and its implications for zinc-air battery efficiency. Moreover, it was observed that increasing starch content enhances the hydrogels' absorption capability, directly enhancing their ionic conductivity. Chain separation in the hydrogels leads to serum expansion that causes the hydrogels to swell and fracture, highlighting the importance of the carbon composition for optimizing electrolyte performance. While these hydrogels may have yielded excellent electrochemical performance, they also suffered from corrosion, meaning that the service life of the battery could be shortened and energy efficiency lowered. They were set in a 12M KOH ionic solution. Tackling this problem, this research delves into chitosan-starch-based biopolymer composite hydrogels functioning as electrolytes in zinc-air batteries, with special attention paid to the effects from different ionic solutions and pH levels and how they affect the carbon-based polymer matrix.

On the other hand, research detailed in [3] delves into the historical and chemical significance of the $ZnCl_2$-NH_4Cl solution, a long-standing electrolyte in electrochemical systems since the 19th century. Its role in stabilizing pH in the neutral range, crucial for zinc-air batteries, is attributed to the interaction between $ZnCl_2$ and NH_4Cl, forming zinc-ammine complexes. These complexes can effectively buffer pH in the 6-10 range, thereby enhancing the fine stability of the electrolyte. The results suggest that when designing dynamic, highly conductive and near-neutral electrolytes for zinc-air batteries it would be vital to take into account not only pH values but also zinc concentration levels so as to reflect an informed understanding about electrolytes in such systems. In this manner, this study aims at the relationship of these biopolymers, derived from renewable sources, with different ionic environments. Therefore, our research could be called the intersection of carbon materials science and sustainable energy storage. The specific ionic environments investigated were aqueous solutions of concentrated ZnCl2, and NH4Cl (a more environmentally friendly alternative with a near-neutral pH) compared to a standard 12M KOH ionic solution. The comprehensive experimental approach employs techniques such as Electrochemical Impedance Spectroscopy (EIS), Cyclic Voltammetry (CV), Infrared (IR) spectroscopy, and X-ray Diffraction (XRD) to examine the electrochemical and structural characteristics of these hydrogels. A key focus is on assessing how variations in the ionic composition and pH of the surrounding solution impact the electrochemical behavior and structural integrity of the hydrogels, thereby influencing their efficacy as electrolytes in ZABs. Notably, the hydrogel electrolyte immersed in a $ZnCl_2$/2.34M NH_4Cl solution at pH 4.45 (as can be seen in Table 1) demonstrates promising ionic conductivities, rivaling those observed in the 12M KOH solution at pH 14 (as it can be acknowledged in Figure. 1).

This research particularly throws light on the substantial role played by the composition of ionic solutions and pH in governing the effectiveness of these carbon-rich biopolymeric hydrogels, thereby setting the way for the development of workable, sustainable electrolytes. With the exploration of $ZnCl_2$-NH_4Cl solution also comes the marching prospect of battery systems that are more eco-friendly and considerably stronger. In such a manner, this study not only deepens our understanding of carbon in the field of energy storage but also points out how crucial it is to adjust the ion environment towards eco-friendly zinc-air batteries. Thus, contributing significantly to carbon materials science, this research emphasizes sustainable approaches in energy storage technology.

Ionic Solution	Measured pH	Electrolyte Code	SR(%)	Ea(eV)	σ(S/cm)
0.51M $ZnCl_2$-2.34M NH_4Cl	5.95	A	689.2	0.110	0.075
0.51M $ZnCl_2$-2.34M NH_4Cl	4.45	B	927.5	0.116	0.128
0.26M $ZnCl_2$-5M NH_4Cl	2.14	D	820	0.115	0.108
3M $ZnCl_2$-7M NH_4Cl	3.85	E	389.7	0.101	0.076
12M KOH	14	F	626.1	0.181	0.178

Table 1: Showing experimental values for Swelling ratio (SR), activation energy (Ea), and conductivity (σ) for electrolytes after hydration in the corresponding ionic solutions. The values for σ were obtained at Temperature = 30°C.

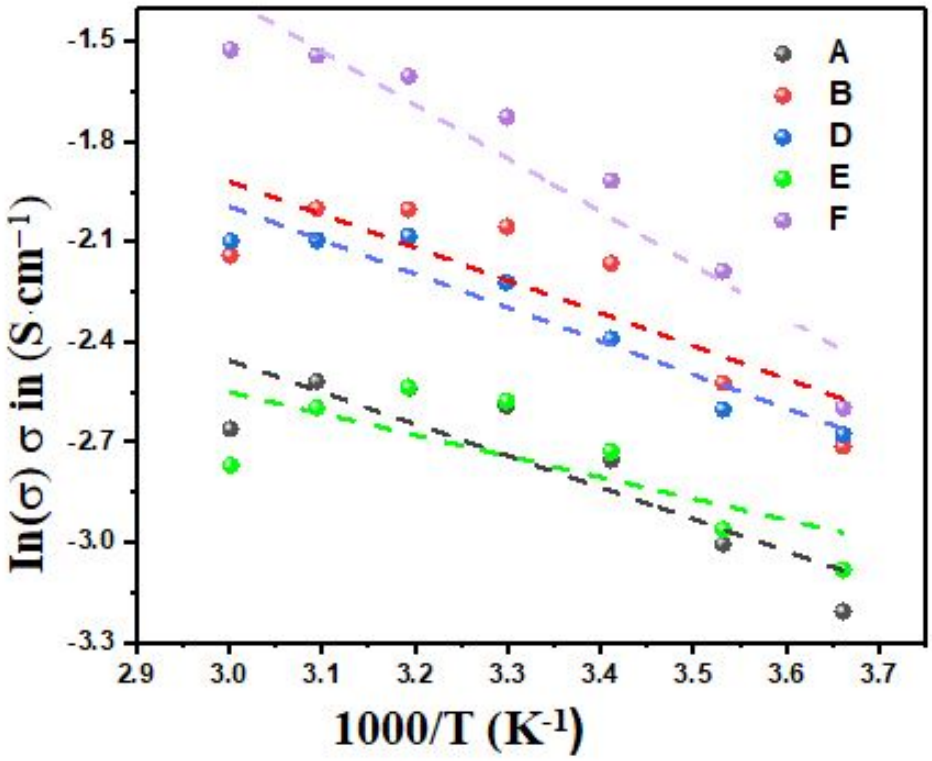

Figure 1: **The variation in ionic conductivity of chitosan-starch electrolytes with changing temperature for all Hydrogel codes.**

References

[1] A. R. Mainar et al., "An overview of progress in electrolytes for secondary zinc-air batteries and other storage systems based on zinc," J Energy Storage, vol. 15, pp. 304–328, Feb. 2018, doi: 10.1016/j.est.2017.12.004.

[2] M. F. B.-C. J. B. L. Á.-C. V. M. C. J. P. T. Authors: María I. Cruz-Balaz, "Synthesis and characterization of Chitosan-Avocado seed starch hydrogels as electrolytes for zinc-air batteries," Journal of Polymer Research, 2023.

[3] S. Clark, A. Latz, and B. Horstmann, "Rational Development of Neutral Aqueous Electrolytes for Zinc–Air Batteries," ChemSusChem, vol. 10, no. 23, pp. 4735–4747, Dec. 2017, doi: 10.1002/cssc.201701468.

Wednesday

Acta Microscopica Vol. 34, Supp. 2, 2025
Abstract Book NSSY 2024 - Galapagos 19-25 May, 2024

Photoemission spectroscopy for characterization of the nanoscale (and a flavor of X-ray absorption spectroscopy).

Paola Ayala[1]
[1] *University of Vienna*
paola.ayala@univie.ac.at

Abstract

X-ray photoelectron spectroscopy (XPS) is a method widely used for analytic understanding of materials. In general, it is one of the best tools for studying the chemical modification of surfaces. The X-ray penetration depth is a particularly important consideration to determine the intrinsic photoemission response of a sample. This explains why measuring nano-structured materials is not as straight forward as using the same technique for bulk materials. Incorrect conclusions can easily be drawn, especially in the assignment of measured binding energies into specific atomic configurations. Starting from the characteristics of pristine materials, my goal of this tutorial will be to provide the fundamental concepts behind photoemission spectroscopy (PES) including lab-based XPS and ultraviolet photoemission spectroscopy (UPS). I will use as example studies on carbon materials (from the bulk to nanostructured species). Given that UPS allows accessing the properties of the valence band of semiconducting materials, I will also provide a short interaction to X-ray absorption and show how it can reveal the conduction band of the systems.

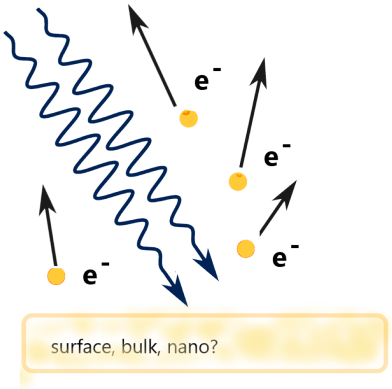

Figure 1: **Photoemission spectroscopy is based on the photoelectric effect. This will be explained more in depth during the corresponding tutorial lecture.**

Acta Microscopica Vol. 34, Supp. 2, 2025
Abstract Book NSSY 2024 - Galapagos 19-25 May, 2024

Local/atomic scale studies of low-dimensional materials by TEM

Raul Arenal

[1] *Instituto de Nanociencia y Materiales de Aragon (INMA), CSIC-U. Zaragoza, 50009 Zaragoza – Spain*

[2] *Laboratorio Microscopias Avanzadas, U. Zaragoza, 50018 Zaragoza - Spain*

[3] *Fundacion ARAID, 50018 Zaragoza – Spain*

arenal@unizar.es

Abstract

Detailed structural and chemical composition analyses, at the atomic scale, of nanomaterials are required in order to determine their impact on the properties of such objects. Transmission electron microscopy (TEM) and in particular, spatially-resolved electron energy loss spectroscopy (SR-EELS) developed in an aberration-corrected TEM, is the most powerful technique to get this information. Indeed, having access to a close to 1 angstrom electron probe, the atomic configuration of these nanomaterials can be obtained [1-10].

In this communication, I will present a selection of recent works involving all these matters. These works will concern the study of the atomic structure & configuration of 1D and 2D atomically thin nanostructures (including nanotubes & graphene/graphene-like material in pristine and hybrid forms) as well as the opto-electronic properties studies carried out via EELS measurements [1-10]. These works will illustrate the excellent capabilities offered by the use of a Cs probe-corrected (S)TEM, combined with the use of a monochromator, to study these properties within a very good spatial resolution. Furthermore, I will also present some recent in-situ TEM-EELS studies showing how powerful this approach can be for allowing the simultaneous measurement of various physical and chemical features of high interest for the study of different phenomena.

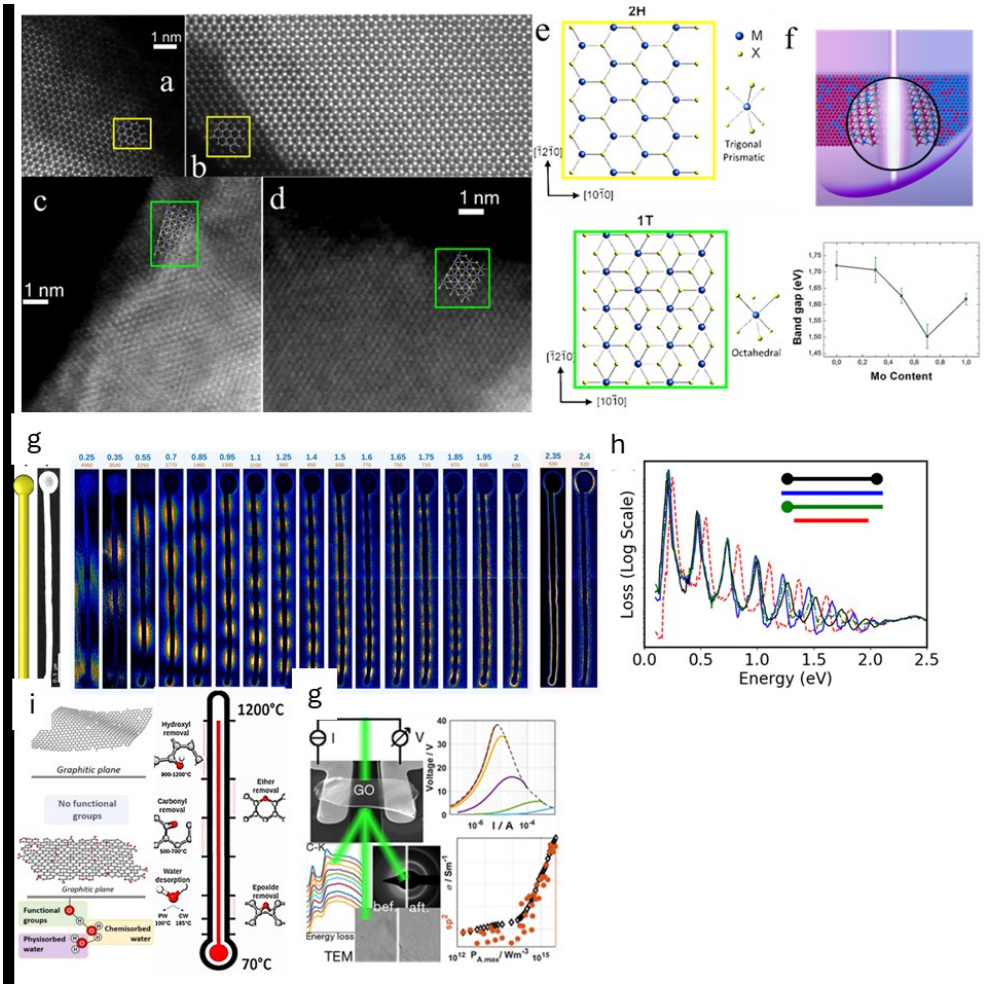

Figure 1: **High-resolution scanning TEM HAADF images of 2H-MoS2 and 2H-WS2 (a and b) and 1T-MoS2 and 1T-WS2 (c and d). The crystal structural models (e) for both phases (2H (highlighted in yellow) and 1T (highlighted in green)) are superimposed on these HRSTEM-HAADF images. (f) Band gap measurement via low-loss EELS studies of few atomically thin MoxW(1-x)S2 layered flakes. (g) From left to right: STEM-HAADF image and NMF components corresponding to Fabry-Perot modes and to the surface modes of the Au NW and the Au NP in an Au half-dumbbell nanostructure. (h) DDA modelled low-loss EEL spectra for a dumbbell and half-dumbbell nanostructures and an Au NW of the same dimensions as well as a shorter Au NW. (i) General schematic on the main results of this study showing the reduction of GO via detailed in-situ heating TEM (HRTEM & EELS) [6]. (b) Reduction of GO via detailed in-situ Joule heating TEM (HRTEM, electron diffraction & EELS) studies and coupled with conductivity investigation by electrical measurements [7].**

References

[1] K.S. Roy, S. Hettler, R. Arenal, L.S. Panchakarla, Mat. Horizons 9, 2115-2127 (2022).

[2] A. Cohen, P. K. Mohapatra, S. Hettler, A. Patsha, K.V.L.V. Narayanachari, P. Shekhter, J. Cavin, J.M. Rondinelli, M. Bedzyk, O. Dieguez, R. Arenal, A Ismach, ACS Nano 17, 5399–5411 (2023).

[3] S. Hettler, M.B. Sreedhara, M. Serra, S.S. Sinha, R. Popovitz-Biro, I. Pinkas, A.N. Enyashin, R. Tenne, R. Arenal, ACS Nano 14, 5445 (2020).

[4] M. B. Sreedharaa, S. Hettler, I. Kaplan-Ashiri, K. Rechav, Y. Feldman, A. Enyashin, L. Houben, R. Arenal, R. Tenne, PNAS 118, e2109945118 (2021).

[5] M. Pelaez-Fernandez, Y.C. Lin, K. Suenaga, R. Arenal, Nanomaterials 11, 3218 (2021).

[6] M. Pelaez-Fernandez, A. Bermejo Solis, A.M. Benito, W.K. Maser, R. Arenal, Carbon 178, 477 (2021).

[7] S. Hettler, D. Sebastian, M. Pelaez, A.M. Benito, W.K. Maser, R. Arenal, 2D Materials 8, 031001 (2021).

[8] A. Kagkoura, R. Arenal, N. Tagmatarchis, Advanced Functional Materials 31, 2105287 (2021).

[9] S. Hettler, M. Sreedhara, M. Serra, S. Sinha, R. Popovitz, I. Pinkas, A. Enyashin, R. Tenne, R. Arenal, ACS Nano 14, 5445 (2020).

[10] R.A. acknowledges financial support from the Spanish Ministry of Science and Innovation MCIN and the Spanish Research Agency AEI (PID2019-104739GB-100/AEI/10.13039/501100011033), Gobierno de Aragon (DGA, E13-23R), and from the European Union H2020 programs “Graphene Flagship-CORE3” (grant Agreement 881603) and ”ESTEEM3” (grant agreement No 823717). These studies have been developed in the Laboratorio de Microscopias Avanzadas (LMA), U. of Zaragoza (Spain).

Acta Microscopica Vol. 34, Supp. 2, 2025
Abstract Book NSSY 2024 - Galapagos 19-25 May, 2024

Interactions of moving charged particle with anisotropic two-dimensional material

Z.L. Miskovic[1], M. Moshayedi[1], M.R. Preciado Rivas[1]
[1] *Department of Applied Mathematics, University of Waterloo, Waterloo, Ontario, Canada*
zmiskovi@uwaterloo.ca

Abstract

We have studied theoretically the interaction of a particle with charge Ze moving with constant velocity vector $\mathbf{v}$ at distance $z_0 > 0$ parallel to the surface of an anisotropic two-dimensional material modeled as doped phosphorene, which occupies the $z = 0$ plane and is supported by an insulating substrate filling the region $z < -h$ (see Fig.1). We considered non-relativistic particle speeds and adopted a dielectric-response formalism to describe the dynamic polarization of the electron-hole system in phosphorene in the non-retarded regime.

We have constructed several models for the density-density polarization function $\chi(\mathbf{q}, \omega)$ of phosphorene, with a dependence on the momentum vector $\mathbf{q} = (q_x, q_y)$ that exhibits strong anisotropy with respect to phosphorene's principal crystalline directions, labeled as the armchair (x axis) and the zigzag (y axis) directions [1-3]. While those models of $\chi(\mathbf{q}, \omega)$ are suitable in the terahertz to the infrared range of frequencies, we also used a local model for the dielectric permittivity of the substrate $\epsilon_s(\omega)$ with a frequency dependence describing the transverse optical phonons in its bulk, represented by SiO_2 [1].

We have calculated the stopping and the image forces acting on the moving particle [1], as well as the electrostatic potential in phosphorene [3], induced by that particle. As a result of the anisotropy of the function $\chi(\mathbf{q}, \omega)$, the stopping force was found to have two components parallel to phosphorene: a longitudinal force F_l in the direction opposing the velocity vector $\mathbf{v}$, and a transverse force F_t perpendicular to it (see the inset to Fig.1), whereas the image force F_i is directed perpendicular to phosphorene. All forces were found to exhibit a strong dependence on the direction of motion of the particle, specified by the angle θ_0 with respect to the armchair direction (x axis).

On the other hand, the induced electrostatic potential in the plane $z = 0$ exhibits an asymmetric wake pattern, which trails behind the projection of the moving particle in the plane of phosphorene, as illustrated by the blue and orange bands in Fig.1 for the direction of motion $\theta_0 = 30°$.

Our findings point to interesting possibilities that may arise in studying the anisotropy of supported and doped phosphorene, e.g., by means of the vibrational and valence aloof beam electron energy loss spectroscopy (EELS) in a monochromated scanning transmission electron microscope or via high-resolution EELS using low-energy electron reflection under grazing incidence upon the surface of phosphorene.

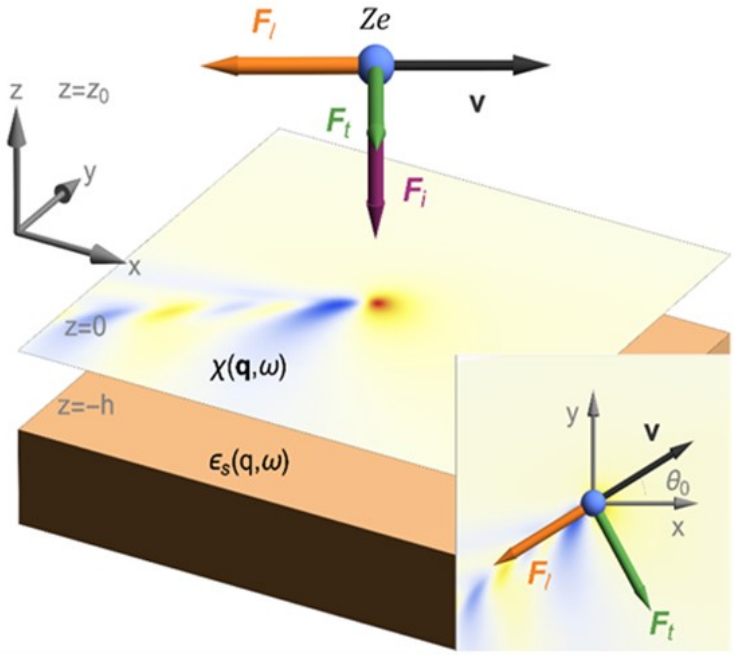

Figure 1: **Schematic diagram of the problem, showing all the quantities that were studied.**

References

[1] Moshayedi M. et al. Phys. Rev. B (2022) (105) (075429).

[2] Miskovic Z.L. et al. Radiat. Eff. Def. Solids (2023) (178) (54).

[3] Miskovic Z.L. et al. Phys. Rev. Res. (2023) (5) (033133).

Acta Microscopica Vol. 34, Supp. 2, 2025
Abstract Book NSSY 2024 - Galapagos 19-25 May, 2024

GOLD RECOVERY FROM ELECTRONIC WASTE USING A NOVEL SEAWATER LEACHING METHOD AND ITS REUSE TO SYNTHESIZE METALLIC NANOSTRUCTURES

Veronica Arellano[1], Hiram Joazet Ojeda Galván[2], Mildred Quintana[3], Armando Encinas[4]

[1] *Universidad Autónoma de San Luis Potosí, Doctorado Institucional en Ingeniería y Ciencia de Materiales, Centro de Investigación en Ciencias de la Salud y Biomedicina, Mexico.*

[2] *Universidad Autónoma de San Luis Potosí, Coordinación para la Innovación y la Aplicación de la Ciencia y la Tecnología (CIACyT), Mexico.*

[3] *Universidad Autónoma de San Luis Potosí, Centro de Investigación en Ciencias de la Salud y Biomedicina (CICSaB), Mexico.*

[4] *Instituto Potosino de Investigación Científica y Tecnológica A.C., División de de Materiales Avanzados, Mexico.*

veroarellanoc@gmail.com

Abstract

It is 13 times more expensive to extract minerals from the Earth than to recycle them since obtaining and processing virgin resources requires industrial quantities of water, chemicals, and fossil fuels [1]. It is expected that 74.7 Mt of electronic waste will be produced worldwide in the next ten years; therefore, to counterbalance the environmental impact of this, we present a protocol for the recovery of gold (Au) from discarded computer processors[2] using diluted nitric acid (HNO3) in seawater [3], and its reuse for the synthesis of gold and gold-copper semispherical nanoparticles. This method presents lower human and environmental risk, compared to the aqua regia leaching method currently used to obtain Au from electronic waste since hydrochloric acid (HCl) is not necessary, and HNO3 can oxidize Cl to Cl2, which can transform Au0 into Au3+, allowing us to prepare HAuCl4, the precursor to synthesize gold nanostructures that can be used for different applications[4]. Furthermore, this work compares the nanostructures synthesized using commercial HAuCl4 versus those fabricated using the precursor obtained from leaching in aqua regia and seawater.

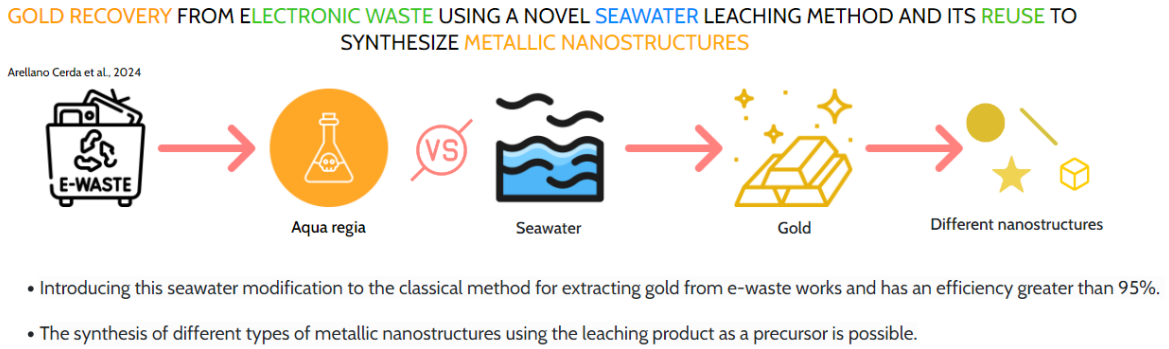

Figure 1: **Graphical Abstract**

References

[1] Zeng, X., Mathews, J. A. & Li, J. Urban Mining of E-Waste is Becoming More Cost-Effective Than Virgin Mining. Environ. Sci. Technol. 52, 4835–4841 (2018).

[2] Wang, R. et al. Recycling gold from printed circuit boards gold-plated layer of waste mobile phones in mild aqua regia system. J. Clean. Prod. 278, (2021).

[3] Hojo, M. MECHANISM OF ENHANCED OXIDATION ABILITY OF DILUTE NITRIC ACID AND DISSOLUTION OF PURE GOLD IN SEAWATER WITH NITRIC ACID. Kharkiv Univ. Bull. Chem. Ser. 33, 6–22 (2019).

[4] Su-Gallegos, J., Magallón-Cacho, L., Ramírez-Aparicio, J. & Borja-Arco, E. Synthesis of Gold Nanoparticles from Gold Coatings Recovered from E-Waste Processors. Materials (Basel). 15, (2022).

Acta Microscopica Vol. 34, Supp. 2, 2025
Abstract Book NSSY 2024 - Galapagos 19-25 May, 2024

New pathways to tailor the properties of carbon nanotubes

Setaro A[1,2], Fiebor A[1], Adeli M[1], Reich S[1]
[1] *Free University Berlin*
[2] *Pegaso University*
setaro@physik.fu-berlin.de

Abstract

Among the various nano-carbon allotropes, single-walled carbon nanotubes (SWNTs) step up for their me- chanical endurance and their optical and electronic properties, trademarks of their quantum nature. SWNTs come in different chiral species, each of them with their distinctive electronic character, providing a rich field to compare theoretical predictions and experimental validations. Despite their structure-properties features have been thoroughly investigated, their customization is still actively under development. Straightforward, reliable, and reproducible protocols to adapt their properties to targeted applications are still missing. Here we focus on the approach we developed to control the amount of charges injected in each SWNTs at the single nanotube level and how to exploit this for targeted applications.

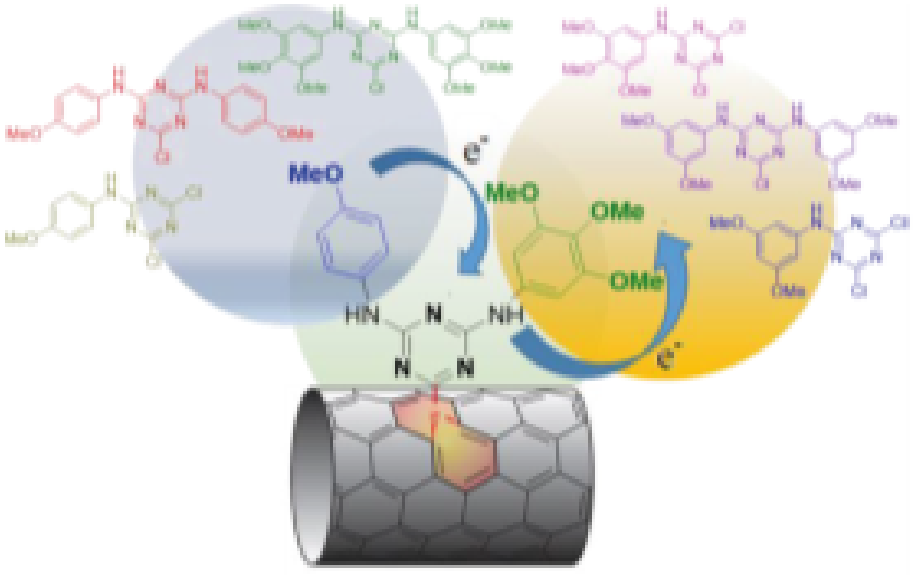

Figure 1: **Attaching different groups onto the SWNTs result in different customization of the tubes.**

Acta Microscopica Vol. 34, Supp. 2, 2025
Abstract Book NSSY 2024 - Galapagos 19-25 May, 2024

Synthesis and characterization of structure-controlled nanotubes

Yohei Yomogida[1]
[1] *Hokkaido University*
yomogida@es.hokudai.ac.jp

Abstract

Recently, two-dimensional semiconductor materials such as transition metal dichalcogenides (TMDCs) has been intensively studied with the aim of obtaining unique optical functions. TMDC has various chemical compositions such as MoS2 and WS2 depending on the combination of transition metal and chalcogen. The physical properties of TMDC vary greatly depending on its composition and structure. For example, when these two-dimensional TMDC form a cylindrical structure, namely TMDC nanotubes, they exhibit unique optical functions different from two-dimensional TMDCs. Until now, we have realized the synthesis, evaluation, and device applications of TMDC nanotubes [1].

In this lecture, we introduce recently developed synthesis technique and discuss the synthesis and characterization of small diameter nanotubes with a diameter of about 10 nm [2] and hetero-nanotubes with controlled chemical composition [3].

The diameter of TMDC nanotubes was controlled by controlling the diameter of their synthetic precursor, oxide nanowires. Figure 1 shows a TEM image of the obtained TMDC nanotubes. Nanotubes with a diameter of about 10 nm were obtained. Small-diameter samples exhibit more red-shifted emission than two-dimensional TMDCs and larger-diameter nanotubes (Figure 2). This is considered to be due to strain effects in the nanotubes.

In addition, by using two types of oxide synthetic precursor, we synthesized heteronanotubes with WS2 on the inside and MoS2 on the outside (Figure 3). We found that WS2/MoS2 heteronanotubes with high crystallinity were obtained, and that the number of layers and crystallinity could be systematically controlled in synthetic process.

References

[1] Y. Yomogida, Y. Kainuma, T. Endo, Y. Miyata, K. Yanagi, Appl. Phys. Lett. 116, pp.203106, (2020)

[2] Md. A. Rahman, Y. Yomogida, A. Ahad, K. Ueji, M. Nagano, A. Ihara, H. Nishidome, M. Omoto, S. Saito, Y. Miyata, Y. Gao, S. Okada, K. Yanagi, Sci. Rep. 13, pp.16959 (2023)

[3] Y. Yomogida, M. Nagano, Z. Liu, K. Ueji, Md. A. Rahman, A. Ahad, A. Ihara, H. Nishidome, T. Yagi, Y. Nakanishi, Y. Miyata, K. Yanagi, Nano Lett. 23, pp.10103-10109 (2023)

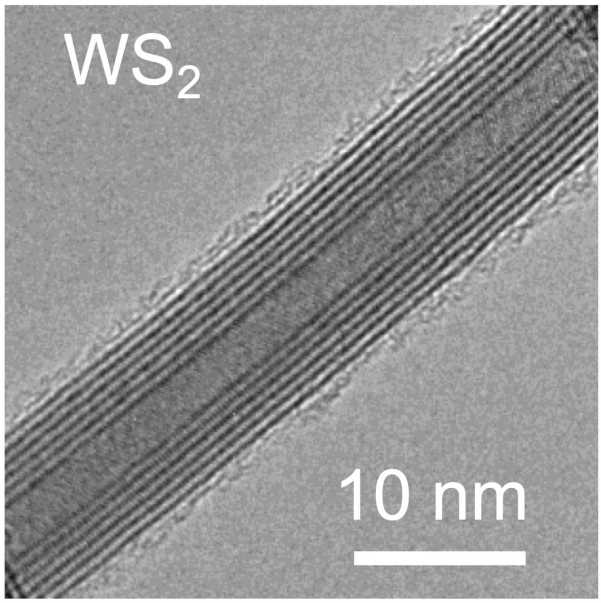

Figure 1: **Transmission electron microscope image of small diameter TMDC nanotubes**

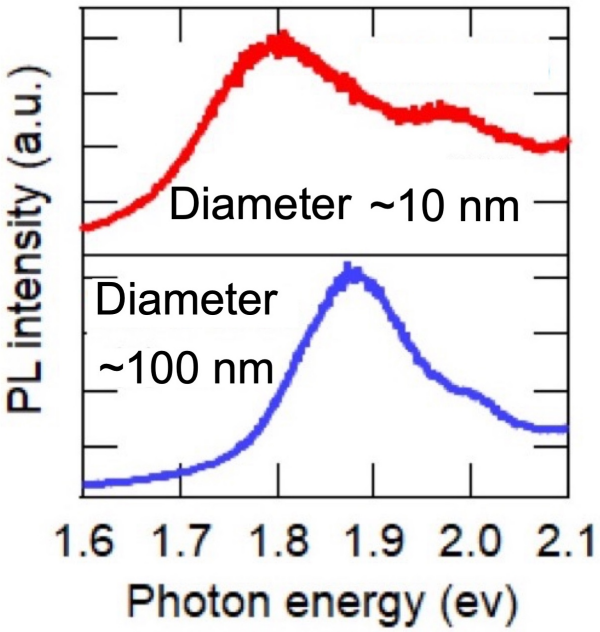

Figure 2: **Photoluminescence spectra for small diameter and large diameter TMDC nanotubes**

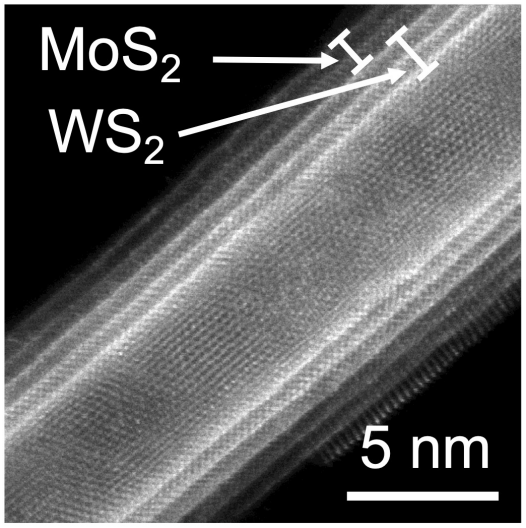

Figure 3: **High Angle Annular Dark Field Scanning Transmission electron microscope image of heteronanotubes**

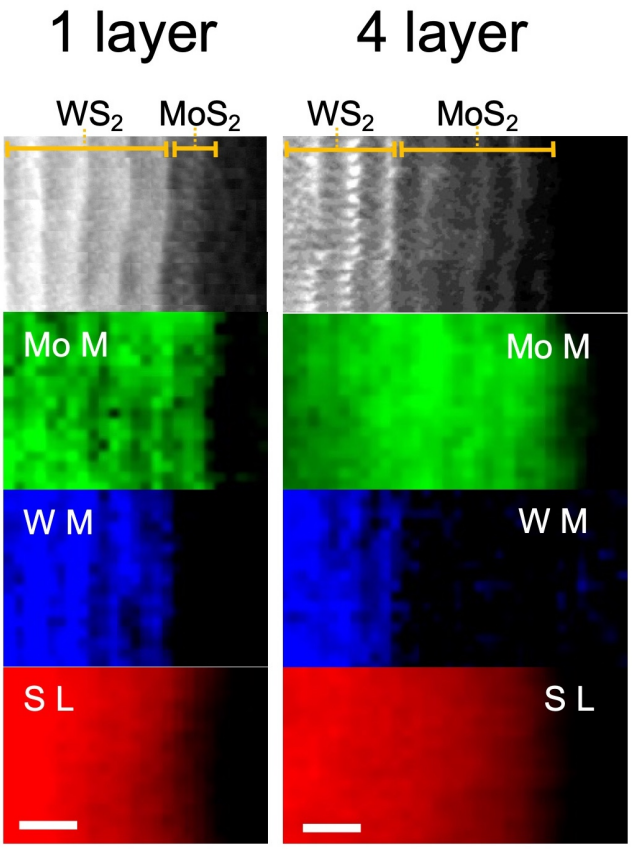

Nanocellulose/Multiwalled Carbon Nanotube Composites for sensing applications

Luis Piedra Marin[1], Jari Koskinen[1]
[1] *Aalto University*
luispiedramarin@gmail.com

Abstract

Two types of nanocellulose materials referred as crystalline and fibrillar with sulfate functional groups are used to disperse commercial multiwalled carbon nanotubes (MWCNT) at different concentration ratios (1:2, 1:1, 2:1). Nanocellulose/MWCNT colloidal aqueous dispersions are drop-cast on tetrahedral amorphous carbon (ta-C) substrates to achieve stable composite electrodes. Their electrochemical properties are studied by employing cyclic voltammetry (CV) and differential pulse voltammetry (DPV) with ruthenium and dopamine as analytes in 10 mM of PBS electrolyte solution. All examined nanocellulose/MWNCNT demonstrated excellent electrochemical stability, reproducibility, and high sensitivity. In addition, both fibrillar and crystalline nanocellulose/MWCNT composite electrodes with concentration ratio 2:1 provided the highest electrochemical active surface area (ECSA) by using Ruthenium as analyte in CV measurements. However, fibrillar nanocellulose/MWCNT provided the highest oxidation and reduction peaks in compared to crystalline nanocellulose/MWCNT. The sensitivity of both nanocellulose/MWCNT composite electrodes were analyzed by employing DPV measurements. The most sensitive composite electrode was the fibrillar nanocellulose/MWCNT 1:1 concentration ratio measured in 1mM of Ruthenium in 10mM of PBS.

References

[1] V. Durairaj et al., "Functionalized Nanocellulose/Multiwalled Carbon Nanotube Composites for Electrochemical Applications," ACS Applied Nano Materials, vol. 4, no. 6, pp. 5842–5853, Jun. 2021, doi: 10.1021/acsanm.1c00774.

[2] V. Durairaj et al., "Multiwalled Carbon Nanotubes/Nanofibrillar Cellulose/Nafion Composite-Modified Tetrahedral Amorphous Carbon Electrodes for Selective Dopamine Detection," Journal of Physical Chemistry C, vol. 123, no. 40, pp. 24826–24836, Oct. 2019, doi: 10.1021/acs.jpcc.9b05537.

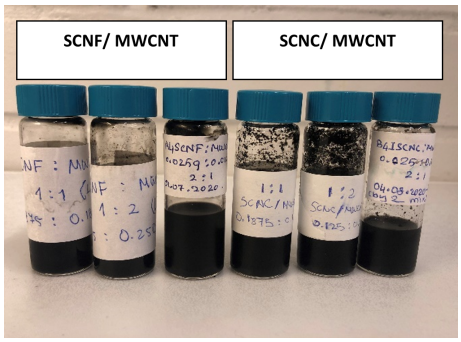

Figure 1: **Photo of SCNF/MWCNT and SCNC/MWCNT suspensions at different concentration ratios (1:1, 1:2, 2:1).**

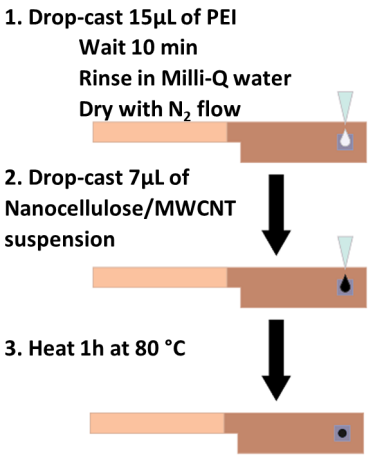

Figure 2: **Nanocellulose/MWCNT composite electrode drop-casting preparation.**

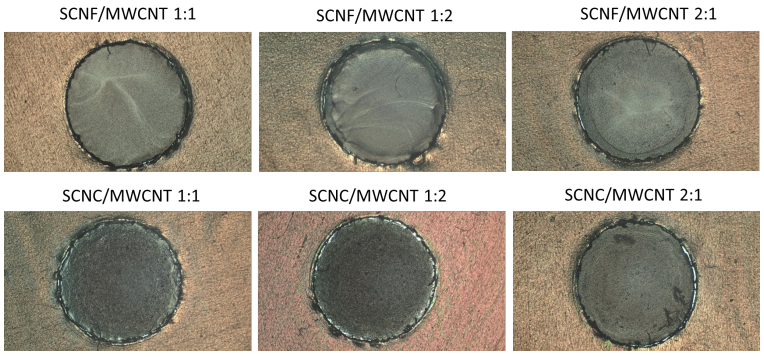

Figure 3: **Optical microscope images of the drop-cast nanocellulose/MWCNT composite electrodes.**

Nitrogen-doped multiwall carbon nanotubes fabricated using a low concentration of catalyst: electrochemical properties

Brenda. I. Orea-Calderón[1], Jenaro L. Varela-Caselis[2], Julio C. Chacón-Torres[3], Florentino. Lopéz-Urías[1], Emilio Muñoz-Sandoval[1,*]

[1] *Advanced Materials Division, IPICYT, Camino a la Presa San José 2055, Col Lomas 4a sección, San Luis Potosí S.L.P., 78216, México.*

[2] *Faculty of Chemical Engineering, Materials Division, Autonomous University of Puebla, 18 sur S/N, Puebla, Mexico.*

[3] *Yachay Tech University, School of Physical Sciences and Nanotechnology, 100119Urcuquí, Ecuador.*

brenda.orea@ipicyt.edu.mx

Abstract

Typically, carbon nanotubes are produced using catalysts by aerosol-assisted chemical vapor deposition (AACVD), but most of the time, this catalyst remains inside them. However, for many applications, it is necessary to remove undesired nanoparticles. In this work, we propose the fabrication of carbon nanotubes using very low amounts of catalyst. Additionally, we incorporated nitrogen atoms into the carbon network using benzylamine. We used 0.05 wt % ferrocene as a catalyst for the growth of nitrogen-doped multiwall carbon nanotubes (N-MWCNTs). AACVD was performed at two temperatures (800 °C and 850 °C) under Ar flow. The morphology, diameter, degree of graphitization, and crystallinity phases present in the N-MWCNTs were analyzed by scanning electron microscopy (SEM), transmission electron microscopy (TEM), Raman spectroscopy, and X-ray diffraction (XRD), respectively. The thermal stability of N-MWCNTs was studied using thermogravimetric analysis (TGA). The concentration of nitrogen was evaluated using X-ray photoelectron spectroscopy (XPS). The TEM results showed that the N-MWCNTs exhibited a bamboo-shaped morphology. Cyclic voltammetry does not present redox processes that are regularly observed in N-MWCNTs.

References

[1] Kumar, M.; Ando, Y. chemical vapor deposition of carbon nanotubes: A review on growth mechanism and mass production. J. Nanosci. Nanotechnol. 2010, 10, 3739–3758.

[2] A. L. Danilyuk et al., "Manifestation of coherent magnetic anisotropy in a carbon nanotube matrix with low ferromagnetic nanoparticle content", New J. Phys. 2015, vol. 17, pp. 023073.

[3] M.I. Ionescu, Y. Zhang, R. Li, H. Abou-Rachid, X. Sun. Hydrogen-free spray pyrolysis chemical vapor deposition method for the carbon nanotube growth: Parametric studies Appl. Surf. Sci. 2011, 258,10,pp. 4563-4568.

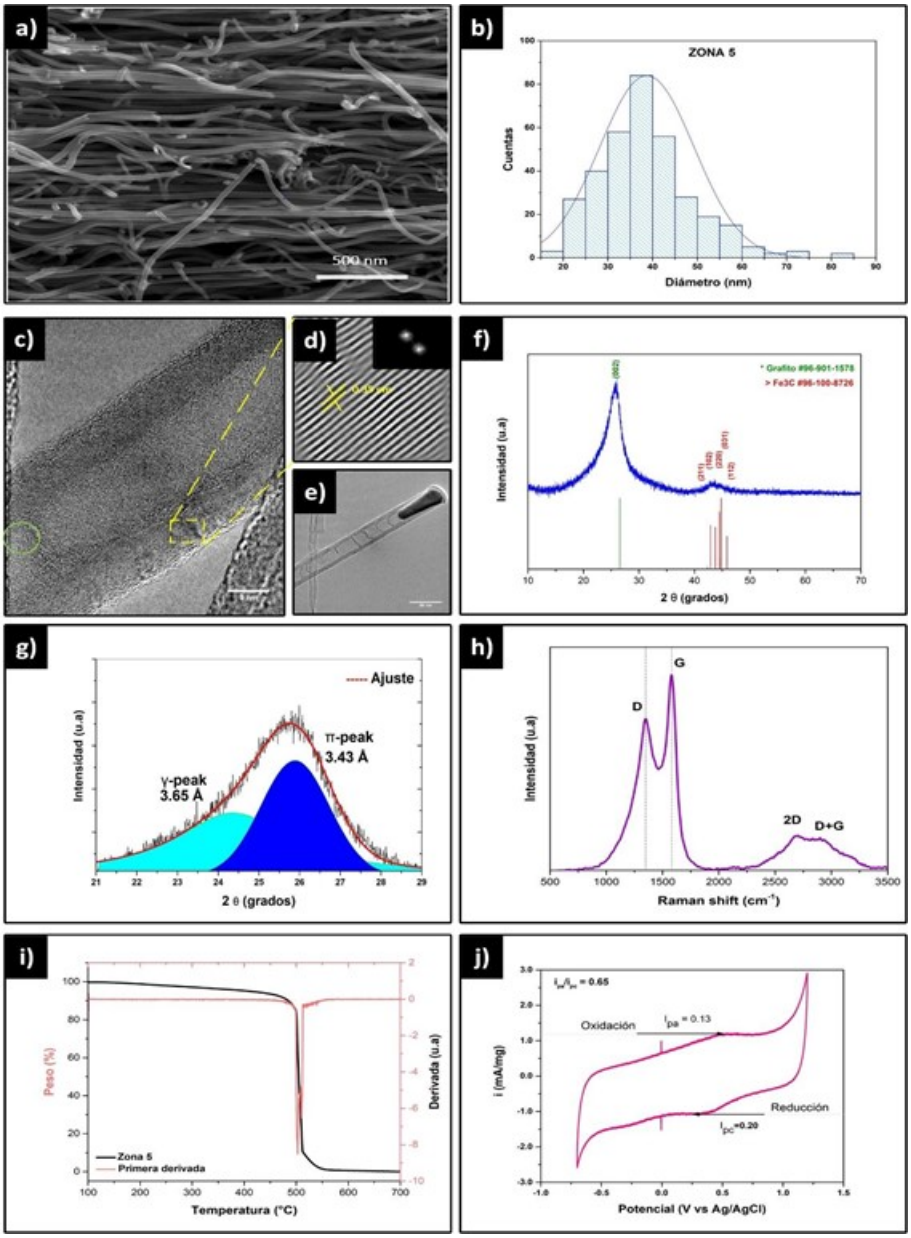

Figure 1: **Corresponding characterizations of the sample with a temperature of 800°C and a flow rate of 3.0 l/min a) micrographs with a magnification of 50000x b) internal morphology of the CNTs c) diffraction pattern and interplanar distance between CNT layers f) peaks characteristic of the graphite and Fe3C phases g) deconvolution of the (002) peak h) bands found by Raman i) weight loss with respect to temperature j) cyclic voltammetry of the N-MWCNTs.**

Thursday

Acta Microscopica Vol. 34, Supp. 2, 2025
Abstract Book NSSY 2024 - Galapagos 19-25 May, 2024

Toward accelerated discovery of new materials

Claudia Draxl[1]

[1] *Humboldt-Universiät zu Berlin, Berlin, Germany*

claudia.draxl@physik.hu-berlin.de

Abstract

Data-centric approaches are becoming an integral part of our research in complementing established traditional paradigms. Given the variety of possible applications in materials science, the potential for gaining new insights through artificial-intelligence (AI) is enormous. The vast amounts of research data produced every day in the field represent a 21st-century gold mine. How can we turn these data into knowledge and value? A FAIR (Findable, Accessible, Interoperable, and Reusable) data infrastructure plays a decisive role, because this gold mine is of little value if the data are not comprehensively characterized and made available. Only then, data can be readily shared and explored through statistical analysis and machine learning. Making data Findable and AI Ready (another interpretation of the acronym) will change the way how science is done today 1. I will show how the NOMAD data infrastructure [2] (see Fig. 1) deals with this complex situation. With selected examples, I will demonstrate how Big Data from either computational or experimental work can be used to find trends and patterns, which would not be possible from single investigations. I will also address the challenges when data potentially come from different sources and will discuss how machine learning can be used for error quantification and data augmentation. Finally, I will ask how we can make use of existing data collections to find materials with desired properties and will show how ML can be combined with established methodology toward nonlinear modeling and classification.

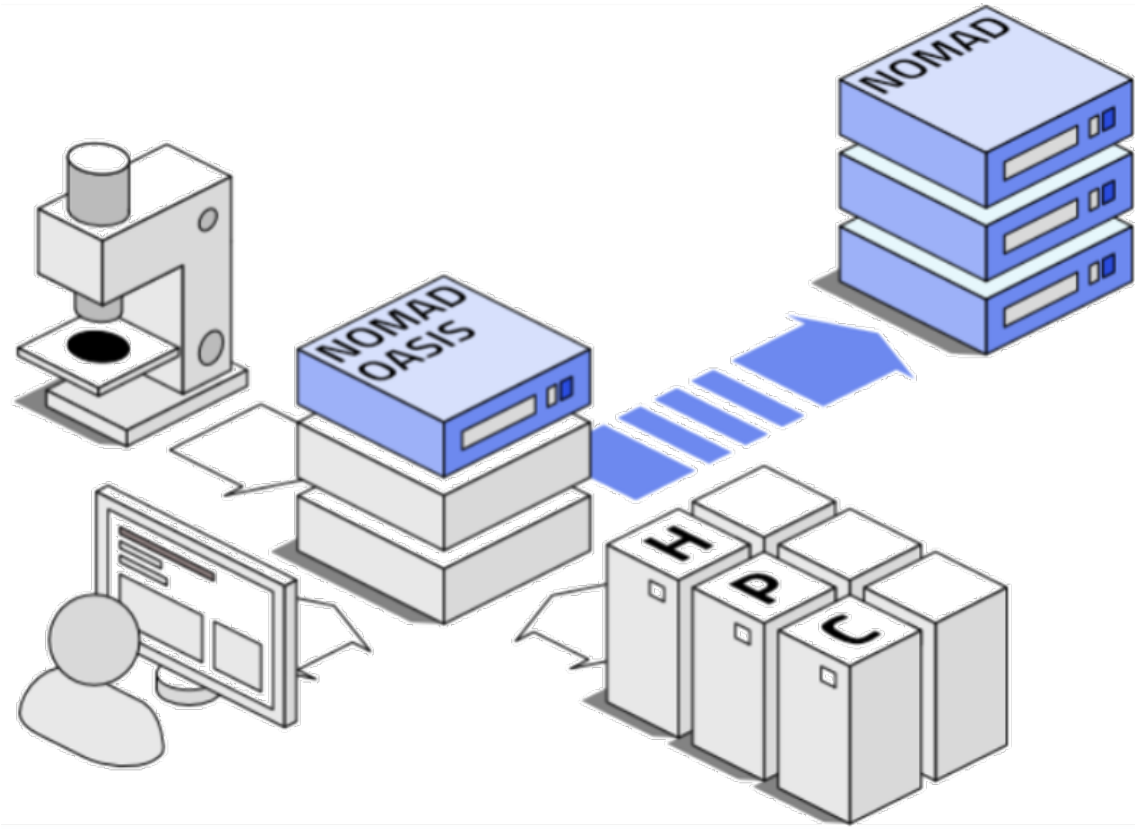

Figure 1: **Concept of the NOMAD data infrastructure.**

References

[1] M. Scheffler, M. Aeschlimann, M. Albrecht, T. Bereau, H.-J. Bungartz, C. Felser, M. Greiner, A. Groß, C. Koch, K. Kremer, W. E. Nagel, M. Scheidgen, C. Wöll, and C. Draxl, Nature **604**, 635 (2022).

[2] M. Scheidgen, L. Himanen, A. Noe Ladines, D. Sikter, M. Nakhaee, A. Fekete, T. Chang, A. Golparvar, J. A. Marquez, S. Brockhauser, S. Brückner, L. M. Ghiringhelli, F. Dietrich, D. Lehmberg, T. Denell, A Albino, H. Näsström, S. Shabih, F. Dobener, M. Kühbach, R. Mozumder, J. Rudzinski, N. Daelman, J. M. Pizarro, M. Kuban, P. Ondracka, H.-J. Bungartz, and C. Draxl, J. Open Source Softw. **8**, 5388 (2023).

Acta Microscopica Vol. 34, Supp. 2, 2025
Abstract Book NSSY 2024 - Galapagos 19-25 May, 2024

Characterization of a Nano Enhanced Phase Change Material Based Sacha Inchi Oil

Juan Francisco Nicolalde[1], Javier Martinez-Gómez, Victor H. Guerrero, Andrés Chico-Proano

[1] *Facultad de Ciecnias Técnicas, Universidad Internacional Del Ecuador UIDe, Quito 170411, Ecuador*

[2] *Mechanical Engineering Area, Signal Theory and Communications Department, Universidad de Alcalá, 28805, Madrid, Spain*

[3] *Department of Materials, Escuela Politécnica Nacional (EPN), Quito 170525, Ecuador*

[4] *Departamento de Ingeniería Química, Escuela Politécnica Nacional (EPN), Quito 170525, Ecuador*

[5] *Facultad de Ingeniería y Ciencias Aplicadas, Universidad Internacional SEK, Albert Einstein s/n and 5th, Quito 170302, Ecuador.*

junicolaldego@uide.edu.ec

Abstract

The energy challenges tha humanity faces demands the development of clean, renewable and efficient technologies. In this way, organic phase change materials are an option that contributes to energy improvement with the utilization of fatty acids that have been found as constituents of Sacha Inchi oil. However, while these natural oils have good stability, working range, and availability, the resulting phase change materials have limitations such as low conductivity. These properties can be improved through the inclusion of nanoparticulate materials . In this way, this research aims to obtain, characterize and evaluate an organic phase change materials of Sacha Inchi enhanced by nanoparticles, which allow to increase their thermal properties. The characterization of the material will includes analysis by UV/Vis for evaluating the degree of dispersion of the nanomaterial. On the other hand, Fourier transform infrared spectroscopy will allows to understand the relationship between the different PCMs and the nanomaterials in terms of the chemical stability of the organic PCMs after the nanoparticles have been incorporated. Differential scanning calorimetry makes it possible to determine the melting and crystallization temperatures, as well as the latent heat of the materials, making possible to know their working ranges and their response to the freeze and melt cycles, their thermal stability and possible super cooling. A thermal conductivity analysis will also be carried out to show its thermal conduction properties after the addition of the nano-particulate, as well as its response to different volumetric fractions. These phase-change materials will exhibit thermal conductivity and specific heat properties superior to those of the base material, thus providing new knowledge of how naturally occurring precursors enable material improvement in engineering

applications with an impact on energy efficiency and renewables. In this way, the present research proposes to contribute to the field of energy efficiency and sustainable use of resources through the characterization of nanoenhanced pahse change materials, which could lead to future solutions to environmental problems in a sustainable way.

Figure 1: **NEPCM**

References

[1] A. Grüneis, M.H. Rümmeli, C. Kramberger, A. Barreiro, T. Pichler, R. Pfeiffer, H. Kuzmany, T. Gemming, B. Büchner, High quality double wall carbon nanotubes with a defined diameter distribution by chemical vapor deposition from alcohol, Carbon N Y. 44 (2006) 3177–3182. https://doi.org/10.1016/j.carbon.2006.07.003

[2] H.J. Basheer, C. Pachot, U. Lafont, X. Devaux, N. Bahlawane, Low-Temperature Thermal CVD of Superblack Carbon Nanotube Coatings, Advanced Materials Interfaces. 4 (2017) 1–9. https://doi.org/10.1002/admi.201700238.

[3] J. Parker, C. Beasley, A. Lin, H.Y. Chen, H. S. P. Wong, Increasing the semiconducting fraction in ensembles of single-walled carbon nanotubes, Carbon 50 (2012) 5093-5098. DOI:10.1016/j.carbon.2012.06.049.

Acta Microscopica Vol. 34, Supp. 2, 2025
Abstract Book NSSY 2024 - Galapagos 19-25 May, 2024

Nano - and microcrystalline luminescent heterometallic Eu(III)-based MOFs as luminescent probes for heavy metal ions

Andrey S. Mereshchenko[1], Stefaniia S. Kolesnik[2]
[1] *Institute of Chemistry, Saint Petersburg State University*
a.mereshchenko@spbu.ru

Abstract

In this work, we reported the morphology and the photoluminescence properties of the three series of microcrystalline heterometallic europium-containing terephthalate metal-organic frameworks synthesized by ultrasound-assisted method from diluted aqueous solutions[1,2]:$(Eu_{1-x}La_x)_2bdc_3nH_2O$, $(Eu_{1-x}Gd_x)_2bdc_3nH_2O$ and $(Eu_{1-x}Lu_x)_2bdc_3nH_2O$ (x = 0–1). The effect of the dopant concentration on the structural properties was revealed. Thus, the La3+ and Gd^{3+}-doped terephthalates are isostructural to $Eu_2bdc_34H_2O$, but the Lu^{3+} doped compounds are isostructural to $Eu_2bdc_34H_2O$ only when the Lu content is lower than 95 at.%; at higher Lu^{3+} content, the new structure namely $Lu_2bdc_32.5H_2O$ was obtained. The unit cell parameters were refined for the compounds corresponding to $Ln_2bdc_34H_2O$ crystalline phase. We observed that the substitution of Eu^{3+} for larger La^{3+} ions increases the unit cell volumes, whereas doping by the smaller Lu^{3+} ion results in a decrease in the unit cell volume. The ionic radius of the Gd^{3+} ion is close to that of Eu^{3+}. Therefore, the unit cell parameters do not change significantly as a result of substitution of Eu^{3+} by Gd^{3+}. The analysis of the morphology of the synthesized materials by scanning electron microscopy has demonstrated that the ultrasound-assisted method results in the formation of particles that have a size of several micrometers and a shape determined by the crystalline phase. In the $(Eu_{1\ x}La_x)_2bdc_34H_2O$ and $(Eu_{1-x}Gd_x)_2bdc_34H_2O$ series, the particles have a similar "leaf" shape and size of approximately 6 × 2 m. In the $(Eu_{1-x}Lu_x)_2bdc_3nH_2O$ series, particles have different shapes depending on the content of lutetium ion. At the Lu^{3+} content below 90 at.%, which corresponds to the $Ln_2bdc_34H_2O$ crystalline phase, the particles have the shape of rods and a size of approximately 4 × 0.8 m. However, in $(Eu_{1-x}Lu_x)_2bdc_3nH_2O$ MOFs with a concentration of Lu^{3+} more than 90% ($Ln_2bdc_32.5H_2O$ crystalline phase), the particles are "brick"-shaped and significantly larger, about 10 × 5 m. At the Lu^{3+} concentration of 90 and 95 at.%, the mixture of "bricks" and "rods" is observed.

All synthesized samples containing Eu^{3+} demonstrated a bright-red emission corresponding to the $^5D_0$-^7F_J (J = 1, 2, 4) transitions of Eu^{3+} ions upon 310-nm excitation to the S_n state of terephthalate ions due to the "antenna" effect.

The fine structure of the emission spectra is determined by the crystalline phase due to the different local symmetry of the Eu^{3+} ions in different types of crystalline structure, namely $Ln_2bdc_34H_2O$ and $Ln_2bdc_32.5H_2O$. In the $(Eu_{1-x}La_x)_2bdc_3nH_2O$ and $(Eu_{1-x}Gd_x)_2bdc_3nH_2O$ series, the photoluminescence quantum yields and $^5D_0$ excited state lifetimes are equal to 11 ± 2% and 0.44 ± 0.01 ms, respectively, and almost do not depend on the content of La^{3+} and Gd^{3+}. The substitution of Eu^{3+} for Lu^{3+} results in an increase in both the photoluminescence quantum yield (up to 23% at the Lu^{3+} content of 95%) and $^5D_0$ excited state lifetime (up to 1.62 ms) in agreement with the phase transition from $Ln_2bdc_34H_2O$ to $Ln_2bdc_32.5H_2O$.

$Eu_2bdc_34H_2O$ nanoparticles were also synthesized in this work by the mixing of low-concentration sodium terephthalate and europium chloride aqueous solutions in the presence of ultrasonication. The average size of nanoparticles was found to be of about 8±2 nm. Thus, the reported $Eu_2bdc_34H_2O$ nanoparticles are the smallest nanosized rare-earth-based MOF crystals, to the best of our knowledge [2]. The nonradiative decay rate of nanocrystalline europium(III) terephthalate was significantly larger that the corresponding values of $Eu_2bdc_34H_2O$ MOFs, which resulted from more efficient quenching of the $^5D_0$ level and Eu^{3+} by the water molecules in aqueous solution due to greater surface-to-volume ratio of nanocrystalline MOF. The Cu^{2+}, Cr^{3+}, and Fe^{3+} ions efficiently and selectively quench the Eu^{3+} $^5D_0{}^7F$ luminescence of nanocrystalline $Eu_2bdc_34H_2O$ MOFs starting from the relatively low concentrations of metal ion: 1 M of Cu^{2+} and 30 μM of Cr^{3+} or Fe^{3+}. The reported nanocrystalline europium(III) terephthalateis one of the most sensitive luminescent MOF-based sensor for Cu^{2+}, Cr $^{3+}$ and Fe^{3+} ions [2]. Therefore, synthesized nanocrystalline $Eu_2bdc_34H_2O$ MOFs can be considered promising luminescent probes for heavy metal ions in waste and drinking water.

References

[1] Kolesnik S.S et al Molecule (2024) (29) (532).

[2] Kolesnik S.S et al Nanomaterials (2021) (11) (2448).

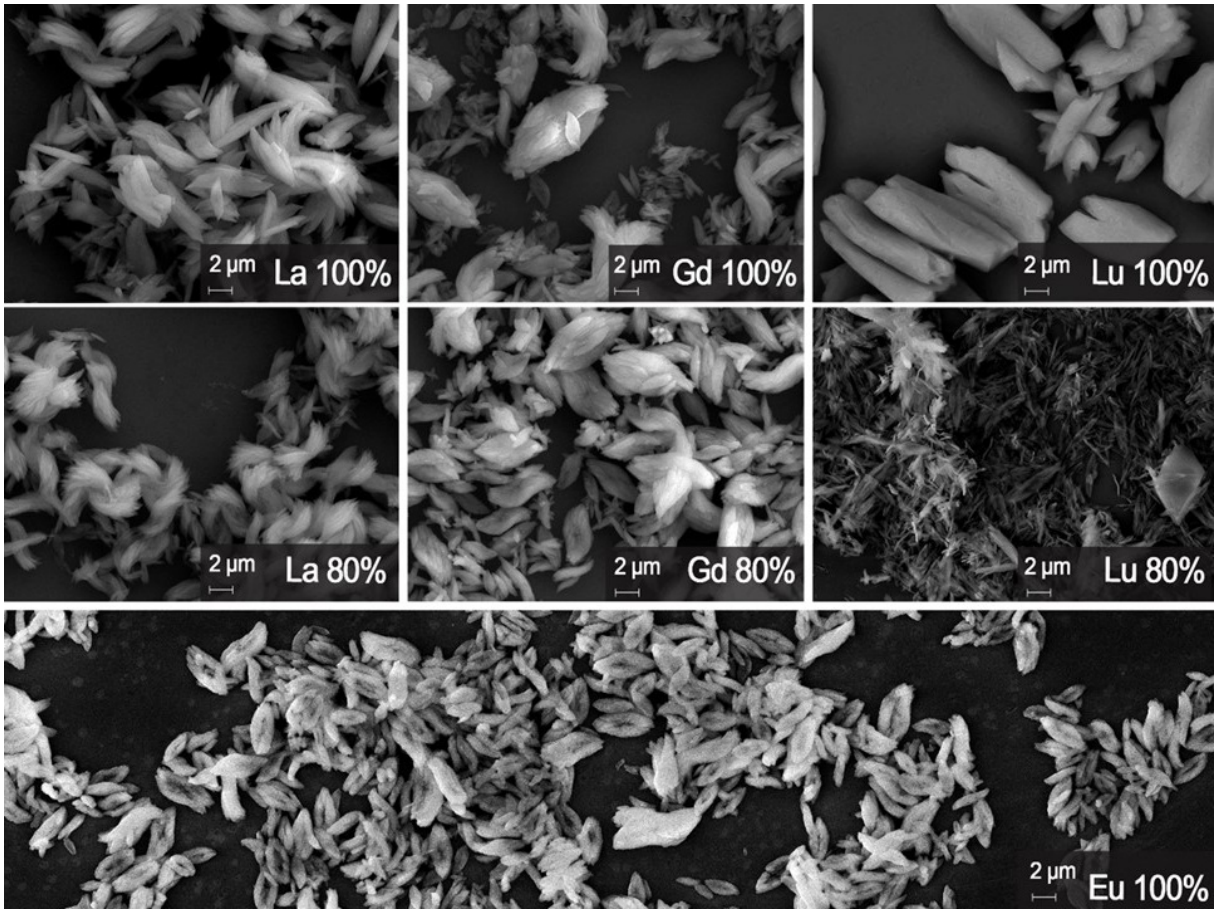

Figure 1: **SEM images of the $(Eu_{1-x}Ln_x)_2bdc_3nH_2O$ (Ln = Lu, La, Gd) microparticles.**

Acta Microscopica Vol. 34, Supp. 2, 2025
Abstract Book NSSY 2024 - Galapagos 19-25 May, 2024

Collective Radial Breathing Modes in Homogeneous Nanotube Bundles

Charlotte Berrezueta-Palacios[1], Dekel Nakar[2], Anna Wroblewska[3], Oisín Garrity[1], Han Li d[5], Nitzan Shadmi[2], Benjamin S. Flavel[4], Ernesto Joselevich[2], Stephanie Reich[1], Georgy Gordeev [1,2]

[1] *Department of Physics, Freie Universität Berlin, Berlin 14195, Germany*

[2] *Department of Molecular Chemistry and Materials Science, Weizmann Institute of Science, Rehovot 7610001, Israel*

[3] *Faculty of Physics, Warsaw University of Technology, Koszykowa 75, 00-662, Warsaw, Poland*

[4] *Institute of Nanotechnology, Karlsruhe Institute of Technology, Kaiserstraße 12, 76131 Karlsruhe, Germany*

[5] *Department of Mechanical and Materials Engineering, University of Turku, Vesilinnantie 5, 20500 Turku, Finland*

[6] *Department of Physics and Materials Science, University of Luxembourg, L-4422 Belvaux, Luxembourg*

email

Abstract

Carbon nanotubes (CNTs) exist in many atomic structures typically grow as mixtures of of many chiralities with a vast variety of properties. Identical CNTs that are arranged into two-dimensional hexagonal lattices, their vibrational properties have been predicted to change with additional low-frequency modes appearing in the Raman spectrum. [1] Up to now, the experimental study of collective vibrations has been limited by a lack of pure homogeneous chirality bundles. We overcome this challenge by employing a self-coil mechanism of a very long CNT that loop into itself during the growth process resulting in a tightly packed hexagonal stack [2]. This lattice is perfectly homogeneous in terms of diameter, chiral twist, and even handedness of the tube. By characterizing and comparing the physical properties of the coil with respect to its tails, the bundling effects are clearly visible. We report on two breathing-like modes for quasi-infinite bundles, compared to the single radial breathing mode characteristic for isolated tubes. The exciton-phonon coupling in these modes is probed with resonant Raman spectroscopy, revealing the same resonance energy for both breathing-like peaks. Additionally, we study the dependence of vibrational coupling on the tube diameter by analysing different tube's diameter coils and other bundling geometries. Our experimental findings align well with previously reported theoretical studies, demonstrating a 1/d scaling for all modes, as well as confirming the relative shift of the modes dependent on intertube interaction. These vibrations provide insight into the role of intertube lattice dynamics in two-dimensional THz-range phononic crystals [3].

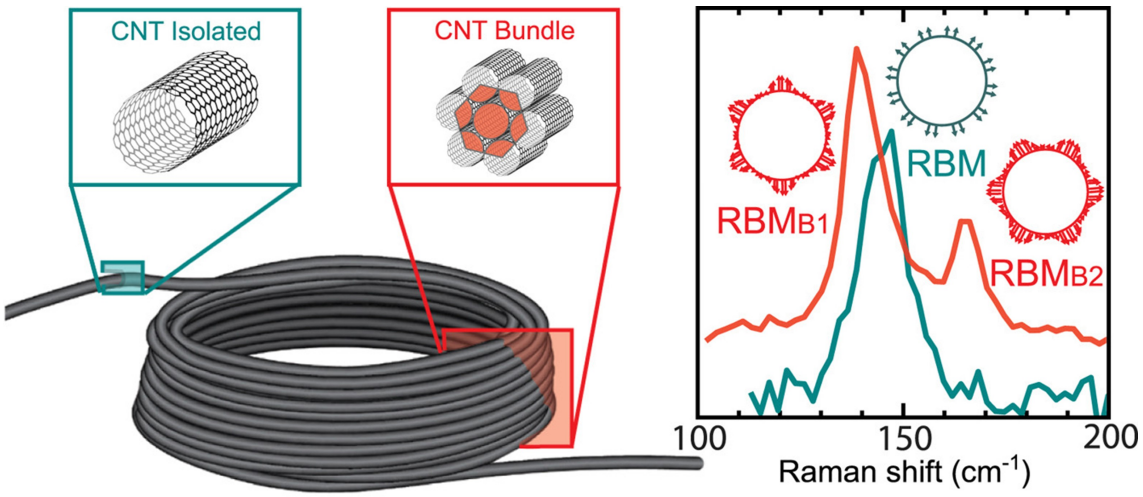

References

[1] Popov, V. N.; Henrard, L. Evidence for the existence of two breathinglike phonon modes in infinite bundles of single-walled carbon nanotubes. Phys. Rev. B 2001, 63, 233407

[2] Nakar, D.; Gordeev, G.; Machado, L. D.; Popovitz-Biro, R.; Rechav, K.; Oliveira, E. F.; Kusch, P.; Jorio, A.; Galvao, D. S.; Reich, S.; others Few-wall Carbon Nanotube Coils. Nano Letters 2019, 20, 953–962.

[3] Berrezueta-Palacios, C., Nakar, D., Wroblewska, A., Garrity, O., Li, H., Shadmi, N., ... & Gordeev, G. (2024). Collective radial breathing modes in homogeneous nanotube bundles. Carbon, 224, 119010.

Acta Microscopica Vol. 34, Supp. 2, 2025
Abstract Book NSSY 2024 - Galapagos 19-25 May, 2024

Magnetic carbon

Hongde Yu[1], **Thomas Heine**[1]
[1] *TU Dresden, School of Science, 01062 Dresden, Germany*
thomas.heine@tu-dresden.de

Abstract

It is generally accepted that carbon is the most versatile element of the periodic table, and it offers a plethora of compounds ranging from biology to materials science. While the list of fascinating properties carbon materials offer is long, they are not yet famous for magnetism.

Indeed, most carbon materials are diamagnetic. Defects, dopants and dangling bonds can introduce paramagnetic centers without the potential to generate magnetic ordering. Recently reported magic-angle twisted bilayer graphene may become ferromagnetic due to a half-filled flat band at the fermi level and spin-orbit coupling [1]. A spectacular early report on magnetic carbon in pressurized fullerenes [2] was found to be caused by defects and the paper has been retracted five years later.

We propose an alternative concept to generate carbon materials with strongly coupled magnetic centers. Our materials are based on molecular triangulene and its derivatives, aromatic molecules intrinsically carrying one or two unpaired electrons. Using covalent linkages that preserve electron conjugation, we construct two-dimensional polymers with honeycomb-kagome lattice. The magnetic coupling between the monomers is facilitated by the linker groups. This has been examined in detail for the dimers [3]. When extending this concept to 2D polymers, we predict magnetic carbon materials with intriguing electronic structure that includes Stoner ferromagnetism with Weyl points at the Fermi level, and Mott-Hubbard insulator antiferromagnetism, which would be the first metal-free ferro- and antiferromagnetic materials with strong magnetic coupling with a Curie/Néel temperature above 250 K [4]. If we use two different building blocks in a heterostructure, we are even able to construct materials where a Curie temperature exceeding 500K.

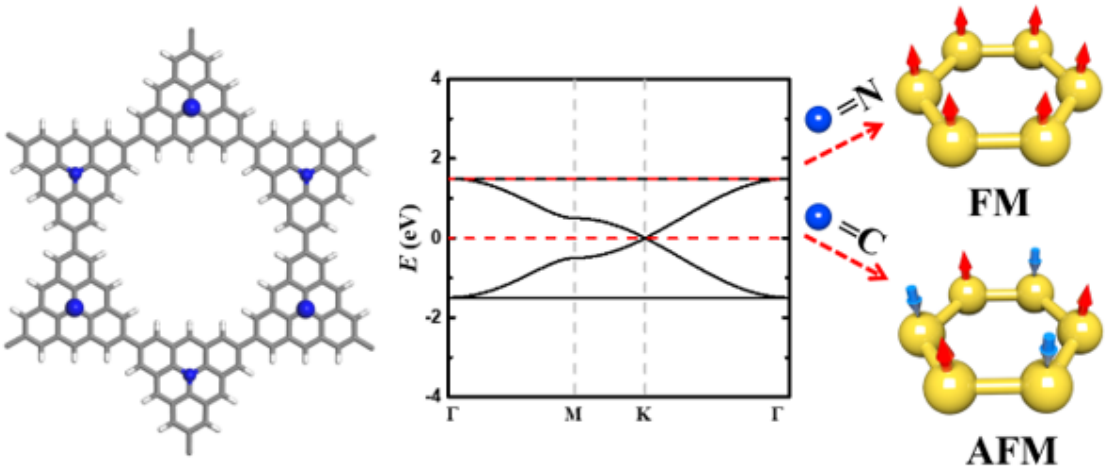

Figure 1: **Sketch to design metal-free ferromagnetic (FM) or antiferromagnetic (AFM) two-dimensional polymers.**

References

[1] A. A. Sharpe E. J. Fox, A. W. Barnard, J. Finney, K. Watanabe, T. Taniguchi, M. A. Kastner, D. Goldhaber-Gordon, ACS Nano 21, 4299 (2021).

[2] T. L. Makarova, B. Sundqvist, R. Höhne, P. Esquinazi, Y. Kopelevich, P. Scharff, V. A. Davydov, L. S. Kashevarova, A. V. Rakhmanina, Nature 413, 716, (2001) (retracted).

[3] H. Yu, T. Heine, J. Am. Chem. Soc. 145, 19303 (2023).

[4] H. Yu, T. Heine, submitted, arxiv: 2311.09026

Acta Microscopica Vol. 34, Supp. 2, 2025
Abstract Book NSSY 2024 - Galapagos 19-25 May, 2024

Understanding light-matter interactions at the nanoscale for plasmon enhanced single-photon emission

Esther Wertz[1]
[1] *Rensselaer Polytechnic Institute*
wertze@rpi.edu

Abstract

The potential of quantum information science is fueling demand for the design and generation of new qubits and devices operating at the single-particle level. One promising approach uses photons as information carriers. Their long decoherence lengths and fast operation speeds offer natural benefits for rapid and safe quantum communication; however, photons typically interact very weakly with matter and thus their manipulation usually require high powers and nonlinear media. One way to strengthen these interactions is to use metallic nanoparticles to enhance electromagnetic fields in their vicinity. Indeed, metal nanoparticles (NPs) sustain a collective oscillation of their free electrons, called a localized surface plasmon resonance (LSPR), when excited by an electromagnetic wave. When this incident wave is resonant with the LSPR frequency, the field intensity is strongly increased in the near field of the NP. Plasmonics thus provides a unique setting for the manipulation of light via the confinement of the electromagnetic field to regions well below the diffraction limit. This has opened up a wide range of applications based on extreme light concentration, including nanophotonic lasers and amplifiers optical metamaterials, biochemical sensing and antennas transmitting and receiving light signals at the nanoscale. Our group is interested in using these NPs to manipulate photons with low powers in an integratable system, however, many difficulties remain in experimentally measuring the shape, size, and enhanced field properties of the localized electromagnetic modes in the vicinity of the NPs due to the limitations of optical microscopy. In this talk, I will discuss how we can unravel the coupling of light to a nano-antenna through single-molecule fluorescence imaging. This technique is a powerful tool to optically study structures beyond the diffraction limit by localizing isolated fluorophores and fitting the emission profile to the microscope point-spread function. By using the random motion of single dye molecules in solution to stochastically scan the surface, and by assessing emission intensity, wavelength, and density of emitters as a function of position, we gain new insight into the properties of these systems and pave the way for the development of better plasmonic devices.

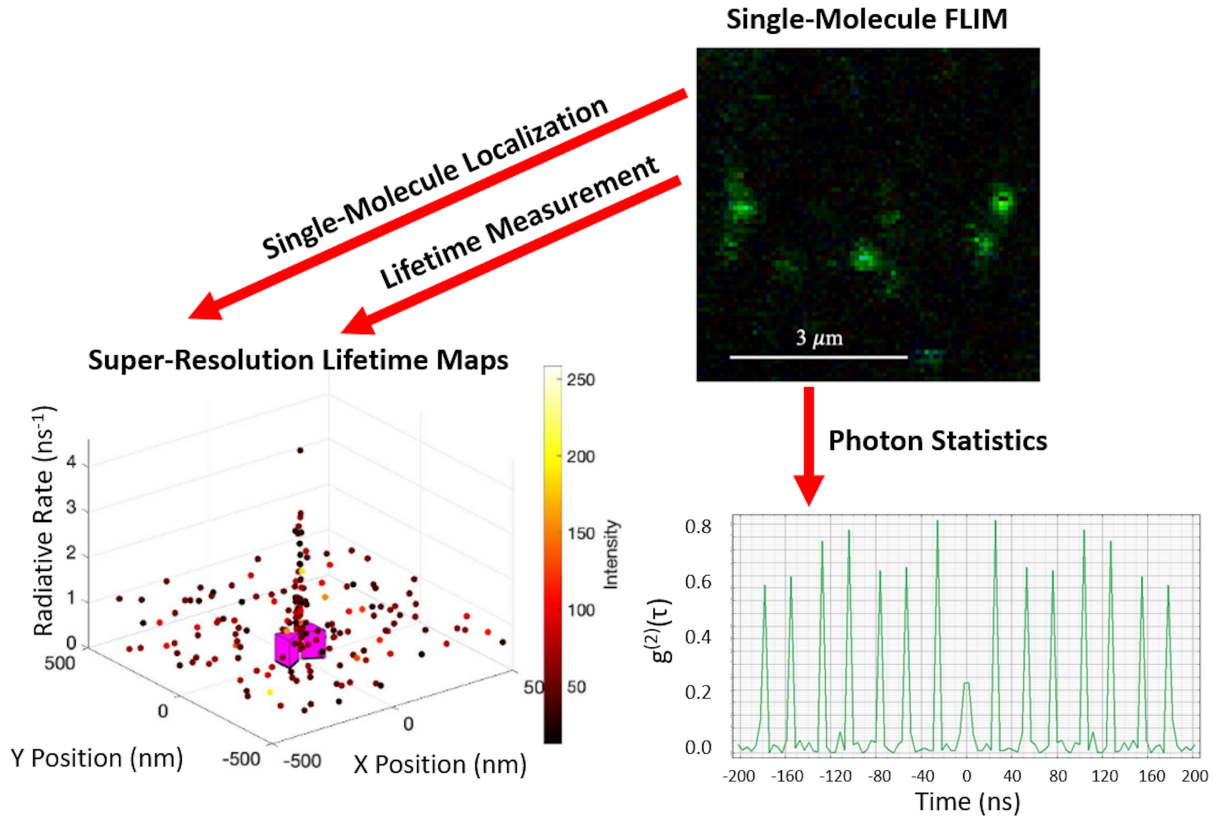

Figure 1: **Single-molecule super-resolution combined with fluorescence lifetime imaging permits the investigation of the changes in emission intensity, radiative rate and photon statistics near plasmonic nanostructures.**

Acta Microscopica Vol. 34, Supp. 2, 2025
Abstract Book NSSY 2024 - Galapagos 19-25 May, 2024

Microbial decontamination of barn surfaces using Engineered Water Nanostructures (EWNS)

Felipe de Jesus Barraza Garcia[1,2], Emilio Muñoz Sandoval[1], Lifeng Zhang[2], Roger E. Bolo[2], Brooke Thompson[3], Shelley Kirychuk[3], Huiqing Guo[4], Bernardo Predicala[5]

[1] *Instituto Potosino de Investigación Científica y Tecnológica A.C., División de Materiales Avanzados, Mexico.*

[2] *University of Saskatchewan, Department of Chemical and Biological Engineering, Canada.*

[3] *University of Saskatchewan, Department of Medicine, Canada.*

[4] *University of Saskatchewan, Department of Mechanical Engineering, Canada.*

[5] *Prairie Swine Centre, Engineering Research Program, Canada.*

felipe3381@hotmail.com

Abstract

Infectious livestock diseases are a major threat to the health and welfare of animals, farm workers and surrounding communities producing a devastating impact on the industry. Current microbial inactivation techniques employed in livestock facilities use oxidizing agents and/or UV radiation, however, these methods are expensive, use toxic chemicals, and produce residual contamination. Engineered water nanostructures (EWNS) technology produces highly charged nanoscale water droplets with encapsulated reactive oxygen species (ROS) for bacterial inactivation through the electrospraying and ionization of reverse osmosis (RO) water (Pyrgiotakis et al., 2012). However, studies on the application of electrosprayers in the decontamination of animal facilities are limited and not fully established (Si et al., 2021).

In this work, an electro-nanospray system was developed for the decontamination of common surfaces found in pig barns including metal, plastic, wood, and concrete. Microbial deactivation of the electro-nanospray device was tested at different conditions in a laboratory-scale on the deactivation of Escherichia coli (E. coli) at a bacterial concentration similar to levels found on pig barn surfaces. Experiments were conducted using an acrylic chamber in which the electro-nanospray system was installed (Fig. 1). The efficacy of the EWNS system in inactivating E. coli was assessed with varying operating conditions such as applied voltage, exposure time, and distance between the counter electrode and the treated surface. Different pig barns surfaces were characterized by scanning electron microscopy and contact angle to understand the different behaviors between the samples.

Fig. 2. depicts the contact angles of a water droplet set on the surface of the coupons, as well as scanning electron micrographs for each of the materials at 30,

500 and 5000 X. According to these results, plastic resulted the least hydrophilic material , followed by metal and wood, while concrete corresponds to a superhydrophilic material and therefore a greater number of possible interactions between these surfaces would be expected. In this way it is expected that surfaces such as plastic and metal have more limited interactions, while wood and concrete may interact more with liquid and/or microbial populations.

The analysis of the efficiency of EWNS to decontaminate surfaces is analyzed in Fig. 3. The EWNS generated by our system to analyze the effect of voltage found that with a voltage of -7.6 kV obtained the highest E. coli reduction (1.44 log) compared to -5.6 and -6.6 kV , which resulted in 1.07 and 1.26 log respectively. On the other hand, for the distance between the counter electrode and the coupon surface (Fig. 3(b)) it was found that the highest microbial inactivation (1.83 log reduction) was obtained at 8 cm distance from the counter electrode. Reducing the distance to 4 and 1 cm decreased the inactivation rate to 1.63 and 1.26 log respectively. Fig. 3(c) shows the highest microbial inactivation for treatment time with 2.66 log reduction at 40 min of treatment. If treatment time is reduced to 30, 15, 10, and 5 minutes, the log reduction drops to 2.58, 1.69, 1.49, and 1.27, respectively. It should be noted that even when there is an increase in inactivation from 30 to 40 min of treatment, the increase was not significant (p¿0.05). Finally, to analyze the effect of surface-dependent inactivation, the highest efficiency conditions were used.

Results showed that porous materials such as wood and concrete showed the highest log reductions with 2.96 and 2.61 respectively. This behavior is associated with the ability of these materials to absorb water in their structure, which limits the presence of E. coli. On the other hand, smooth materials such as metal and plastic had logarithm reductions of 2.02 and 1.61 respectively, which implied reductions of 99.05 and 97.64 for metal and plastic. This behavior indicates that a smoother surface maintains favorable conditions for the presence of E. coli. The difference between the total number of bacteria before and after testing plastic and metal surfaces is associated with electrochemical corrosion processes in metals that oxidize, producing OH-free radicals that interact with microorganisms (Bazli et al., 2020). These results show the potential of EWNS technology as a microbial decontamination method for the treatment of surfaces in animal confinement facilities. However, in-barn tests are needed for the implementation of these systems.

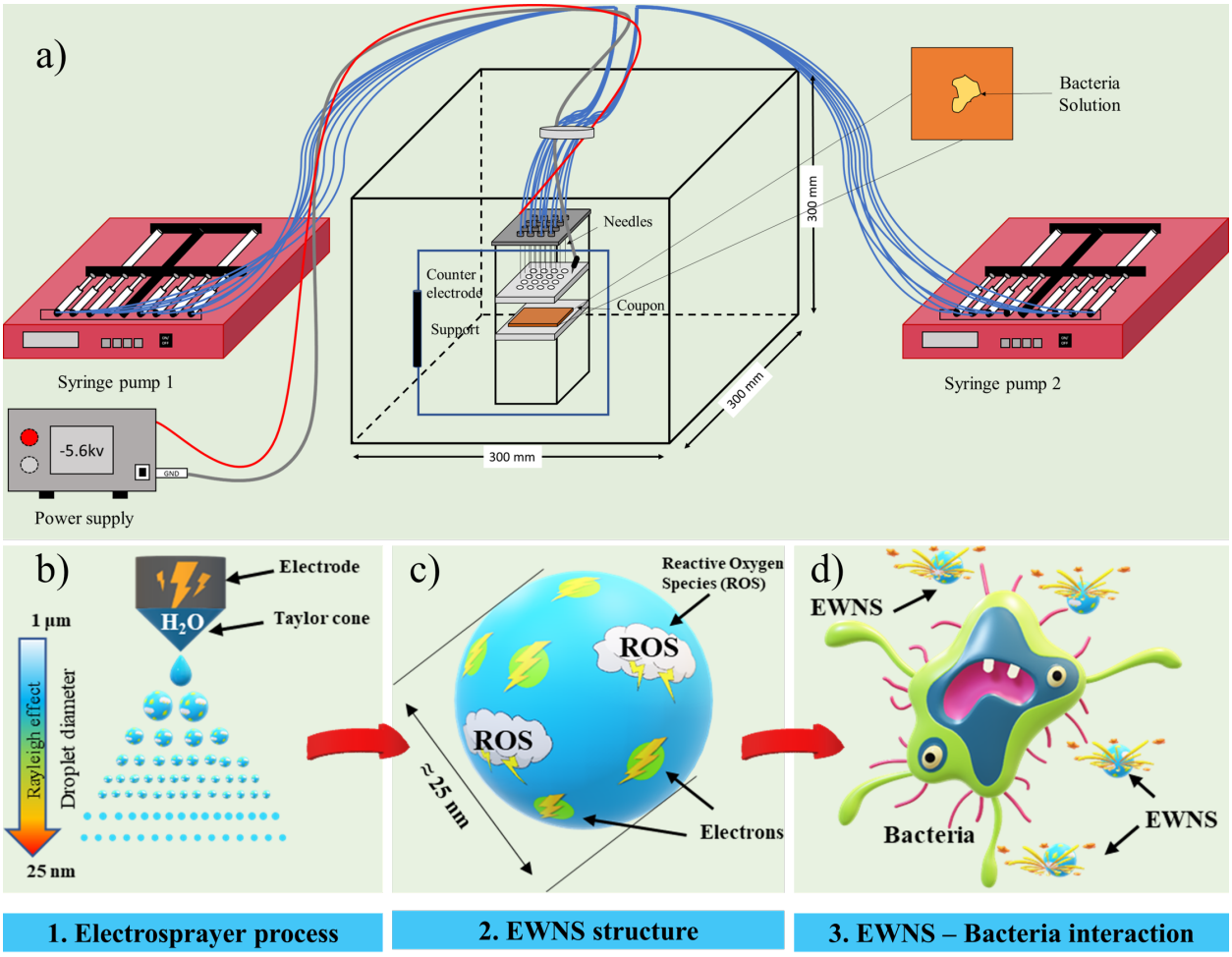

Figure 1: **Schematic diagram of surface decontamination through EWNS. (a) Electronanosprayer system. (b) Electrospray process, (c) EWNS structure, (d) EWNS – Bacteria interaction.**

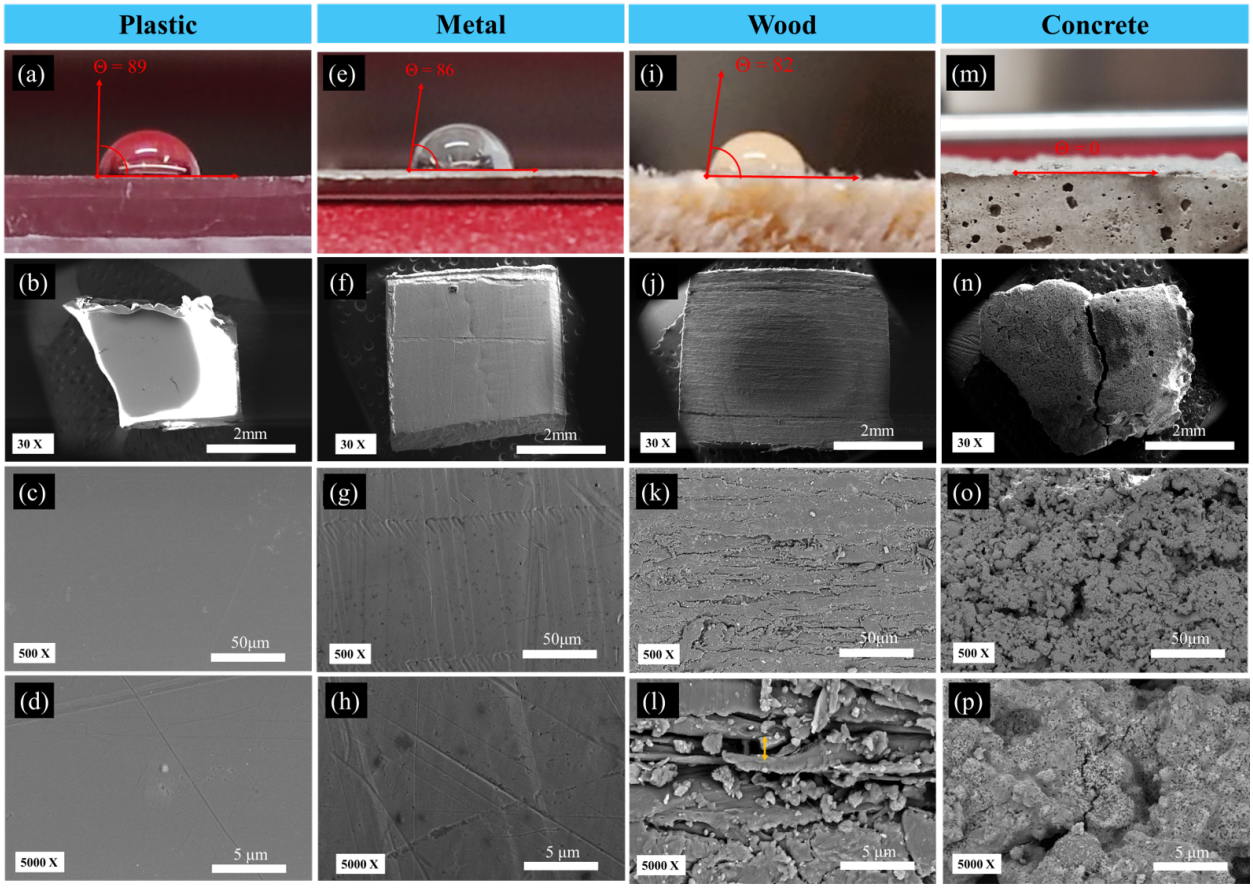

Figure 2: **Surface characterization by contact angle and SEM microscopy for the coupons of the different materials: a-d) plastic, e-h) metal, (i-l) wood, and (m-p) concrete, respectively.**

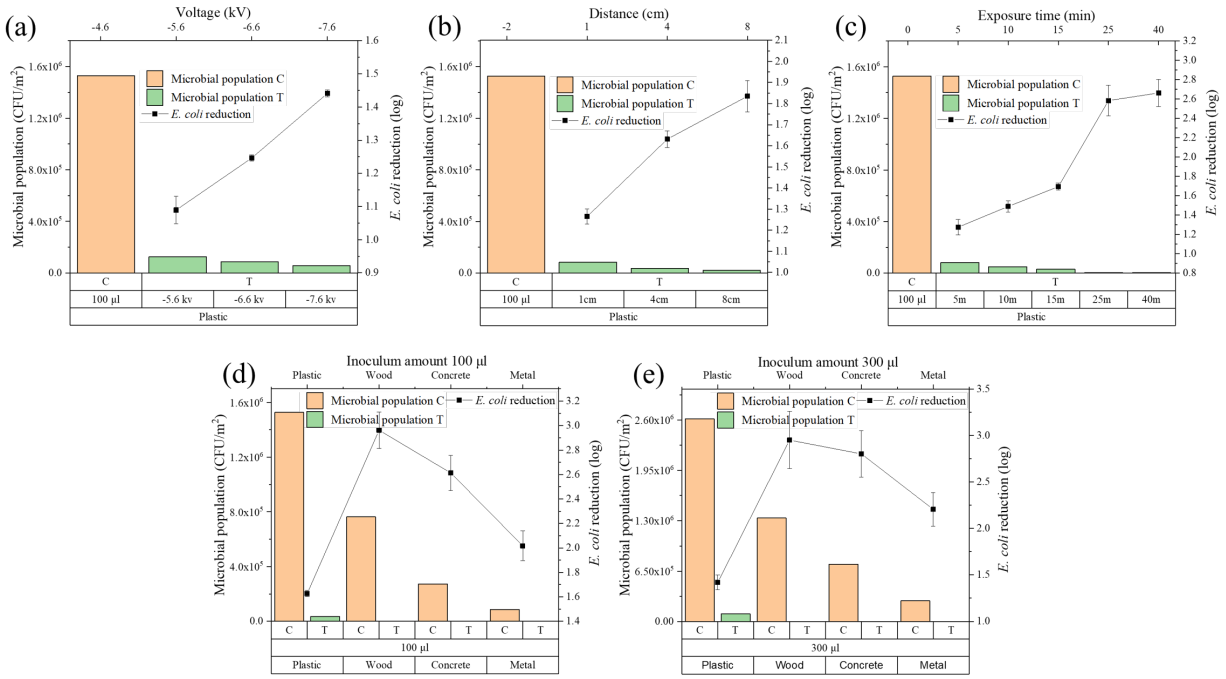

Figure 3: **Effect of different parameters tested on the microbial inactivation of E. coli. (a) applied voltage, (b) distance between counter electrode and coupon surface, (c) exposure time and (d-e) surface type.**

References

[1] G. Pyrgiotakis, J. McDevitt, T. Yamauchi, y P. Demokritou, A novel method for bacterial inactivation using electrosprayed water nanostructures, J. Nanoparticle Res., vol. 14, n.o 8, p. 1027, ago. 2012, doi: 10.1007/s11051-012-1027-x.

[2] Y. Si et al., "Effects of Operating Parameters on the Efficacy of Engineered Water Nanostructures (EWNS) in Inactivating Escherichia coli on Stainless-Steel Surfaces", Trans. ASABE, vol. 64, núm. 6, pp. 1913–1920, 2021, doi: 10.13031/trans.14645.

[3] Bazli, L., Yusuf, M., Farahani, A., Kiamarzi, M., Seyedhosseini, Z., Nezhadmansari, M., Aliasghari, M., Iranpoor, M., 2020. Application of composite conducting polymers for improving the corrosion behavior of various substrates: A Review. J. Compos. Compd. 2, 228–240. https://doi.org/10.29252/jcc.2.4.7

Acta Microscopica Vol. 34, Supp. 2, 2025
Abstract Book NSSY 2024 - Galapagos 19-25 May, 2024

Synthesis and characterization of fluorescent carbon quantum dots derived from citric acid as potential optical sensor for the detection of metallic cations.

M. Belén Cánchig[1], Manuel Caetano[1], Thibault Terencio[1], Juan Pablo Saucedo[1]
[1] *CATALYSIS THEORY SPECTROSCOPY Research Group (CATS), School of Chemical Sciences & Engineering, Yachay Tech University, San Miguel de Urcuquí, Hacienda San José s/n, Urcuquí 100115, Ecuador*
maria.canchig@yachaytech.edu.ec

Abstract

Environmental water pollution resulting from toxic metal ions has emerged as a significant and serious issue in the environment. Any substance (metal or anion) can be deemed a "pollutant" when it appears in an undesirable location or is present in a form or concentration that results in harmful effects on humans or the environment [1] . Some examples of such metals and metalloids encompass lead, cadmium, mercury, arsenic, chromium, copper, selenium, nickel, silver, zinc, aluminum, cesium, cobalt, manganese, molybdenum, strontium, and uranium [2]. The consequences of this water pollution have driven researchers to develop methods for identifying and measuring metal ion contaminants. These can be classified in three main groups: spectroscopic, electrochemical and optical techniques. Furthermore, specific detection methods are qualitative and involve toxic or radioactive elements, while electrochemical determination requires complex electrode fabrication [3]. Consequently, there is a strong demand for simple and cost-effective techniques to detect metal ions and anions.

Carbon quantum dots (CQDs), as fluorescent nanomaterials based on carbon, have gained significant interest in several optical applications because of their small size and properties, such as high chemical stability, excellent water solubility, low cost, and interesting optical properties. In fact, recently relevant application of quantum dots gained attention due to the announcement of the Nobel Prize in chemistry in 2023, by the discovery and the development of quantum dots. Which have applications in nanotechnology as light sources of televisions and LED lamps, and can also guide surgeons when they remove tumor tissue, among many other things. The photoluminescent properties of carbon dots present clear opportunities in the context of sensing applications.

Then, the main issue of this work is to investigate how the combination of synthetic method and the modification of the starting material affected the nature and fluorescence properties of CDs and consequently their ability to sense cations and or

anions. Modifications of the starting material were performed using diethylenetriamine, ethylenediamine and L-Cysteine as heteroatom-doped. Interestingly, select doped agents helps to increase the response of CDs to specific cations as Fe(III) and Pb(II) (Figure 1).

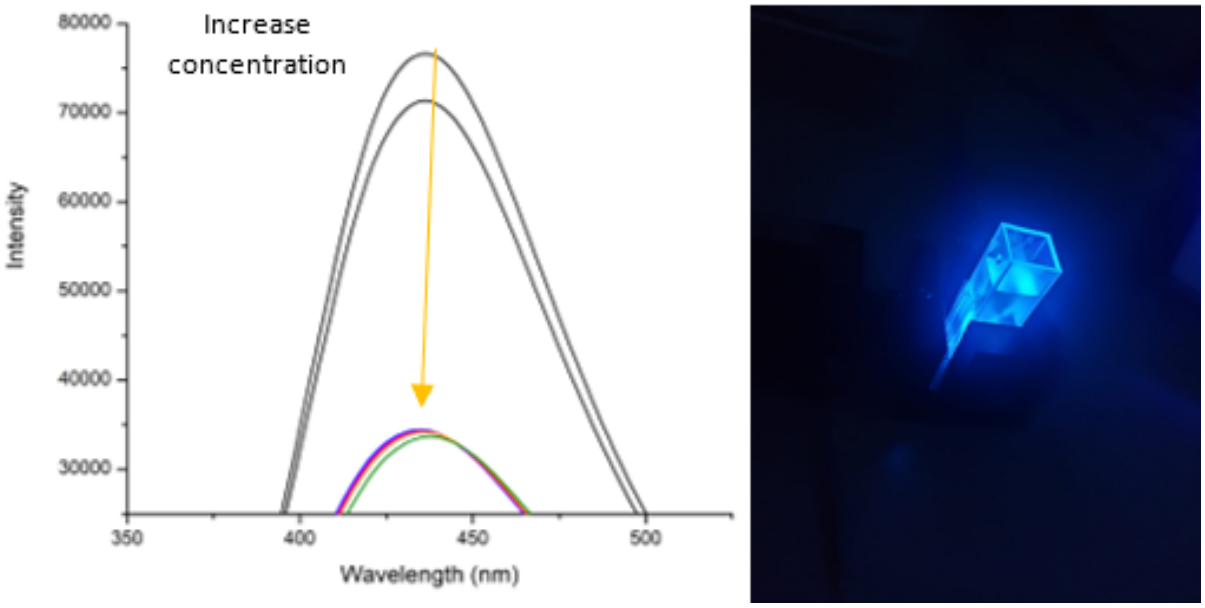

Figure 1: **The change of fluorescence of CDs L-cystein solution with different lead concentrations.**

References

[1] M. I. Lone, Z. L. He, P. J. Stoffella, and X. E. Yang, "Phytoremediation of heavy metal polluted soils and water: Progresses and perspectives," Journal of Zhejiang University: Science B, vol. 9, no. 3. pp. 210–220, Mar. 2008. doi: 10.1631/jzus.B0710633.

[2] Y. Xie et al., "Effect of heavy metals pollution on soil microbial diversity and bermudagrass genetic variation," Front Plant Sci, vol. 7, no. MAY2016, May 2016, doi: 10.3389/fpls.2016.00755.

[3] M. B. Gumpu, S. Sethuraman, U. M. Krishnan, and J. B. B. Rayappan, "A review on detection of heavy metal ions in water - An electrochemical approach," Sensors and Actuators, B: Chemical, vol. 213. Elsevier B.V., pp. 515–533, Jul. 05, 2015. doi: 10.1016/j.snb.2015.02.122.

Friday

Acta Microscopica Vol. 34, Supp. 2, 2025
Abstract Book NSSY 2024 - Galapagos 19-25 May, 2024

Density Functional Theory: a crash course

Vincent Meunier[1]

[1] *Engineering Science and Mechanics Department, The Pennsylvania State University*

vincent.meunier@psu.edu

Abstract

This tutorial talk on Density Functional Theory (DFT) provides an accessible and comprehensive introduction to a pivotal method in the computational modeling of electronic structures in physics and chemistry. DFT is celebrated for its unique blend of accuracy and computational efficiency, making it indispensable for studying the electronic properties of atoms, molecules, and solids. The talk begins with a historical overview, tracing DFT's development from quantum mechanical principles to its current prominence. It then dives into the theoretical underpinnings, including the Hohenberg-Kohn theorems, which establish the ground-state energy of a system as a functional of the electron density, and the Kohn-Sham equations, which operationalize this principle for practical calculations.

The presentation aims to demystify the complex mathematics behind DFT, presenting it in an approachable manner that emphasizes intuition and physical understanding. Key concepts such as exchange-correlation functionals, the role of approximations in practical implementations, and the limitations and strengths of DFT are discussed.

This talk is designed to equip participants with a foundation in DFT, enabling them to appreciate its capabilities and to be able to understand the limitations and strength of the method.

During the optional afternoon session, I will go through illustrative examples to enable attendees see how DFT is applied to solve real-world problems in materials science, chemistry, and nanotechnology.

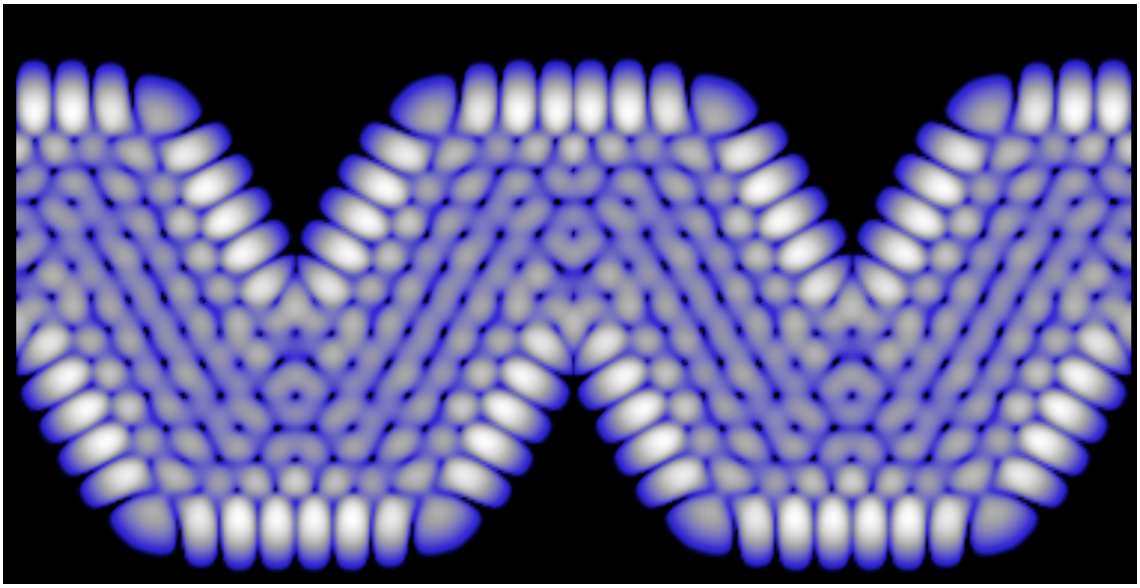

Figure 1: **Density of charge in a chevron-type carbon nanoribbon, calculated using density functional theory.**

Acta Microscopica Vol. 34, Supp. 2, 2025
Abstract Book NSSY 2024 - Galapagos 19-25 May, 2024

From Bio to Nano - New methods for producing carbon nanostructures.

Julio C. Chacón-Torres[1], M. Daniela Serrano-Larrea, Andrea C. Landázuri

[1] *School of Physical Sciences and Nanotechnology, Yachay Tech University, Urcuquí 100119, Ecuador*

[2] *Chemical Engineering Department, Applied Circular Engineering & Simulation Group (GICAS), Universidad San Francisco de Quito USFQ, Diego de Robles y Vía Interoceánica, P.O. Box 17-0901, Quito, Ecuador.*

jchacon@yachaytech.edu.ec

Abstract

"The evolution of green synthesis methods for the obtention of carbon-based nanomaterials has led to a novel research line that aims to recover waste biomaterials for a second use as advanced carbon nanostructures. A circular economy is a key factor in Latin America and developing countries, which is why optimizing the recovery of valuable biomaterials is crucial. For instance, biomaterials contain high amounts of cellulose, starch, lignin, and polysaccharides with a high carbon yield (¿50 weight percent). These biomaterials can be used as natural and inexpensive precursors for generating carbon nanomaterials through the correct physicochemical treatment and processing. These carbon nanomaterials have been categorized into hydrochars, biochars, hard carbon, and carbon fibers based on their nanostructural properties, which include porosity, crystallinity, morphology, functionalization, and dispersion ability. The uniqueness of these nanostructures can only be revealed through non-destructive characterization techniques that reveal their intrinsic structural fingerprint.

Here, I will summarize the fundamental factors to consider when treating biomaterials for the synthesis of carbon nanostructures. I will show three main advanced nanostructures obtained from organic biomolecules: hard carbon, hydrochars, and graphene. I will present their structural differences as observed when comparing their Raman spectra, whose main vibrations reveal inherent crystallinity and functionalization patterns. These observed characteristics were confirmed through the use of X-ray photoelectron spectroscopy (XPS) and X-ray diffraction (XRD) analyses. Finally, through electron microscopy techniques, the porosity and complex three-, and two-dimensional crystalline structures have been unveiled confirming a potential novel route for the synthesis of advanced carbon nanostructures based on biomaterials."

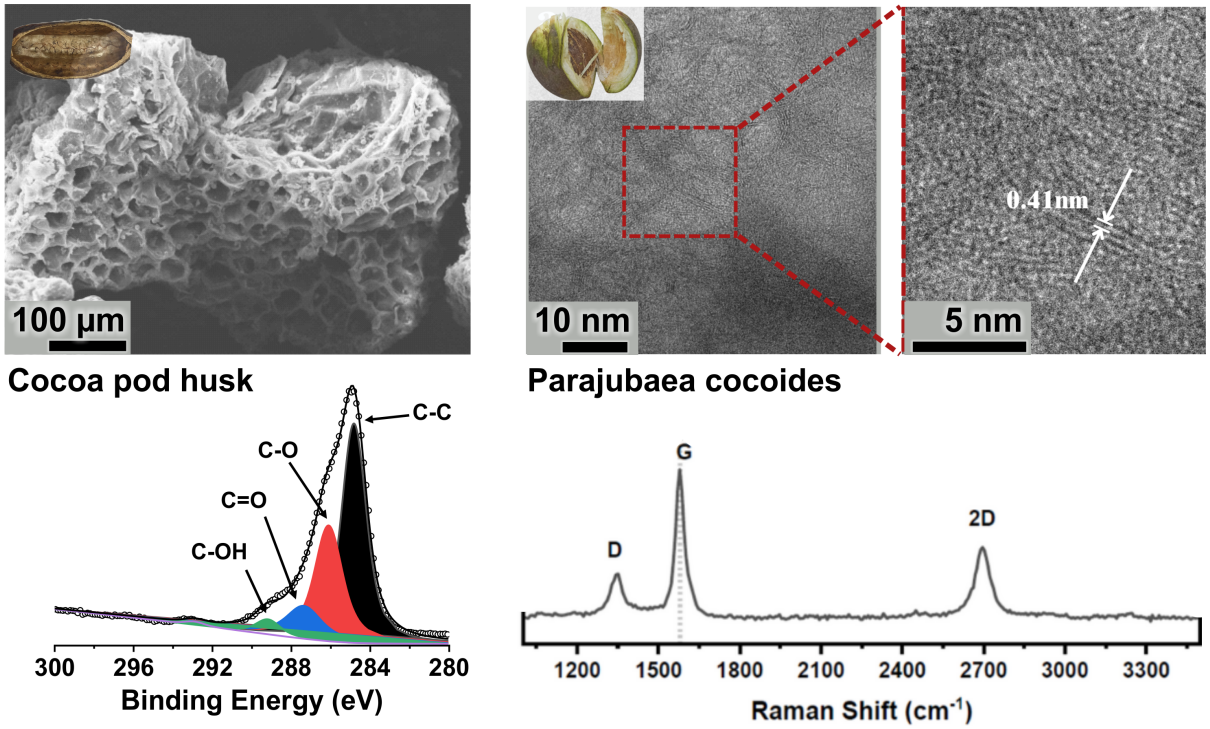

Figure 1: **Microscopic SEM image from hydrochars obtained from the cocoa pod husk confirmed by a C-OH feature within the C1s spectrum. Microscopic TEM image from hard carbon obtained from a parajubaea cocoides confirmed by a graphitic Raman spectrum with interplanar distances of around 0.4 nm.**

Acta Microscopica Vol. 34, Supp. 2, 2025
Abstract Book NSSY 2024 - Galapagos 19-25 May, 2024

β-casein nanostructures as a natural platform for cancer targeting

Garaiová Zuzana[1], Kráľová Isabel[1], Šubjaková Veronika[1], Zvarík Milan[1], Velísková Martina[1], Hianik Tibor[1]

[1] *Department of Nuclear Physics and Biophysics, Faculty of Mathematics, Physics and Informatics, Comenius University, Bratislava, Slovakia*

garaiova.zuzana7@gmail.com

Abstract

β-casein (β-CN) represent a promising platform having the potential to function as a natural drug delivery system [1]. The amphiphilic structure of β-CN self-assemble into micellar structures with a hydrophobic internal environment capable of solubilizing hydrophobic compounds in aqueous solution.

Curcumin is a compound occurring naturally in rhizomes of turmeric plant (Curcuma longa L.) that has been studied for its potential anti-cancer properties as well as for enhancing its low water solubility with the help of nanocarriers.

Research in the field of cancer treatments focuses on the application of highly specialized aptamer-based drug delivery systems. Aptamers are short nucleic acid sequences which can fold into the unique structure and bind targets, e.g. oncomarker receptors, with high affinity and specificity [3]. More importantly, funcionaliztion of β-casein structures with aptamers has not been studied in sufficient details so far.

In this work, within the project VEGA1/0554/23, we focused on studying the interaction of β-casein with 1) curcumin, 2) sgc8c DNA aptamers fluorescently labeled (Atto542) and conjugated with a cholesteryl-TEG linker (Chol-sgc8c-Atto542), that specifically bind to protein tyrosine kinase 7 (PTK7), which is highly expressed in the membranes of the leukemic cells [4].

β-casein micelles were prepred from β-casein (2 mg/ml) in sodium-phosphate buffer (10 mmol/l, pH 7). The filtered micelles were incubated with curcumin (50μM dissolved in ethanol) or with aptamers (2 μmol/l) under constant stirring for 2h at laboratory temperature (approx. 20 oC). The prepared formulations were analyzed by UV-VIS, fluorescence spectrophotometry and size exclusion chromatography.

1)β-CM interacted with curcumin, its solubilization has been demonstrated by several complementary methods, including visual observation.

2)β-CM interacted with Chol-sgc8c-Atto542 aptamers. The fluorescent signal corresponding to shorter elution time of β-casein decreased for the complexed sample of β-casein + Chol-sgc8c-Atto 542, and the fluorescence signal from the aptamer

was partly shifted to this region. Obtained results suggest potential of β-CN micelles to encapsulate curcumin and functionalization with cholesteryl-aptamers.

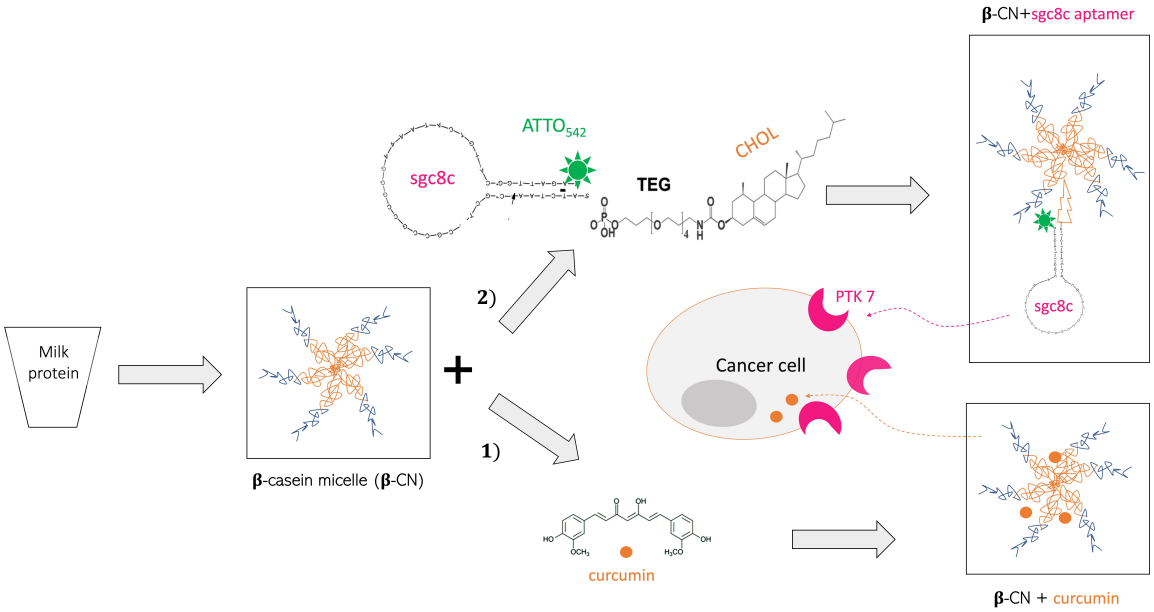

Figure 1: **Schematic representation of β-casein micelle modified by 1) curcumin and 2) sgc8c DNA aptamers fluorescently labeled (Atto542) and conjugated with a cholesteryl-TEG linker (Chol-sgc8c-Atto542), that specifically bind to protein tyrosine kinase 7 (PTK7), which is highly expressed in the membranes of the leukemic cells.**

References

[1] Li, M. et al. Food Hydrocolloids (2019) (96) (653-662).

[2] Fu, Z. et al. Int. J. of Molec. Sci. (2020) (21(23)) (9123)

[3] Poturnayová, A. et al. Chemphyschem (2019) (20(4)) (545-554).

Acta Microscopica Vol. 34, Supp. 2, 2025
Abstract Book NSSY 2024 - Galapagos 19-25 May, 2024

Clinical research and botanic medicine: The journey from the conception of an idea up to the birth of a new product. A history before and beyond

Gabriela M. Castillo B.[1], Jaroslav Trávnik[2]
[1] *Clinical Data Science Department. Premier Research s.r.o.*
[2] *Travnicek produkty -Ing. Jaroslav Trávnik. Slovakia*
Gabriela.Castillo@premier-research.com

Abstract

Historically, the evolution of clinical research goes over a long and fascinating path, moving from dietary therapy, legumes and lemons to drugs. As an anecdotic discovery, we can recall the crucial role that natural remedies shared by most of the world's cultures had in the current development of clinical trials and drugs. These remedies have either with the times become embedded in current holistic medical paradigms, been determined to be unsafe or ineffective and abandoned, or been consumed into more modern clinical practices [Barrett J.S. (2022) Fundamentals of drug development. The History of Drug Development, John Wiley & Sons, pp 5].

The born of a new pharmaceutical drug, biological product or medical device starts with the discovering by design, accidentally, or can be obtained when a company or institution applies for a patent. It could be also the result of the characterization in preclinical studies, or the outcome of a clinical development plan. Each study in a clinical development program addresses one or more research questions which suggest how the study needs to be designed. Each trial has also a specific timeline and purpose and this purpose changes as a clinical development program proceeds (Fig. 1). Clinical trials build upon the knowledge gained in the nonclinical development programs and on data from preceding trials. After basic approach of clinical trial was described in 18th century, true efforts were made to refine the design and statistical aspects. These were followed by changes in regulatory and ethics settings [Bhatt A. Perspect. Clin. Res. (2010) (1) (6)].

Premier Research is a global clinical research organization dedicated to helping top innovators turn big ideas into life-changing treatments from benchtop to bedside. The company target working area is divided into the following fields: Haematology-oncology, Neuroscience, Specialty areas (rare disease, pediatrics, dermatology, women's health, general medicine), MedTech (medical device, diagnostics, digital therapeutics) and Consulting (strategic development). An example

of an innovative project is the Canary speech's vocal biomarker technology developed by one customer which unlocks voice as a vital sign, leading a new era of machine learning in healthcare. Some other examples of recently successfully projects developed in collaboration by Premier Research are the following: A phase 2 vitiligo study project, and a project about an oral liquid formulation for recovery after gastrointestinal surgery.

Alternatively, there is another approach to develop a product intended to be a supportive or complementary treatment using natural ingredients. This is the example of small start-ups or family companies working within the field of marketing of botanicals in foods and supplements. In most of the cases, the path to be followed is different as those drugs or devices that saw the light under the directives governing classical drug development. However, scientific research about medicinal properties of the botanical foods, regulations, guidelines, and ethical concerns are an interesting topic of convergence on this approach as well. To illustrate this scenario with an example, I would like to present the case of a small company based in Slovakia- Travnicek products, which is dedicated to manufacturing creams, tinctures and essential oils using dragon's blood-sangre de drago (Croton lechleri) resin from Ecuadorian rainforest as basis material in combination with other plants known for having healing properties [Sánchez García, M., Quilumbango Grijalva, C. (2021). Anticancer Secondary Metabolites Found in Native Ecuadorian Plant Species Uncaria tomentosa DC. (Rubiaceae), Croton lechleri Müll. Arg. (Euphorbiaceae), and Equisetum giganteum L. (Equisetaceae). Springer, Cham, pp 377].

Marketing of botanicals in foods and food supplements in the European Union (EU) is subject to several provisions of food law, which cover aspects of safety, production, labelling and product composition, including the use of additives and maximum levels of contaminants and residues (i.e. Directive 2004/24/EC).

The fulfilment of such requirements brings to the light interesting opportunities for the Academy and the scientific community to initiate collaboration projects with this kind of companies. Studies about levels of contamination and residues present in the natural raw materials, as well as samples characterization and optimization of the methods of extraction are crucial for an adequate development of such botanic products, or in a near future for the participation of such product on a clinical trial. An example as such initiative is the analyzed sample of a mixture of cannabis (produced in Slovakia by Travnicek products) and croton lechleri resin (originally from Ecuador), which showed an enhanced profile of cannabinols and terpenoid compounds (Fig 2.). These findings could be studied in detail to bring out further insights about the improvement of medicinal properties of both plant and resin, precisely due to its combination.

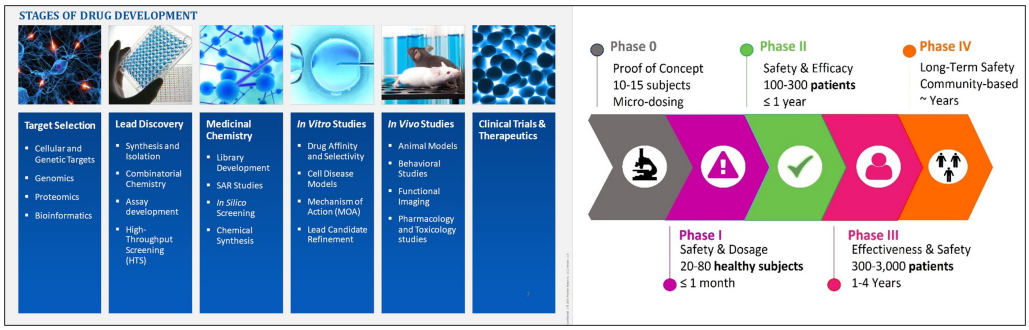

Figure 1: **Drug discovery process. Left: Stages of drug development. Right: Clinical trials phase stages. Taken from Premier Research LLC 2014, version 1.0 (SharePoint portal).**

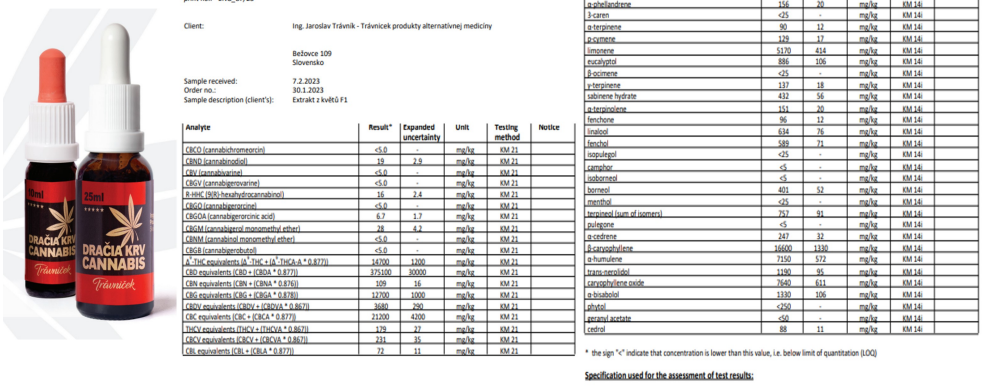

Figure 2: **Extract from the analytical composition of a sample containing croton lechleri (sangre de drago) resin and cannabis extract produced by Travnicek products done at Department of Chemistry and Analysis, Institute of Chemical Technology, Prague under supervision of Prof. Dr. Jana Hajšlová.**

References

[1] Bhatt A. Perspect. Clin. Res. (2010) (1) (6).

[2] Barrett J.S. (2022) Fundamentals of drug development. The History of Drug Development, John Wiley & Sons, pp 5.

[3] Sánchez García, M., Quilumbango Grijalva, C. (2021). Anticancer Secondary Metabolites Found in Native Ecuadorian Plant Species Uncaria tomentosa DC. (Rubiaceae), Croton lechleri Müll. Arg. (Euphorbiaceae), and Equisetum giganteum L. (Equisetaceae). Springer, Cham, pp 377.

Acta Microscopica Vol. 34, Supp. 2, 2025
Abstract Book NSSY 2024 - Galapagos 19-25 May, 2024

The Past and Future of Carbon Science and Technology

Mauricio Terrones[1]

[1] *Department of Physics, Department of Chemistry, Department of Materials Science and Engineering and Center for 2-Dimensional & Layered Materials. The Pennsylvania State University, University Park, Pennsylvania 16802, USA.*

mut11@psu.edu

Abstract

First, we will give a general historical introduction of Carbon Science and Technology with emphasis in Nanoscience and the impact of great Carbon scientists. We will then provide an overview of current research challenges and trends in carbon science. One of the objectives of this talk is to motivate carbons scientists to discover and synthesize novel materials with unprecedented properties, and to fabricate novel functional devices. In particular, materials with different hybridization states will be discussed. These include 1) sp linear carbon chains, 2) sp2-graphene nanoribbons, 3) sp3-low-dimensional systems (flexible diamonds), and 4) three-dimensional (3D) graphene-based structures that are highly conducting, very robust and can operate at temperatures ranging from 77K to 1173K.

We will also discuss the synthesis of carbon nanotubes and nanotube networks using different dopants during chemical vapor deposition (CVD). In particular, the effects of sulfur, boron and nitrogen during growth will be summarized. It will be demonstrated that it is indeed possible to assemble novel micro-fluidic devices using nitrogen doped aligned carbon nanotubes. These devices can be used to trap and enrich human and animal viruses that could be then identified using genomic sequencing and Raman spectroscopy. This enrichment method coupled to Raman virus identification constitutes an innovative system that could be used to quickly track and monitor viral outbreaks in real-time.

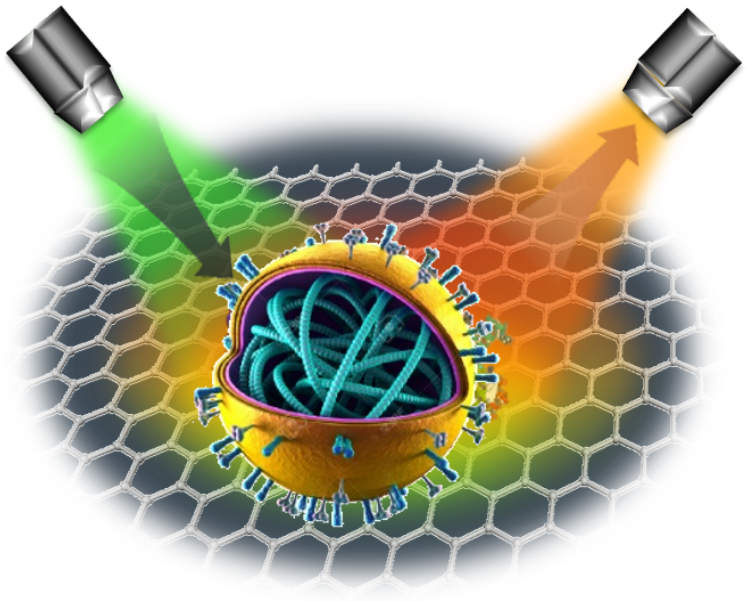

Figure 1: **Image representing a virus that is being studied under Raman spectroscopy.**

References

[1] Y.-T. Yeh, Y. Tang, A. Sebastian, A. Dasgupta, N. Perea-Lopez, I. Albert, H. Lu, M. Terrones, S.-Y. Zheng. (2016) "Tunable and Label-Free Virus Enrichment for Ultra-sensitive Virus Detection Using Carbon Nanotube Arrays". Science Advances 2: e1601026.

[2] Y.-T Yeh, K. Gulino, Y. Zhang, A. Sabestien, T.-W. Chou, B. Zhou, Z. Lin, I. Albert, H. Lu, V. Swaminathan, E. Ghedin, M. Terrones, M. (2020) "A rapid and label-free platform for virus capture and identification from clinical samples". Proceedings of the National Academy of Sciences (PNAS) 117, 895-901.

[3] J. Ye, M. Terrones, et. al. (2022). "Accurate virus identification with interpretable Raman signatures by machine learning". Proceedings of the National Academy of Sciences 119 (23), e2118836119.

Acta Microscopica Vol. 34, Supp. 2, 2025
Abstract Book NSSY 2024 - Galapagos 19-25 May, 2024

Stable BDD-based photoanodes for the degradation of emerging contaminants and microplastics by photoelectrochemistry.

Patricio J. Espinoza-Montero[1]

[1] *Escuela de Ciencias Químicas, Pontificia Universidad Católica del Ecuador, Quito 170525, Ecuador.*

pespinoza646@puce.edu.ec

Abstract

The need for new clean technologies (chemically green) for the treatment of water contaminated with recalcitrant compounds (pesticides, herbicides, antibiotics, drugs, microplastics, etc.) has gained momentum in recent years, including photoelectrocatalysis (PEC). PEC belongs to the advanced oxidation processes, which are capable of degrading persistent organic matter and inactivating microorganisms through reactive oxygen species (ROS) generated by the microorganisms. PEC can be divided into the following stages: i) light is absorbed on a crystal-lattice, photocatalytic thin film supported on a conductive substrate (photoelectrode) (light energy ¿ photocatalyst band gap), generating electron-hole charge carriers (e-/h+); ii) e- is extracted from the photoanode's conduction band minima (CBM) through external circuit, applying an external bias potential to avoid recombination and making h+ available; iii) h+ -mediated redox reactions occur (h+ are expected to have enough energy to oxidize water to form hydroxyl radicals (OH) or oxidize organic matter directly) [1].This lecture will address the preparation of photoanodes based in TiO2 on boron-doped diamond (BDD), their characterization and their application in the degradation of diclofenac, glyphosate and microplastics. In addition, the long-term stability of this photoanode will be presented [2,3].

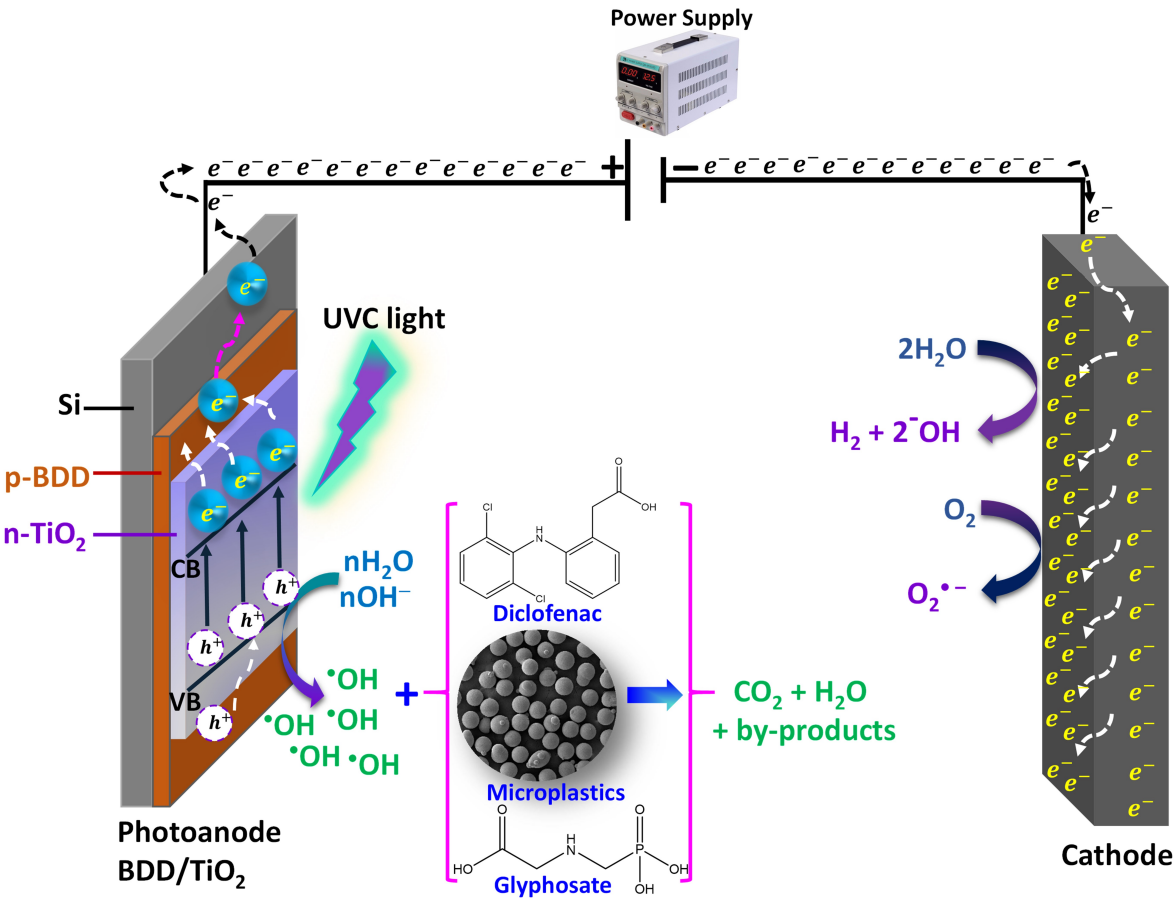

Figure 1: **Photoelectrocatalysis process**

References

[1] Quilumbaquin, W., Castillo-Cabrera, G. X., Borrero-González, L. J., Mora, J., Valle, V., Debut, A., ... & Espinoza-Montero, P. J. (2024). Photoelectrocatalytic degradation of high-density polyethylene microplastics on TiO2-modified boron-doped diamond photoanode. iScience, e 27, 109192.

[2] Alulema-Pullupaxi, P., Fernández, L., Debut, A., Santacruz, C. P., Villacis, W., Fierro, C., & Espinoza-Montero, P. J. (2021). Photoelectrocatalytic degradation of glyphosate on titanium dioxide synthesized by sol-gel/spin-coating on boron doped diamond (TiO2/BDD) as a photoanode. Chemosphere, 278, 130488.

[3] Sigcha-Pallo, C., Peralta-Hernández, J. M., Alulema-Pullupaxi, P., Carrera, P., Fernández, L., Pozo, P., & Espinoza-Montero, P. J. (2022). Photoelectrocatalytic degradation of diclofenac with a boron-doped diamond electrode modified with titanium dioxide as a photoanode. Environmental Research, 212, 113362.

Acta Microscopica Vol. 34, Supp. 2, 2025
Abstract Book NSSY 2024 - Galapagos 19-25 May, 2024

Highly specific peptide-nanoparticle conjugates towards HeLa and MDA-MB-231 cancer cells.

Verónica Quilumba-Dutan[1], Clara Carreón-Álvarez[2], Sergio Hidalgo-Figueroa[3], Rubén López-Revilla[3], Eugenia Valsami-Jones[4], Swaroop Chakraborty[4], José Luis Rodríguez-López[1]

[1] *Instituto Potosino de Investigación Científica y Tecnológica. Advanced Materials Department*

[2] *Universidad de Guadalajara. Departamento de Ciencias Naturales y Exactas*

[3] *Instituto Potosino de Investigación Científica y Tecnológica. Molecular Biology Department*

[4] *University of Birmingham. School of Geography, Earth, and Environmental Sciences*

veronica.quilumba22@gmail.com

Abstract

Breast and cervical cancer are the most diagnosed and the major causes of cancer cases and deaths in women (Sung et al., 2021). Cancer treatments include surgical tumor resection complemented by radiotherapy and/or chemotherapy. However, surgery is contraindicated to remove small tumors and complementary methods usually have limited therapeutic effects and severe side effects due to their low specificity. (Debela et al., 2021). Current research efforts aim to identify ligands targeting cancer-specific biomarkers to improve therapeutic selectivity for efficient and safer cancer treatments. Peptides stand out as candidates for targeted therapy due to their high specificity and ability to bind to sites where small molecules cannot, low immunogenicity, rapid tissue penetration, stability at room temperature, ease of synthesis, lower manufacturing costs, and their potential application as peptide-drug conjugates or imaging agents, particularly for cancer treatment (Fu et al., 2023). For this reason, this work aimed to isolate peptides with high affinity to cell-surface proteins of the MDA-MB-231 (MDA) breast cancer cell line and the HeLa cervical cancer cell line combining the phage display technology and the in silico method of molecular docking to improve the specificity of photothermal multibranched gold nanoparticles (MBAuNPs) towards cancer cells. For this purpose, we isolated 44 phage clones displaying high-affinity peptides to the surface of MDA and/or HeLa cells, from an M13KE 12-mer peptide phage-display library. Through a systematic review, we identified a set of plasma membrane proteins overexpressed in breast and cervical cancer cells. Via a virtual screening, we explored the molecular interaction between the 44 isolated peptide sequences and selected biomarkers, and we quantified this interaction using energy-scoring functions based on the Amber force field to obtain a ranking of the most specific ligands. Results showed that six sequences, from the set of 44 peptides, appeared repeatedly during

the screening in HeLa (2 sequences) and MDA (4 sequences) cells. Three consensus sequences were also identified, CS1 in HeLa, and CS2 and CS3 in MDA, and a shared sequence appeared screened in both cell lines. These results suggested that these sequences have more affinity to receptors on the surface of the cells. On the other hand, Annexin A2, Epidermal growth factor receptor, CD44, CD146, and Integrin alpha V were identified as potential biomarkers in Hela cells, as well as Vimentin, Annexin A1, Annexin A5, and Galectin-1 in MDA cells. Results obtained from the virtual screening, and after the visualization of the conformational modes, suggested that the interactions with peptide ligands occurred mostly with the CD44 biomarker in HeLa and the Annexin A5 biomarker in MDA, which was corroborated by the quantification of the ligand-receptor interaction. Finally, the peptides with the highest affinity to specific cell-surface proteins will be synthesized to create a peptide-nanoparticle conjugated system (MBAuNPs-Pep12) and the cytotoxic profile will be evaluated to establish their potential use in multimodal treatment against breast and cervical cancer

References

[1] Sung H. et al. CA: a cancer journal for clinicians. (2021) (71) (209-249)

[2] Debela D. et al. SAGE open medicine. (2021) (9)

[3] Fu C. et al. Acta pharmaceutica Sinica. B (2023) (13) (498–516)

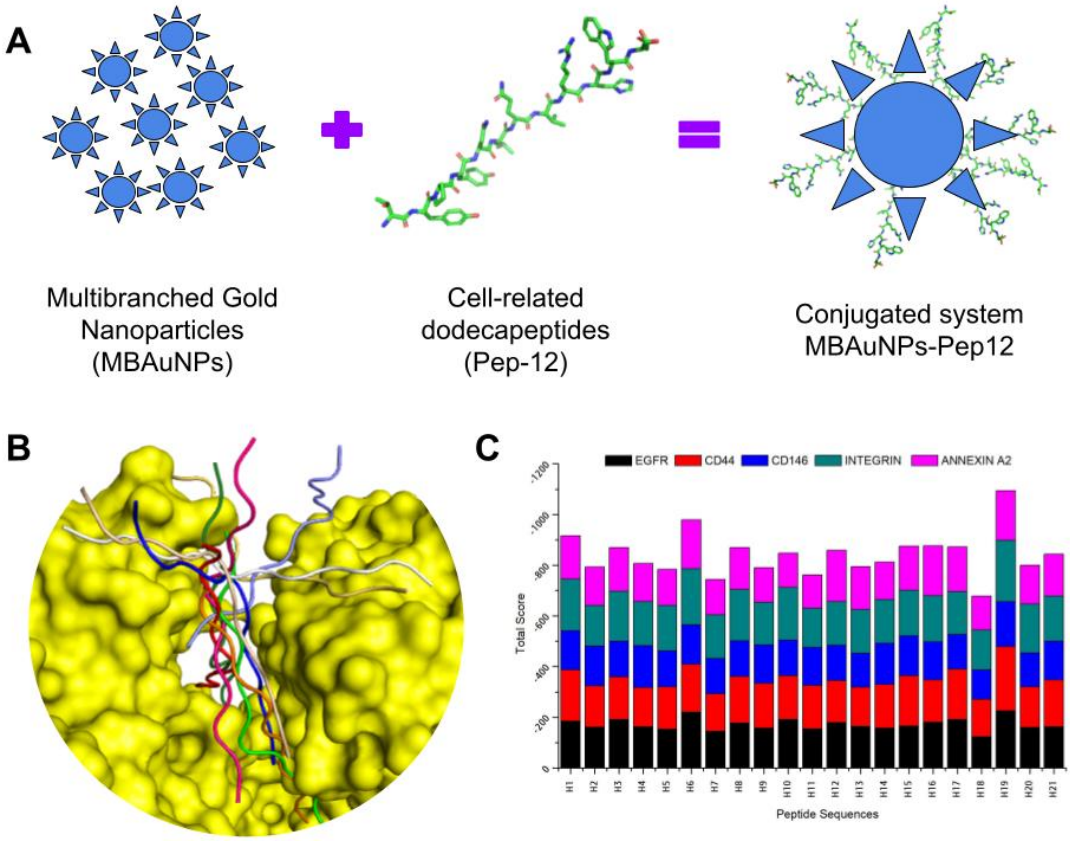

Figure 1: **Graphical abstract of the work. A. Hypothetical diagram of the nanostructured system MBAuNPs-Pep12 and its constituents. B. Different conformational modes were obtained after the virtual screening between an overexpressed biomarker (in yellow) found on the plasma membrane of HeLa cells and a specific peptide (in colors) obtained using phage display technology. The conformational modes show the most probable ways in which a single peptide interacts with the biomarker. This interaction can be quantified using energy score functions. C. Total scores obtained after molecular docking between 21 peptides screened using HeLa cells and overexpressed biomarkers in HeLa cells. The scores quantify the ligand-receptor interaction.**

Acta Microscopica Vol. 34, Supp. 2, 2025
Abstract Book NSSY 2024 - Galapagos 19-25 May, 2024

Monday

Poster Session

Acta Microscopica Vol. 34, Supp. 2, 2025
Abstract Book NSSY 2024 - Galapagos 19-25 May, 2024

Nanodiamond-doped biopolymer electrolytes for enhanced performance in zinc-air batteries

Juan Carlos Vallejo Jurado[1], María Fernanda Bósquez-Cáceres[1,2], Vivian Morera[1], Lorena Álvarez-Contreras[3], Juan P. Tafur[4]

[1] *School of Chemical Sciences and Engineering, Yachay Tech University, Urcuquí 100119, Ecuador*

[2] *School of Physical Sciences and Nanotechnology, Yachay Tech University, Urcuquí 100119, Ecuador*

[3] *Centro de Investigación en Materiales Avanzados S. C., Complejo Industrial Chihuahua, Chihuahua C. P. 31136, México*

[4] *Departamento de Ingeniería Mecánica, Química y Diseño Industrial, Escuela Técnica Superior de Ingeniería y Diseño Industrial (ETSIDI), Universidad Politécnica de Madrid (UPM), Ronda de Valencia 3, 28012 Madrid, Spain*

juan.vallejo@yachaytech.edu.ec

Abstract

Zinc-air batteries (ZABs) have garnered significant attention as viable energy storage solutions across diverse applications. These batteries utilize zinc as the negative metal electrode and an air-breathing positive electrode, capitalizing on the inherent safety, cost-effectiveness, and widespread availability of zinc [1]. To advance ZAB prototypes for scalable commercial use, a crucial element is the selection of an electrolyte that is cost-effective, environmentally friendly, exhibits low toxicity, nonflammability, a large stable potential window, and the capacity to deliver high specific energy and ionic conductivity values. Biopolymers emerge as promising candidates for electrolytes due to their inherent qualities such as high flexibility, commendable performance, cost-effectiveness, compatibility with solvents, and film-forming ability. Specifically, the combination of Chitosan (CS) and carboxymethylcellulose (CMC), employing a cross-linker like citric acid, can yield intermolecular complexes, leading to hydrogels with the ability to absorb ionic solutions such as a KOH solution. Nanocomposite polymer electrolytes (NCPEs) are gaining interest in electrochemical devices due to the advantages offered by dispersed fillers. These nanocomposites can establish space charge regions, induce local electric fields, and enhance amorphousness, thereby achieving higher ionic conductivity by minimizing impediments to ion passage [2]. In the pursuit of improved ionic conductivity, the choice of nanoparticles becomes essential in ensuring compatibility with the desired electrolyte characteristics. Nanodiamonds (NDs) arise as a promising option, leveraging their superior mechanical and thermal properties, rich surface chemistry, and biocompatibility, making them an excellent filler material for composites. This research proposes the synthesis of CS-CMC membranes

doped with diamond nanoparticles (NDs) to produce a biocompatible electrolyte for ZAB manufacturing. The primary objective is to assess the electrochemical and structural impacts of NDs on hydrogel performance when applied as electrolytes for energy storage devices. Characterization through ATR-FTIR, XRD, TGA, and electrochemical tests reveals that the addition of diamond nanoparticles enhances ionic conductivity. However, at weight percentages of 2% and 4% NDs, detrimental effects are observed in both ionic conductivity and electrochemical stability. This is attributed to a low ND dispersion and accumulation hindering ion passage and weak zone generation compromising stability. Optimal results are achieved at 0.5% to 1.5% weight percentage, with the highest ionic conductivity observed at 1% wt of NDs (0.527 S cm-1). The relationship between ionic conductivity values and the percentage of KOH 12M ionic solution absorption is graphically depicted in Figure 1. Comparisons with previous works indicate a similar behavior, with these nanocomposite biopolymer electrolytes showcasing crucial attributes for zinc or magnesium-based batteries, potentially finding applications in rechargeable cells. The use of such biopolymer electrolytes holds promise for advancing green technologies, steering away from non-biodegradable, toxic materials prevalent in current commercial batteries.

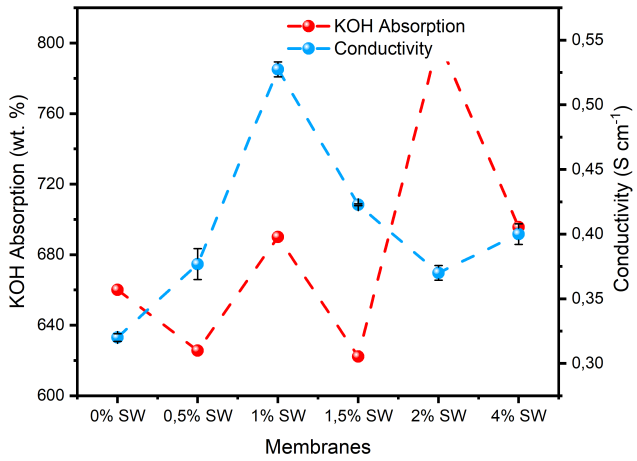

Figure 1: **Relationship between the ionic conductivity values and the percentage of absorption of 12M KOH solution of hydrogels at different NDs content.**

References

[1] Cruz-Balaz, María I., et al. "Synthesis and characterization of Chitosan-Avocado seed starch hydrogels as electrolytes for zinc-air batteries." Journal of Polymer Research 30.6 (2023): 189.

[2] Bósquez-Cáceres, María Fernanda, et al. "Nanocomposite Polymer Electrolytes for Zinc and Magnesium Batteries: From Synthetic to Biopolymers." Polymers 13.24 (2021): 4284.

Acta Microscopica Vol. 34, Supp. 2, 2025
Abstract Book NSSY 2024 - Galapagos 19-25 May, 2024

Cadmium adsorption on iron-doped biochar derives from Guadua angustifolia residues through a dual experimental and theoretical approach

Diana Ramos[1], Lola De Lima[1] , Terencio Thibault[1]
[1] *School of Chemical Sciences and Engineering, Yachay Tech.*
diana.ramos@yachaytech.edu.ec

Abstract

In the pursuit of sustainable environmental remediation solutions, the conversion of agricultural residues into functionalized biochar presents a promising avenue for the adsorption of heavy metal contaminants. This work delineates the synthesis, characterization, and application of iron-doped biochar derived from Guadua angustifolia residues for cadmium removal from aqueous solutions. Utilizing pyrolysis and hydrothermal carbonization, biochar samples were produced and subsequently doped with iron via incipient wetness impregnation to achieve various concentrations of iron. The doping process involved dissolving iron in a mixture of nitric and hydrochloric acids, followed by application to the biochar samples, which were then treated under specific conditions in a Chemical Vapor Deposition (CVD) oven to ensure uniform distribution of iron.

For the synthesis, Guadua angustifolia residues have some processes, size reduction and standardization to a specific particle size range. This preparatory step was critical for achieving consistent biochar properties and ensuring the effectiveness of subsequent doping. The hydrothermal carbonization process involved treating the biomass with phosphoric acid under controlled conditions to produce Hydrochar (HC), while Pyrochar (PC) was synthesized through pyrolysis in an inert atmosphere, reaching temperatures conducive to the structural transformation of the biomass into biochar. These synthesis methods were carefully optimized to enhance the biochar's physicochemical properties, making it an ideal candidate for iron doping and heavy metal adsorption.

The modified biochar's structural and chemical properties were analyzed through X-ray Photoelectron Spectroscopy (XPS), Raman Spectroscopy, X-ray Diffraction (XRD), and Fourier Transform Infrared Spectroscopy (FTIR). Theoretical models, complemented by Density Functional Theory (DFT) calculations, provided insights into the interaction mechanisms between the iron sites and cadmium ions, affirming the empirical findings and guiding the optimization of the biochar for enhanced heavy metal adsorption.

Experimental investigations into the cadmium adsorption capabilities of the iron-doped biochar revealed that specific iron concentrations significantly influence the adsorption efficiency. Optimal conditions for cadmium adsorption were established through systematic variation of parameters such as adsorbent dosage, initial solution pH, and initial cadmium concentration. The findings indicate that biochar samples with 0.2% and 1.3% iron content exhibit superior adsorption capacities, underscoring the role of iron in facilitating the removal of cadmium ions.

Notably, the study emphasizes that iron content exceeding 2% does not proportionally enhance the biochar's adsorption capacity, likely due to the aggregation of iron particles which may hinder effective interaction between the biochar surface and cadmium ions. This observation underscores the necessity for precise control over the doping process to optimize the material's performance for heavy metal remediation.

The research aligns with the conference themes in the development of bio-based materials for environmental applications. The integration of nanoscale modifications through iron doping and the comprehensive characterization of the resultant materials contribute to the broader discourse on advanced materials processing and characterization.

This study not only advances our understanding of biochar's potential in environmental remediation but also highlights the significance of interdisciplinary approaches in tackling pollution through innovative material science. By leveraging agricultural waste, this work contributes to the development of sustainable and efficient solutions for heavy metal removal, embodying the principles of a circular economy.

References

[1] Navas-Cárdenas, C., Caetano, M., Endara, D., Jiménez, R., Lozada, A. B., Manangón, L. E., ... & Villasana, Y. (2023). The Role of Oxygenated Functional Groups on Cadmium Removal using Pyrochar and Hydrochar Derived from Guadua angustifolia Residues. Water, 15(3), 525.

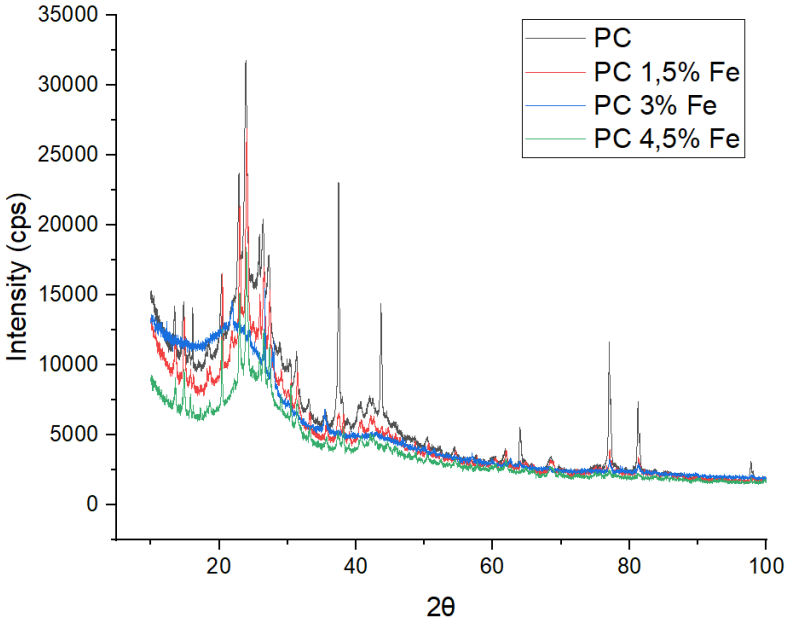

Figure 1: **XRD pattern of PC and iron doped PC samples at different concentrations.**

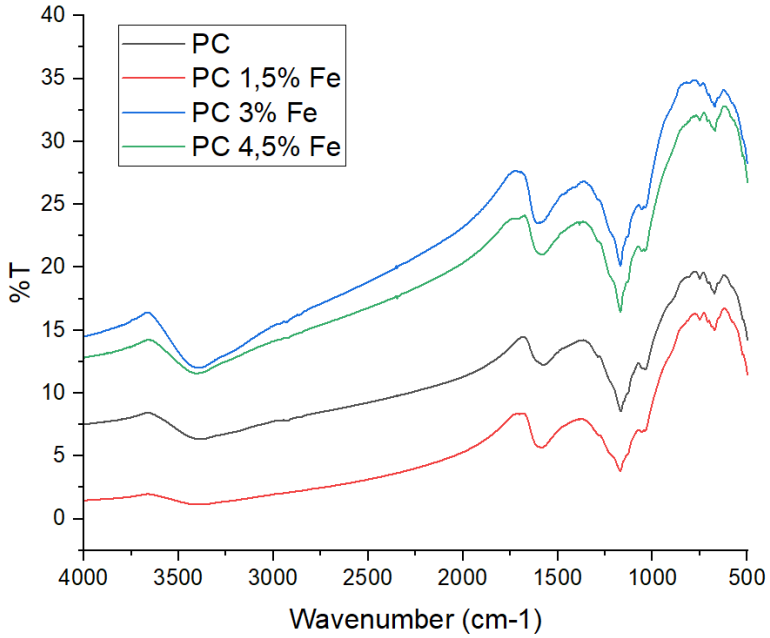

Figure 2: **FTIR pattern of PC and iron doped PC samples at different concentrations.**

Acta Microscopica Vol. 34, Supp. 2, 2025
Abstract Book NSSY 2024 - Galapagos 19-25 May, 2024

Chitosan nanoparticles as a sustainable and eco-friendly solution to enhance horticultural crops

Yara Tahìs Montalvo[1], Sandra Naranjo[1], Roxana Taco[1], Gema Gonzalez[2]

[1] *Universidad de las Fuerzas Armadas- ESPE. Department of Earth Sciences and Construction.*

[2] *School of Physical Sciences and Nanotechnology, Yachay Tech University, Urcuqui, 100119, Ecuador*

ytmontalvo@espe.edu.ec

Abstract

The challenge of increased food demand today has promoted the implementation of excessive agricultural practices in an attempt to multiply crop yield and productivity. The progressive intensification in the use of chemical fertilizers has inadvertently led to a decrease in the soil's response to these agrochemicals due to its degradation caused by the accumulation and subsequent leaching of toxic compounds and residual mineral salts left by the fertilizers (Mehta et al., 2022). On the other hand, the majority of its main components such as N (nitrogen), P (phosphorus), and K (potassium) are not fully utilized by crops as a large fraction of them disperses into the environment, resulting in environmental pollution, economic loss, and contamination (Saberi et al., 2024).

In this context, the search for efficient methodologies to ensure the effective delivery and absorption of nutrients in crops has led to the synthesis of biopolymer-based nanomaterials for use as controlled release systems for agrochemicals. Chitosan, a polycationic polysaccharide derivative of deacetylated chitin, is a natural polymer with unique properties of superabsorbency, biodegradability, and non-toxicity, making it an ideal precursor for the synthesis of chitosan nanoparticles (NPQ) as nano-carriers that enhance the stability of fertilizer components and allow for their gradual and sustained release, achieving the application of agrochemicals in low doses and with fewer treatments (Ingle et al., 2022).

This study focused on the synthesis of NPQ as a polymeric matrix for the encapsulation of NPK fertilizer used as a test fertilizer. The method applied was ionic gelation involving the ionic crosslinking of the chitosan's cationic structure with the anionic structure of a crosslinking compound, sodium tripolyphosphate (TPP), in various concentrations of NPQ/TPP with constant vigorous agitation. Subsequently, the NPK fertilizer was incorporated into a 100 ppm solution under temperature conditions of 60°C. Two types of nanoparticles were obtained: NPCS - TPP (without fertilizer) and NPCS - NPK (with fertilizer), whose characterization was carried out using Fourier-transform infrared spectroscopy (FTIR) to confirm the formation of chitosan nanoparticles and the entrapment of the fertilizer in the

polymeric matrix, in comparison to the spectrum of pure chitosan. Preliminary results showed the formation of nanoparticles with chitosan due to the similarity of the spectra. Further characterization is intended to be carried out using scanning electron microscopy to observe particle size and morphology, as well as fertilizer release analysis, water absorption capacity, and finally to evaluate the promotion of plant development.

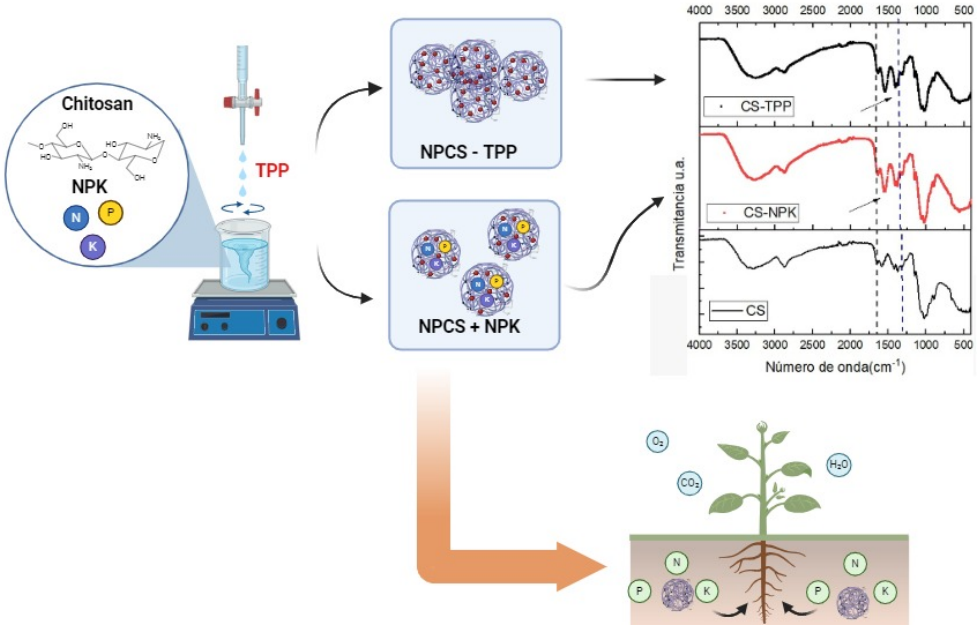

Figure 1: **Sustainable Agriculture**

References

[1] Ashraf, U., Zafar, S., Ghaffar, R., Sher, A., Mahmood, S., Noreen, Z., Maqbool, M. M., Saddique, M., & Ashraf, A. (2022). Impact of nano chitosan-NPK fertilizer on field crops. In D. S. Kumar & S. V. Madihally (Eds.), Role of Chitosan and Chitosan-Based Nanomaterials in Plant Sciences (pp. 165–183). Elsevier.

[2] Doval R., Torres S., Tenorio A.,Gómez A., Valencia A(2023).Chitosan: Properties and Its Application in Agriculture in Context of Molecular Weight. MDPI. México.Polymers 15(13), 2867; https://doi.org/10.3390/polym15132867.

[3] Ingle, P. U., Shende, S. S., Shingote, P. R., Mishra, S. S., Sarda, V., Wasule, D. L., Rajput, V. D., Minkina, T., Rai, M., Sushkova, S., Mandzhieva, S., & Gade, A. (2022). Chitosan nanoparticles (ChNPs): A versatile growth promoter in modern agricultural production. Heliyon, 8(11), e11893. https://doi.org/10.1016/j.heliyon.2022.e11893

Acta Microscopica Vol. 34, Supp. 2, 2025
Abstract Book NSSY 2024 - Galapagos 19-25 May, 2024

Super decorated carbon nanotubes grown on copper substrates by CVD

Brenda Verónica Padilla Teniente[1], Emilio Muñoz Sandoval[1], Ismailia Leilani Escalante García[2], Juan Luis Fajardo Díaz[3]

[1] *Advanced Materials Division, IPICYT, Camino a la Presa San Jose 2055, San Luis Potosí, 78216, Mexico*

[2] *Chemical Sciences Academic Unit, Autonomous University of Zacatecas, Carretera Zacatecas-Guadalajara Km. 6, Ejido la Escondida, Zacatecas, 98160, Mexico*

[3] *Global Aqua Innovation Center, Shinshu University*

brenda.padilla@ipicyt.edu.mx

Abstract

TSince their invention [1], carbon nanotubes have been widely studied in different areas of knowledge, in order to enhance their properties and also their possible applications in everyday life. This is why in this work we were able to synthesize carbon nanostructures, including carbon nanotubes, on copper substrates at different temperatures ranging from 750 °C to 950 °C, using chemical vapor deposition (CVD), that is, a total of 5 syntheses were made at different temperatures, all with the same synthesis time of 80 minutes. There are few investigations of carbon nanotubes grown directly on copper and researchers argue that the growth of carbon nanotubes is not possible without an additional thin film, however, in this work we have shown that it is possible [2]. By scanning electron microscopy we observed that as the temperature is varied the nanostructures are modified, but in all cases super-decorated growths are obtained in a single step. A Raman spectroscopy analysis is also carried out, which provides us with great information about nanostructures. Likewise, both copper and carbon nanotubes are studied to consider whether temperature affects the crystalline phases of copper and, in turn, the growth of our nanostructures. Subsequently, it is characterized in electrochemistry to study its possible applications in supercapacitors or batteries [3].

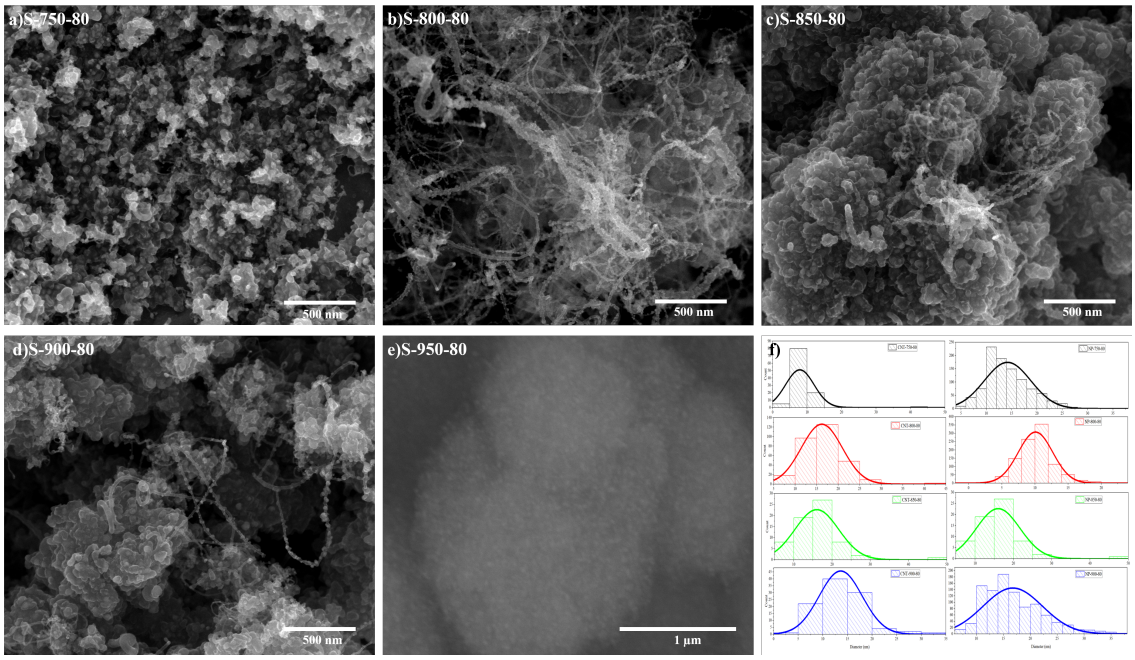

Figure 1: **SEM images at secondary electron for the five samples corresponding each temperature. a) 750 °C, b) 800 °C, c) 850 °C, d) 900 °C, e) 950 °C, f) distribution graphs of the average diameters, on the left side are the graphs for the nanotubes and on the right side are the graphs for the nanoparticles**

References

[1] S. Ijima S. Helical microtubules of graphitic carbon. Nature 354(6348), 56, 1991

[2] Atthipalli et al., 2011. Gowtam Atthipalli, Rigved Epur, Prashant N. Kumta, Mengjin Yang, Jung-Kun Lee, and Jennifer L. Gray. Nickel Catalyst-Assisted Vertical Growth of Dense Carbon Nanotube Forests on Bulk Copper. J. Phys. Chem. C 2011, 115, 3534–3538. dx.doi.org/10.1021/jp108624n

[3] Juan Luis Fajardo-Díaz et al., 2019.Fajardo-Díaz, Juan L., Durón-Torres, S.M., López-Urías, F., Muñoz-Sandoval, E., 2019. Synthesis, characterization and cyclic voltammetry studies of helical carbon nanostructures produced by thermal decomposition of ethanol on Cu-foils. Carbon 155, 469–482. https://doi.org/10.1016/j.carbon.2019.09.015

Acta Microscopica Vol. 34, Supp. 2, 2025
Abstract Book NSSY 2024 - Galapagos 19-25 May, 2024

Synthesis and physical characterization of Carbon Quantum Dots from watermelon seed towards a biological application

Puchaicela Marlene[2], Spencer Lilian[1], Chimborazo Johnny.[2]

[1] *Yachay Tech University. School of Biological Sciences and Engineering*

[2] *Yachay Tech University. School of Physical Sciences and Nanotechnology.*

marlene.puchaicela@yachaytech.edu.ec

Abstract

Carbon Quantum Dots (CQDs) have emerged as an innovative alternative for drug delivery when integrated into hydrogels intended for wound dressings. This approach leverages the exceptional properties of CQDs, such as their ability for controlled release, precise targeting, and real-time monitoring, based on their inherent biocompatibility and distinctive fluorescence. The synthesis of CQDs is a crucial process that explores various methodologies, from laser ablation to hydrothermal synthesis (1), with the latter being the simplest and most cost-effective. Green synthesis, especially using biomass like watermelon seeds, proves advantageous from economic, environmental, and technological perspectives, contributing to circular economy principles and enabling biomedical applications.

The methodology used in this work comprises four consecutive phases. In the first phase, CQDs are synthesized using the hydrothermal method (figure 1). The second phase involves physical characterization of CQDs using several techniques, including Ultraviolet-visible spectroscopy (UV-vis), scanning electron microscopy (SEM), dynamic light scattering (DLS), atomic force microscopy (AFM), Raman spectroscopy, Fourier transform infrared spectroscopy (FTIR), X-ray photoelectron spectroscopy (XPS), and fluorescence microscopy (2). In the third phase, hydrogels are prepared with Polyvinyl Alcohol Fully Hydrolyzed and Hydroxypropyl Methylcellulose. The final phase involves assays to evaluate CQDs' antimicrobial activity and cytotoxicity when used in pure form or when integrated into the mentioned hydrogels (figure 2).

The hydrothermal synthesis study revealed a 30 mg/ml concentration of CQDs. The CQDs exhibited a primarily round, almost spherical morphology, confirmed by SEM. In SEM, their size was 142 nm; however, DLS indicated a size of approximately 500 to 1000 nm. To make sense of these results, zeta potential analysis was conducted, showing a value of 2.35 mV trending towards zero, suggesting that the sizes found in both SEM and DLS are aggregations. AFM analysis was performed to confirm the size of CQDs, revealing a size of 10 nm. In Raman results, two predominant peaks were observed around 1340 and 1590, commonly attributed to

the disordered D-band and crystalline G-band, respectively. The FTIR spectrum analysis reveals the presence of various functional groups in CQDs, such as hydroxyl, amine, C-H (sp2) and C-H (sp3) bonds, carbonyl, alkene/alkyne, amide, ether, and C-O bonds. XPS confirmed the presence of Carbon, Nitrogen, and Oxygen in CQDs. Finally, fluorescence studies demonstrated high fluorescence over time in the blue range.

Regarding biological application, it was found that CQDs alone do not exhibit antimicrobial activity. On the other hand, CQDs alone and when embedded with HPMC are non-toxic at concentrations of 0.03, 0.3, and 0.5 mg/ml. Conversely, when combined with PVA, they exhibit slight toxicity. CQDs' potent photoluminescence and low cytotoxicity make them excellent candidates for hydrogel drug delivery.

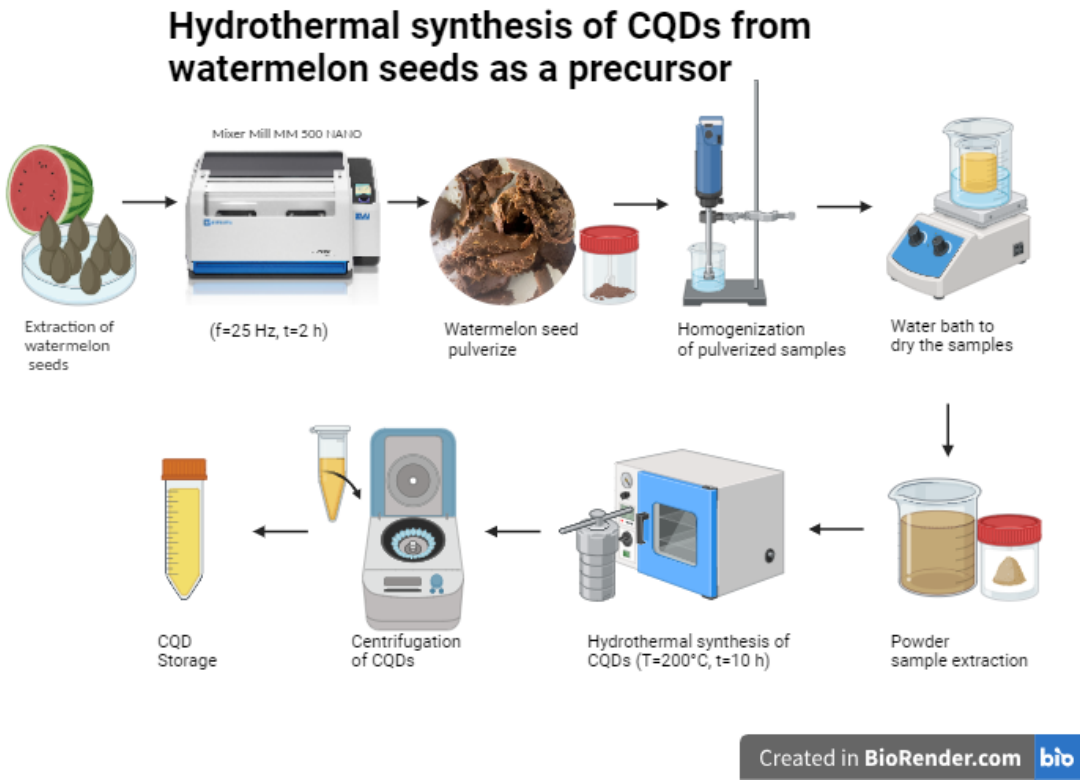

Figure 1: **Synthesis of Carbon Quantum Dots through the hydrothermal method using watermelon seeds as a precursor.**

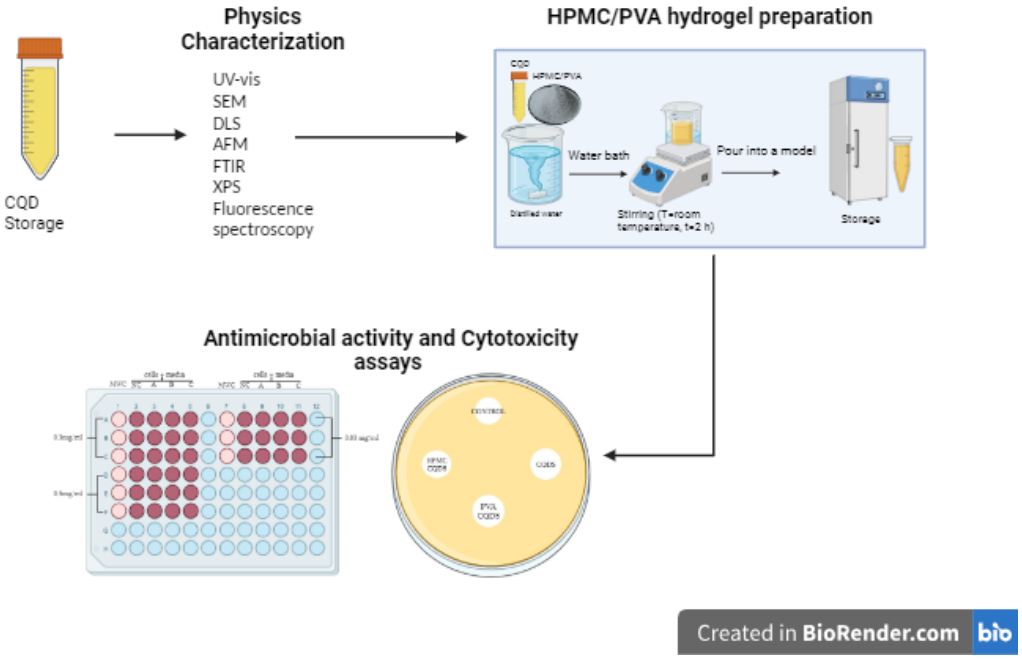

Figure 2: **The methodology used after the hydrothermal synthesis of CQDs comprises physical characterization, preparation of hydrogels, and antimicrobial activity and cytotoxicity tests.**

References

[1] Singh I. et al. J. Pharm. Sci. (2018) (15) (2)

[2] Sousa H.et al. Nanomaterials. (2021) (11) (3)

Acta Microscopica Vol. 34, Supp. 2, 2025
Abstract Book NSSY 2024 - Galapagos 19-25 May, 2024

Novel Soft Matrices for Magnetic Microwave Absorption: Plasticine-Based Composites

Daniela Abigail López Mireles[1], Joaquín de la Torre Medina[2], Armando Encinas Oropeza[1]

[1] *Instituto Potosino de Investigación Científica y Tecnológica A.C.*

[2] *Instituto de Investigaciones en materiales UNAM Unidad Morelia*

daniela.lopez@ipicyt.edu.mx

Abstract

Today, due to continued technological advancement, the increasing prevalence of electronic products and communications based stations has led to an increase in the electromagnetic radiation emitted by these devices. The widespread use of electromagnetic waves within this frequency spectrum has now emerged as a major contributor to electromagnetic interference, creating challenges and raising concerns about potential environmental impacts. In the literature we can find solutions to this issue based on materials with wave absorption properties however materials exhibiting these characteristics often present drawbacks, which include limited flexibility, high density, susceptibility to corrosion. In this work, we propose the use of moldable plasticine as a soft matrix to fabricate magnetite and nickel composites which are materials used for microwave absorption. The plasticine was mixed with the magnetic material until it was uniformly integrated in different concentrations achieving an economical synthesis and operational simplicity in addition to obtaining a material with wave absorption properties while having the mechanical properties of plasticine. The results show that the material has very good wave absorption properties in the GHz range. This study demonstrates that plasticine is a practical and cost-effective option for use as a soft matrix for specialized microwave absorbing applications.

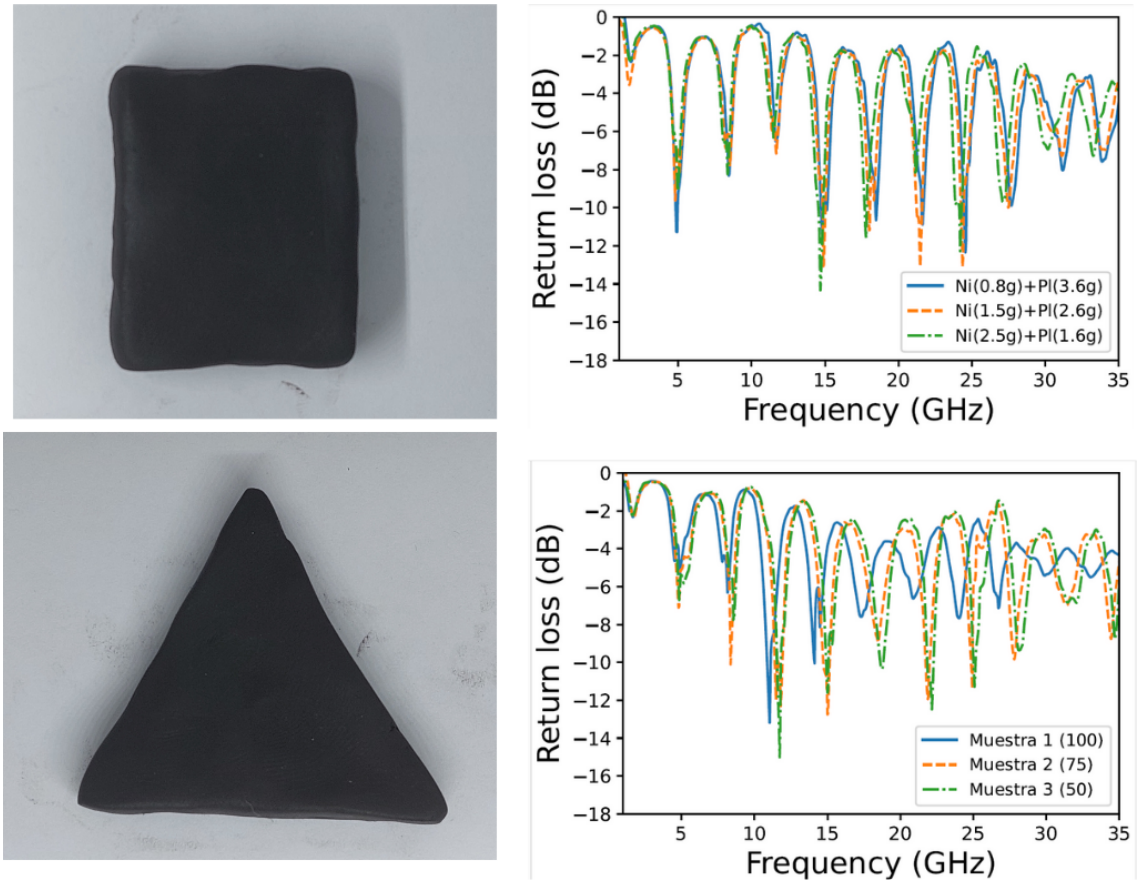

Figure 1: **The figure shows the magnetic plasticine and the curves for return loss of the sample**

References

[1] Abdul Momin, S., & Jaafar, M. (2022). High Thermal Conductivity of Plasticine-Based Nanocomposites Developed Using Simple Fabrication for Heat Management in Electronic Devices. Advanced Engineering Materials, 24(1), 2100662. https://doi.org/[DOI del artículo]

Enlarged hexagonal vertically multilayer MoS2 nanoflakes synthesized by chemical vapor deposition

Omar F. de-Leon-Ibarra[1], Juan Luis Fajardo-Díaz[2], Florentino López-Urías[1], Emilio Muñoz-Sandoval*[1]

[1] *Advanced Materials Department, IPICYT, Camino a presa San José 2055, Lomas 4a sección, San Luis Potosí, San Luis Potosí, 78216 Mexico.*

[2] *Global Aqua Innovation Center and Research Initiative for Supra-Materials, Shinshu University,* small *4-17-1 Wakasato, Nagano, 380-8553, Japan.*

omar.deleon@ipicyt.edu.mx

Abstract

MoO_3 decomposes at 800°C wholly and quickly. On the other hand, sulfur is a non-metal with a decomposition temperature around 450° C. Therefore, MoS_2 fabrication by chemical vapor deposition needs two hot zones, one for MoO_3 and the other for sulfur. Researchers regularly have also used salts as additives to improve the catalyst performance. The MoS_2 2D nanomaterials need besides complicated processes to be transferred to other substrates for characterization. In this work, a one-hot zone, no salt use, and a simple transference process for applications and characterizations have achieved the fabrication of new geometries of perpendicular MoS_2 flakes.

References

[1] N. Thomas et al., "2D MoS2: structure, mechanisms, and photocatalytic applications," Materials Today Sustainability, vol. 13, Sep. 2021, doi:10.1016/J.MTSUST.2021.100073.

[2] M. P. C. Taverne et al., "Conformal CVD-Grown MoS2 on Three-Dimensional Woodpile Photonic Crystals for Photonic Bandgap Engineering," ACS Applied Optical Materials, vol. 1, no. 5, pp. 990–996, May 2023, doi: 10.1021/ACSAOM.3C00055.

[3] A. S. Konopatsky et al., "Carbothermal-reduction-assisted CVD synthesis of layered MoS2 nanosheets on activated carbon support: Implication for photocatalysis," J Alloys Compd, vol. 934, pp. 167867–167867, Feb. 2023, doi: 10.1016/J.JALLCOM.2022.167867.

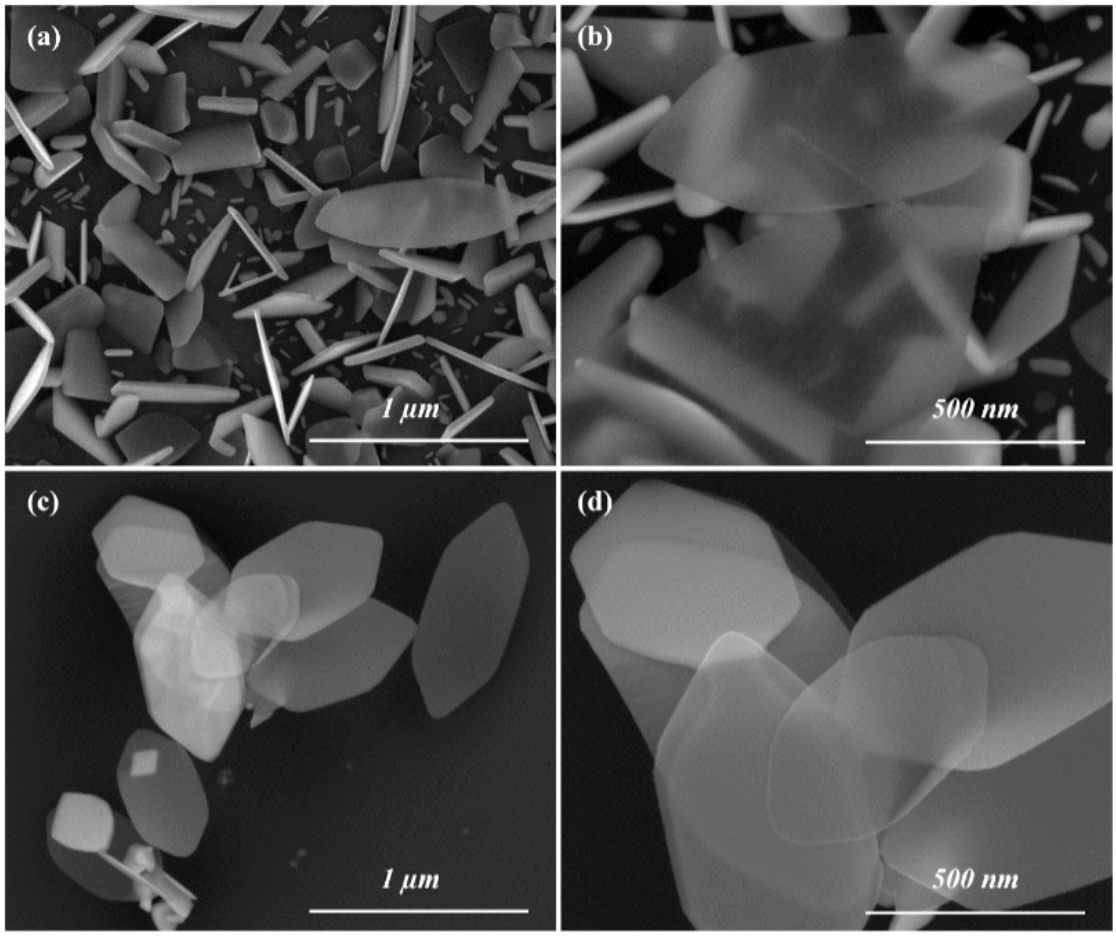

Figure 1: **(a) Secondary SEM image depicting MoS 2 -N3 nanostructures, synthesized through the Chemical Vapor Deposition (CVD) method, exhibiting a distinctive perpendicular orientation to the substrate. (b) Close-up view of enlarged hexagonal MoS 2 -N3 nanostructures, each approximately 1 μm in size, positioned at top the vertically aligned samples. The reduced thickness of these hexagonal structures is suggested by their apparent transparency. (c) MoS 2 -E3 samples captured at the cooler end of the reactor. The image highlights a nearly perfect hexagonal structure (indicated by the red arrow), representative of the samples that migrated from the Si/SiO 2 substrate to the colder zone (∼300 °C) at the terminal end of the quartz tube. (d) Zoomed-in view of part (c), providing a magnified view of the hexagonal MoS 2 -E3 structure, with a side length of 400 nm, from the previously mentioned section of the reactor.**

Acta Microscopica Vol. 34, Supp. 2, 2025
Abstract Book NSSY 2024 - Galapagos 19-25 May, 2024

Graphene-Enhanced Raman detection of pharmaceuticals in water

Nayeli Y. Gómez-Castillo[1], Julio C. Chacón-Torres[2]

[1] *Yachay Tech University, School of Biological Sciences and Engineering, 100119 Urcuquí, Ecuador*

[2] *Yachay Tech University, School of Physical Sciences and Nanotechnology, 100119 Urcuquí, Ecuador*

nayeli.ng1530@gmail.com

Abstract

Research on pharmaceutical pollution in aquatic systems [1] affirms that pharmaceutical residues have been found in almost all environmental matrices worldwide, including polar regions, in ultra-low concentrations ranging from ng/L to μg/L. Even at these ultra-low concentrations, their presence in water has raised concerns among stakeholders regarding the potential risks to human health. So, there is a need for a sensible biosensor capable of detecting these trace levels of pharmaceuticals to enforce ecotoxicological risk assessments and protect the population from involuntary exposure [2,3]. Nowadays, only three commonly used techniques are employed for the detection of pharmaceutical pollution: gas chromatography-mass spectrometry (GC-MS), gas chromatography-tandem mass spectrometry (GC-MS/MS), and liquid chromatography-tandem mass spectrometry (LC-MS/MS). However, these are time-consuming methods that require expensive reagents, technology, and highly specialized users. In this work, we implemented the use of Raman spectroscopy as a fast, non-destructive, non-invasive, and optimal characterization technique to trace the characteristic fingerprint of pharmaceuticals dissolved in water. We developed a novel Raman spectroscopy metrology to detect ultra-low concentrations of five pharmaceuticals: ibuprofen, naproxen, acetaminophen, azithromycin, and amoxicillin. This metrology consisted of drop-casting the solution of pharmaceuticals on a monolayer of graphene on a quartz substrate and analyzing it using a micro-Raman spectrometer. We found that the supramolecular interaction of graphene with a drop of ultralow-concentrated pharmaceuticals triggered the Graphene Surface Enhanced Raman Spectroscopy (GSERS) response, allowing for the detection of pharmaceuticals within a low concentration limit of 100 μg/mL. The enhancement observed for GSERS in the G- and 2D-lines reached up to 48 times, derived from the molecular interaction of both molecules (graphene and the pharmaceutical). In addition, the graphene substrate enhanced the pharmaceutical bands and quenched its fluorescence, allowing the identification of the pharmaceutical's characteristic spectrum, which, in turn, can be used as a marker of the pharmaceutical presence as a sensor. Thus, this project brings an absolutely innovative tool for the detection of ultra-low concentrated pharmaceuticals when deposited in graphene. This discovery opens doors to a better understanding of

the pollutant sources, distribution patterns, and ecological and eco-toxic effects of pharmaceuticals. Therefore, it contributes to the preservation of public sanity, pharmaceutical pollution research, and water quality monitoring.

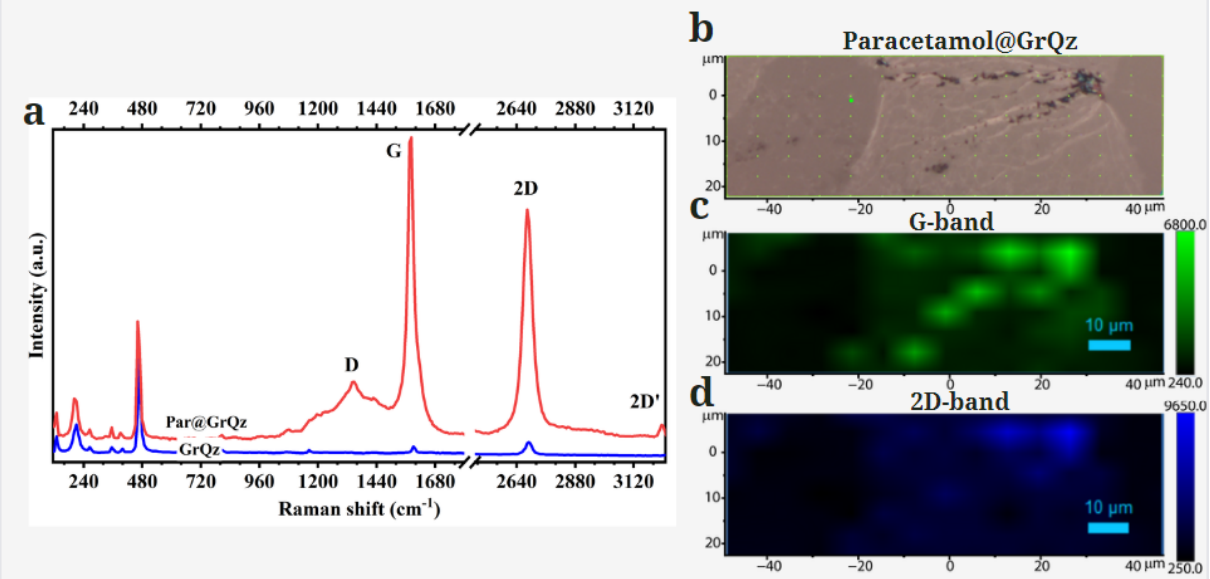

Figure 1: **SERS phenomenon of paracetamol on graphene substrate. a) Raman spectra of Paracetamol@GrQz and GrQz. b) Micrograph of paracetamol@GrQz. c) Raman map of the G band. d) Raman map of the 2D band.**

References

[1] M. Patel, R. Kumar, K. Kishor, T. Mlsna, C. U. Pittman Jr, and D. Mohan, "Pharmaceuticals of emerging concern in aquatic systems: chemistry, occurrence, effects, and removal methods," Chemical reviews, vol. 119, no. 6, pp. 3510–3673, 2019.

[2] A. Wennmalm and B. Gunnarsson, "Public health care management of water pollution with pharmaceuticals: environmental classification and analysis of pharmaceutical residues in sewage water," Drug information journal: DIJ/Drug Information Association, vol. 39, no. 3, pp. 291–297, 2005.

[3] H. Sanderson, D. J. Johnson, T. Reitsma, R. A. Brain, C. J. Wilson, and K. R. Solomon, "Ranking and prioritization of environmental risks of pharmaceuticals in surface waters," Regulatory toxicology and pharmacology, vol. 39, no. 2, pp. 158–183, 2004

Acta Microscopica Vol. 34, Supp. 2, 2025
Abstract Book NSSY 2024 - Galapagos 19-25 May, 2024

Synthesis: and Characterization of Samarium Doped Hydroxyapatite and Preliminary Cytotoxicity Study

Stephanie N. Enríquez[1], Gema González Vásquez[1], Sarah Briceño[1], Lenin Ramirez Cando[2]

[1] *Yachay Tech University, School of Physical Sciences and Nanotechnology*

[2] *Yachay Tech University, School of Biological Sciences and Engineering*

stephanie.enriquez@yachaytech.edu.ec

Abstract

Tydroxyapatite (HAp) is a commonly used biomaterial in biomedical applications and the main constituent of bone tissue. This inorganic compound exhibits an affinity for substitutions, enhancing its unique properties (1). By replacing Ca^{2+} ions with lanthanides, such as samarium (Sm), the material gains improved antimicrobial and biological characteristics (2). Sm has luminescent properties and a strong affinity for bone mineral (3), making it suitable for drug delivery systems and bio-imaging. This research focuses on synthesizing samarium-doped hydroxyapatite (Sm:HAp) with biocompatible features. $Ca_{10-x}Sm_x(PO_4)_6(OH)_2$ was substituted with (xSm= 0, 0.05, 0.1, 0.5, 1.0) and then calcined at 200°C, 400°C, 600°C, and 800°C. Samples were characterized using Fourier-transform infrared spectroscopy (FTIR), Raman spectroscopy, scanning electron microscopy (SEM), x-ray diffraction (XRD), and photoluminescence spectroscopy. Biocompatibility was assessed through cytotoxicity studies, such as Trypan Blue and MTT assays. The results show the successful integration of Sm^{3+} ions into the HAp structure, with visible fluorescence. The response of neuroblastoma cells was dependent on the Sm content, especially noticeable in composites with higher Sm^{3+} concentrations.

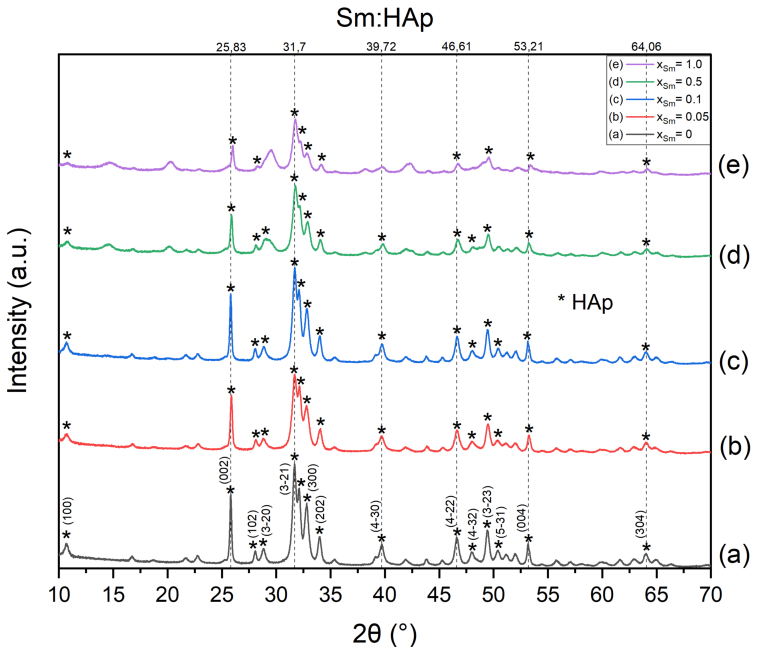

Figure 1: **XRD pattern of Sm:HAp at different samarium concentrations (x_{Sm} = 0, 0.05, 0.1, 0.5, 1.0).**

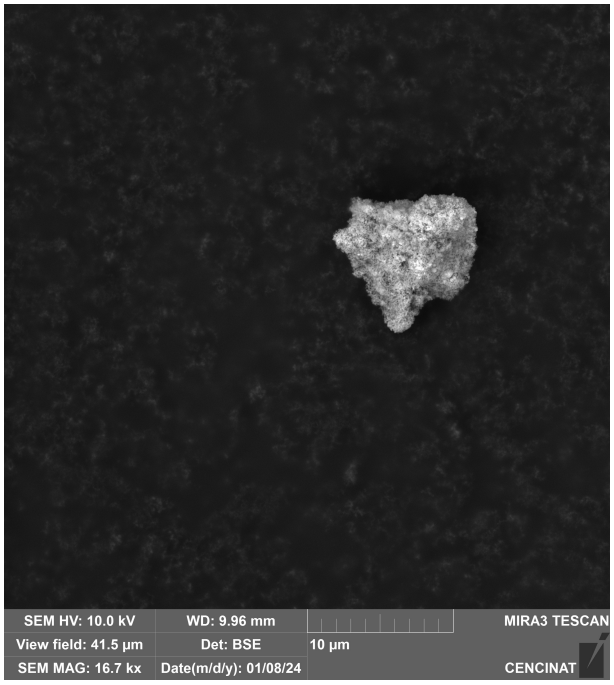

Figure 2: **SEM image at 16.7 kx magnification of Sm:HAp with x_{Sm}= 0.5 calcined at T = 800°C**

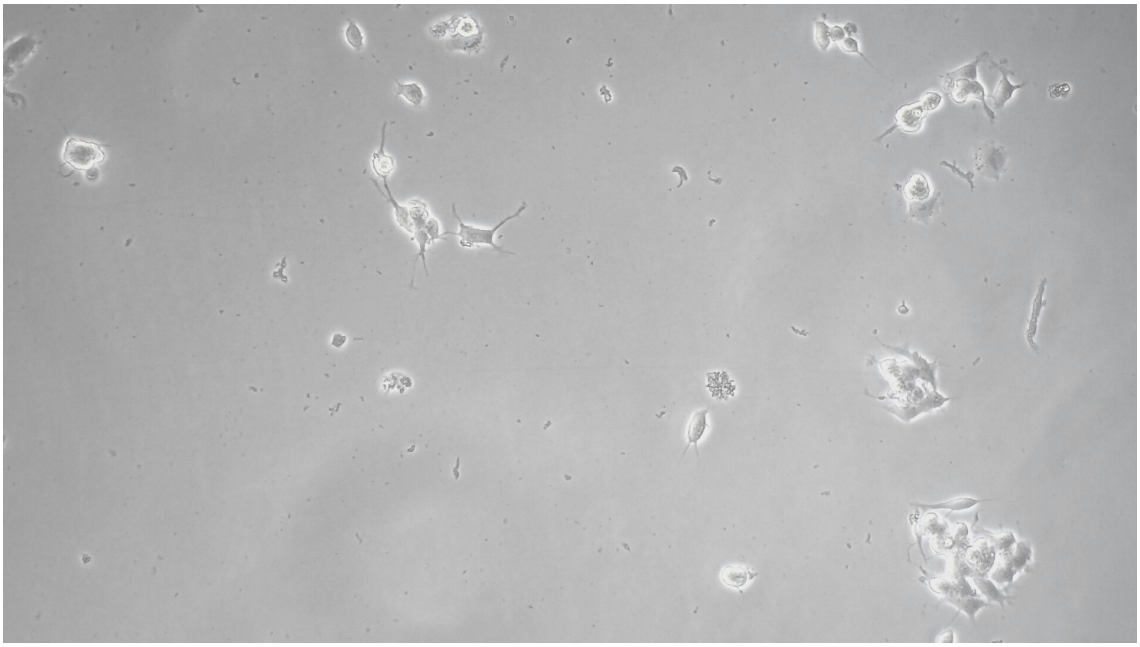

Figure 3: **Images obtained from an inverted microscope at 20X magnification that show cell viability evaluation of SH-SY5Y treated for 24 h with Sm:HAp sample (x_{Sm} = 0.5, T = 400°C) treatment at concentrations of 5 µM.**

References

[1] Uskokovi, V. (2015). The role of hydroxyl channel in defining selected physicochemical peculiarities exhibited by hydroxyapatite. RSC advances, 5(46), 36614-36633. https://doi.org/10.1039/C4RA17180B

[2] Ciobanu, S.C.; Iconaru, S.L.; Predoi, D.; Prodan, A.M.; Predoi, M.V. Physico-Chemical Properties and In Vitro Antifungal Evaluation of Samarium Doped Hydroxyapatite Coatings. Coatings 2020, 10, 827. https://doi.org/10.3390/coatings10090827

[3] Wieszczycka, K., Staszak, K., Woniak-Budych, M. J., & Jurga, S. (2019). Lanthanides and tissue engineering strategies for bone regeneration. Coordination Chemistry Reviews, 388, 248-267. https://doi.org/10.1016/j.ccr.2019.03.003

Acta Microscopica Vol. 34, Supp. 2, 2025
Abstract Book NSSY 2024 - Galapagos 19-25 May, 2024

Charge transport in graphene-molecule-gold single-molecule junction

Gaby Balcázar[1], Henrry Osorio[1]
[1] *Escuela Politécnica Nacional, Departamento de Física*
gaby.balcazar@epn.edu.ec

Abstract

Molecular electronics is an interdisciplinary field that integrates physics, chemistry, biology, materials science, and engineering. This field aims to develop electrical devices using molecules or molecular assemblies as essential components. Therefore, this field constitutes a viable solution to overcome the miniaturization limits of present-day CMOS (complementary metal-oxide semiconductor) technology, extending the efficiency and miniaturization of electronic systems to a molecular scale [1]. In contrast to conventional CMOS-electronic devices, molecular devices offer increased processing and storage capacity, enhancing performance at a reduced cost and occupying a smaller physical space. In addition, this approach holds the promise of transforming electronic technology by harnessing the quantum properties of molecules. While research on metal-molecule-metal molecular junctions employing metals such as gold, silver, platinum, aluminum, and copper (Au, Ag, Pt, Al, Cu) has provided a comprehensive understanding of the fundamentals for studying and manufacturing molecular-scale electronic components, recent attention has shifted toward the study of carbonaceous-based molecular junctions [2]. This approach uses the notable advantages of carbonaceous electrodes over metallic electrodes. Specific carbonaceous electrodes, including graphene, carbon nanotubes (CNT), reduced graphene oxide (rGO), etc., exhibit remarkable electrical, mechanical, thermal, and optical properties, encompassing high electrical conductivity, mechanical strength, thermal conductivity, optical transparency, and more. [1] Beyond their chemical stability and resilience against oxidation, carbonaceous electrodes also showcase exceptional compatibility with a wide range of chemical compounds, rendering them suitable for manipulating molecules in experiments and devices. Specifically, graphene electrodes can establish strong connections with individual molecules using either covalent bonds (amide and C–C bond) or non-covalent bonds, like van der Waals (vdW) and π-π stacking interactions. [2] In this contribution, we study single-molecule junctions formed from 4,4'-biphenyl dithiol molecular bridges on a graphene electrode. The graphene film (on copper substrate) was obtained using the chemical vapor deposition (CVD) technique. We evaluate electrical conductance in graphene-molecule-gold junctions employing the scanning tunneling microscopy (STM) based I(s) method. [2] In brief, an STM tip approached close to the substrate (graphene) so that the target molecule could

bind between the gold tip and the substrate. Then, the tip is rapidly retracted, and a current (I) versus distance (s) curve is recorded. Hundreds of such junction-making and breaking curves are analyzed statistically in histograms to yield the conductance. [3] The acquired data undergoes meticulous statistical analysis to determine the mean conductance of the molecular junction. We then systematically compare these results with experimental conductance values available in the literature for molecular systems featuring various electrodes and several molecules. In summary, this contribution enhances our understanding of the experimental findings, contributing valuable insights to the broader field of molecular electronics using graphene electrodes. This study paves the way for using graphene as nanoelectrodes to evaluate charge transport at the molecular level.

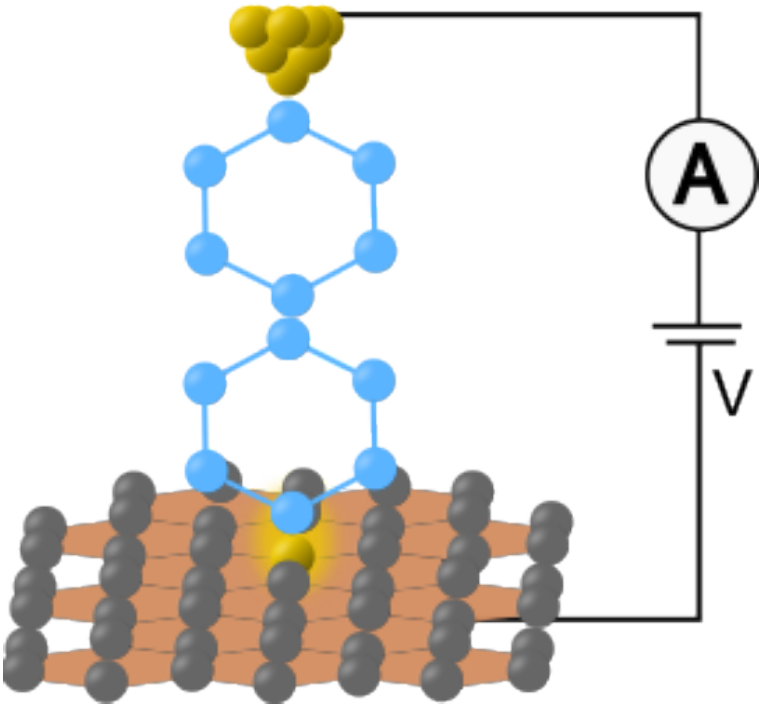

Figure 1: **Schematic diagram of the molecular junction (graphene-4,4'-biphenyl-dithiol-gold) studied in this research.**

References

[1] Yu X. et al. Nature Reviews Materials. (2017) (2) (17046)

[2] Zhao S. et al. Nano Research. (2021) (1)

[3] Zang Q. et al. J. Phys. Chem. C. (2018) (6) (7527)

Acta Microscopica Vol. 34, Supp. 2, 2025
Abstract Book NSSY 2024 - Galapagos 19-25 May, 2024

A Study on the Optimum Conditions of Rice Husk Ash to Improve Concrete Strength

Francisco Darquea[1], Alex X. Jerves[2], Jorge Albuja[3]

[1] *Universidad Católica de Cuenca*

[2] *Pontificia Universidad Católica del Ecuador*

[3] *Fundación INSPIRE*

francisco.darqueac@ucacue.edu.ec

Abstract

Researchers are constantly seeking high-strength and higher quality materials for construction because of the widespread use of filler aggregates in construction. The use of cement to enhance the mechanical properties of concrete is responsible for high carbon dioxide emissions, which are highly polluting for the planet.

The objective of this research project is to examine the effect of modifying cement percentages by employing rice husk ash as a filler, which can enhance the structural properties of cement, to generate a nanostructured cement composite. The incorporation of different percentages of rice husk ash will be demonstrated through various laboratory tests on how the physical-mechanical characteristics of cement are affected. In addition, the modulation of the mechanical properties of cement are directly dependent on the morphological and chemical characteristics of the rice husk ash, which will be introduced as a main variable in the cement composite formation.

Previous research has shown that adding up to 7.5% hull ash to concrete mixtures significantly increases compressive strength, however, it also increases water absorption. To guarantee that there is an increase in the compressive strength, the silica content obtained when calcining the rice husk must be as high as possible. For this purpose, research carried out recommends that the calcination temperature be between 400 °C and 800 °C. [1]

For the development of this research, it is necessary to propose multidisciplinary activities, starting with the identification of the local and regional geology of the place where the materials are extracted from, their physical properties, mineralogical composition, structure and chemical composition. To get an insight in these analyses, advanced characterization techniques are required such as XPS, Raman and FTIR spectroscopic techniques. In addition, mechanical testing based on standardized ISO 1920-4 are conducted to prove the effects of the rice husk filler. Finally, the analysis of results will be carried out using statistical and data analysis methods.

Hence, the project has a multidisciplinary approach, applying sciences such as Geology, Lithology, Mechanics of materials, Chemistry, Statistics and environmental sustainability.

Figure 1: **A Study on the Optimum Conditions of Rice Husk Ash to Improve Concrete Strength**

References

[1] Taku JK, Amartey YD, Kassar T. Comparative Elemental Analysis of Rice Husk Ash Calcined at Different Temperatures Using X-ray Flourescence (XRF) Technique. American Journal of Civil Engineering and Architecture [Internet]. 2016;4(1):28-31. Disponible en: http://pubs.sciepub.com/ajcea/4/1/4

Acta Microscopica Vol. 34, Supp. 2, 2025
Abstract Book NSSY 2024 - Galapagos 19-25 May, 2024

Synthesis and characterization of chitosan-alginate bio-composites derived from endemic algae for efficient removal of Escherichia Coli in water

Dayanna Baque[1], Óscar Almeida[2], Julio C. Chacón-Torres[3]

[1] *Yachay Tech University, School of Biological Sciences and Engineering, 100119 Urcuquí, Ecuador*

[2] *Yachay Tech University, School of Chemical Sciences and Engineering, 100119 Urcuquí, Ecuador*

[3] *Yachay Tech University, School of Physical Sciences and Nanotechnology, 100119 Urcuquí, Ecuador*

ayanna.baque@yachaytech.edu.ec

Abstract

Chitosan and alginate are biopolymers that have been extensively studied for their potential applications in removing contaminants from water. Chitosan has some advantageous properties, such as biocompatibility, biodegradability, and antibacterial activity. Likewise, alginate is recognized for its capability to form hydrogels and has good ion exchange capacity. Overall, they exhibit notable efficacy with a high capacity and a high affinity for various pollutants. [1]. Existing water treatment techniques do not remove every microorganism that grow in this environment. In developing countries, potable water contains substantial amount bacteria, such as Escherichia coli, due to inefficient and inaccessible purification systems [1]. Therefore, this work focuses on the synthesis and characterization of chitosan-alginate bio-composites with the main objective of developing an effective filter for removing Escherichia coli to enhance water quality. For the synthesis of biocomposites, commercial chitosan and calcium alginate extracted from Eichornia crassipies and Azollia filiculoides, endemic algae of Yaguarcoha lagoon were used. Alginates were extracted by a dynamic maceration, further treated with formaldehyde and ethanol, to isolate the alginate compound, which is treated with calcium chloride and freeze-dried to obtain the alginate powder. The methodology for the synthesis of biocomposites was adapted from [2]. The preparation of chitosan-alginate (CHs-ALG) solution was performed using a cross-linking component to maintain the composite's stability. It was subsequently converted into beads by dropping the suspension into a 0.5M NaOH solution. The viscous beads were thoroughly washed with distilled water until achieve a neutral pH and then dried in an oven at 60°C for two hours. The bio-composite beads were systematically characterized by Fourier Transform Infrared Spectroscopy (FTIR), RAMAN spectroscopy, and X-ray Photoelectron Spectroscopy (XPS) to describe the chemical composition, molecular structure, and surface properties of the CHs-ALG beads.

FTIR analysis provided insights into the chemical bonds and molecular structure of the CHs-ALG beads. In the chitosan spectrum, the functional groups amino (3500-3200 cm-1), carbonyl (around 1750 to 1680 cm-1) and hydroxyl (around 3600 to 3200 cm-1) were identified. In the alginate the main groups are shown, such as hydroxyl (around 3600 to 3200 cm-1), C-H stretching (around 3110 and 2900 cm-1), and the carboxylate (around 1650-1400 cm-1). The biocomposite shows both characteristic functional groups. Additionally, Raman spectroscopy contributed valuable information on molecular vibrations, confirming the composition and structural properties of the synthesized biocomposites. The presence of chitosan and alginate peaks in the synthesized biocomposites, these being Amide-II (1376 cm-1), Amide-I (1659 cm-1) and C-H (2888 cm-1) corresponding to chitosan were identified. Meanwhile, the COO symmetric stretching (1444 cm-1), and COO asymmetric stretching (1678 cm-1) correspond to alginate. However, due to the fluorescence phenomena of biological sample its peaks are not shown. Moreover, the application of XPS facilitated the analysis of the surface chemical composition and elemental states of the CHs-ALG beads, offering a deeper understanding of the surface chemistry and identification of elemental constituents present in the beads. Finally, the design of the filtration system consisted of three layers: commercial activated carbon, clay and synthesized biocomposites. The most relevant findings showcase the successful synthesis of CHs-ALG beads with a potential for efficient removal of E. coli from water. The biocomposites exhibited promising attributes, as confirmed by FTIR, Raman, and XPS analyses, validating their chemical composition, molecular structure, and surface properties. In conclusion, this study presents a systematic method for synthesizing and characterizing chitosan-alginate bio-composites sourced from endemic algae, offering a sustainable solution for the elimination of E. coli from water. The detailed methodology and thorough characterization contribute valuable insights to the advancement of sustainable water treatment solutions.

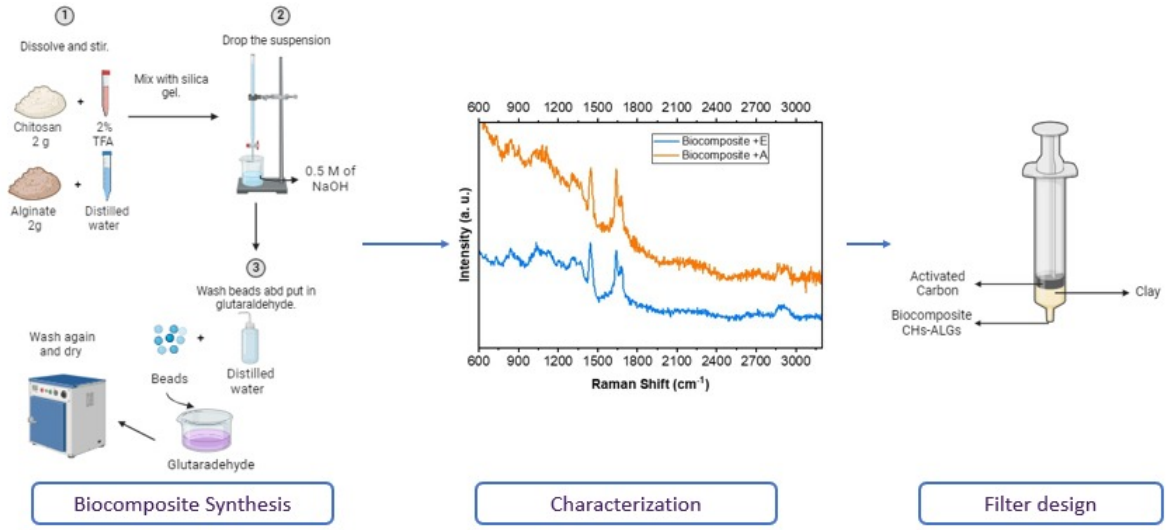

Fig 1. Illustration of synthesis, characterization and filter design of CHs-ALGs biocomposite.

Figure 1: **Illustration of Synthesis, characterization and filter design CHs-ALGs biocomposites.**

References

[1] D. Garg, C.B. Majumder, S. Kumar, B. Sarkar, Removal of Direct Blue-86 dye from aqueous solution using alginate encapsulated activated carbon (PnsAC-alginate) prepared from waste peanut shell, J. Environ. Chem. Eng. 7 (2019), 103365https://doi.org/10.1016/j.jece.2019.103365

[2] Quesada, H. B., de Araújo, T. P., Vareschini, D. T., de Barros, M. A. S. D., Gomes, R. G., & Bergamasco, R. (2020). Chitosan, alginate and other macromolecules as activated carbon immobilizing agents: a review on composite adsorbents for the removal of water contaminants. International Journal of Biological Macromolecules, 164, 2535-2549.

Acta Microscopica Vol. 34, Supp. 2, 2025
Abstract Book NSSY 2024 - Galapagos 19-25 May, 2024

Comparing the theoretical calculated spectra of retinol (C20H30O) with the experimental spectra

Iván P. Urbano[1], Mowbray Duncan[1]
[1] *Yachay Tech*
ivan.urbano@yachaytech.edu.ec

Abstract

In this study, we investigate the interesting comparison between theoretical calculations and experimental data in the context of retinol. The aim is to assess the accuracy of theoretical models by comparing the calculated spectra with the experimental spectra. Can theoretical calculations accurately predict the electronic and vibrational transitions in retinol? This open question guides our research and directs our approach. We employ the Atomic Simulator Environment (ASE) to obtain theoretical vibrational frequencies and perform molecular relaxation using density functional theory (DFT). Our findings aim to shed light on the agreement between theoretical and experimental spectra and the significance of our results.

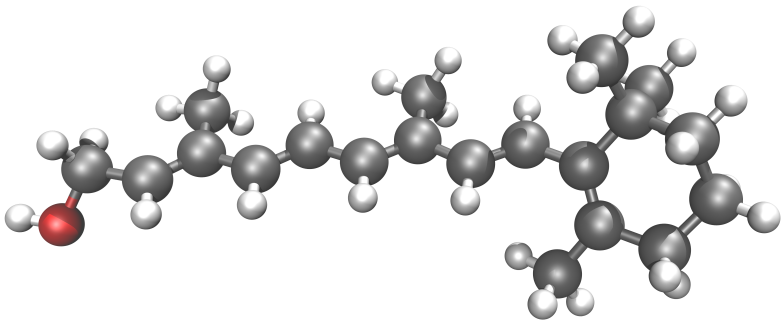

Figure 1: **Retinol molecule relaxed using LCAO**

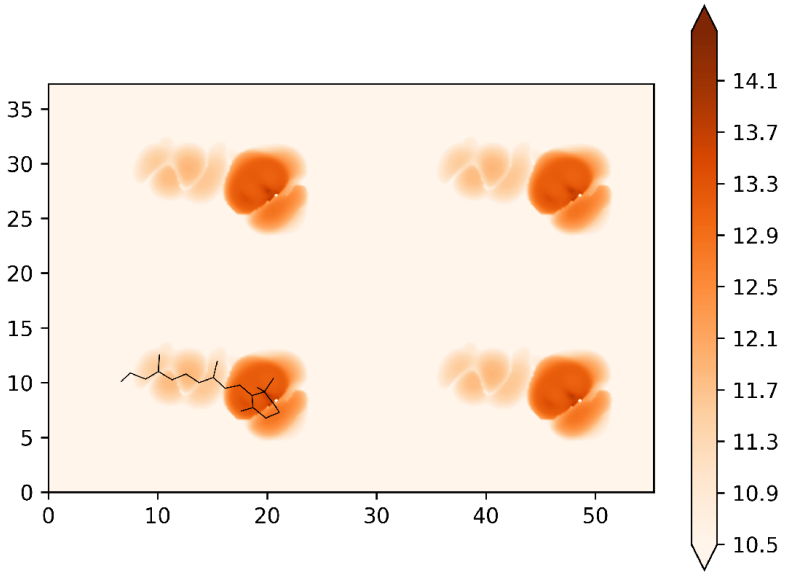

Figure 2: **Theoretical STM image.**

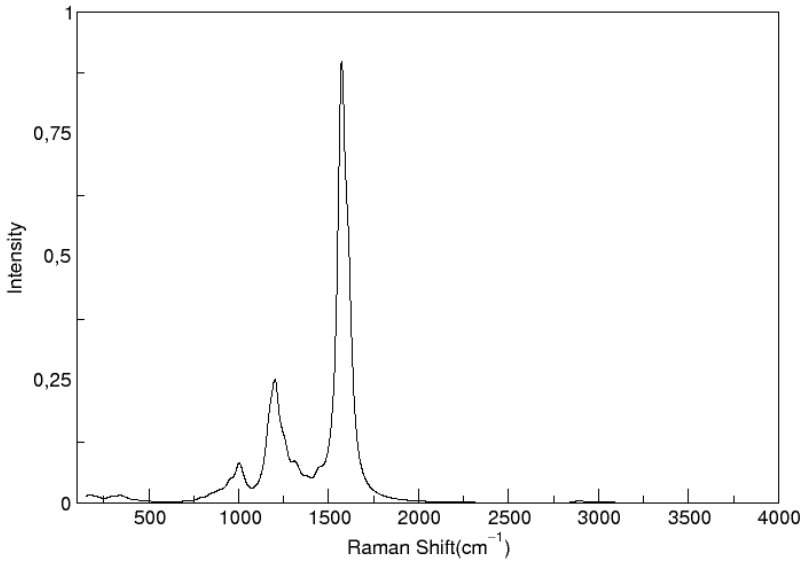

Figure 3: **Theoretical FTIR spectra of retinol**

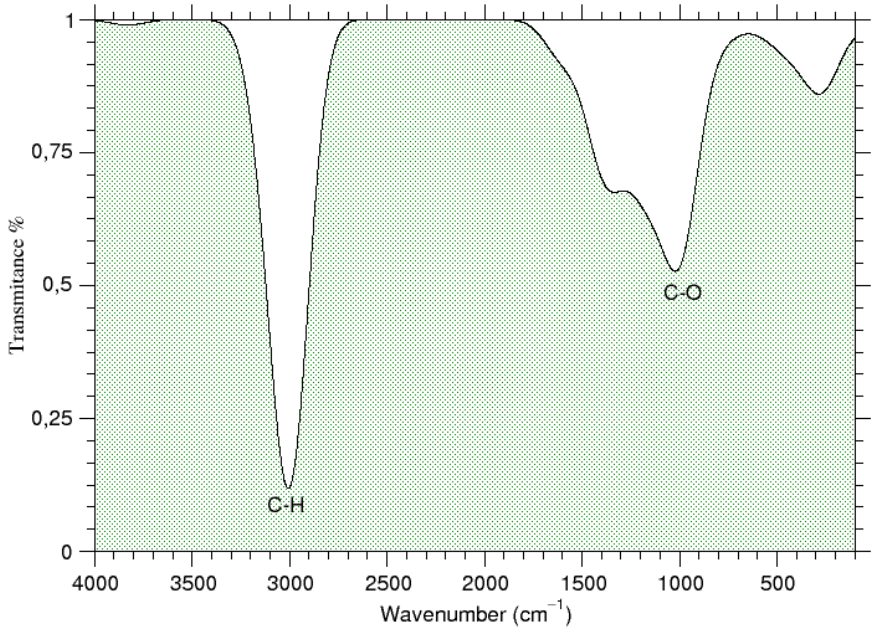

Figure 4: **Theoretical Raman spectra**

References

[1] Failloux, N., Bonnet, I., Baron, M-H., & Perrier, E. (2003). Quantitative Analysis of Vitamin A Degradation by Raman Spectroscopy. Applied Spectroscopy, 57(9), 1117-1122.

[2] Kochan, K., Marzec, K. M., Maslak, E., Chlopicki, S., & Baranska, M. (2015). Raman spectroscopic studies of vitamin A content in the liver: a biomarker of healthy liver. Analyst, 140(7), 2074-2079. doi:10.1039/C4AN01878H

[3] Kim, H., Hu, Y., Jeong, D., Jun, B-H., Cho, E., & Jung, S. (2016). Synthesis, characterization, and retinol stabilization of fatty amide-β-cyclodextrin conjugates. Molecules, 21(7), 963.

Acta Microscopica Vol. 34, Supp. 2, 2025
Abstract Book NSSY 2024 - Galapagos 19-25 May, 2024

Emerging copper-pyridyl nanoporous network MoF analysis

Gustavo Campi[1], Alisson Ceccatto[2], Abner de Siervo[2], Duncan Mowbray[1]

[1] *School of Physical Sciences and Nanotechnology Yachay Tech University, Urcuqui, Ecuador*

[2] *Institute of Physics Gleb Wataghin State University of Campinas UNICAMP, Campinas, Brazil*

gustavo.campi@yachaytech.edu.ec

Abstract

This research explores the intriguing realm of nanoporous materials, particularly Metal-Organic Frameworks (MoFs), known for their unique capabilities in gas separation, catalysis, and potential in organic photovoltaic devices. The study examines the molecular adsorption of 1,3,5-tris[4-(pyridine-4-yl)phenyl]benzene (TPyPB) on Cu(111), a process leading to MoF formation on the surface, influenced by the methodologies discussed in [2] forming an electronic structure. Performing annealing during the 2D synthesis creates this bonding mode [4], forming a bonding mode of N-Cu-N and connecting the organic nanoporous network to the surface of the Cu(111). The investigation encompasses on-surface synthesis, high-resolution scanning tunneling microscopy (STM), Density Functional Theory (DFT), and Time-Dependent Density Functional Theory (TDDFT-k-omega [1]) for the Optical Absorption Spectrum (OAS), Optical Conductivity Spectrum, and excitonic densities. Finally, the research utilizes Fourier Transform Infrared Spectrum and Resonant Raman Spectroscopy to characterize the material's vibrational modes and bond stiffness, aiming to unravel the complex electronic interactions of this nanoporous network structure. This work comprehensively analyzes the bonding properties and electronic properties insight with DOS and PDOS along important optoelectronic activity in the transition phases found on OAS.

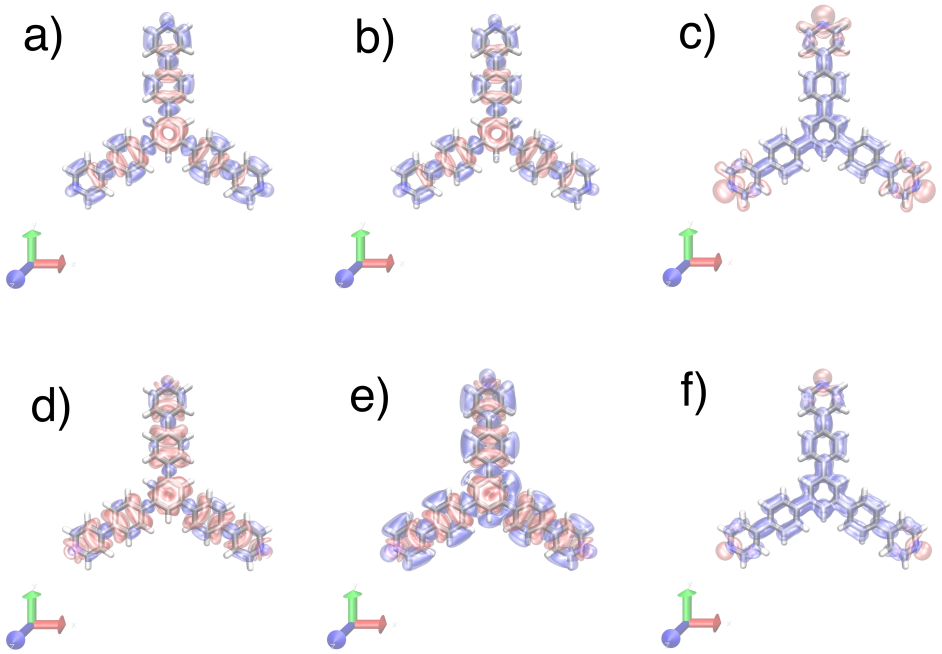

Figure 1: **Electrons are represented in blue and holes represented in red a),b),c) Describe the excitonic density at 4.10 eV for the x,y, and z axes. d),e),f) Describe the excitonic density at 4.47 eV for the x,y, and z axes.**

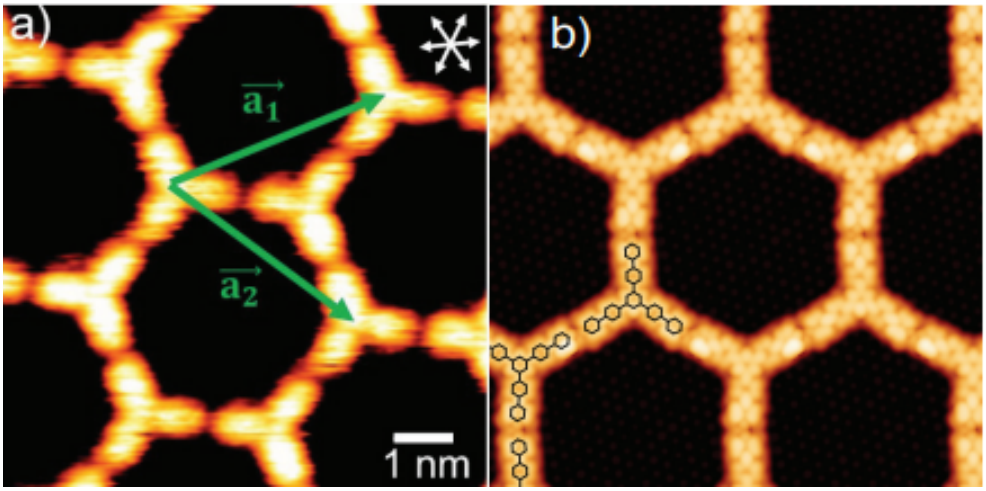

Figure 2: **a) High-resolution STM image of the honeycomb of TPyPB netwrok with lattice vectors (VBias = -1.4 eV), b) STM simulation (VBias = -0.41 eV at HOMO)**

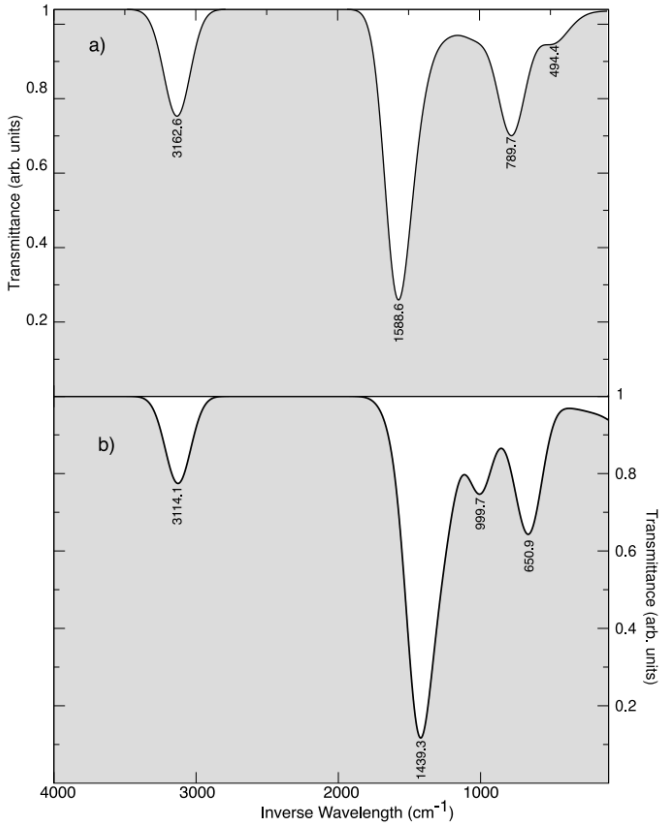

Figure 3: **FT-IR Spectrum; a) spectrum of TPyPB in the gas phase, b) spectrum of TPyPB on Cu(111)**

References

[1] Keenan Lyon, María Rosa Preciado-Rivas, Camilo Zamora-Ledezma, Vito Despoja, and Duncan John Mowbray. Lcao-tddft-k-ω: Spectroscopy in the in the optical limit. Journal of Physics: Condensed Matter, 32(41):415901, 2020.

[2] Weihua Wang, Xingqiang Shi, Shiyong Wang, Jun Liu, Michel A. Van Hove, Pei Nian Liu, Rui-Qin Zhang, and Nian Lin. Cooperative Modulation of Electronic Structures of Aromatic Molecules Coupled to Multiple Metal Contacts. Phys. Rev. Lett. 110, 046802 – Published 23 January 2013.

[3] Sebastian Stepanow, Nian Lin,* Dietmar Payer, Uta Schlickum, Florian Klappenberger, Giorgio Zoppellaro, Mario Ruben, Harald Brune, Johannes V. Barth, and Klaus Kern. Surface-Assisted Assembly of 2D Metal–Organic Networks That Exhibit Unusual Threefold Coordination Symmetry*. Coordination Chemistry DOI: 10.1002/anie.200603644

Acta Microscopica Vol. 34, Supp. 2, 2025
Abstract Book NSSY 2024 - Galapagos 19-25 May, 2024

Assessing Climate Change Impacts on the Galapagos Islands: A Decadal Analysis Using Regional Climate Model Version 5 (RegCM5)

Arianna J. Paredes[1], Oscar Chimborazo[1]
[1] *Yachay Tech University*
arianna.paredes@yachaytech.edu.ec

Abstract

The Galapagos Islands, a unique and ecologically critical archipelago, are renowned for their extraordinary biodiversity and significant contribution to evolutionary biology. However, these islands are increasingly vulnerable to the impacts of climate change, making the study of their climatic patterns crucial for conservation and ecological understanding (Duenas et al., 2021). This paper employs the Regional Climate Model version 5 (RegCM5) to analyze the current and near-future climatic conditions of the Galapagos.

Our analysis involved two simulation periods: the present (2010-2020) and the near future (2020-2030), with each phase commencing at 00:00 UTC on January 1st. The first year of each simulation served as a spin-up and was excluded from the analysis. The model configuration was standardized for both periods, with a focus on a 15 km resolution grid covering the Galapagos region (Figure 1).

We employed a non-hydrostatic model core with pressure vertical coordinates and the MM5 Horizontal Arakawa-B Grid for the dynamic core. The radiation parametrization utilized the NCAR CCM3 scheme. For the representation of the planetary boundary layer and cumulus convection, the non-local boundary layer Holtslag scheme and a mixed convection scheme [Grell (1993) over land, Emanuel and Zivkovic-Rothman (1999) over ocean] were used as suggested by Reboita et al. (2014). Notably, the Community Land Model version 4.5 (CLM4.5) was selected for its enhanced representation of terrestrial processes.

Our findings highlight significant climatic changes impacting the Galapagos Islands, with considerable implications for their delicate ecosystems. The study not only contributes to the understanding of regional climate dynamics but also underscores the urgency of climate change mitigation efforts in preserving these ecologically significant islands.

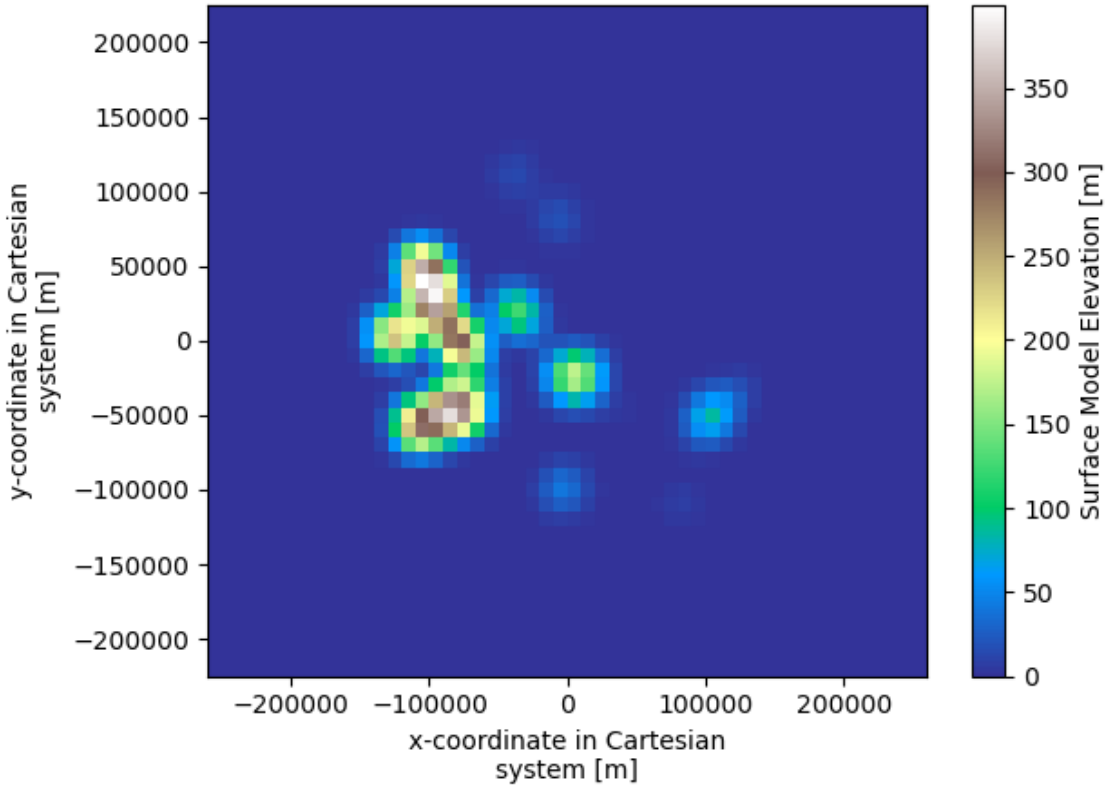

Figure 1: **Topographic Map of Galapagos Island Generated by RegCM5 with 15 km Grid Resolution. This detailed elevation map showcases the varied terrain of the Galapagos Island, providing insights into its geological features. It is the domain of the simulations.**

References

[1] Dueñas, A., Jiménez-Uzcátegui, G., & Bosker, T. (2021). The effects of climate change on wildlife biodiversity of the Galapagos Islands. Climate Change Ecology, 2, 100026.

[2] Reboita, M. S., Fernandez, J. P. R., Llopart, M. P., da Rocha, R. P., Pampuch, L. A., & Cruz, F. T. (2014). Assessment of RegCM4. 3 over the CORDEX South America domain: sensitivity analysis for physical parameterization schemes. Climate Research, 60(3), 215-234.

Acta Microscopica Vol. 34, Supp. 2, 2025
Abstract Book NSSY 2024 - Galapagos 19-25 May, 2024

Improving mechanical properties of Chitosan films: Sustainable eco-friendly packaging

Paula Dayana Ponce[1], Thibault Terencio[1], Carlos Loyo[1], Floralba Lopez[1]
[1] *CATS INVESTIGATION GROUP (Catalysis Theory & Spectroscopy, YachayTech, Urcuqui, Ecuador)*
paula.ponce@yachaytech.edu.ec

Abstract

Chitosan, known for its biodegradability and biocompatibility, is a versatile material with broad applications. In this study, we incorporated different proportions of glycerol and propylene carbonate into chitosan films to investigate their combined impact on structural and mechanical attributes. To elucidate structural alterations induced by these additives, we employed specifically Infrared Spectroscopy and X-ray Diffractometry. These methods meticulously probed the molecular and crystalline structures of the chitosan films, unveiling impactful structural differences. The mechanical properties of these films were tested by a UTM machine, revealing a noteworthy enhancement in various mechanical attributes. This augmentation suggests a synergistic effect arising from glycerol and propylene carbonate addition, fortifying the mechanical performance of the chitosan films. DFT modeling allow us to propose a chemical structure related to the observed polymerization changes that gave the material their unexpected structural properties. The structural and mechanical enhancements observed in the chitosan films are particularly relevant in sustainable packaging solutions, where the demand for environmentally friendly materials is ever-growing. In conclusion, this study reveals the intricate interplay of additives in chitosan films and underscores their potential for transformative applications, especially in eco-friendly and sustainable solutions across diverse sectors.

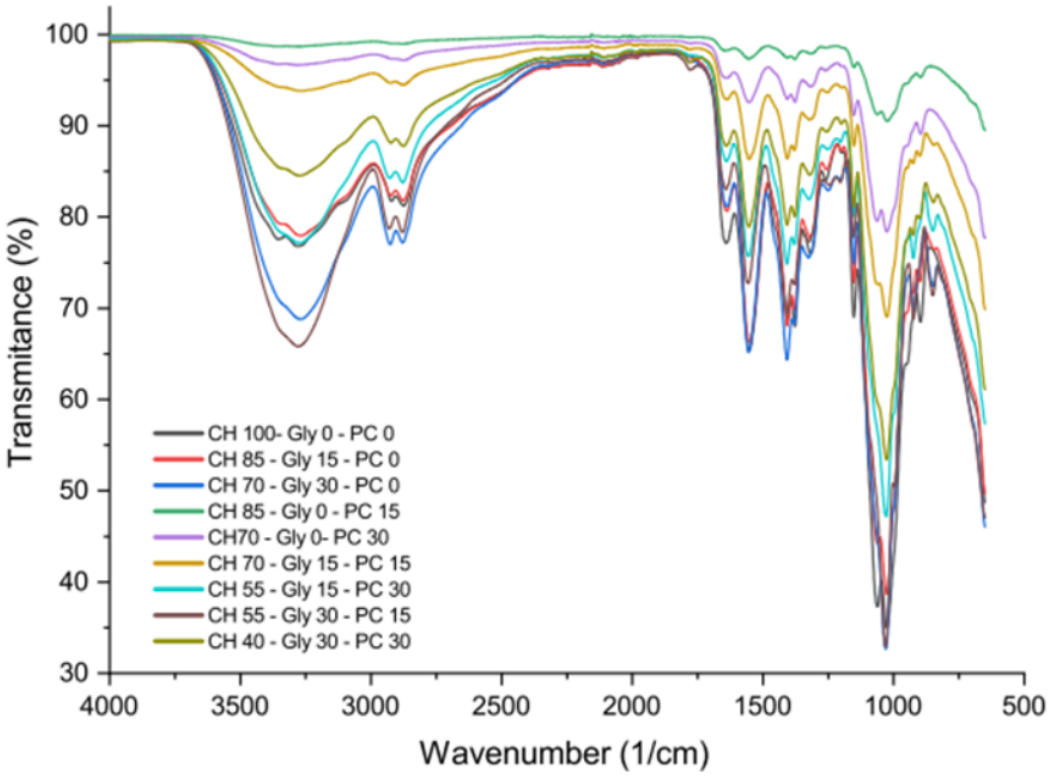

Figure 1: **IR spectrum for samples at different concentrations**

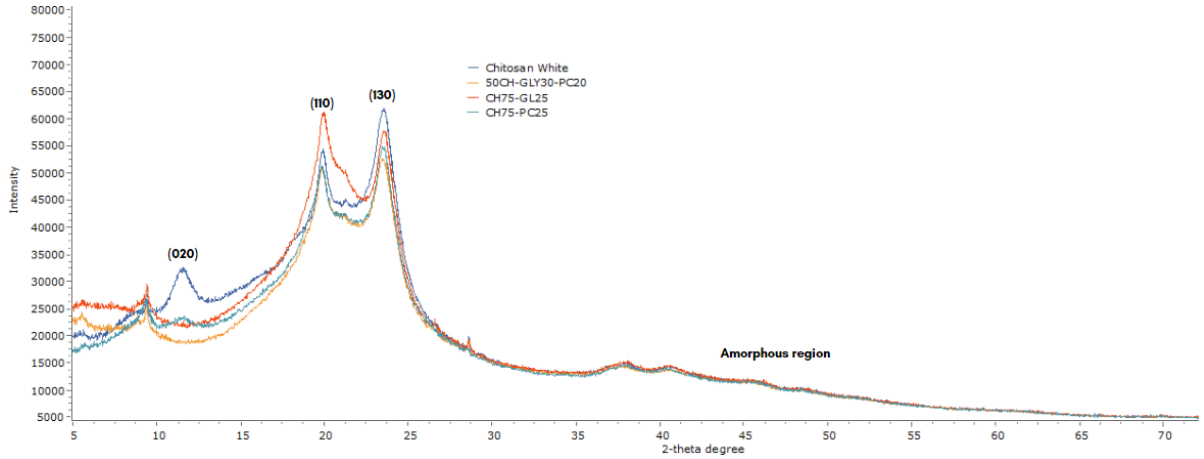

Figure 2: **XRD contrast for films crystallinity at different concentrations**

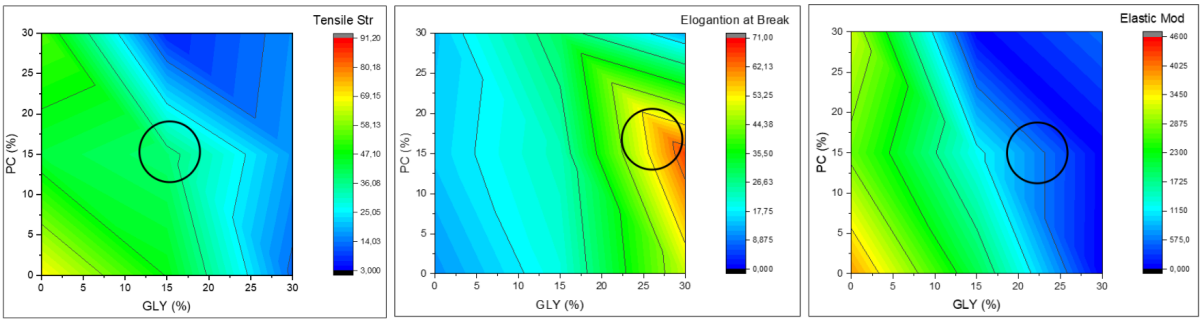

Figure 3: **Mechanical Properties Characterization**

References

[1] Ibrahim, M. A.; Alhalafi, M. H.; Emam, E.-A. M.; Ibrahim, H. M.; Mosaad, R. M. A Review of Chitosan and Chitosan Nanofiber: Preparation, Characterization, and Its Potential Applications. Polymers 2023, 15 (13), 2820–2820. https://doi.org/10.3390/polym1513282.

[2] Wasina Thakhiew, Manida Champahom, Sakamon Devahastin, & Somchart Soponronnarit. (2015). Improvement of mechanical properties of chitosan-based films via physical treatment of film-forming solution. Journal of Food Engineering, 158, 66–72. https://doi.org/10.1016/j.jfoodeng.2015.02.027.

[3] Yasunari Ikezawa; Toshiyuki Ariga. In Situ FTIR Spectra at the Cu Electrode/Propylene Carbonate Solution Interface. Electrochimica Acta 2007, 52 (7), 2710–2715. https://doi.org/10.1016/j.electacta.2006.09.050.

Acta Microscopica Vol. 34, Supp. 2, 2025
Abstract Book NSSY 2024 - Galapagos 19-25 May, 2024

Prediction of liposomes' physicochemical properties through nano-QSPR: Investigating the impact of liposome structure on its zeta potential

Kamila Jarzynska[1], Agnieszka Gajewicz-Skretna[1], Krzesimir Ciura[1,2,*], Tomasz Puzyn[1,*]

[1] *University of Gdansk. Faculty of Chemistry*

[2] *Medical University of Gdansk. Faculty of Pharmacy.*

kamila.jarzynska@phdstud.ug.edu.pl

Abstract

Amphiphilic lipids can be arranged into nanoscale spherical structures, called liposomes, which have potential use in several pharmaceutical applications. They are particularly useful in targeted drug delivery as nanocarriers due to their biocompatibility, biodegradability, and low immunogenicity1. To optimize liposome design, it is essential to comprehend the factors that affect their physicochemical properties. In this study, we have presented the kernel-weighted local polynomial regression (KwLPR) nano-quantitative structure-property relationships (nano-QSPR) model to predict the zeta potential (ZP) based on the structure of 12 liposome formulations, including 1,2-dioleoyl-sn-glycero-3-phosphoethanolamine (DOPE), 3β-[N-(N',N'-dimethylaminoethane)-carbamoyl]cholesterol (DC - Chol), 1,2-dioleoyl-3-trimethylammonium-propane (DOTAP), and L-α-phosphatidylcholine (EPC). The developed model has shown strong fit (R^2 = 0.96, $RMSE_C$ = 5.76), flexibility ($Q^2_{CVloo} = 0.83$, $RMSE_{CVloo} = 10.77$), and predictive power ($Q^2_{Ext} = 0.89$, $RMSE_{Ext}$ = 5.17). Furthermore, we have established the formula for computing molecular nanodescriptors for liposomes, based on constituent lipids' molar fractions. Through the correlation matrix and principal component analysis (PCA), we have identified two key structural features affecting liposomes' zeta potential: hydrophilic-lipophilic balance (HLB) and enthalpy of formation Lower HLB values, which indicate a more lipophilic nature, are associated with a higher zeta potential and greater stability. Conversely, higher enthalpy of formation reflects a reduced zeta potential and decreased stability of liposomes. Our research has demonstrated that the nano-QSPR approach provides a better understanding of how the composition and molecular structure of liposomes affect their zeta potential. This fills a gap in ZP nano-QSPR modeling methodologies for nanomaterials (NMs). Our proof-of-concept study is the first step in developing a comprehensive and computationally-based system for predicting the physicochemical properties of liposomes, which are one of the most important drug nano-vehicles.

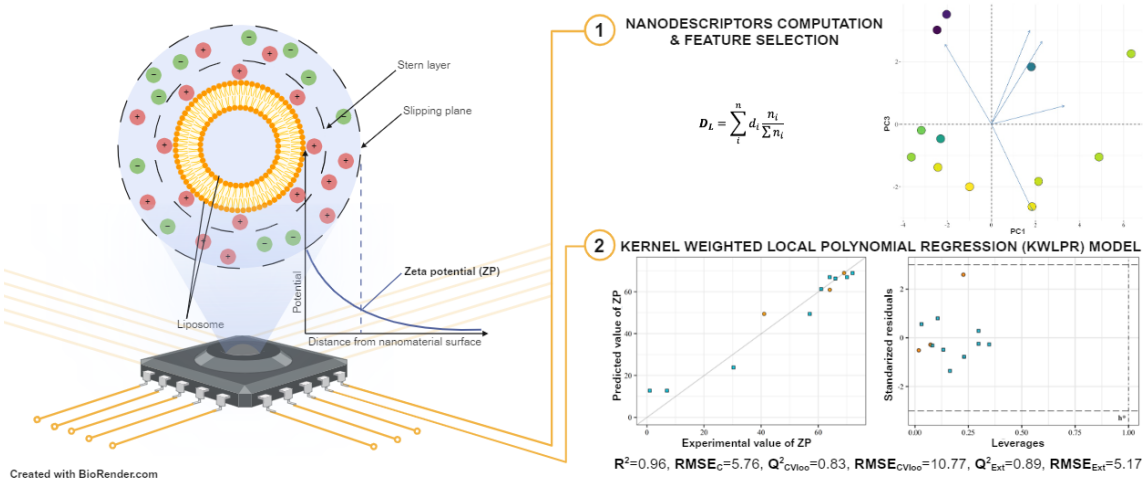

Figure 1: **Graphical abstract of the study.**

References

[1] Guimarães D. et al. Int J Pharm (2021) (601) (120571).

Acta Microscopica Vol. 34, Supp. 2, 2025
Abstract Book NSSY 2024 - Galapagos 19-25 May, 2024

Study of the Antioxidant Activity of Andean Species with Ethnobotanical Use for Skin Diseases

Milene González[1], Vivian Morera[1]

[1] *Yachay Tech University, School of Chemical Sciences and Engineering, 100119 Urcuquí, Ecuador*

milene.gonzalez@yachaytech.edu.ec

Abstract

Plant extracts have been used for medicinal and therapeutic purposes in various cultures worldwide due to their rich content of phenolic compounds such as flavonoids, terpenoids, and tannins, which have been shown to have benefits for the skin, acting as antioxidants, protecting the skin from damage caused by free radicals. This study assesses the antioxidant and toxic capacity of four native Andean plant species in Ecuador: *Juglans neotropica* Diels, *Duranta triacantha* Juss, *Mikania sp*, and *Brugmansia aurea* Lagerh. The total content of phenols and flavonoids, antioxidant capacity, and toxicity of each plant's methanolic and methanolic hydrolyzed extracts were evaluated. The methods used included (a) Total flavonoid content (TFC), (b) Total phenolic content (TPC), (c) 2,2-diphenyl-1-picrylhydrazyl (DPPH) radical scavenging assay, (d) 2,2'-casino-bis (3-ethylbenzothiazoline-6-sulfonic acid) (ABTS) radical scavenging assay, (e) Ferric ion reducing antioxidant power (FRAP) assay, (f) Brine shrimp lethality assay, (g) Fourier transform infrared spectroscopy (FT-IR), and (h) High-performance liquid chromatography (HPLC). The results demonstrated that all four species contain phenols, flavonoids, and antioxidant capacity, with *Juglans neotropica* Diels having the highest values being: TFC: 292.40 mg QE/g DE, TPC: 270.57 mg GAE/DE, DPPH: 517.54 µg/mL IC_{50}, ABTS: 182.33 µg/mL IC_{50}, and FRAP: 544.60 mg TE/g DE for methanolic extracts. On the other hand, the results for acid hydrolysis for *Juglans neotropica* Diels were TFC: 164.59 mg QE/g DE, TPC: 365.72 mg GAE/DE, DPPH: 630.26 µg/mL IC_{50}, ABTS: 84.63 µg/mL IC_{50}, and FRAP: 736.49 mg TE/g DE and for basic hydrolysis were TFC: 406.30 mg QE/g DE, TPC: 503.33 mg GAE/DE, DPPH: 356.06 µg/mL IC_{50}, ABTS: 61.22 µg/mL IC_{50}, and FRAP: 1072.10 mg TE/g DE. The methanol extract of *Juglans neotropica* Diels is non-toxic in concentrations of less than or equal to 1 mg/mL, while its acid and basic hydrolysis extracts are toxic. From the infrared spectrum, it was determined that all extracts contain alcohols and amines as functional groups, and their vibrations correspond to the following bonds: C-H, C=O, N-H, and C=C, characteristics of phenolic compounds. These results were corroborated with high-performance liquid chromatography, where most extracts observed common phenols such as ferulic

acid, gallic acid, and chlorogenic acid. This study suggests that the species studied have a favorable profile for future research.

Plant Specie	Concentration (ug/mL)	% Inhibition		
		Mac	AH	BH
J. Neotropica	10	11.06	-	-
	50	26.10	-	40.81
	100	43.55	54.41	81.76
	250	81.98	83.11	-
	500	98.86	-	-
	600	98.86	-	-
D. Triacantha	10	15.74	-	-
	50	21.13	-	-
	100	27.66	39.76	57.99
	250	42.41	64.57	90.28
	500	65.81	-	-
	600	-	-	-
M. Sp.	10	13.19	-	-
	50	21.84	25.71	30.49
	100	31.91	67.11	70.85
	250	46.52	-	-
	500	64.68	-	-
	600	68.65	-	-
B. Aurea	10	12.91	-	-
	50	13.33	-	-
	100	15.74	51.12	49.48
	250	23.26	79.37	75.78
	500	33.33	-	-
	600	38.44	-	-
Trolox	10	31.77	-	-
	50	38.86	-	-
	100	49.50	-	-
	200	64.25	-	-
	300	77.16	-	-
	400	87.51	-	-
	500	93.33	-	-

Figure 1: **Percentage of inhibition of the ABTS method for the four plant extracts according to the extraction method.**

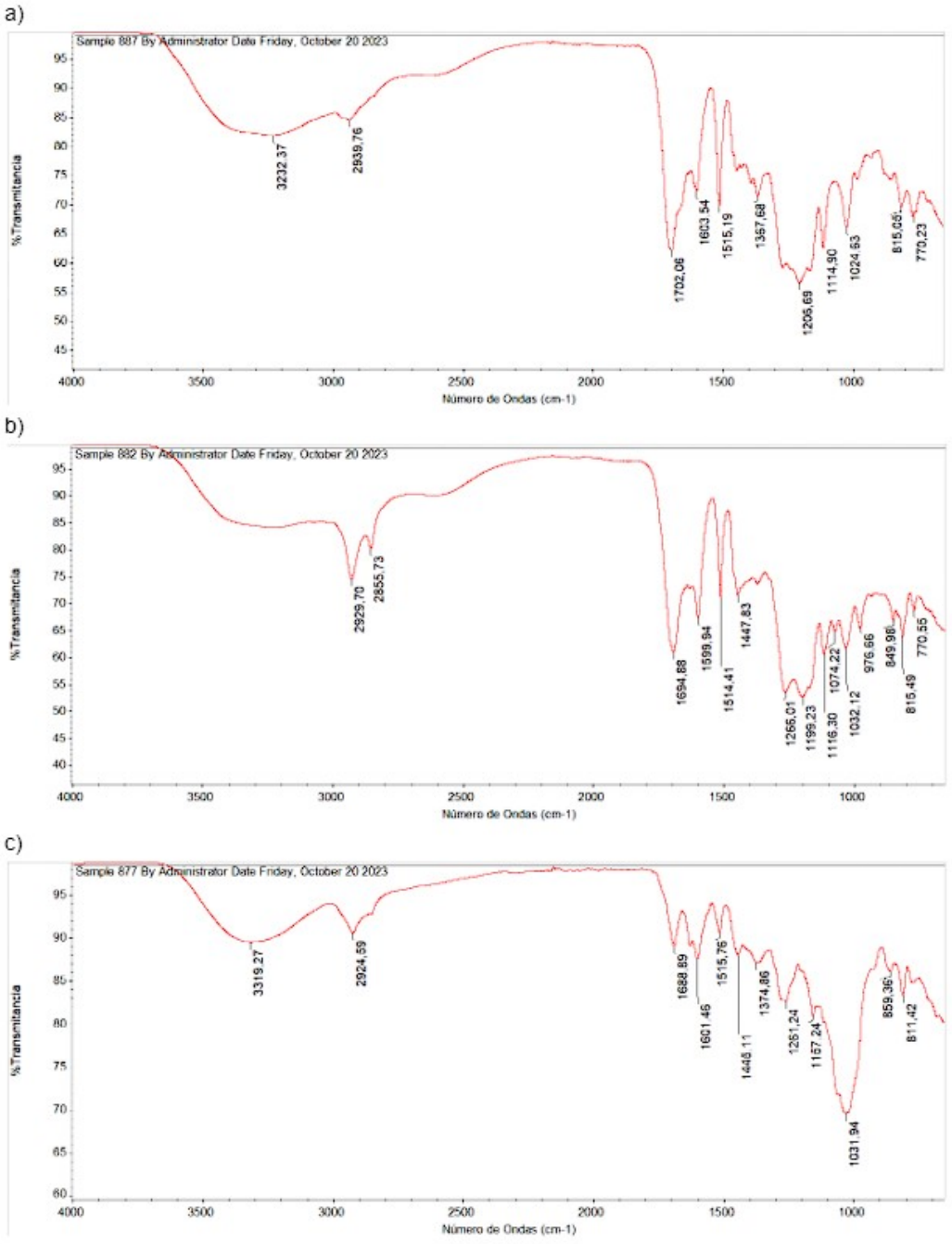

Figure 2: **Ir-Spectrum of different extraction methods for Duranta triacantha.**

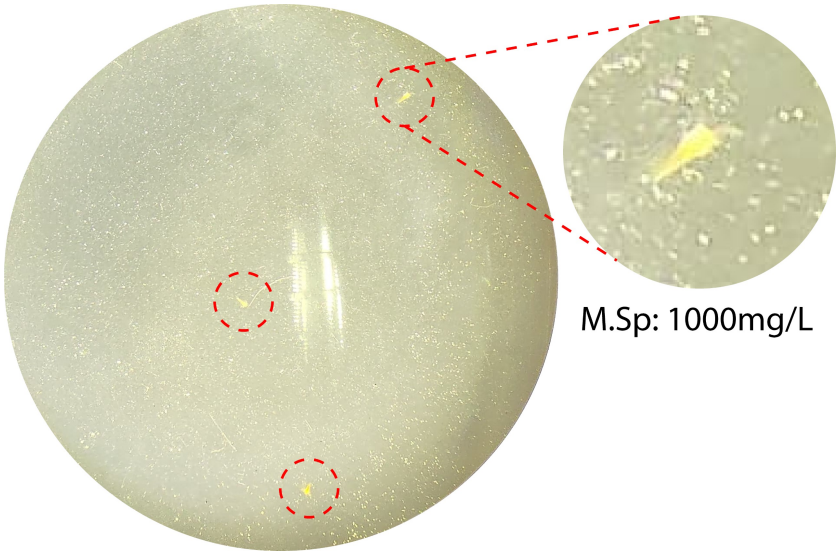

Figure 3: **Mortality of brine shrimps at a concentration of 1000 mg/L for the methanolic extract of Mikania Sp.**

References

[1] Neagu, O. M., Ghitea, T., Marian, E., Vlase, L., Vlase, A. M., Ciavoi, G., Fehér, P., Pallag, A., Bácskay, I., Nemes, D., Vicaș, L. G., Teușdea, A., & Jurca, T. (2023)

[2] Dawid-Pać, R. (2013).

[3] Antunes Filho, S., dos Santos, M. S., dos Santos, O. A. L., Backx, B. P., Soran, M. L., Opriş, O., Lung, I., Stegarescu, A., & Bououdina, M. (2023).

Acta Microscopica Vol. 34, Supp. 2, 2025
Abstract Book NSSY 2024 - Galapagos 19-25 May, 2024

Comparative study on methylene blue removal in the presence of eco-friendly adsorbents

Fernando Vega[1], Melanie Cedeño[1], Javier Cevallos[1], Joana Bahamonde[1], Daniela Serrano[1], Julio C. Chacón-Torres[1]

[1] *School of Physical Sciences and Nanotechnology, Yachay Tech University, 100119 Urcuquí, Ecuador.*

fernando.vega@yachaytech.edu.ec

Abstract

Methylene blue (MB) is one of the principal bench markers to evaluate the absorption performance of materials in aqueous solutions. MB is a cationic organic dye used in a wide range of manufacturing activities, including the food, pharmaceutical, and textile industries [1]. Due to its extensive use, effluents from these industries have been discharged into aquatic environments, representing a significant threat to ecosystems and human health [2]. For this reason, the enhancement of methods to decrease the concentration of MB is crucial. Adsorption stands out as a cost-effective, easily handled, and non-toxic method with selective adsorption capabilities, making it highly attractive for MB removal [3]. In this study, a comparative analysis of MB removal performance with different adsorbents was carried out. Four main eco-friendly adsorbents were studied: (i) Hard carbon (HC) synthesized from coconut shell, (ii) Ecuadorian endemic natural clays (clay A and B), (iii) Hydroxyapatite (HAp) synthesized from $CaCl_2$ and $(NH_4)_2HPO_4$, and (iv) Clay-HAp composites (clay@HAp). The composites used during this study were prepared with three different formulations of HAp/clay A and HAp/clay B in proportions of 1:2, 1:1, and 2:1. The samples were first characterized by X-Ray Diffraction (XRD) to determine their crystallographic structure where the characteristic peaks of hydroxyapatite, clays, and the crystalline-amorphous components of hard carbon were found on each case. Raman spectroscopy, Fourier transform infrared spectroscopy (FTIR), and X-ray photoelectron spectroscopy (XPS) were also conducted to provide information on the chemical composition, molecular structure and surface properties of the constitutes for the eco-friendly. The adsorption study was carried out using UV-Vis spectroscopy by exposing the absorbents to methylene blue solutions as a function of time during 2 hours. The results showed that Clay A has potential for MB degradation under dark conditions, achieving a removal efficiency of 72.35%. In a second place, hard carbon revealed a removal efficiency of 60%. These results suggest that the minerals present in Clay A, primarily muscovite, kaolinite and dolomite, exhibit a notable cationic adsorption capacity, promoting enhanced removal of MB. Meanwhile, the HC structure, characterized by

the presence of both graphitic and amorphous components facilitated the formation of active sites for the MB. After two hours, the clay@HAp composites exhibited an efficiency of less than 40%, indicating that, despite a positive interaction between clay and HAp, their synergy does not stimulate the formation of new active sites. Finally, HAp and Clay B showed adsorption capacities lower than 25%, thus showing low affinity towards organic cationic MB dye. Despite the study's limited duration of two hours, the results obtained offer valuable information on the effectiveness of various materials as new bioadsorbents for the removal of methylene blue. Therefore, novel materials are proposed, which possess the essential potential to address current challenges and optimize methodologies for water treatment in a way that is sustainable and scalable.

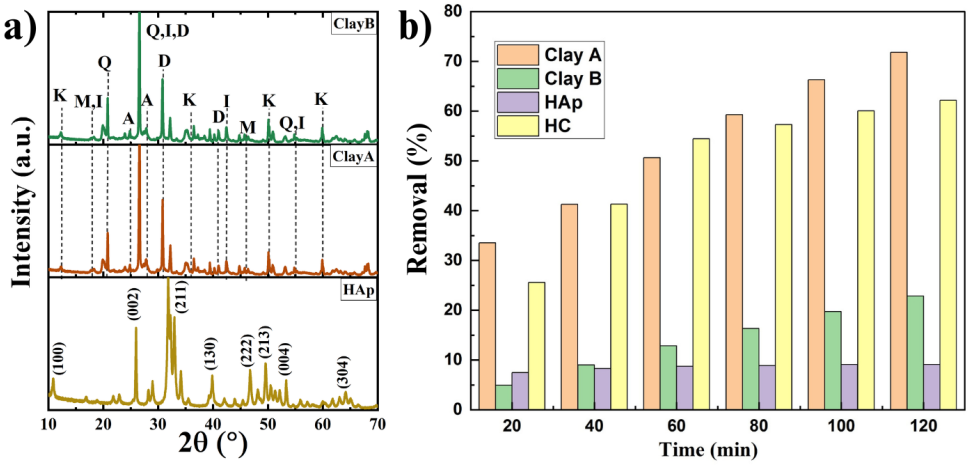

Figure 1: **X-ray and absorbance analisis of pristine materials (a) X-ray diffraction of ClayA, ClayB and Hydroxyapatite (Hap) describing the characteristic peaks of Hap and minerals present in clay A and B. Kaolinite (K), muscovite (M), illite (I), quartz (Q), albite (A), and dolomite (D) are the minerals found in clay A and B. (b) Removal efficiency of MB as a function of time for the different materials as pristine.**

References

[1] I. Khan et al., Review on Methylene Blue: Its Properties, Uses, Toxicity and Photodegradation, Water, vol. 14, n.o 2, p. 242, ene. 2022, doi: 10.3390/w14020242.

[2] P. O. Oladoye, T. O. Ajiboye, E. O. Omotola, y O. J. Oyewola, Methylene blue dye: Toxicity and potential elimination technology from wastewater, Results Eng., vol. 16, p. 100678, dic. 2022, doi: 10.1016/j.rineng.2022.100678.

[3] E. Santoso, R. Ediati, Y. Kusumawati, H. Bahruji, D. O. Sulistiono, y D. Prasetyoko, Review on recent advances of carbon based adsorbent for methylene blue removal from waste water, Mater. Today Chem., vol. 16, p. 100233, jun. 2020, doi: 10.1016/j.mtchem.2019.100233.

Acta Microscopica Vol. 34, Supp. 2, 2025
Abstract Book NSSY 2024 - Galapagos 19-25 May, 2024

Glucose as an emerging precursor for the synthesis of high quality graphene

José D. Pizha[1], HJ Ojeda-Galván[2,3], M Quintana[2,3], Julio C. Chacón-Torres[1]

[1] *Yachay Tech University. School of physical sciences and nanotechnology*

[2] *Universidad Autónoma de San Luis Potosí. Centro de Investigación en Ciencias de la Salud y Biomedicina*

[3] *Universidad Autónoma de San Luis Potosí. Facultad de Ciencias*

jose.pizha@yachaytech.edu.ec

Abstract

Graphene is a two-dimensional sheet of carbon atoms arranged in a honeycomb sp^2 pattern, where valence electrons covalently bond in-plane. This structural arrangement gives graphene excellent thermal conductivity, mechanical stiffness, optical transparency, and high charge carrier mobility. These unique properties make graphene a promising material for various applications, including electronics, energy storage, sensors, and biomedical devices [1]. However, since the pioneering work of Geim and Novoselov in 2004 the main drawback in implementing graphene into electronics has been the high cost and limited yield of production [2, 3]. Thus, there still exist a need for the development of simple methods to prepare high-quality graphene sheets on a large yield. In this work, we propose an alternative method for large-scale production of high-quality graphene sheets by using vaporization and calcination of a glucose within $FeCl_3$. In a beaker, glucose and $FeCl_3$ were dissolved in deionized water obtaining a yellow-colored solution further evaporated resulting in a black solid powder, denoted as $g@FeCl_3$. The material was placed in a small alumina boat and subjected to calcination treatment in a furnace at 1000 °C under an inert environment. The material obtained was characterized using Raman spectroscopy, X-ray photoelectron spectroscopy (XPS), atomic force microscopy (AFM), and transmission electron microscopy (TEM). Raman spectroscopy analyses confirm the presence of graphene's characteristic vibration modes, while AFM and TEM revealed uniform and wide surface mono-layer flakes between 10-20 µm. This indicates high-quality graphene with a large surface area, surpassing common literature results obtained using dicyandiamide as a template for bottom-up graphene synthesis. These findings open novel research venues for understanding the growth mechanism of template-free graphene synthesis. In summary, the present method offers a promising approach for large-scale graphene synthesis, with excellent quality and surface characteristics, using glucose as carbon precursor that could become part of nanostructured biosensising functional devices.

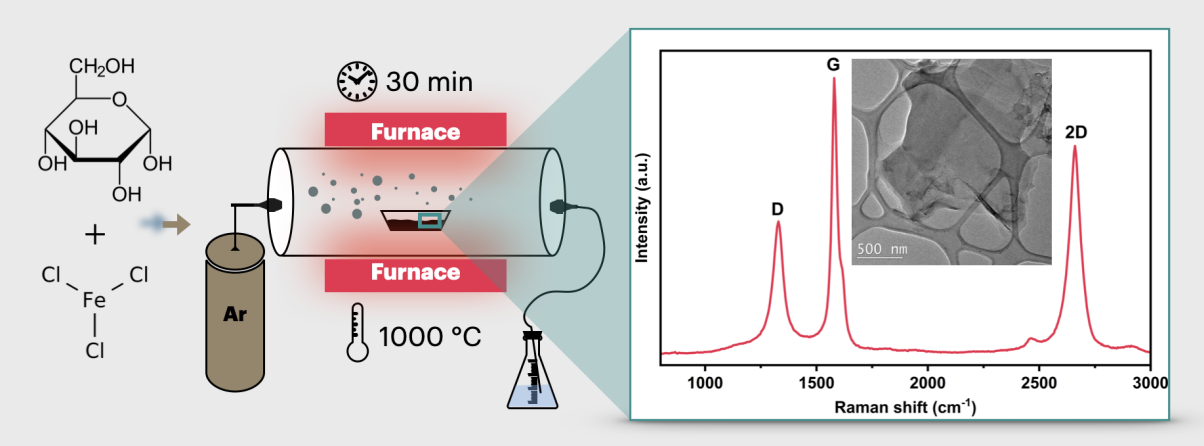

Figure 1: **Illustrates the representative schema of graphene synthesis using glucose and iron chloride via Chemical Vapor Deposition, followed by characterization using Raman spectroscopy and transmission electron microscopy.**

References

[1] Bazylewski P., & Fanchini G. (2019) 1.13-graphene: Properties and applications, Oxford, Academic Press, (pp. 287-304).

[2] Zhang B. et al. (2014). Large-scale production of high-quality graphene using glucose and ferric chloride. Chemical science, 5(12), 4656

[3] Lavin-Lopez M. P. et al. (2015). Thickness control of graphene deposited over polycrystalline nickel. New Journal of Chemistry, 39(6), 4414.

Acta Microscopica Vol. 34, Supp. 2, 2025
Abstract Book NSSY 2024 - Galapagos 19-25 May, 2024

Selenium nanoparticles stabilized in tannic acid: An innovative approach for combating infections caused by H. pylori or Candida albicans

López-Cabaña Zoraya[1], Pariguana- Begazo Manuel[2], Parra-Sepúlveda Cristian[3], González-Gutiérrez Liz[3], García-Cancino Apolinaria[3], Alderete-Triviños Joel[1]

[1] *Biomaterials and Molecular Design Laboratory, Chemistry Institute of Natural Resources, University of Talca, Chile.*

[2] *PhD Program in Science, R&D Bioactive Products, Chemistry Institute of Natural Resources, University of Talca, Chile.*

[3] *Bacterial Pathogenicity Laboratory, Department of Microbiology, Faculty of Biological Sciences, University of Concepción, Chile*

zlopez@utalca.cl

Abstract

Selenium is an essential trace elemental in the diet, required for maintenance of health and growth. Give that the least toxic form of selenium is elemental Se, its nano-form has attracted significant attention. In recent years, selenium nanoparticles (SeNps) attracted the interest of many researchers due to their biocompatibility, bioavailability and low toxicity. Several studies have pointed out the ability of SeNps to exhibit anticancer, antioxidant, antibacterial and anti-biofilm properties. So far, remarkable antimicrobial activity of these nanoparticles have been evidenced against pathogenic bacteria, fungi and yeasts. Metal nanoparticles, for example, gold and silver, have immense medicinal benefits but are costlier to synthesis, whereas the synthesis of SeNps is economical. SeNps have been synthesized in various forms such as nanowires, nanorods and nanotubes through sonochemical, microwave, hydrothermal methods[1]. In humans, fungal and bacterial infections are responsible for causing a wide range of diseases to life-threatening. Infections caused by Helicobacter pylori (H. pylori), a Gram-negative microaerobic bacterium that colonizes the human stomach, it has been associated with gastrointestinal diseases including chronic gastritis, peptic ulcer, gastric carcinoma. On the other hand, Candida albicans is the most common pathogenic fungus that affects the oral cavity, skin, reproductive tract, and gastrointestinal tract. These microbial infections that cause great health concerns are due that most of the pathogenic organisms have become drug-resistant because of the constant utilization of a wide range of antibiotics[2]. In this study, we discuss the synthesis of SeNps using tannic acid as reducing and stabilizing agent, and explores their potential as a novel strategy against bacterial (H. pylori) and fungal (Candida albicans) infections. Tannic

acid, a plant derived polyphenolic compound, is one such agent which embodies characteristics of being harmless and environmentally friendly combined with being a good reducing and stabilizing agent, these gives an eco-friendly agent to the green synthesis of SeNps. The synthesis of SeNps by tannic acid was conducted by interacting a solution of sodium selenite (10 mM) and tannic acid (TA) (6 and 13 mM) under slightly basic conditions (pH=8). The reaction mixture was kept under magnetic stirring at 70°C for 2 h. Following the formation of the red precipitate, this was centrifugate at 1000 rpm for 30 min. Subsequent washed with 70% etanol and acetone were performed to eliminate excess reactants and the solid was dried at 50°C for 2 h. Antibiotic susceptibility was evaluated through the agar dilution method to ascertain the minimum bactericidal concentration (MBC) of Clarithromycin, Metronidazole, Levofloxacin, Tetracycline, and Amoxicillin. Minimum nhibitory concentration (MIC) values were determined based on the ninth version of the European Committee on Antimicrobial. In the well diffusion inhibition assay, wells were made in the agar with a 6 mm sterile punch, which were filled with aliquots of approximately 70 μL of the solutions to be tested at different concentrations. The microbial suspensions used were adjusted to 6x108 CFU/mL and spread on Müeller-Hinton agar plates supplemented with 5% horse blood. The plates were cultured at 37°C under microaerobiosis conditions for 48-72 h. The final halo size was obtained by subtracting the well size (6 mm) from the zone of inhibition. The characteristic absorption band of the SeNps is shown in Figure 1. Appearance of a maximun at 266 nm in the absorption band as well as the red color of the colloidal suspension (Fig. 1, the inset) shows formation de selenium nanoparticles[3]. The XRD pattern of SeNPs has been depicted in Figure 2, which shows broader peak without any sharp Bragg's peaks and thus, it specifies that synthesized red elemental SeNPs is certainly amorphous in nature, which is in agreement with previous reports[1]. The SeNPs exhibited significant antibacterial activity against H. pylori isolates both sensitive and resistant to clarithromycin, with MIC values ranging between 75 and 150 µg/ml as verified in Tabla 1. In general, the MIC of the nanoparticles against clarithromycin-resistant isolates was within the range of 150 µg/ml. This results demonstrate the potential of SeNps as novel antimicrobial agents for the treatment of diseases caused by H. pylori and candida albicans.

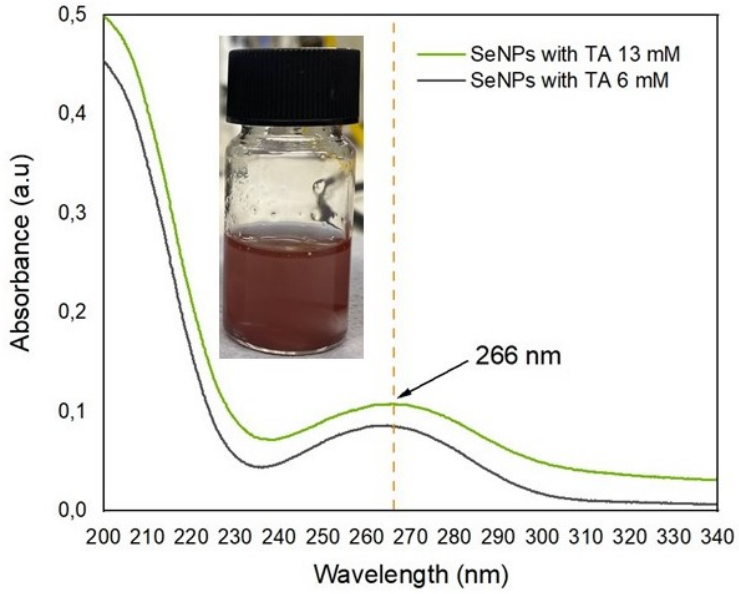

Figure 1: **Absorption spectrum of SeNps. The inset show red color of the colloidal suspension**

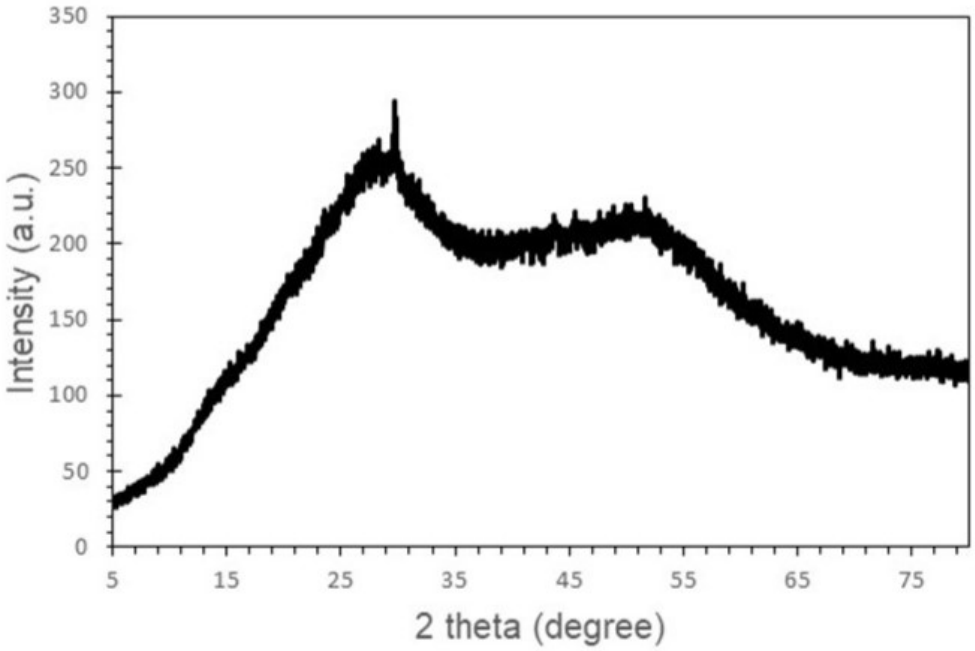

Figure 2: **X-ray diffraction (XRD) pattern of SeNps synthesized with tannic acid 13mM**

	Selenium Nanoparticles	
Pathogenic bacteria	MIC ug/ml	MBC ug/ml
H. pylori ATCC 43504	75	150
H. pylori clinical strain 219A	75	150
H. pylori clinical strain 239A	37,5	75
H. pylori clinical strain 240A	75	150

Figure 3: **Minimum inhibitory concentration and maximum bactericidal concentration in pathogenic strains of H pylor ATCC and clinical strains resistant to antibiotics**

References

[1] Khanna P.K. et al. Mater. Adv. (2022) (3) (1415).

[2] Emran T.B. et al. J. Infection Public Health (2021) (14) (1750).

[3] Moghadam T.T. et al. Nature Research. (2020) (10) (510).

Acta Microscopica Vol. 34, Supp. 2, 2025
Abstract Book NSSY 2024 - Galapagos 19-25 May, 2024

Fabrication: of PVP fibers loaded with CoFe2O4 nanoparticles via electrospinning

Vinicio Javier Cevallos[1], Raúl Dávalos[2,3], Werner Bramer[1], Gema González[1], Sarah Briceño[1]

[1] *Yachay Tech University, School of Physical Sciences and Nanotechnology, 100119 Urcuquí, Ecuador*

[2] *Yachay Tech University, School of Biological Sciences and Engineering, 100119 Urcuquí, Ecuador*

[3] *Biological and Environmental Sciences and Engineering Division, King Abdullah University of Science and Technology (KAUST), Thuwal, Saudi Arabia*

vinicio.cevallos@yachaytech.edu.ec

Abstract

The recent developments in nanotechnology and semiconductors have increased interest in the electrospinning technique and its uses in sensor fabrication. Electrospinning is one of the most powerful and facile fabrication methods for producing organized and complex uniform fibers of synthetic and natural polymers with diameters ranging from micro to nanometers [1]. Polyvinylpyrrolidone (PVP), a synthetic polymer, has taken significant attention due to its highly water/organic solvents-soluble, excellent film formation ability, and non-toxic behavior, which make it one of the most important materials used in paints, electronics, and biomedical engineering [2]. Nowadays, adding nanostructured materials into a polymer matrix provides shorter pathways for electrons transfer along the nanofibers' longitudinal axis, improving sensing performance [3]. The aim of this work is to fabricate nanofibers of PVP loaded with $CoFe_2O_4$ nanoparticles (5, 10, 15, 20, and 25 nm) by electrospinning technique to study the electrical properties of the fiber composites as a potential material for biosensing. The experimental procedure began synthesizing nanoparticles of $CoFe_2O_4$ at different sizes (5, 10, 15, 20, and 25 nm) by hydrothermal method. Then, PVP (Mw 1300000 g/mol) solution at 10 wt% was prepared in ethanol and stirred at 500 rpm for 30 min. Subsequently, $CoFe_2O_4$ (5, 10, 15, 20, 25 nm) nanoparticles were added to the PVP solution and sonicated for 3 minutes 50 seconds with a 90% amplitude. PVP and composite solutions were transferred to electrospinning equipment to obtain nanofibers of each. Structural and composition properties were observed by Optical microscopy, Raman spectroscopy, Fourier Transform Infrared spectroscopy (FTIR), and Thermogravimetric analysis (TGA). The results showed the formation of PVP smooth fibers free from beads loaded with cobalt ferrite nanoparticles. Electrical properties were characterized using a homemade electrical device applying a voltage range from 421 to 100 V. Considering an applied voltage of $\sim$ 421 V, the PVP fibers showed a

resistance of 52.61 GΩ in contrast to PVP/$CoFe_2O_4$ (5,10,15,20,25 nm) composite fibers that exhibited a resistance range from 0.99 to 5.31 GΩ. Subsequently, at a low voltage value of ∼ 100 V, the resistance of PVP fibers could not be measured due to electrons not flowing through the polymer matrix. Nevertheless, PVP/$CoFe_2O_4$ (5,10,15,20,25 nm) showed a resistance range from 1.48 to 7.13 GΩ. It indicates that adding cobalt-ferrite nanoparticles into a polymeric matrix helps electrons flow. Then, an average voltage analysis against the resistance was done where PVP fibers had the highest resistance value (121.58 GΩ) due to their insulating properties. PVP/$CoFe_2O_4$ (5,10,15,20,25 nm) exhibited a resistance reduction of two orders of magnitude, being PVP/$CoFe_2O_4$ (20nm), the composite fibers which had the lowest resistance (1.20 GΩ). To sum up, voltage as a function of resistance characterization analysis showed that the resistance is inversely proportional to the applied voltage, and the electrical properties of PVP are improved when the cobalt ferrite nanoparticles are added.

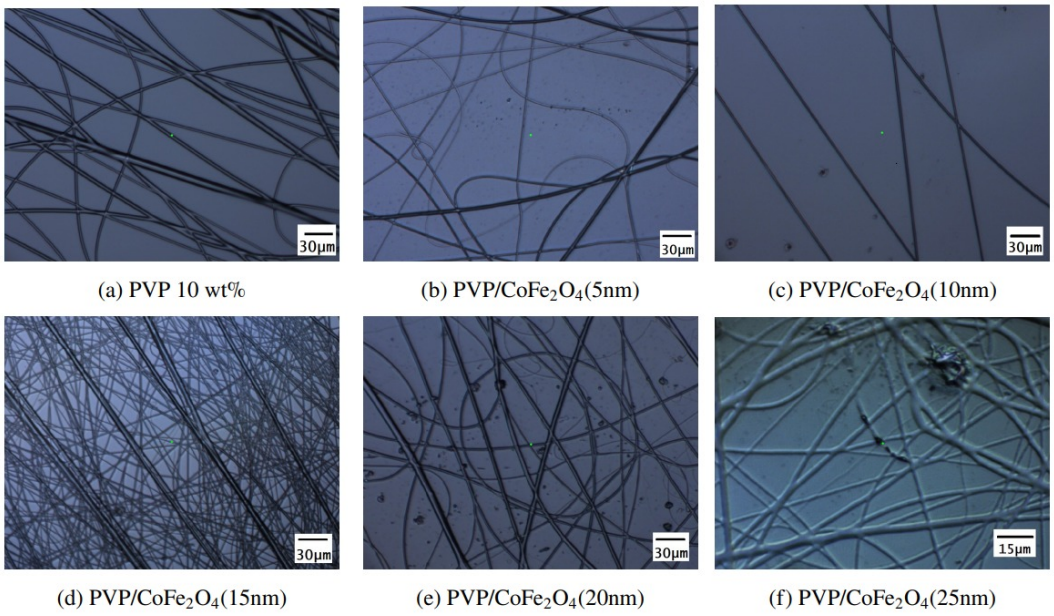

(a) PVP 10 wt% (b) PVP/$CoFe_2O_4$(5nm) (c) PVP/$CoFe_2O_4$(10nm)

(d) PVP/$CoFe_2O_4$(15nm) (e) PVP/$CoFe_2O_4$(20nm) (f) PVP/$CoFe_2O_4$(25nm)

Figure 1: **Optical images of PVP and PVP/CoFe2O4 fibers**

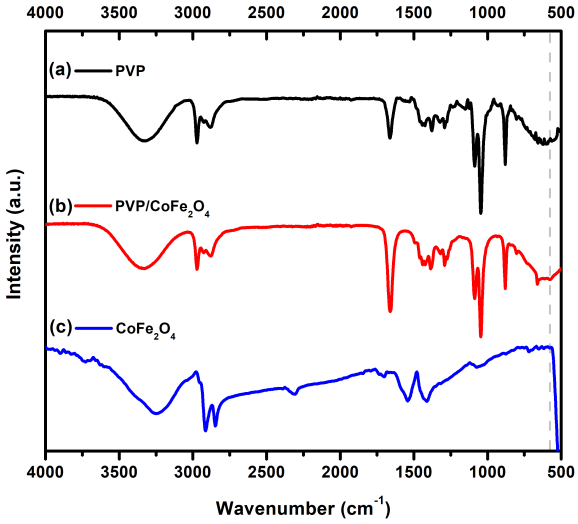

Figure 2: **FTIR spectra of PVP fibers, PVP/CoFe2O4 fibers, and nanoparticles of CoFe2O4.**

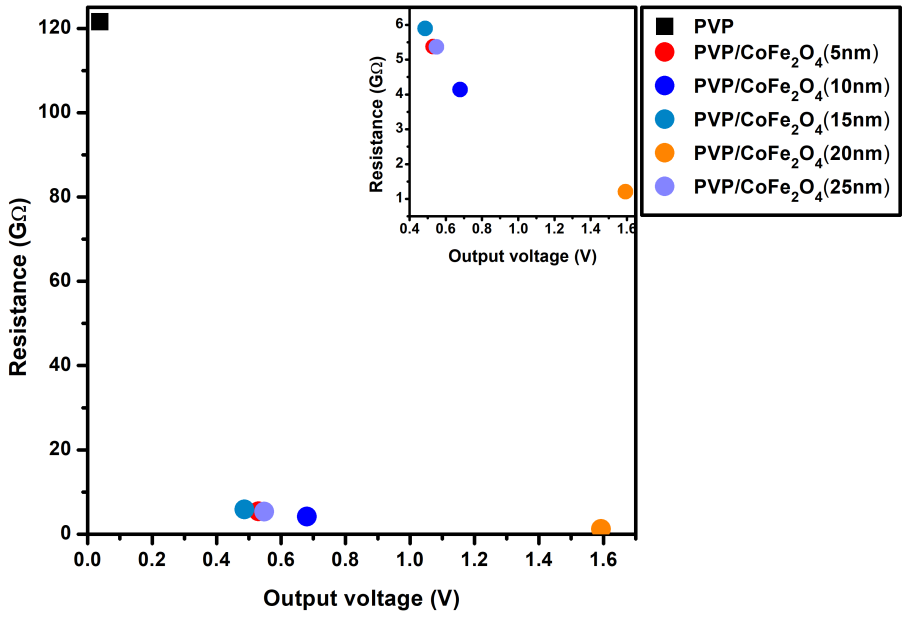

Figure 3: **Average analysis of voltage against resistance of PVP and PVP/CoFe2O4 fibers.**

References

[1] Utkarsh, Hegab, H., Tariq, M., Syed, N. A., Rizvi, G., & Pop-Iliev, R. (2020). Towards analysis and optimization of electrospun PVP (polyvinylpyrrolidone) nanofibers. Advances in Polymer Technology, 2020,1-9.

[2] Dhatarwal, P., & Sengwa, R. J. (2021). Investigation on the optical properties of (PVP/PVA)/Al2O3 nanocomposite films for green disposable optoelectronics. Physica B: Condensed Matter, 613, 412989.

[3] Wang, Z.; Wu, S.; Wang, J.; Yu, A.; Wei, G. Carbon nanofiber-based functional nanomaterials for sensor applications. Nanomaterials 2019, 9, 1045.

Acta Microscopica Vol. 34, Supp. 2, 2025
Abstract Book NSSY 2024 - Galapagos 19-25 May, 2024

Composite Graphene Aerogel Electrodes with Polyaniline for Capacitive Deionization

Suelem Soares dos Santos[1], Evaldo José Corat[1]
[1] *Instituto Nacional de Pesquisas Espaciais*
suelemsoares3609@gmail.com

Abstract

Deionization holds diverse applications, particularly in environmental contexts, where it stands out for adsorption aimed at removing ions from salts and metals in water, employing a simple and low-cost system based on the Helmholtz double layer filling. In other words, it is a technique where ions are attracted and stored on the surface of electrodes, with the electrodes subjected to a constant external voltage or current that attracts ions to the electrode surface. Subsequently, electrode recovery occurs by reversing the electrode polarization or applying a short circuit.

The electrodes commonly used are based on carbon materials due to the formation of electrical double-layer capacitance (EDLC), resulting in the formation of the Helmholtz double layer at the electrode-electrolyte interface, allowing for the electrostatic storage of charges. Various forms of carbon have been investigated for the electrosorption of electroactive materials, including activated carbon, activated carbon fabric, titania-modified carbon cloth, carbon felt, carbon black, sintered activated carbon, carbon nanotubes, and carbon aerogels.

Carbonaceous material is highly attractive for electrode production due to its extensive surface area, providing a higher quantity of active sites for charge storage during the ionic adsorption process, in addition to being cost-effective. These are often enhanced using conductive polymers and transition metal oxides to increase energy efficiency and adsorption capacity through faradaic charge resulting from rapid electrochemical reactions.

The use of conductive polymers stands out as one of the most promising approaches due to their high theoretical charge storage capacity and good conductivity, which are highly beneficial for improving the energy efficiency of the process. Polyaniline (PAni) is a conductive polymer with different oxidation states and electrochromic properties that vary with the potential of each state, known as fully reduced leucoemeraldine (containing only nitrogens as amines), fully oxidized pernigraniline (containing nitrogens as imines), and base emeraldine, which is partially oxidized and can be converted to emeraldine salt through protonation with organic or inorganic acids. Additionally, PAni has great prospects in adsorption applications because the inherent cationic amine groups and imine groups in

polymeric chains can electrostatically interact with anionic pollutants.

Electrodes containing PAni were developed with the aim of enhancing conductivity and charge storage in electrodes for capacitive deionization. This is because the redox reactions that occur in the polymer involve the faradaic electron transfer process, generating pseudocapacitance in carbon-based electrodes, thus increasing the specific capacitance of these materials.

This work involved the production of graphene aerogel, a low-density carbonaceous material with a wide surface area, good electrical conductivity, and specific capacitance, for electrode production by using it as a base material. Subsequently, an electrochemical deposition of PAni was performed on the material to form the composite.

Morphological analysis of the samples was investigated by Field Emission Scanning Electron Microscopy (FEG-SEM) (TESCAN MIRA 3), composition analysis by Energy Dispersive Spectroscopy (EDS) (Oxford/X-Max) at 5 kV, and structural analysis by Raman Spectroscopy (Horiba Scientific LabRAM HR Evolution) using a 514 nm wavelength excitation laser. Electrochemical characterization was conducted on an AUTOLAB potentiostat from Metrohm (PGSTAT-302N) with NOVA version 2.1.6 software used for data acquisition.

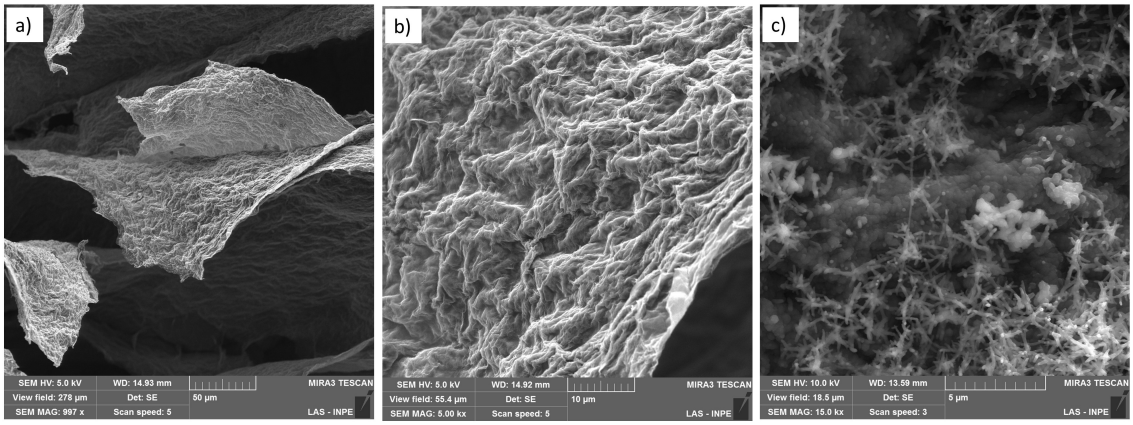

Figure 1: **Scanning Electron Microscopy. a) and b) graphene aerogel at different magnifications, c) graphene aerogel with electro-deposited PAni.**

Acta Microscopica Vol. 34, Supp. 2, 2025
Abstract Book NSSY 2024 - Galapagos 19-25 May, 2024

Alginate-based encapsulation for enhanced Rss51 phage delivery: A sustainable approach to combat Ralstonia solanacearum

Chilcañan-Ramos, M.[1], Anrango-Méndez A.[1], Guerrero-Haro, M.[1], Motoche-Monar C.[1], Castillo, J.A.[1], Camacho-Casanova F.[2]

[1] *School of Biological Sciences and Engineering, Yachay Tech University, Urcuquí 100115, Imbabura, Ecuador*

[2] *Department of Pharmacology, School of Biological Sciences, Universidad de la Concepción, Concepción, Chile.*

mayra.chilcanan@yachaytech.edu.ec

Abstract

Bananas, potatoes, and tomatoes collectively serve as cornerstones of the Ecuadorian economy, accounting for a significant portion of cultivated land. Specifically, bananas (Musa paradisiaca sp., AAB Simmonds) contribute 20.57% of this land, ranking as the country's second most significant perennial crop [1]. However, managing R. solanacearum, a pathogen affecting all banana varieties, as well as potatoes and tomatoes, poses a formidable challenge in today's agricultural sector. This pathogen is notorious for inducing Banana Moko, accelerating plant wilting, inhibiting growth, triggering vascular necrosis, and ultimately causing extensive losses in nearly entire banana plantations by colonizing the vascular system of the plants. This challenge profoundly impacts the country's economy and its citizens, given the pivotal role of bananas, potatoes, and tomatoes in exports.

While traditional chemical alternatives exist, they are fraught with limitations and raise environmental and health concerns for farmers. In light of these challenges, phage therapy emerges as a promising approach, harnessing the unique ability of bacteriophages to selectively infect and destroy specific bacteria. However, the susceptibility of these phages to environmental conditions prompts the need for innovative solutions. Thus, this study proposes an innovative strategy that explores the versatility of alginate, a copolymer abundant in seaweed and certain bacteria. Alginate's unique features, such as biocompatibility, biodegradability, and non-toxicity, make it an ideal material for developing encapsulation systems [2]. Utilizing alginate, we aim to design beads as carriers for phages to investigate their potential impact upon release in banana crops. This approach aims to enhance the stability and effectiveness of phage delivery to the environment, prolonging their shelf life. Additionally, it provides a controlled release mechanism, optimizing phage dissemination in the crop environment. This offers a sustainable and environmentally friendly solution, addressing the limitations of conventional chemical methods.

To encapsulate phages (fig 1), a 2% alginate solution was prepared, to which Rs551 phages were added. This alginate/phage solution was then meticulously added drop by drop into a CaCl2 solution using sterilized pipettes [3]. The resulting beads were filtered for subsequent use. The gel-forming nature of alginate effectively entraps the phages, enabling a controlled release and interaction with pathogens. Finally, the stability of the encapsulated phages was assessed by storing them at different temperatures. At a 2% alginate concentration, we observed a higher phage diffusion rate and superior mechanical characteristics, including a diameter of approximately 4.7 mm, pores with an average diameter of 148 micrometers, and excellent stability. This formulation successfully encapsulated Rs551 phages, measuring about 1200 nm in length and 7 nm in width. The Rs551 phage was encapsulated and stored at 4 degrees Celsius and diffusion tests were conducted for encapsulated phages.

The encapsulated phage exhibited stable viability at 4 degrees Celsius but lost potency after 30 days. This suggests the encapsulation process influenced storage requirements, warranting further investigation for optimized storage conditions, improving mechanical properties of the alginate beads, and finally exploring this phage delivery mechanism in plants. Overall, phage encapsulation with an alginate solution emerges as a promising and eco-friendly strategy for combating agricultural pathogens, contributing to the advancement of sustainable agricultural practices.

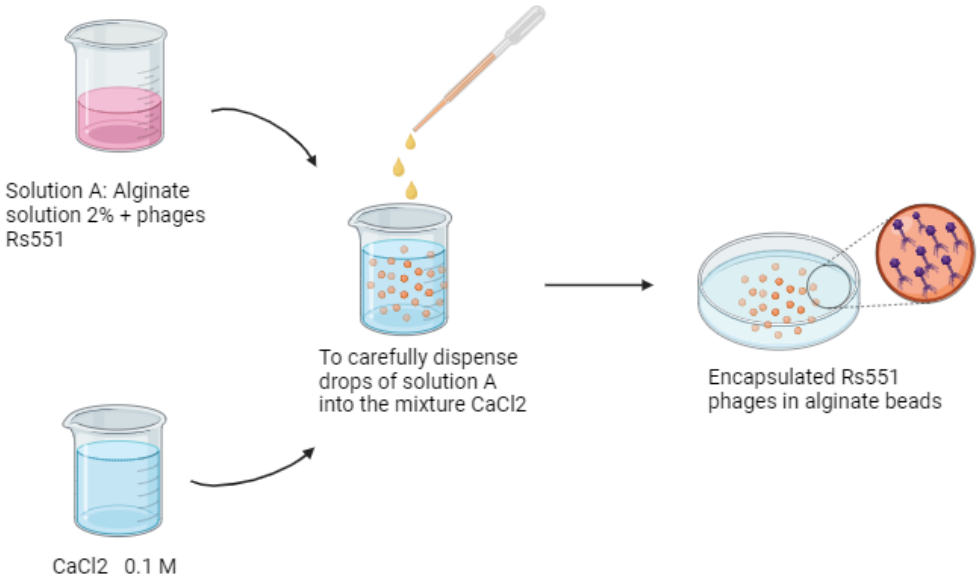

Figure 1: **Rs551 phages encapsulation methodology.**

References

[1] Prior, P., Ailloud, F., Dalsing, B.L. et al. Genomic and proteomic evidence supporting the division of the plant pathogen Ralstonia solanacearum into three species. BMC Genomics 17, 90 (2016). https://doi.org/10.1186/s12864-016-2413-z

[2] R. Abka-khajouei, L. Tounsi, N. Shahabi, A. K. Patel, S. Abdelkafi, and P. Michaud, "Structures, Properties and Applications of Alginates," Marine Drugs, vol. 20, no. 6. MDPI, Jun. 01, 2022. https://doi.org/10.3390/md20060364

[3] Blas Chumacero, S. (2023).Encapsulación de fagos en perlas de alginato para el delivery de fagoterapia en acuicultura contra vibrios. Disponible en https://repositorio.uchile.cl/handle/2250/194462.

Acta Microscopica Vol. 34, Supp. 2, 2025
Abstract Book NSSY 2024 - Galapagos 19-25 May, 2024

Wednesday

Poster Session

Acta Microscopica Vol. 34, Supp. 2, 2025
Abstract Book NSSY 2024 - Galapagos 19-25 May, 2024

Synthesis and Reduction of Strontium Sulfate for Phosphorescence Application with Underproduction of Aluminates

Francia Reyes-Grajeda[1], Javier Morales-Mendoza[2]

[1] *Universidad Tecnológica de Chihuahua Sur. Nanotechnology Department*

[2] *Centro de Investigación de Materiales Avanzados. Materials engineering and chemistry.*

franciareyesmrg@gmail.com

Abstract

Mexico is the third place in the world in the production of celestite, which is made up of 98% strontium sulfate (SrSO4), a ceramic material that, among its applications, is used to produce strontium carbonate (SrCO3). They also have functional applications, as in the case of strontium chromate and strontium chloride, applied in pigments and toothpastes respectively. These compounds are also obtained with reduced strontium sulfate, in the form of strontium sulfide (SrS). Strontium has thermoluminescent properties, so it maintains applications in this branch, in addition, it is an element that, in its base form, is usually reactive, which gives it prominence in applications such as fireworks and flares (Secretaría de Economía, 2013).

While the feasibility of the material continues to be investigated, it is also looking for ways to produce it where it has a lower environmental impact, since current reduction processes, such as direct synthesis and black ash, lead to carbon emissions and high energy levels for good performance (Kang and Lee 2021).

Currently, as reduction and processing options, thermometallic and mechanical milling reductions are in the focus of research, which are based on using a metal as a reducing agent in a system at elevated temperatures to initiate and continue the reaction, in addition, these metals will be used as by-products in the form of metal oxides (Takacs 2002); Mechanical grinding, due to the high levels of kinetic energy it contains in its cycles, is considered as a viable means and method for reducing compounds. The most accessible precursor metals for this type of process are aluminum (Al) and magnesium (Mg) (Setoudeh and Welham 2012). However, the recycling of aluminium today is a mainstay for the world's ecology, so in this proposal, a focus is given to this same element.

Strontium (Sr) is known to be sensitive to reacting exothermicly, which helps in this type of procedure, but means that the process must be operated cautiously,

especially with magnesium, which shares this character. However, aluminum, as a reducing agent in this methodology, has not presented a concise phase, but produces various by-products such as aluminates and other tertiary compounds, rather than a particular obtaining of reduced strontium sulfate, and alumina (Al2O3) (Setoudeh and Welham 2011).

SrSO4 could not be obtained in its mineral form, so it was synthesized by two methods: one solid and one solid-liquid.

The reduction was tested in times starting at 20 minutes, and was successfully achieved in times greater than 50 minutes. Where the formation of an aluminate is observed, and a successful reduction; In these experiments, various characterization tests were carried out, such as X-ray diffraction, physical-optical analysis, and Rietveld refinements, which verified the composition of the samples, in addition, the amount of each of them was verified by making a solution with agitation and temperature, being 53% of the Strontium Sulphate and 47% of the aluminate obtained.

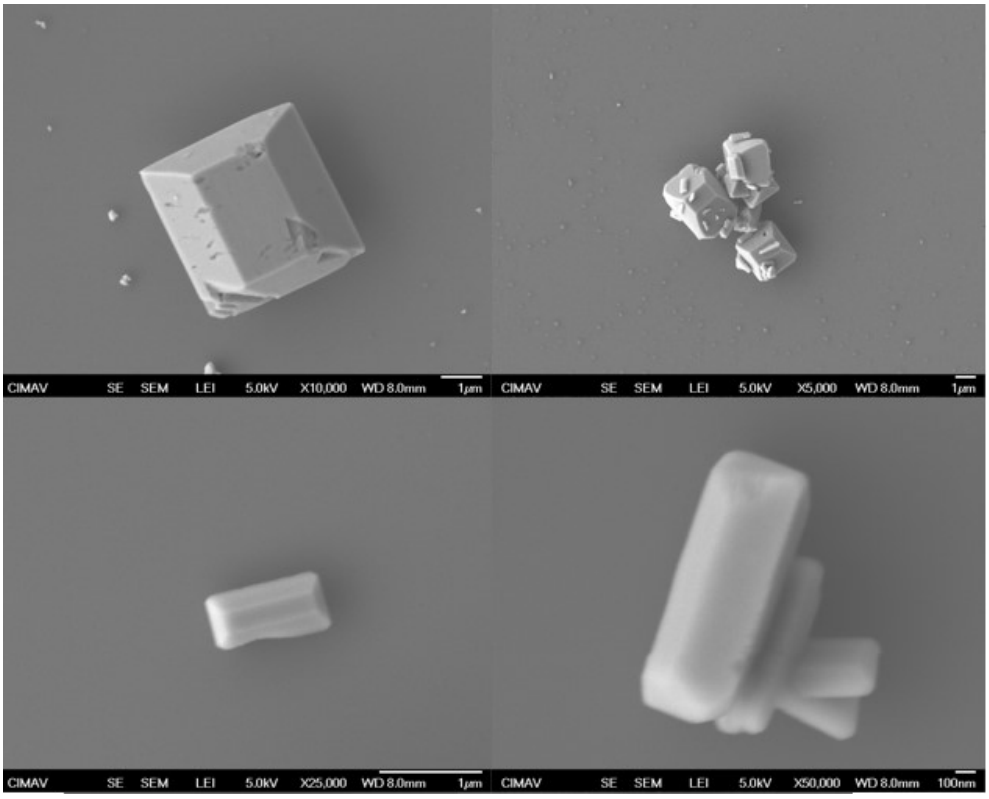

Figure 1: **Obtained Strontium Sulfate Morphology.**

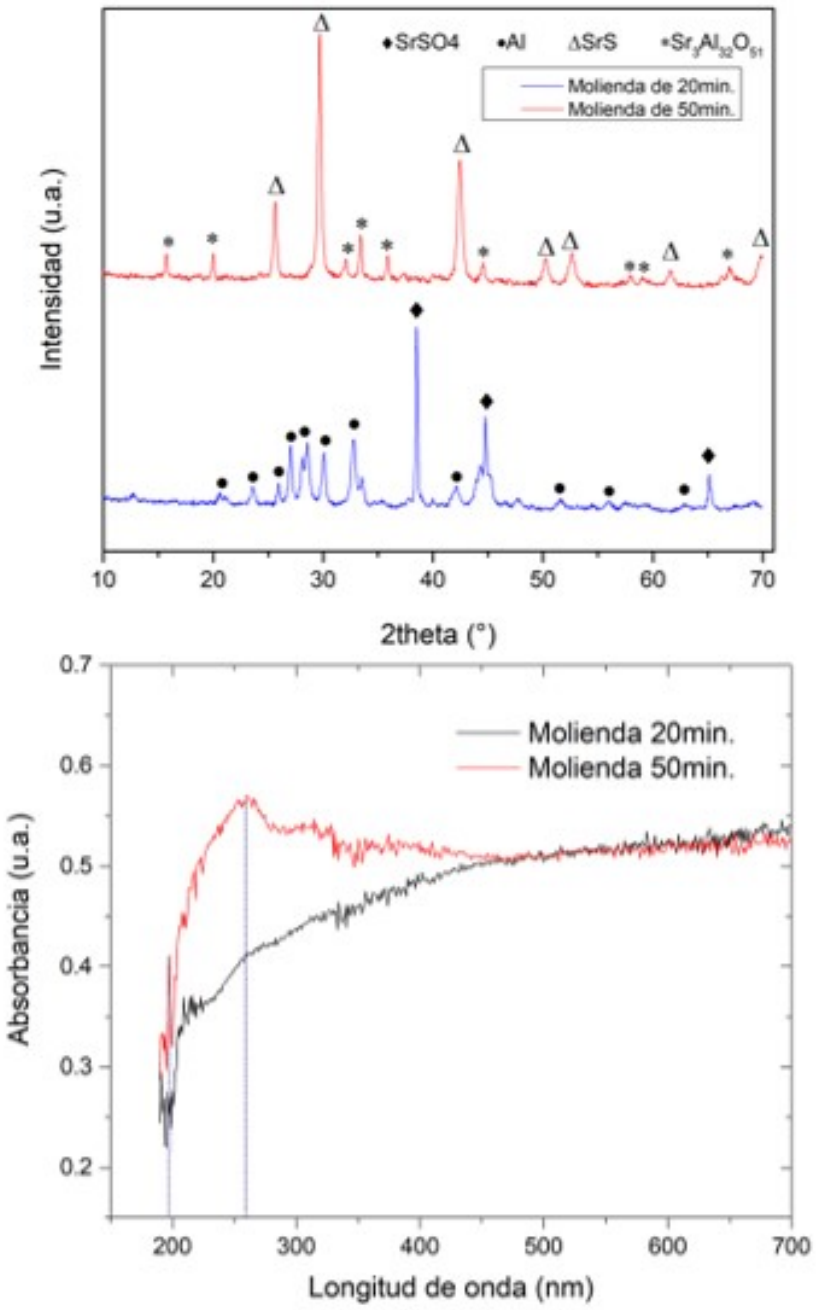

Figure 2: **X-Ray diffraction of the obtained strontium sulfate.**

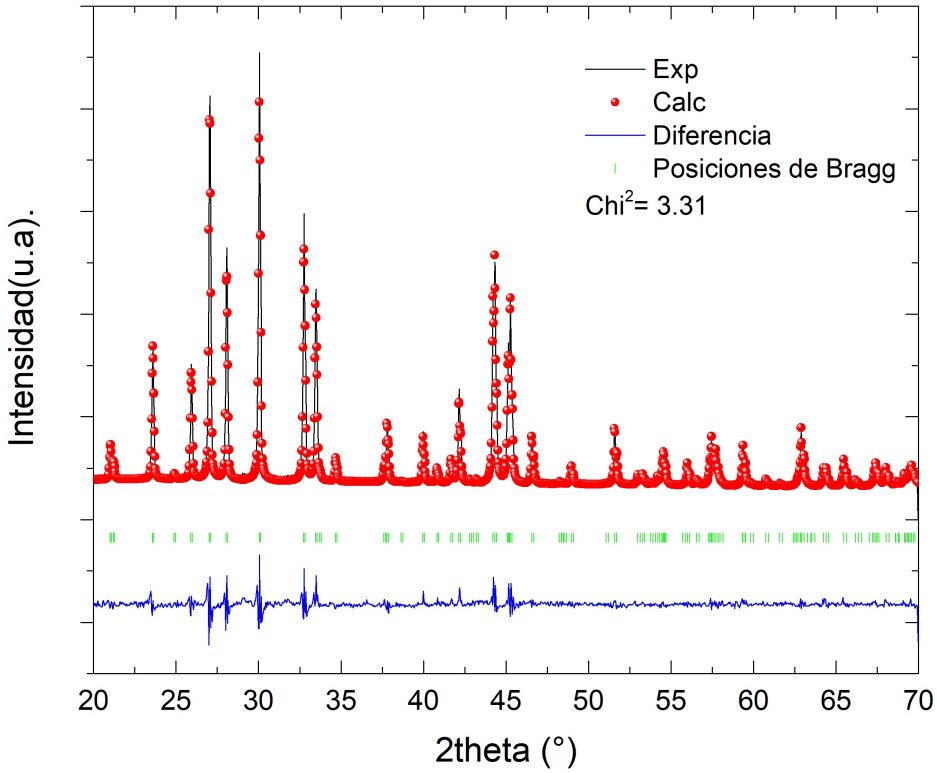

Figure 3: **Comparison of the mechanical grinding, x-ray diffraction pattern and UV-Vis absorption test.**

References

[1] Kang, Jungshin, and Jin-Young Lee. 2021. "Production of SrCO3 from SrSO4 through the Black Ash Process." Resources Recycling 30(5):49–56. doi: 10.7844/kirr.2021.30.5.49.

[2] Secretaría de Economía. 2013. Perfil de Mercado de La Celestita.

[3] Setoudeh, N., and N. J. Welham. 2011. "Ball Milling Induced Reduction of SrSO4 by Al." International Journal of Mineral Processing 98(3–4):214–18. doi: 10.1016/j.minpro.2010.12.002.

Acta Microscopica Vol. 34, Supp. 2, 2025
Abstract Book NSSY 2024 - Galapagos 19-25 May, 2024

Advancing zinc-air battery technologies: exploring the impact of novel drying strategies and potassium hydroxide concentrations in the electrochemical properties of CMC-CS-CA hydrogels as electrolytes

María Fernanda Bósquez-Cáceres[1,2], María Isabel Cruz-Balaz[1], Vivian Morera[1], Marvin Ricaurte[1], Lorena Álvarez-Contreras[3], Juan P. Tafur[1,4]

[1] *Grupo de Investigación Aplicada en Materiales y Procesos (GIAMP), School of Chemical Sciences and Engineering, Yachay Tech University, Urcuquí 100119, Ecuador*

[2] *School of Physical Sciences and Nanotechnology, Yachay Tech University, Urcuquí 100119, Ecuador*

[3] *Centro de Investigación en Materiales Avanzados S. C., Complejo Industrial Chihuahua, Chihuahua C. P. 31136, Mexico*

[4] *Departamento de Ingeniería Mecánica, Química y Diseño Industrial, Escuela Técnica Superior de Ingeniería y Diseño Industrial (ETSIDI), Universidad Politécnica de Madrid (UPM), Ronda de Valencia 3, 28012 Madrid, Spain*

mbosquez@yachaytech.edu.ec

Abstract

With the rapid increase in demand for energy with a flexible and portable approach, electrolytes are one of the limiting components of electrochemical energy storage devices that are receiving more attention as their physical and chemical properties play a vital role in the device's performance. Hydrogel-based electrolytes are emerging as novel materials for cell's use due to their diverse 3D porous network, flexible structure, and tunable properties. In the present work, the hydrogel composed of carboxymethylcellulose (CMC) and chitosan (CS) biopolymers, and citric acid (CA) chemical crosslinker has been synthesized using two independent drying techniques: casting process, and freezing-thawing strategies with subsequent lyophilization process. The latter approach of freezing strategies lead to the development of microporous structures through the formation of crystallites, intending to increase the absorption and chemical crosslinking capacity [1]. These biopolymers are capable of forming intermolecular complexes that lead to hydrogels that absorb ionic solutions, such as potassium hydroxide, used as an ion source to improve the ionic conductivity of the system, so that the conduction process can occur. Hence, the prepared hydrogels were soaked in two different molar concentrations (8M and 12M) of potassium hydroxide (KOH) for 24 h to form ionic conductor hydrogel electrolytes. Subsequently, structural characterization tests of FTIR, TGA, SEM and swelling behavior were carried out to analyze and contrast the proposed syn-

theses' effects on the hydrogels' performance for the desired application. The structural characterization confirmed adequate doping between the ionic salt and the hydrogels. SEM micrographs showed the highly porous morphology of the lyophilized hydrogel in comparison to its casting counterpart that exhibited a chapped surface with granules, pleats, and few orifices. The membranes were electrochemically evaluated through PEIS and CV techniques. Through electrochemical characterization, an increase in ionic conductivity and current is evident when the cross-linked hydrogels were immersed in the ionic solutions. The maximum ionic conductivity achieved was 0.65 S/cm by the $L50_8M$ hydrogel at 30 °C. Finally, the hydrogels were tested in a zinc-air battery (ZAB) prototype, obtaining a specific capacitance of 2045 mAh/g for the $L50_8M$ hydrogel (Figure 1). Furthermore, the results demonstrate the promising potential of these hydrogels as electrolytes for green storage devices and highlight the importance of carefully considering the drying strategies, the soaking time, and KOH concentration when designing and developing next-generation ZABs.

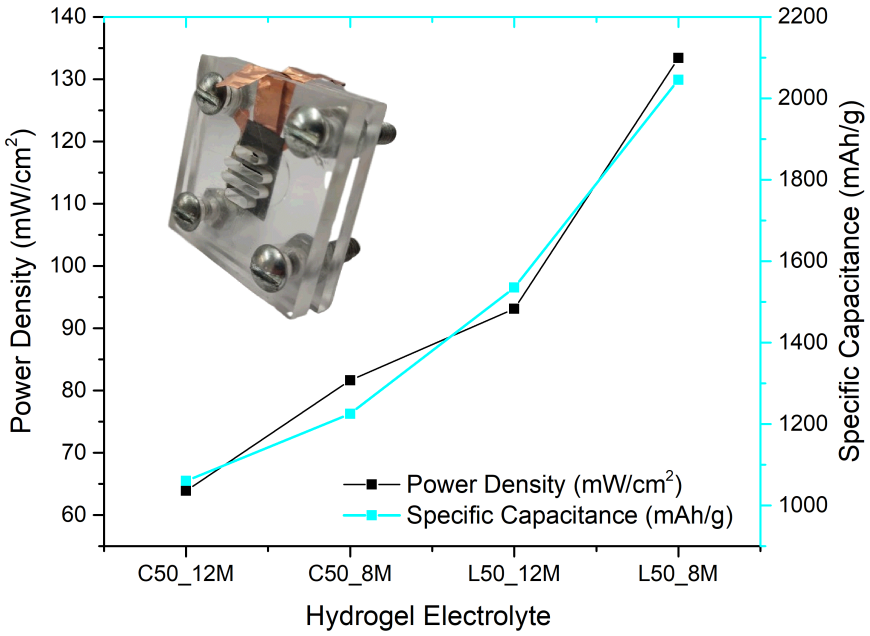

Figure 1: **Power density and specific capacitance values for the batteries operated with Zn foil as anode and Pt/C as cathode with the synthetized hydrogels.**

References

[1] Bósquez-Cáceres, María Fernanda, et al. "Enhancing Electrochemical Performance of Zinc-Air Batteries Using Freeze Crosslinked Carboxymethylcellulose-Chitosan Hydrogels as Electrolytes." J. Electrochem. Soc. 170(6), (2023): 060502. https://doi.org/10.1149/1945-7111/ACD876.

Acta Microscopica Vol. 34, Supp. 2, 2025
Abstract Book NSSY 2024 - Galapagos 19-25 May, 2024

Bound States Solutions to the Klein-Gordon equation for spin-zero particles with the Woods-Saxon potential well

Alexis Garzón[1], Clara Rojas[1]
[1] *School of Physical Sciences and Nanotechnology, Yachay Tech University, Urcuqui*
alexis.garzon@yachaytech.edu.ec

Abstract

In the study of particles that move close to the speed of light, the complex theory of Relativistic Quantum Mechanics is employed. These relativistic wave equations enable us to comprehend various phenomena such as bound states, transmission resonances, and superradiance. In this theoretical framework, the Klein-Gordon (KG) equation is the most used equation to describe spin-zero particles (spinless bosons), since its scalar function and it does not possess any internal degrees of freedom, that is the case of the Higgs boson. Discovered at the Large Hadron Collider (LHC) at CERN in 2012, the Higgs boson is a fundamental scalar boson with a mass of 125 GeV [1]. The Klein-Gordon equation is solved in the presence of a spatially one-dimensional Woods-Saxon potential well to obtain the bound state solutions, and discussions are held on the pair creation mechanism and the antiparticle bound state.

The Woods-Saxon potential well used in this study is illustrated in Fig. 1. For a given value of the width parameter L, as the shape parameter 'a' increases, it plays a crucial role because it exhibits a smoothed-out form of the square well potential [2]. This choice of potential brings about several advantages. Notably, the one-dimensional Klein-Gordon equation becomes solvable in terms of special functions, significantly enhancing the tractability of studying bound states and scattering processes [3].

The one-dimensional Klein-Gordon equation to be solved is expressed in natural units. The bound state solutions are considered for values less than zero and greater than zero, facilitating the selection of regular wave functions to determine the corresponding energy eigenvalues. In this short-range potential, negative solutions can be correlated with the spontaneous production of experimentally observable antiparticles, thus emphasizing the Klein-Gordon theory as a valuable generalization of Schrödinger's theory [4].

The obtained results indicate a turning point, as shown in Fig. 2, at a specific value of V_0, where a bound antiparticle state emerges and subsequently merges with the bound particle state. This forms a state with zero norm at $V_0 = V_{cr}$, ultimately vanishing from the spectrum [2]. The numerical solutions of the energy equation

were obtained using FindRoot in Mathematica, exploring various potentials and restricting the analysis to a short range ($2.34620 < V_0 < 2.34630$) to observe the intriguing phenomenon of the vanishing spectrum. The comprehensive exploration of these theoretical concepts and numerical results contributes to the broader understanding of particle behavior at relativistic speeds within the framework of Quantum Mechanics.

In conclusion, applying Relativistic Quantum Mechanics and the Klein-Gordon equation is essential for understanding the behavior of spin-zero particles, as exemplified by the Higgs boson discovered at CERN. Using a Woods-Saxon potential well improves tractability, revealing its smoothed shape with the 'a' shape parameter. The resulting bound-state solutions, analyzed for both positive and negative values, provide insights into the spontaneous production of antiparticles. The observed turning point and subsequent vanishing spectrum at $V_0 = V_{cr}$, as illustrated in Fig. 2, emphasize the significance of the Klein-Gordon theory. The numerical solutions obtained further contribute to our comprehensive understanding of particle dynamics at relativistic velocities within the framework of Relativistic Quantum Mechanics.

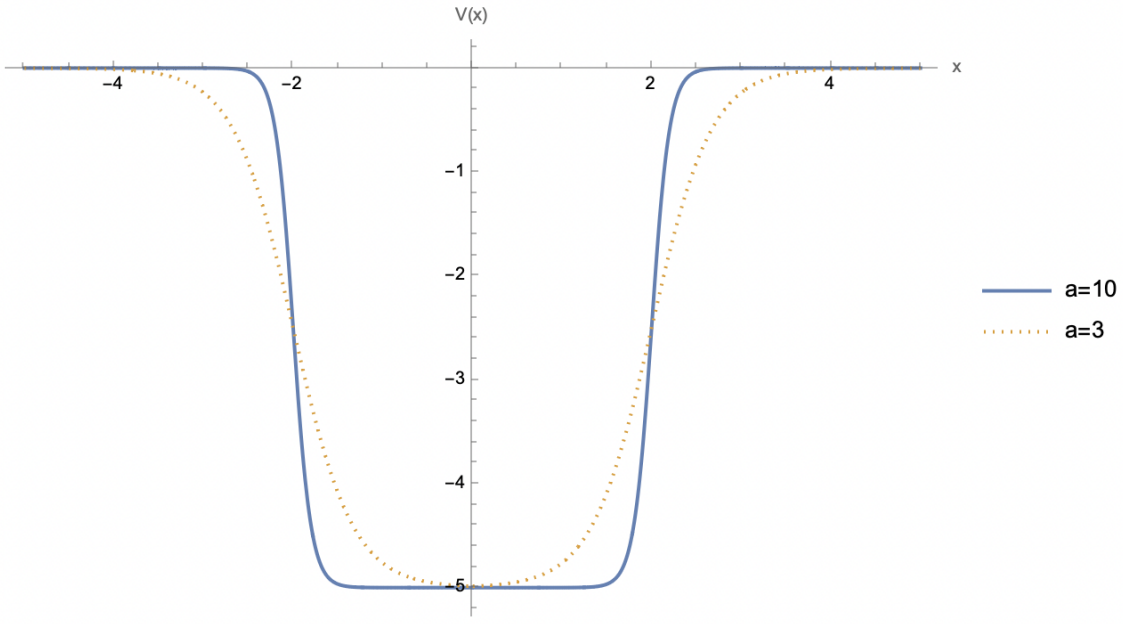

Figure 1: **The Woods-Saxon potential barrier for L = 2 with a = 10 (solid line) and a = 3 (dotted line).**

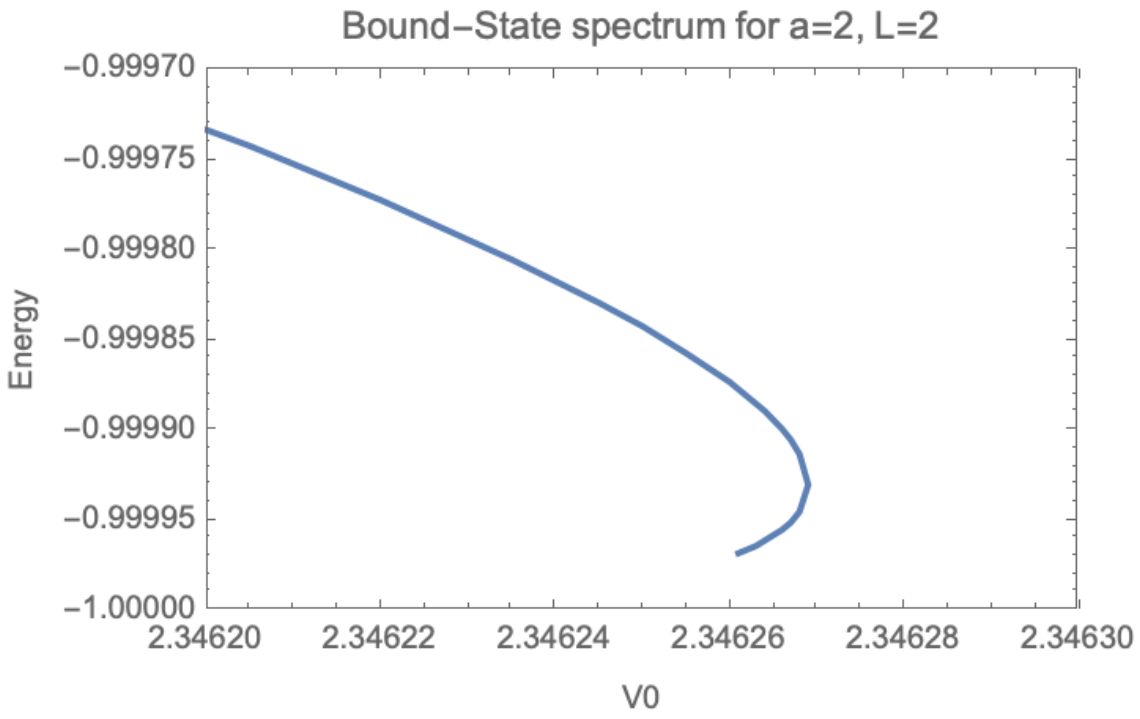

Figure 2: **Bound-state spectrum for L = 2 and a = 2.**

References

[1] Bass, S.D., De Roeck, A. & Kado, M. The Higgs boson implications and prospects for future discoveries. Nat Rev Phys 3, 608–624 (2021). https://doi.org/10.1038/s42254-021-00341-2

[2] Rojas, C., & Villalba, V. M. (2006). The Klein-Gordon equation with the Woods-Saxon potential well. Revista mexicana de física, 52, 127-129.

[3] Gonul, B., & Koksal, K. (2006). A note on the Woods-Saxon potential. arXiv preprint nucl-th/0605077.

3D Raman spectroscopy as novel detection tool for simulated epidermal tissues

Joselin E. Guananga[1], Samantha V. Loor[1], Julio C. Chacón-Torres[1]

[1] *School of Physical Sciences and Nanotechnology, Yachay Tech University, Urcuquí 100119, Ecuador.*

joselin.guananga@yachaytech.edu.ec

Abstract

The application of Raman spectroscopy on epidermal polymers emerges as a promising tool for characterization, resembling simulated tissues. This study focuses on implementing 3D mapping using Raman spectroscopy in epidermal polymers, with the potential to explore their capabilities in cancer detection using carbon nanotubes as biomarkers, by acting as biological indicators, they not only offer greater precision in the identification of possible signs of cancer, but also open new perspectives for the advancement of biomedical research [**?**]. This work aims to analyze the capacity of 3D Raman spectroscopy mapping, as a tool for evaluating spectral peak intensities in epidermal polymers with a three-dimensional approach. In addition, a precise spatial localization of carbon nanotubes as cancer biomarkers was performed. Raman spectroscopy with a 785 nm laser was used for this procedure to conduct 3D mappings in epidermal polymers in a volume of around 30 to 34 µm in "x," 31 to 39 µm in "y," and 70 µm in "z." The heterojunction of polymers was formed by a layer of silicone (Epi-Derm), used as a skin regenerative patch developed to mitigate hypertrophic scars and keloids. Subsequent polymer layers were deposited by drop casting employing synthetically produced: i) 4% NIPA-2% MBA [**?**], and ii) 2% VCL -2% PEGDA [**?**], these polymers were specifically selected to simulate the composition of epidermal tissues, bearing similarity to the structure of human skin. However, it is essential to highlight that this choice constitutes a first approximation in the initial stage, preparatory to more detailed analyzes involving real tissues. This preliminary approach lays the foundation for deeper investigations, serving as an initial platform in simulating biological conditions before proceeding to evaluations with authentic tissue samples. Throughout the mapping process, considerations were made for intensities in a three-dimensional environment, optimizing experimental conditions to enhance the sensitivity and spatial resolution of Raman spectroscopy based on the relative intensities of the Silicon peaks in order to describe the penetration depth of the Raman laser. The choice of this wavelength is justified for its ability to penetrate biological samples and reveal detailed information about molecular vibrations avoiding fluorescence effects. Our first results show the capability to fine measure the characteristic finger print of

silicone and (i) and (ii) polymers. As a function of penetration (z direction of the mapping) we could describe the incremental intensity of the deeper layers in the construction of the heterojunction. These layers are distinguished through a color palette that encompasses green and blue hues, reflecting the spatial location of the distinctive spectral peaks of each polymer. In this way, we were able to identify the individual layers of each polymer or their specific locations in a three-dimensional volume, allowing the detection of a spatial distribution of nanotubes in polymeric media. Based on these findings, conclusions can be drawn regarding the efficacy of Raman spectroscopy through the 3D mapping technique in providing essential information that contributes to the design and development of more precise and personalized therapeutic approaches and methodologies within the biomedical field.

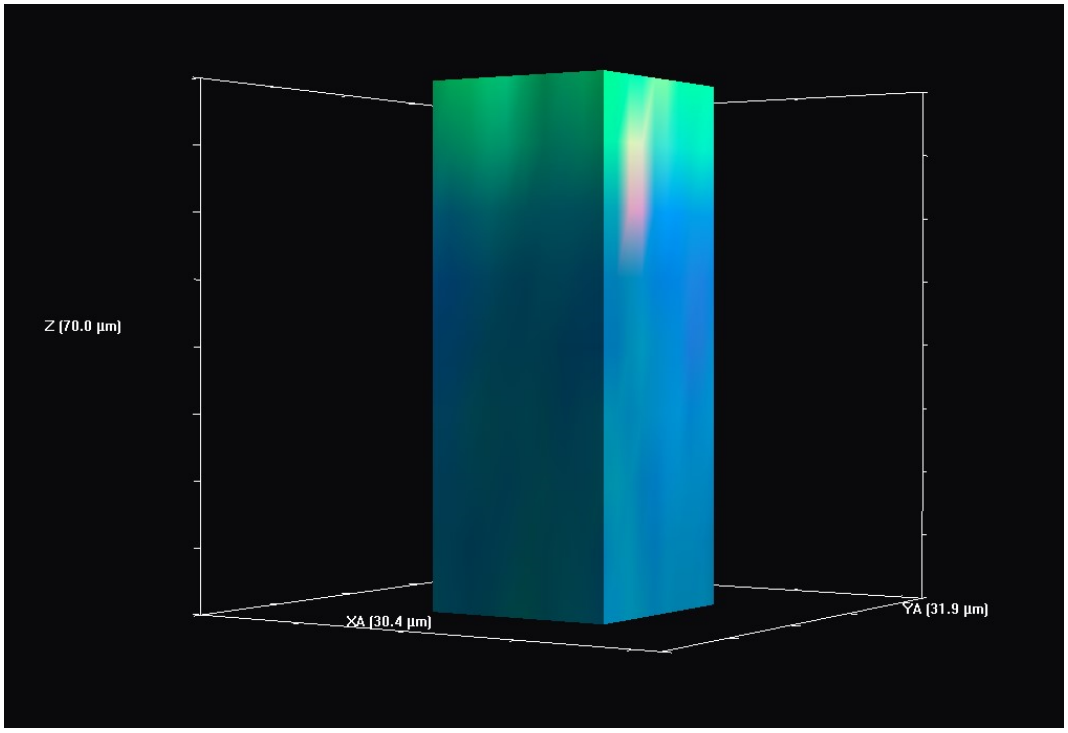

Figure 1: **Raman mapping from the polymer heterojunction, with a specific focus on layering involving a 4% NIPA-2%MBA layer superimposed on a silicone sheet (Epi-Derm). The color variations clearly denote the stratification of the polymers. In the upper region, the predominance of the 4% NIPA-2%MBA polymer stands out with an approximate thickness of 18 µm. The lower spectral colorimetry (blue) distinctively reveals the characteristic presence of silicone focused on the analysis of the peak at 740 cm^{-1}.**

References

[1] M. Utsav. Literature survey on carbon nanotubes and their potential applications in cancer treatment, 14th IEEE International Conference on Nanotechnology. (2014), pp. 678-681, doi: 10.1109/NANO.2014.6968038.

[2] N. Zhang, S. et al. Phase Transition Effects on Mechanical Properties of NIPA Hydrogel. Polymers (Basel). (2018). (10) (358). doi: 10.3390/polym10040358. PMID: 30966393; PMCID: PMC6414852.

[3] M. Puertas, et al. (2016) New bioactive polymers for tissue engineering. Proceedings of the XXXIX Congress of the Iberian Society of Biomechanics and Biomaterials, pp. 69.

Acta Microscopica Vol. 34, Supp. 2, 2025
Abstract Book NSSY 2024 - Galapagos 19-25 May, 2024

Characterization and application of diatoms doped with titanium oxide nanoparticles for environmental bioremediation

Ariel Ojeda[1], Sarah Briceño[1], Gema Gonzalez[1]
[1] *Yachay Tech University. Physics and Nanotechnology Department*
ariel.ojeda@yachaytech.edu.ec

Abstract

This study proposes an innovative solution for environmental bioremediation, incorporating diatoms doped with titanium dioxide (TiO2) nanoparticles. Focusing on the current situation of Yahuarcocha lagoon, the ability of these modified diatoms to purify pollutants is meticulously evaluated, with an emphasis on the elimination of harmful cyanobacteria. Through photocatalysis processes, the decomposition of methylene blue (methylene chloride) as a model molecule was investigated, demonstrating the effectiveness of the treated diatoms in environmental purification.

The generation of nanostructured TiO2 was carried out using ultrasonic synthesis techniques, supported by the work of Nguyen Trung [1] and Hassanjani-Roshan [2]. Detailed characterization of the doped diatoms was performed using ultraviolet-visible spectroscopy (UV-VIS) and X-ray diffraction analysis (XRD), as evidenced in the spectra of Figure 1, which showed the anatase and rutile phases of TiO2. This analysis was complemented with the use of Qualx software for phase identification and the Scherrer equation to estimate the size of the nanoparticles. The average particle size calculation was performed using the Origin software, which allows us to calculate the average particle size using the full width at half maximum (FWHM) of all discernible peaks, resulting in an average size of 80 nanometers.

Scanning electron microscopy (SEM) allowed detailed observation of the nanoparticles as shown in Figure 2 and the morphology of the diatoms, including the pore diameter and the surface distribution of the nanoparticles as shown in Figure 3. Various diatom structures were identified, highlighting one of 32.23 μm in length, another of 17.86 μm, and several smaller ones down to 4.42 μm in length, with an average diameter of 6.32 µm and a pore size of 0.16 μm. Additionally, energy-dispersive X-ray analysis (EDX) was used to determine the chemical composition, and transmission electron microscopy (TEM) for a thorough examination of the nanoparticles.

To verify the improvement in the water quality of the lagoon, atomic absorption spectroscopy (AAS) was used, which facilitated the quantification of the reduction of heavy metals. This approach proposes a sustainable and effective strategy for

treating contaminated water bodies, such as Yahuarcocha lagoon, severely impacted by the discharge of wastewater, chemicals, and solid waste, deteriorating water quality and negatively affecting aquatic life.

This work directly addresses current environmental challenges, offering a novel technique for water purification and ecological restoration. The implementation of TiO2-doped diatoms not only constitutes progress in bioremediation but also highlights the potential of nanotechnology solutions to combat and reduce water pollution, marking a milestone in the search for efficient and environmentally friendly methods for the preservation of our aquatic resources.

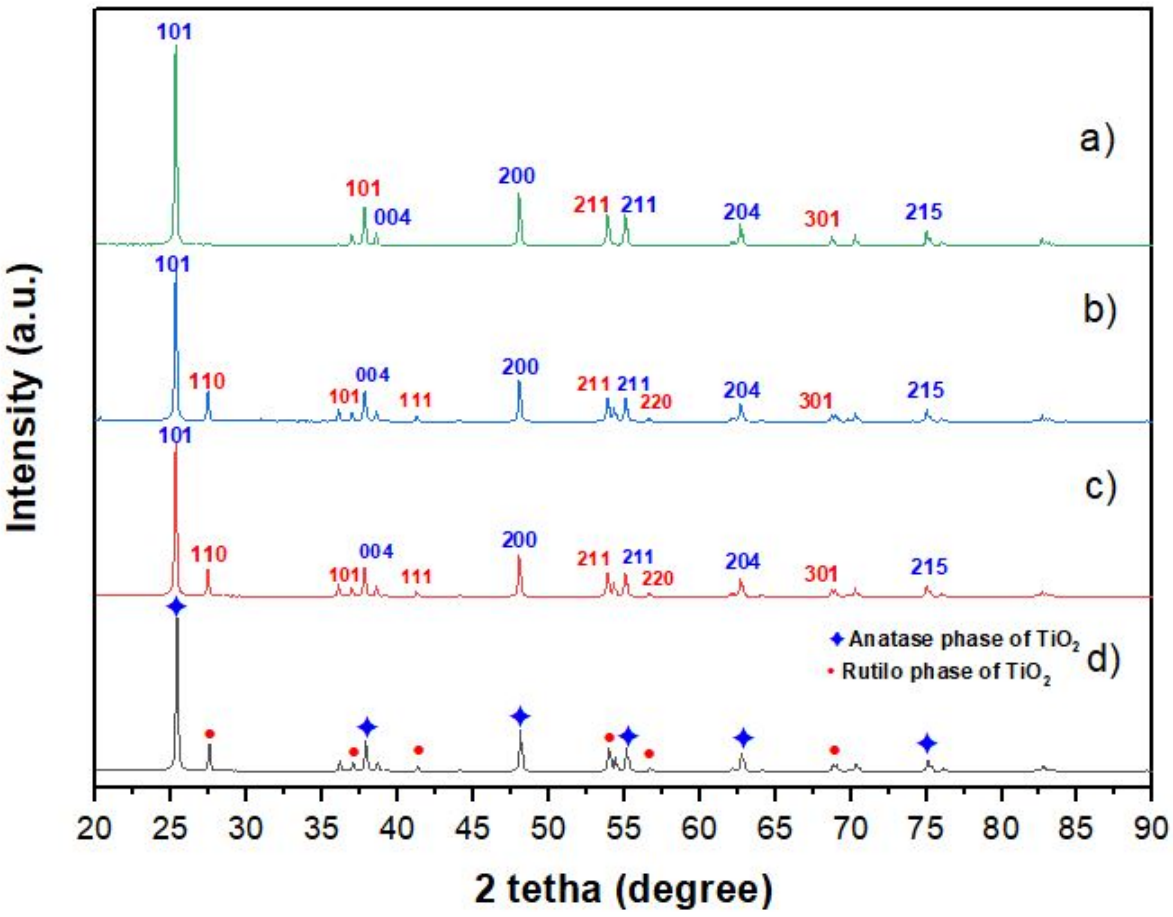

Figure 1: **XRD analysis**

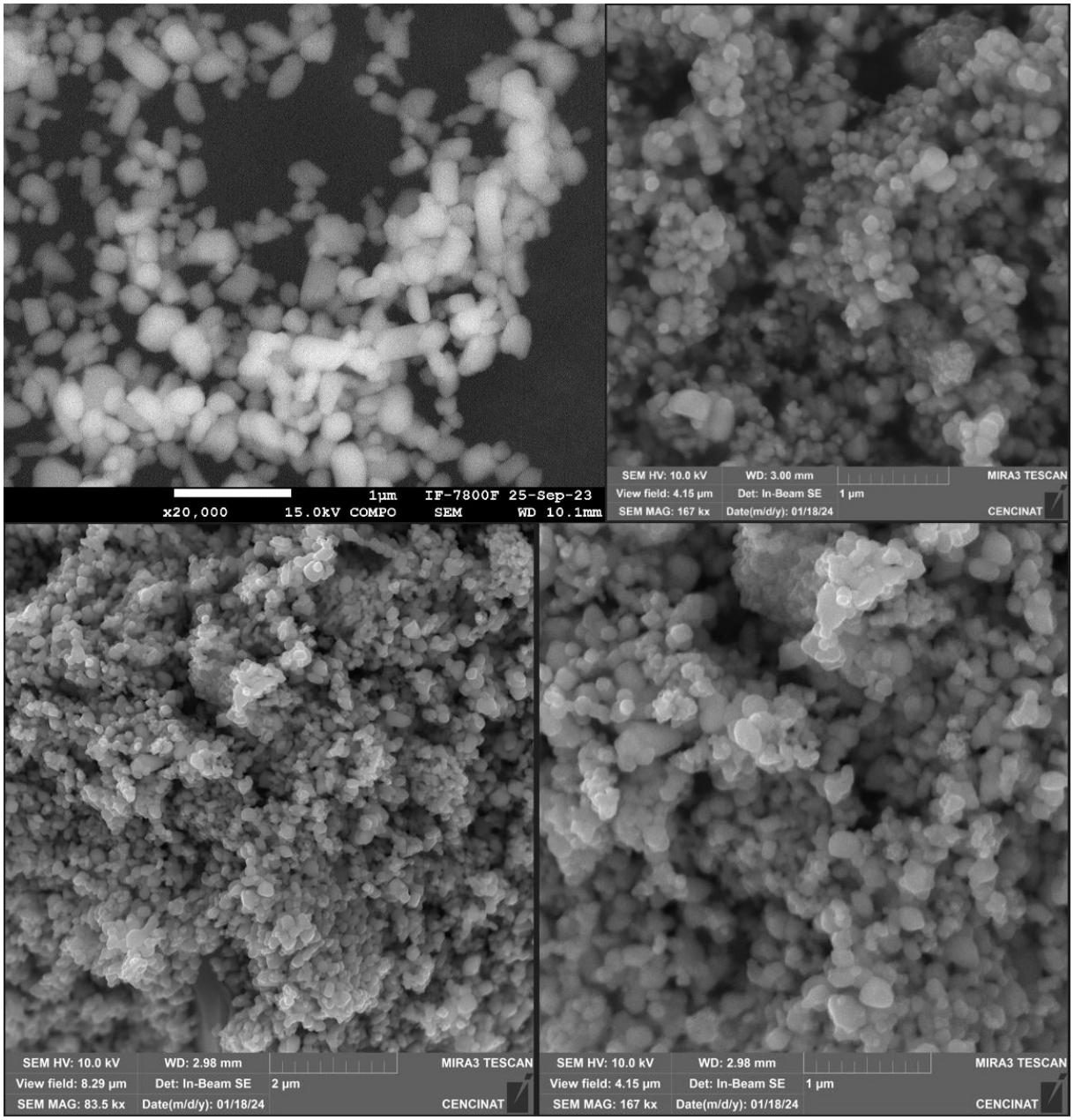

Figure 2: **SEM of TiO2 Nps analysis**

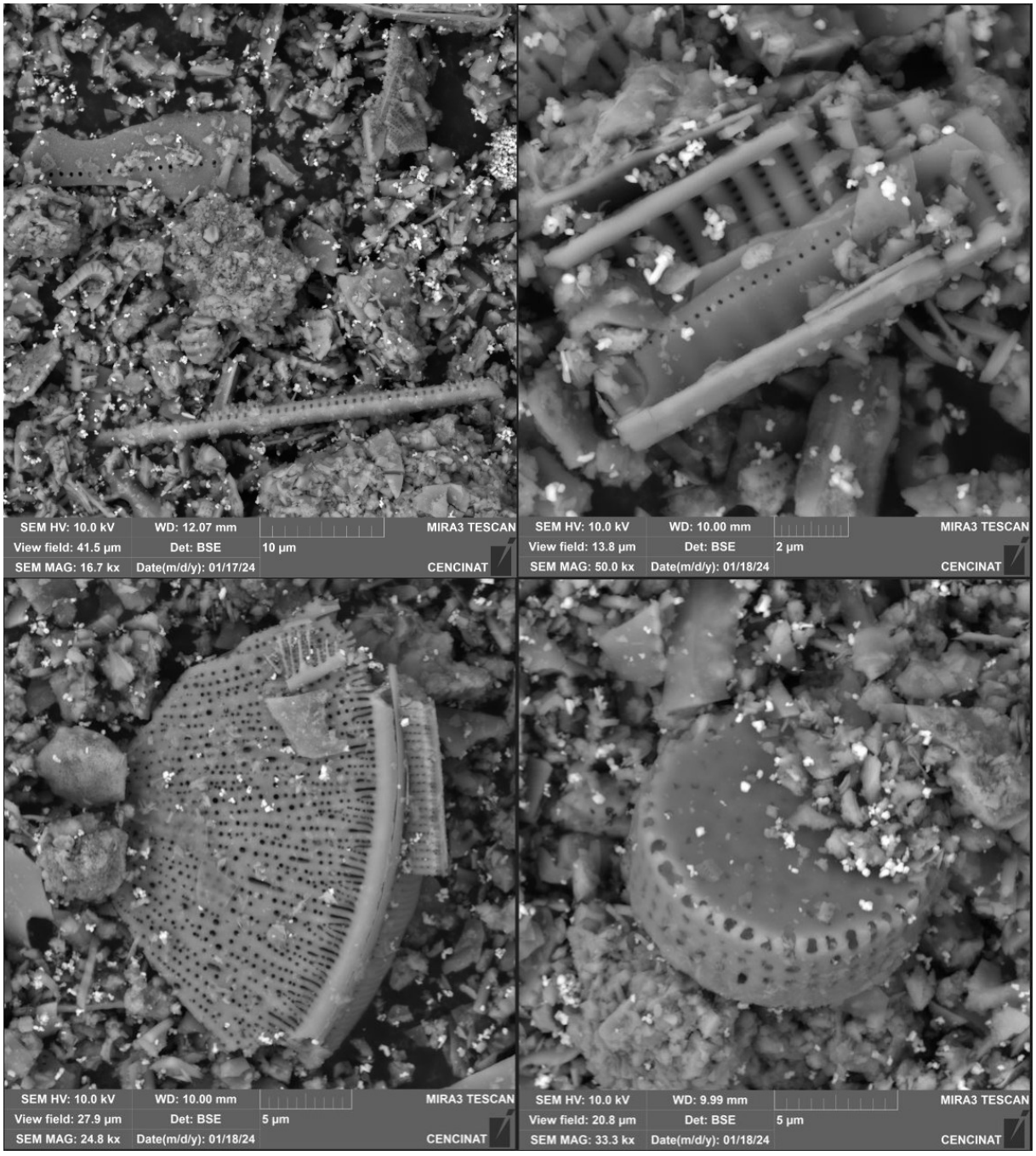

Figure 3: **SEM of Diatom decored with TiO2 Nps**

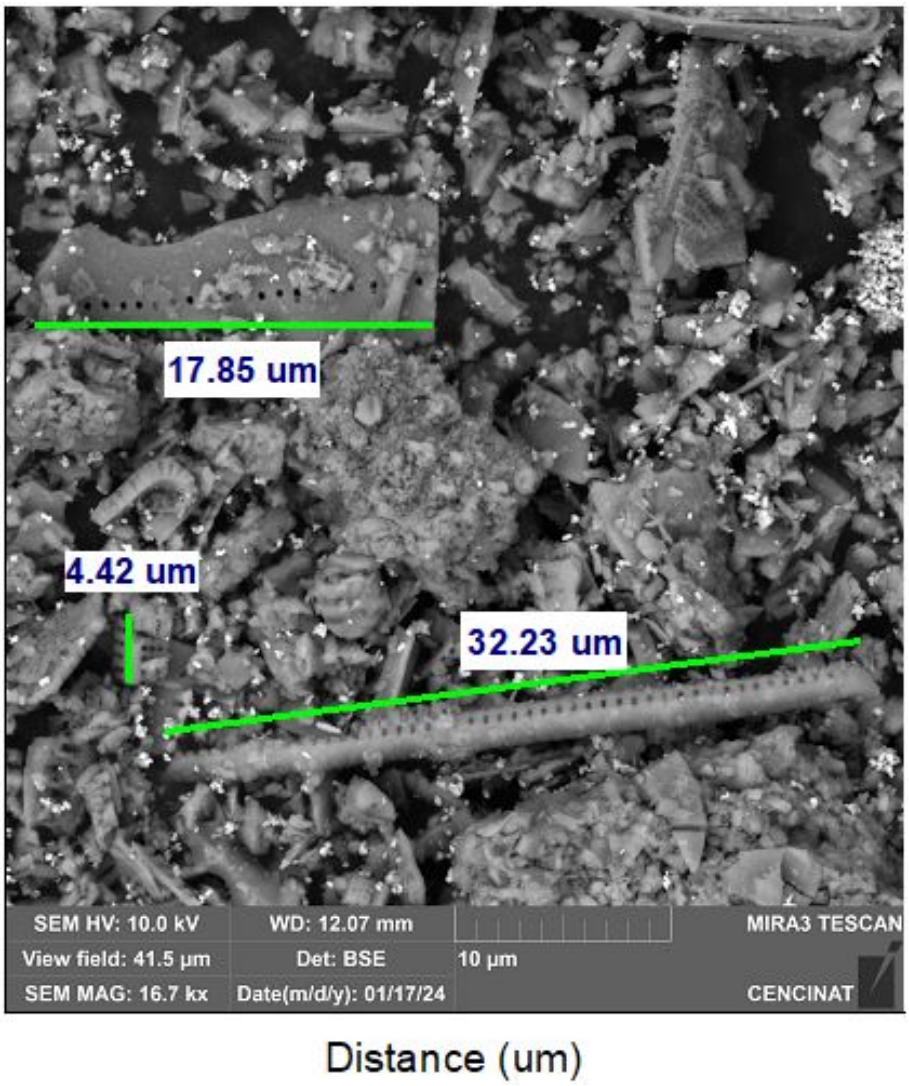

Figure 4: **Diatom size calculation**

References

[1] Duong, Nguyen & Dai Vuong, Le & Nguyen Manh, Son & Tuyen, Ho & Chuong, Truong. (2017). The synthesis of TiO 2 nanoparticles using sulfuric acid method with the aid of ultrasound. Nanomaterials and Energy. 6. 1-7. 10.1680/jnaen.17.00009.

[2] Amir Hassanjani, Seyed Kazemzadeh, Mohammmad Vaezi, and Ali Shokuhfar. Effect of sonication power on the sonochemical synthesis of titania nanoparticles. Journal of Ceramic Processing Research, 12(3), 299–303, 2011.

Acta Microscopica Vol. 34, Supp. 2, 2025
Abstract Book NSSY 2024 - Galapagos 19-25 May, 2024

Systematic Analysis of the Nanostructure and Mechanical Properties of Bamboo Guadua angustifolia Kunth

Anderson Rivadeneira[1], Vladimir Bonilla[1,2], Cristian Quijia[1]
[1] *Universidad de Investigación de Tecnología Experimental Yachay*
[2] *Universidad UTE*
aprivadeneira@yachaytech.edu.ec

Abstract

The Ecuadorian territory is highly exposed to earthquakes and their consequences. On April 16, a devastating earthquake struck down rural communities of Ecuador, underscoring the critical importance of using appropriate building materials in risk areas to seismic events. This natural disaster brought to light the vulnerabilities in conventional construction practices and highlighted the need for more resilient materials, such as bamboo. Bamboo, known for its flexibility, strength, and sustainability, has emerged as a viable alternative in seismic architecture. Its inherent properties enable structures to absorb seismic shocks more effectively, minimizing damage and potentially saving lives. The earthquake's aftermath serves as a stark reminder of the urgent need to reevaluate and adapt building practices to better withstand the forces of nature, particularly in regions like Ecuador that are prone to seismic activity. The inappropriate use of materials and construction methods often leads to building collapse or severe damage resulting in substantial human and economic losses when a natural disaster occur. This study aims to address a part of this issue by exploring the potential of Guadua Angustifolia Kunth specimen mechanical properties, as a seismically resistant building material. The methodology employed involved analyzing the 3D nanostructure response of samples of bamboo to uniaxial stress in each orthogonal direction. This was achieved using the Bruker SkyScan 2211 X-ray nanotomographer, equipped with a Tungsten (w) source and Material Testing Stage MTS-3. The results of this study confirm significant insights into the nano-level strength of bamboo. Some samples of traditional buildings materials using in Ecuador such as concrete were tested with the same conditions, its samples respond to mechanical properties less than the third part of the bamboo samples. A multivariate analysis was conducted comparing the obtained mechanical properties to measured physical qualities such as thickness, internode length, culm diameter etc. It was observed that the bamboo's strength correlates with its fiber density, with the thicker bottom part containing more fiber compared to the thinner-walled top. The concentration of fiber near the outer wall of the bamboo culm contributed to better resistance in the mechanical experiments.

Besides, the compression strength was found to be related to the internode distance and the cross-sectional area of the culm, while flexure strength was associated with the thickness at the culm level. Also, the culm diameter or the number of nodes appeared to have no significant impact on flexure strength. In conclusion, this study highlights the different qualities of Guadua Angustifolia Kunth specimen sections. This specimen of bamboo could be considerate as a suitable and appropriate material for buildings in earthquake-prone areas. This research not only contributes to the understanding of bamboo as a building material but also promotes its application in enhancing the resilience of infrastructures against earthquakes.

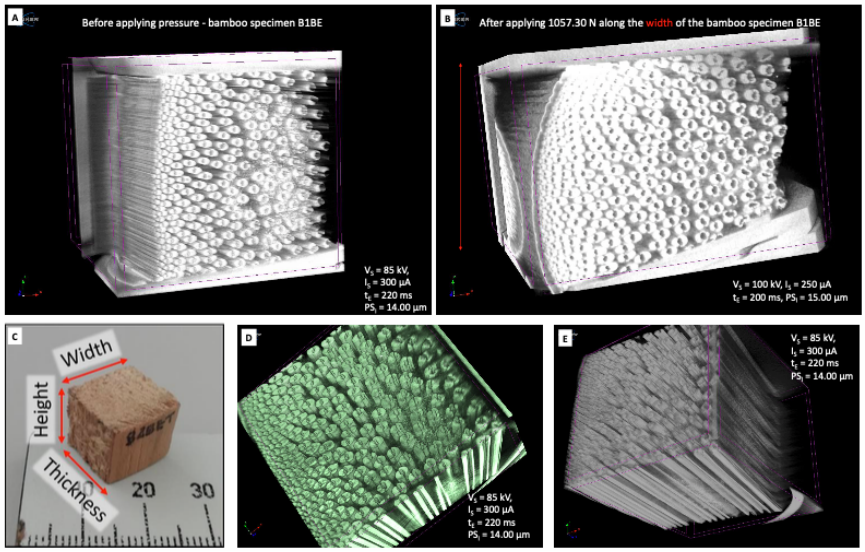

Figure 1: **Example of the nanotomographer results. A) 3D view of the sample before and B) after applying pressure along the width of a 1 cc bamboo specimen shown in C). In D and E two different views of the same sample in it's initial state. VS = source voltage IS = source current , tE = exposure time and PSI = image pixel size.**

References

[1] Drunen, N., Cangas, A., Rojas, S., & Kaminski, S. (2016). Post-earthquake report on bamboo structures and recommendations for reconstruction with bamboo on the Ecuadorian coast. Beijing: International Bamboo and Rattan Organisation.

[2] Hu, D., Song, B., Dang, L., & Zhang, Z. (2018). Effect of strain rate on mechanical properties of the bamboo material under quasi-static and dynamic loading condition. Composite Structures, 200, 635-646.

[3] Tan, T., Rahbar, N., Allameh, S. M., Kwofie, S., Dissmore, D., Ghavami, K., & Soboyejo, W. O. (2011). Mechanical properties of functionally graded hierarchical bamboo structures. Acta biomaterialia, 7(10), 3796-3803.

Acta Microscopica Vol. 34, Supp. 2, 2025
Abstract Book NSSY 2024 - Galapagos 19-25 May, 2024

Chitosan – collagen – cerium hydroxyapatite nanoparticles composite for antibiotic delivery

Amauta Quilumbango[1], Sarah Briceño[1], Gema Gonzales[1]
[1] *School of Physical Sciences and Nanotechnology*
amauta.quilumbango@yachaytech.edu.ec

Abstract

This research delves deeply into the process of fabricating composite films, amalgamating chitosan, collagen, and Cerium hydroxyapatite nanoparticles, with the overarching goal of enabling the controlled release of gentamicin. The primary focus lies in scrutinizing the nuanced effects stemming from the manipulation of the chitosan-to-collagen ratio within these composite films. This exploration spans across various ratios, ranging from the purity of chitosan (100/0) to a blend with 25% collagen (75/25) and eventually an equal distribution of chitosan and collagen (50/50 v/v), all while integrating hydroxyapatite into the composite matrix, Sionkowska, A., Kaczmarek, B., & Gadzala-Kopciuch, R. (2016). Gentamicin release from chitosan and collagen composites. (35) (353-359). The methodological approach adopted involves the embedding of the antibiotic within the composite film matrix, precisely achieving a concentration of 20 mg in 10 ml of the composite solution. Subsequently, a delicate drying process ensues, meticulously executed within an oven set at a gentle $30C$. This methodical procedure yields composite films endowed with a diverse spectrum of mechanical properties and release capacities, thereby elucidating the intricate interplay between the constituent materials. Furthermore, this investigation introduces cerium-loaded hydroxyapatites into the 50/50 composite blend varying the percentage of cerium loaded in the hydroxyapatite, from 0% to 25 %. Broadening the horizons of inquiry to encompass the influence of this additional element on the dynamic release kinetics of gentamicin over time, simulated within a body-like fluid environment. Thanks to their fluorescence characteristics cerium will allow a monitoring of the recuperation process. A notable revelation stemming from this exhaustive investigation is the emergence of a discernible pattern elucidating the intricate relationship between the chitosan concentration within the composites and the corresponding release kinetics of the drug. Specifically, a diminishing chitosan concentration correlates with a deceleration in the rate of drug release, ultimately culminating in a peak release observed after an extended incubation period. This phenomenon is exemplified by the 100/0 chitosan/collagen blend, wherein maximum release capacity is achieved after a span of nine days, shedding profound light on the temporal dynamics of drug release

mechanisms within these complex composite matrices. The characterization techniques include Fourier Transformation Infrared Spectroscopy (FTIR) for chemical bonding details, Raman spectroscopy for vibrational analysis, Scanning Electron Microscopy (SEM) for morphological studies, Energy-Dispersive X-ray Spectroscopy (EDS) for elemental analysis, Fluorescence Microscopy and Ultraviolet-visible spectroscopy (UV-Vis) for assessing optical properties and the release results. The highest percentage of release observed after a two-hour period was attained by a composite featuring a 1:1 ratio of chitosan to collagen, supplemented with 25% Ce-HAp, achieving a peak release rate of up to 98%. An in-depth examination across various parameters provides valuable insights into the desorption mechanisms and the intricate drug interactions within these nanocomposite films.

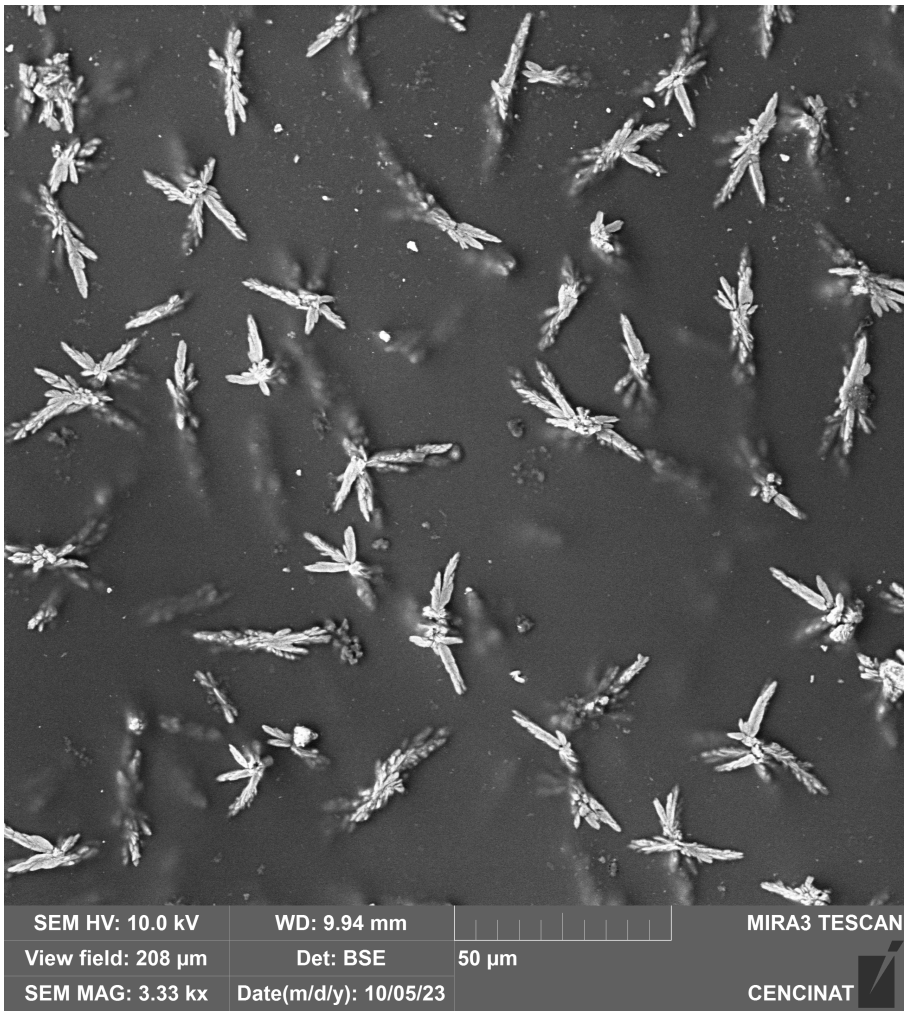

Figure 1: **SEM image of 50 chitosan/50 collagen and Ce-hydroxyapatite composite films. Composite with 0% Ce loaded in the hydroxyapatite.**

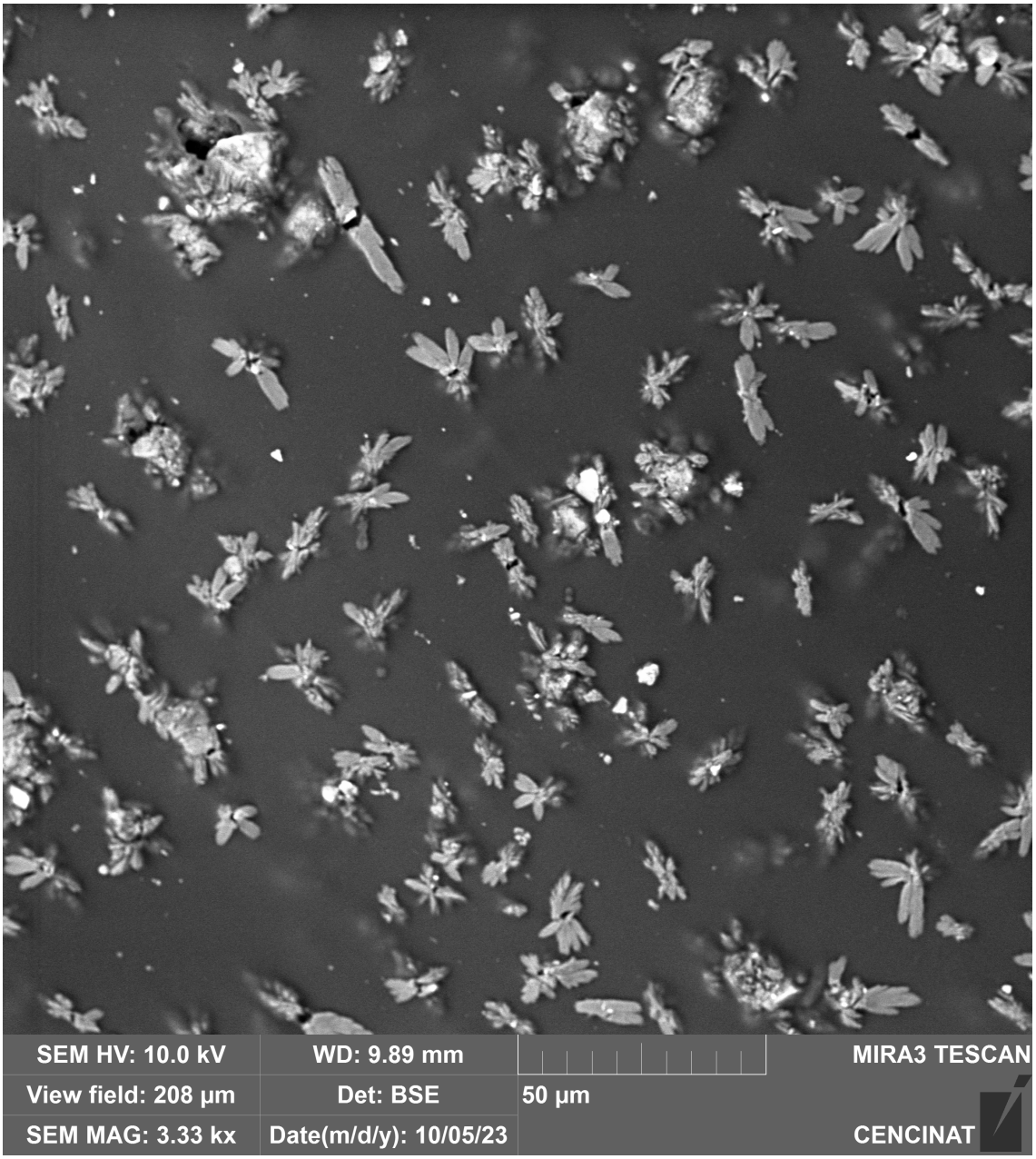

Figure 2: **SEM image of 50 chitosan/50 collagen and Ce-hydroxyapatite composite films. Composite with 10% Ce loaded in the hydroxyapatite.**

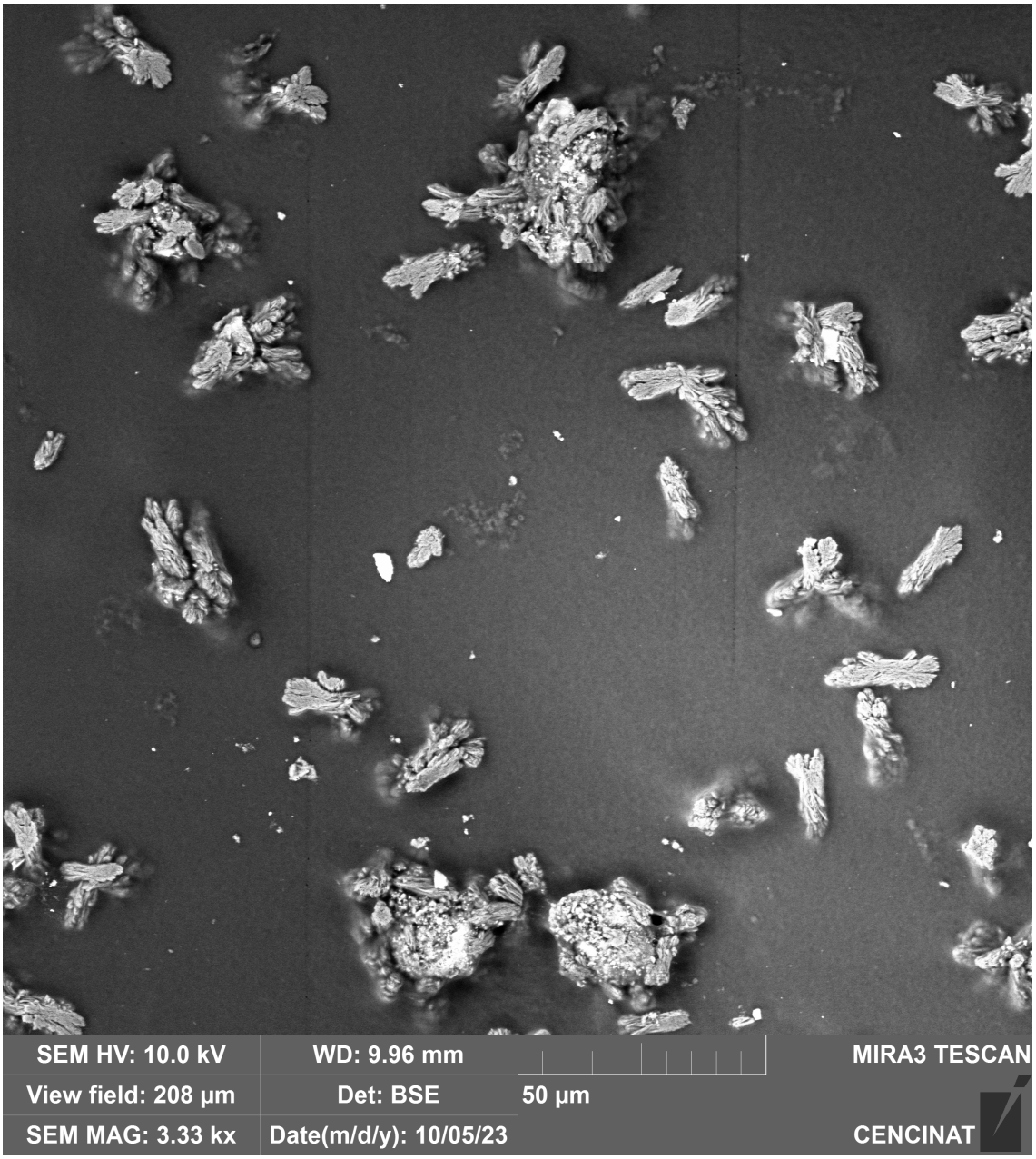

Figure 3: **SEM image of 50 chitosan/50 collagen and Ce-hydroxyapatite composite films. Composite with 15% Ce loaded in the hydroxyapatite.**

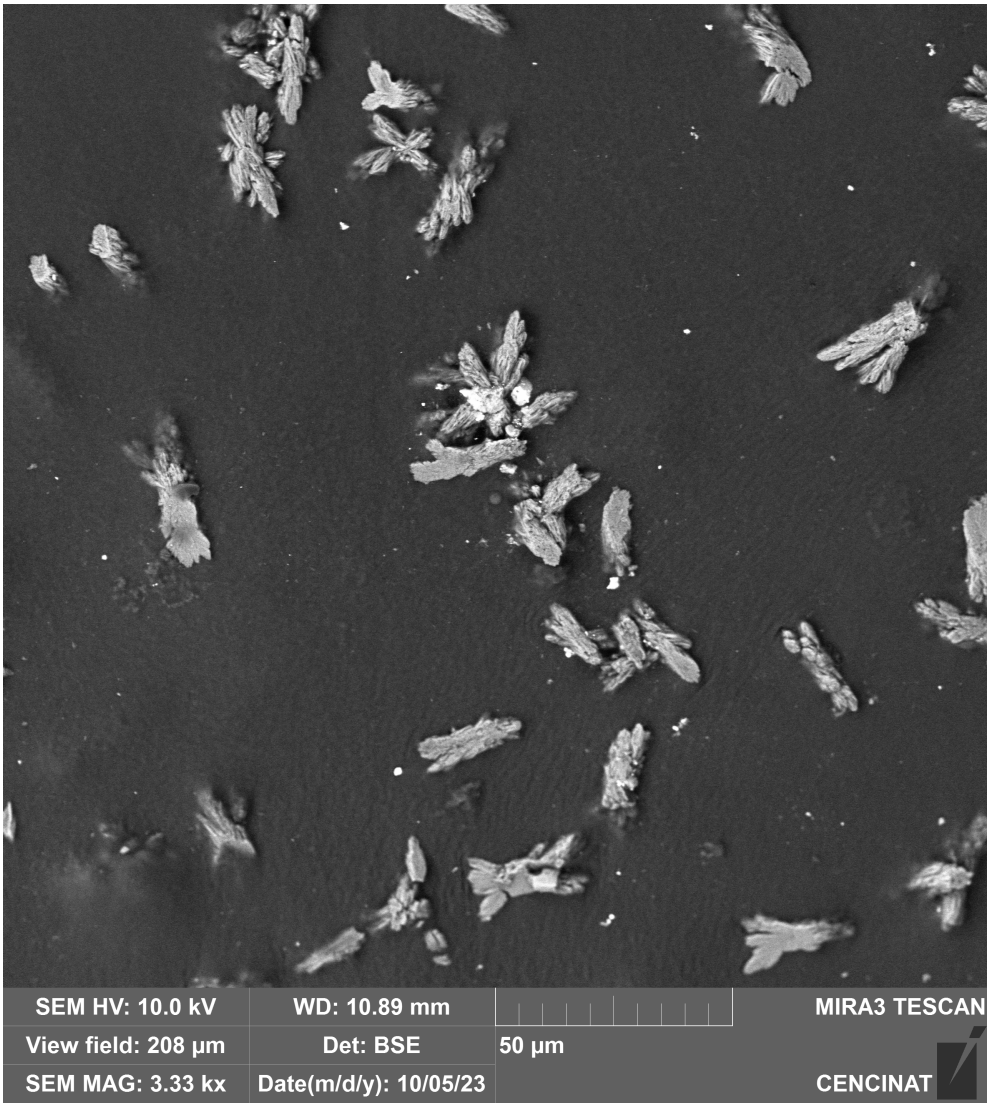

Figure 4: **SEM image of 50 chitosan/50 collagen and Ce-hydroxyapatite composite films. Composite with 25% Ce loaded in the hydroxyapatite.**

References

[1] Sionkowska, A., Kaczmarek, B., & Gadzala-Kopciuch, R. Gentamicin release from chitosan and collagen composites.(2016) (35) (353-359).

Acta Microscopica Vol. 34, Supp. 2, 2025
Abstract Book NSSY 2024 - Galapagos 19-25 May, 2024

Green synthesis of silver nanoparticles using Vitis vinifera natural extract and evaluation of their antibacterial activity

Karla Chaglla[1]

[1] *School of Biological Sciences & Engineering, Universidad Yachay Tech, Urcuquí, 100650, Ecuador*

karla.chaglla9817@gmail.com

Abstract

Antibiotic resistance poses a significant threat to human health, exacerbated by the rampant misuse and overuse of antimicrobials, which are primary drivers of pathogen evolution towards drug resistance (World Health Organization, 2021). The inherent biocidal potential of silver nanoparticles (AgNPs), attributed to the release of silver ions that disrupt microbial membranes and interfere with vital cellular processes, underscores their precise and valuable contribution to combating resistant pathogens (Cheon et al., 2019). This research aims to synthesize and characterize AgNPs through green synthesis using the Vitis vinifera leaves extract, varying the pH of the extract to optimize the synthesis process. Additionally, the study aims to investigate the antimicrobial efficacy of these AgNPs against two antibiotic-resistant pathogens.

The nanoparticle synthesis was carried out by adding dropwise Vitis vinifera leaf extract to AgNO3 (1 mM). The pH of the aqueous extract was adjusted with NaOH in a range of 3.0 to 12.0 pH. Biosynthesized AgNPs were characterized by Ultraviolet-visible spectroscopy (UV-vis), Fourier transform infrared spectroscopy (FT-IR), X-ray photoelectron spectroscopy (XPS) and Transmission electron microscopy (TEM). The antimicrobial activity of AgNPs was evaluated using the disk diffusion method against Escherichia coli ATCC 25922 and Staphylococcus aureus ECBI-UITEY strains.

The formation of the nanoparticles was first confirmed with a visual color change in the reaction mixture from light yellow to dark brown, indicating the formation of AgNPs, then confirmed with the UV-vis spectrum analysis. The color of the mixture intensified as the pH value of the extract increased (Figure 1a). Depending on the experimental pH conditions (3.0, 7.0, 9.0, 12.0 pH), the AgNPs exhibited a characteristic absorption peak at 407, 409, 442, and 451 nm, confirming the synthesis of the nanoparticles. Figure 1b shows that the absorption peaks shifted to shorter wavelengths and became narrower with the elevated pH value, possibly due to a reduction in the size of the silver particles. The bioreduction of silver ions (Ag+) to Ag nanoparticles (Ag0) was favored by the primary and secondary metabolites in the aqueous extract of Vitis vinifera leaves that act as reducing, stabilizing, and

protective agents. FT-IR spectrum confirms that hydroxyl and carbonyl groups present in polyphenolic compounds, flavonoids, terpenoids, and proteins present in the extract have a high binding capacity with metal and are responsible for the reduction of silver ions and the stabilization of AgNPs (Figure 2a). XPS survey of the AgNPs showed the presence of C (52.2%), O (27.9%), Ag (6.3 %), and other elements ($\leq$ 5%) (Figure 2b). The lower atomic concentration of silver does not necessarily imply a lower presence of AgNPs since several factors can influence the interpretation of the results, including the nature of the biomolecules present in the extract and the limitation of the sampling depth of the XPS characterization technique. The strong signal of Ag 3d, with an energy of 367 eV, confirms the existence of silver in its metallic form. The peaks at 373.8 eV y 367.8 eV are attributed to metallic Ag. Furthermore, the energy separation between the Ag3d peaks is equivalent to 6.0 eV, corresponding to metallic silver Ag0 (Figure 2c). The C1s high-resolution spectrum in Figure 2d deconvolutes into three peaks at the electron binding energies of 288.5, 286.3, and 284.8eV due to C=O, C-O, and C-C, respectively. TEM micrographs showed that the nanoparticles had a spherical morphology with an average size of 20.42nm, 14.52nm and 5.24nm according to the synthesis pH (Figure 3). Figure 4a shows the size of the inhibition halos formed around the discs loaded with AgNPs. The results revealed that the antibacterial effect of AgNPs was greater in the case of S. aureus than E. coli when the discs were immersed in 50 ul of AgNPs (20ug/ml), the zone of inhibition was highest in S. aureus with 27 mm, followed by E. coli with 24 mm (Figure 4b).

This study successfully biosynthesized spherical AgNPs using Vitis vinifera leaf extract. Additionally, the promising antibacterial results against antibiotic-resistant strains underscore the potential of AgNPs as effective agents. This research marks a significant step towards sustainable nanoparticle synthesis and contributes to the advancement of sustainable antimicrobial strategies in the fight against antibiotic resistance.

References

[1] World Health Organization. (2021). Antimicrobial Resistance. https://www.who.int/news-room/fact-sheets/detail/antimicrobial-resistance

[2] Cheon, J. Y., Kim, S. J., Rhee, Y. H., Kwon, O. H., & Park, W. H. (2019). Shape-dependent antimicrobial activities of silver nanoparticles. International Journal of Nanomedicine, Volume 14, 2773–2780. https://doi.org/10.2147/IJN.S196472

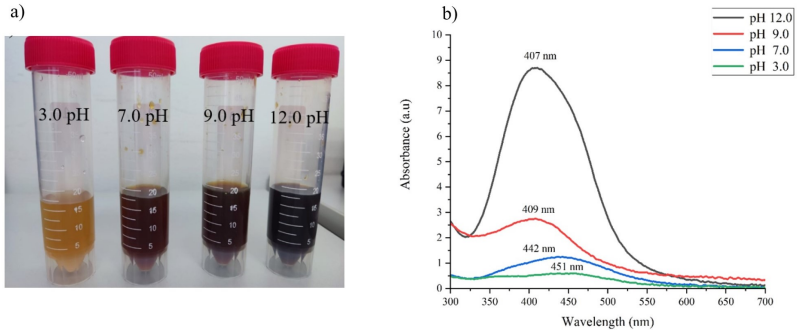

Figure 1: **(a) Color change and (b) UV-vis spectra of AgNPs showing absorbance depending on the pH values of the extract.**

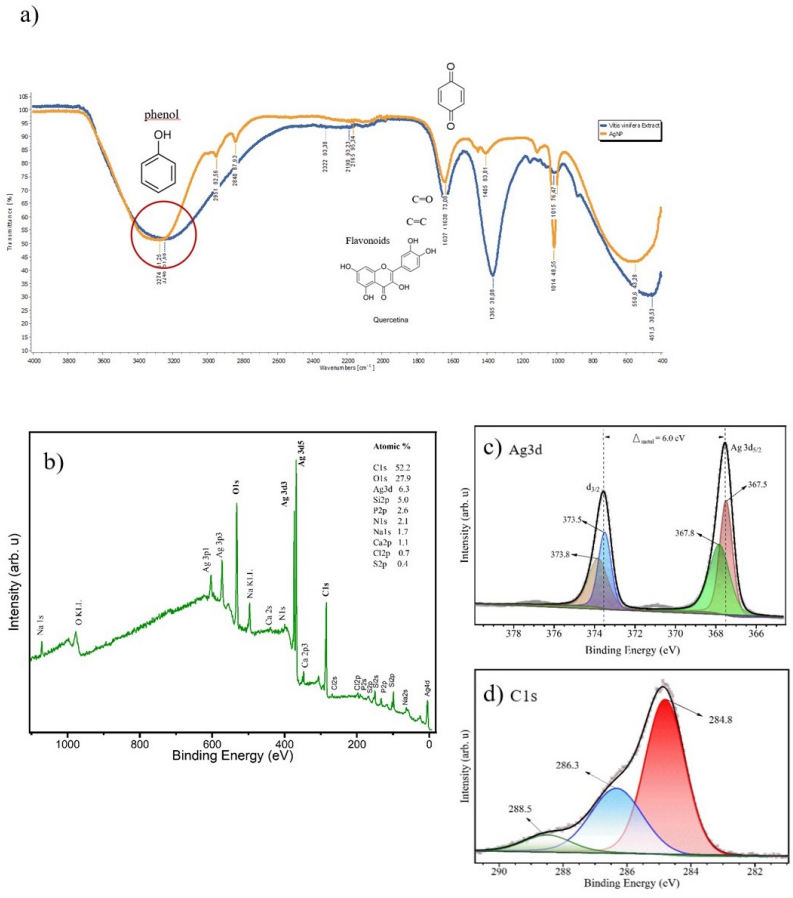

Figure 2: **(a) FT-IR spectra of leaves extract, and AgNPs biosynthesized; (b) XPS survey spectrum of the nanoparticles. (c) High-resolution XPS spectrum of the Ag 3d, (d) high-resolution XPS spectrum of the C1s.**

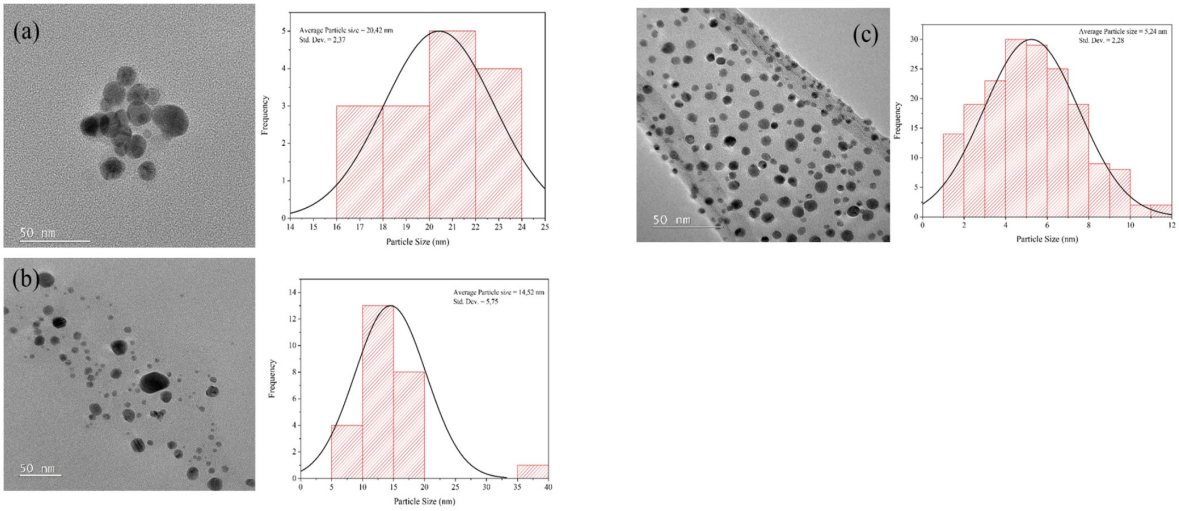

Figure 3: **TEM images of silver nanoparticles synthesized from Vitis vinifera leaf extract at various pH values: (a) 7.0 pH, (b) 9.0 pH, and (c) 12.0 pH.**

Test Strain	Zone of inhibition (mm)						
	1	2	3	4	5	6	7
	10ul AgNPs	20ul AgNPs	30ul AgNPs	50ul AgNPs	Extract	AgNO3	Ampicillin (50 ug/ml)
A) E. coli	20	22	23	24	7	8	33
B) S. aureus	25	26	27	27	7	10	45

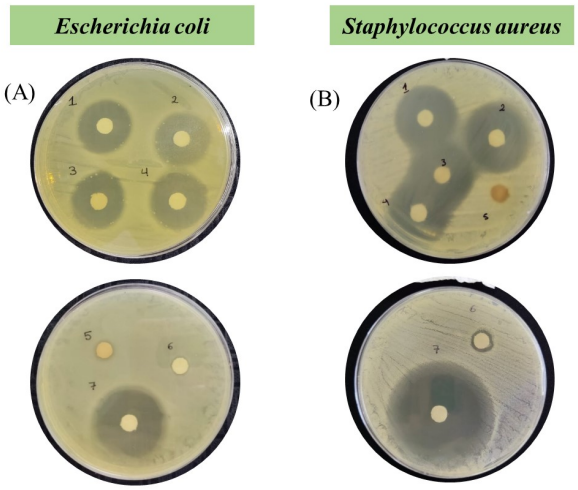

Figure 4: **(a) Table with the values of the zone of inhibition (mm) of silver nanoparticles; (b) Antibacterial activity of AgNPs by Vitis vinifera leaf extract against (A) E. coli (B) S. aureus. The discs were soaked with 1) 10ul AgNP, 2) 20ul AgNP, 3) 30 ul AgNP, 4) 50 ul AgNP, 5) Vitis vinifera extract, 6) AgNO3, and 7) Ampicillin.**

Acta Microscopica Vol. 34, Supp. 2, 2025
Abstract Book NSSY 2024 - Galapagos 19-25 May, 2024

Interface boundary interactions in polymer heterostructures

Samantha V. Loor[1], Joselin E. Guananga[1], Julio C. Chacón-Torres[1]
[1] *School of Physical Sciences and Nanotechnology, Yachay Tech University, Urcuquí 100119, Ecuador*
samantha.loor@yachaytech.edu.ec

Abstract

Polymeric materials emerge as a substitute for epidermal tissue, which do not require a specific permit for their production in a laboratory for skin *in situ* studies. NIPA and PVCL hydrogels have been tested for thermo-responsive characteristics and biocompatibility, but their properties at the boundary interface with a substrate have not been tested. To characterize these hydrogels 3D mapping Raman spectroscopy promises to give information a few millimeters down the hydrogel to the border between the hydrogel and substrate, which facilitates the study for inner multilayer boundary heterostructures [1]. This investigation analyzes the boundary interaction from three hydrogels: 4% NIPA-2% MBA (23-005), 2% VCL-2% PEGDA (23-006), and 4% NIPA (23-004) [2]. To unveil additional characteristics of PVCL and NIPA hydrogels were used as a coating of a silicon surface, then, they were mapped by the 3D Raman technique and selecting the deeper interface layer were they joint. For the purpose of testing boundary interface properties, hydrogels were synthesized by emulsion; then, there were 3 samples left to dry by drop casting, and other 3 samples dried over silicone (Epi-Derm), which is used as a skin regenerative to treat hypertrophic scars and keloids; when fully dried, each of the samples was characterized with 3D Raman Spectroscopy. By analyzing this experimental data, it is possible to extract the boundary interactions of these hydrogels to explain the existence of covalent or Van der Walls interaction between the layers. Using Origin Pro, the hydrogels' behavior at each interface was observed as a 3D surface and documented. It is expected to obtain a 3D complete mapping where the change in the intensities would allow us to identify the change in vibrational energies of molecular bonds present at different deepness that could simulate a multilayer skin system like in the hydrogel/ EpiDerm structure. The future potential implementation of this project goes to optimizing the use of interlayers analyses employing Raman 3D mapping to identify the molecular interaction between skin layers and cancer cells without having to perform a surgery or X-ray tomography. This approach is a simple, fast and reliable method to study cancer treatment and molecular interactions for these complex bio systems.

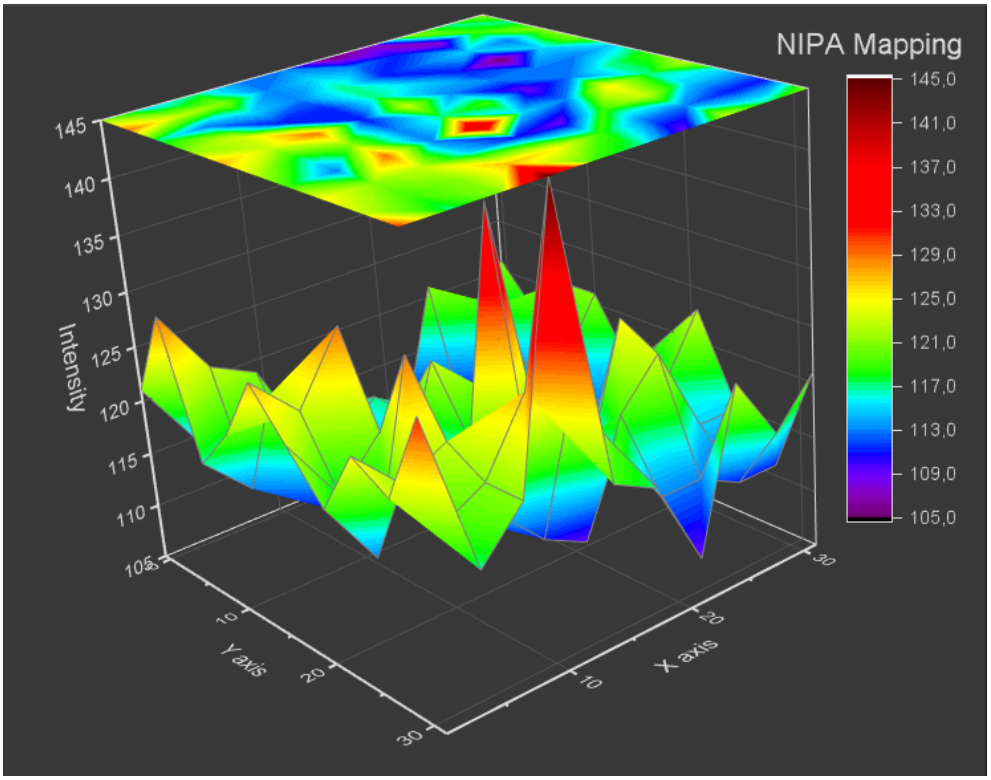

Figure 1: **Raman mapping of 15 hours from 4% NIPA-2% MBA (23-005) hydrogel superimposed onto an EpiDerm substrate with a specific focus on layer at -20 μm. The change in intensity denoted by a change in color represents the presence of the interface between the hydrogel and the substrate. Red colorimetry denotes high intensity at a specific peak at ~1500 cm^{-1} corresponding to the EpiDerm.**

References

[1] Daniel, Amuthachelvi, et al. J. Raman Spectrosc. 45 (2014) 541-549.

[2] Romero J. et al. Rev. Bionatura 6 (2021) 1712-1719.

Acta Microscopica Vol. 34, Supp. 2, 2025
Abstract Book NSSY 2024 - Galapagos 19-25 May, 2024

Kinetics Study of Acid-Catalyzed Cleavage of Carbon-Oxygen Bonds

Cristina Rubio[1], Jacob Sitterly[2], Justin Nhan[2], Thibault Terencio[1], Robert Brainard[2]

[1] *Yachay Tech University, School of Chemical Science and Engineering, Urcuqui, Ecuador.*

[2] *University at Albany, College of Nanoscale Science and Engineering, Albany NY, US.*

cristina.rubio@yachaytech.edu.ec

Abstract

The manufacturing process of modern microelectronic devices is dependent upon the use of polymer photoresists in several crucial steps. Photolithography has traditionally been limited by the minimum feature size achieved by the wavelength of light and materials used [1]. Acid-catalyzed cleavage of carbon-oxygen bonds is a key step in the image-formation reactions of DUV, EUV, and 193-nm photoresists. Exposure to light in these chemically amplified photoresists produces a sulfonic acid that catalyzes the breaking of a C-O bond, resulting in a polymer-bound carboxylic acid and a carbocation [2]. The carbocation then decomposes to regenerate the catalytic acid. These reactions provide the solubility switch that drives the formation of nanoscale features. Acid-catalyzed C-O bond cleavage reactions have also been central to resist platforms, such as MANA, CAMP, DD-CAMP, and Acid Amplifiers, which group members have studied or created. C-O bond cleavage leads to the deprotection of a base-soluble functional group, such as a phenol or carboxylic acid. Lowering the activation energy of the C-O bond cleavage reaction can achieve several lithographic benefits. By implementing these lower activation energy monomers into the EUV photoresists, lower processes can be achieved, reducing acid diffusion and improving resolution and process windows [3].

This work describes a detailed study of the kinetics of these acid-catalyzed deprotection reactions in solution-phase in sealed NMR tubes. A kinetic study was conducted to describe the acid-catalyzed deprotection of three esters with strong, medium, and weak sulfonic acids. Solutions comprised 100 mM and 1 mM concentrations of ester and sulfonic acid in a C6D6/CD3CN solvent mixture. Solutions were sealed in 5 mm NMR tubes and immersed in oil baths for 5-30 minutes at different temperatures, and ^{1}H NMR followed the extent of the reaction. First-order reaction kinetics over several temperatures are shown for each combination of acid and ester. The Ehtyl cycle pentyl acetate (ECPA) with the strongest acid (nonaflate acid) showed the fastest reaction rate, while the medium strength acid ((Trifluoromethyl) benzenesulfonic acid) decomposed slowly. The natural log of the rate constants was plotted against the reciprocal temperature in Kelvin (1/T),

yielding four activation energy plots (Figure 1). Interestingly, as we can observe in the Arrhenius plot, the rates of these reactions are influenced more by their entropy than by their enthalpy (Figure 3).

Moreover, an approach to modeling these important reactions using ORCA software has been described. This modeling predicts the activation energies and LogA of catalyzed and uncatalyzed C-O bond-breaking reactions. To verify the capabilities of this modeling approach, the modeled predictions of activation energies were compared against experimental values. Specifically, the kinetic parameters of C-O bond breaking of commonly used 193-nm monomers were predicted as catalyzed by three different sulfonic acids (Figure 2).

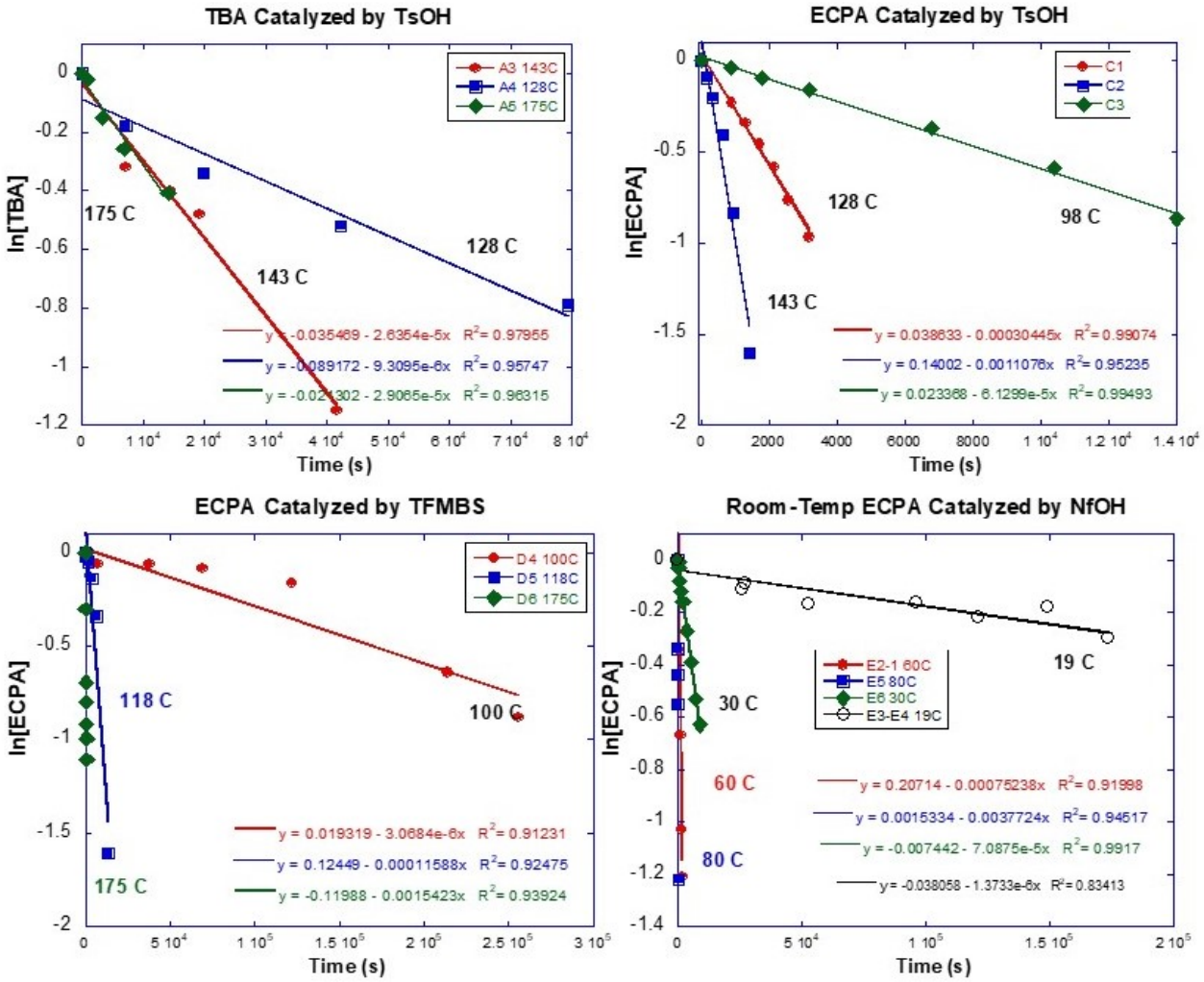

Figure 1: **1H NMR Kinetics Plots for the four different reactions performed with success in the different combinations of esters-acid.**

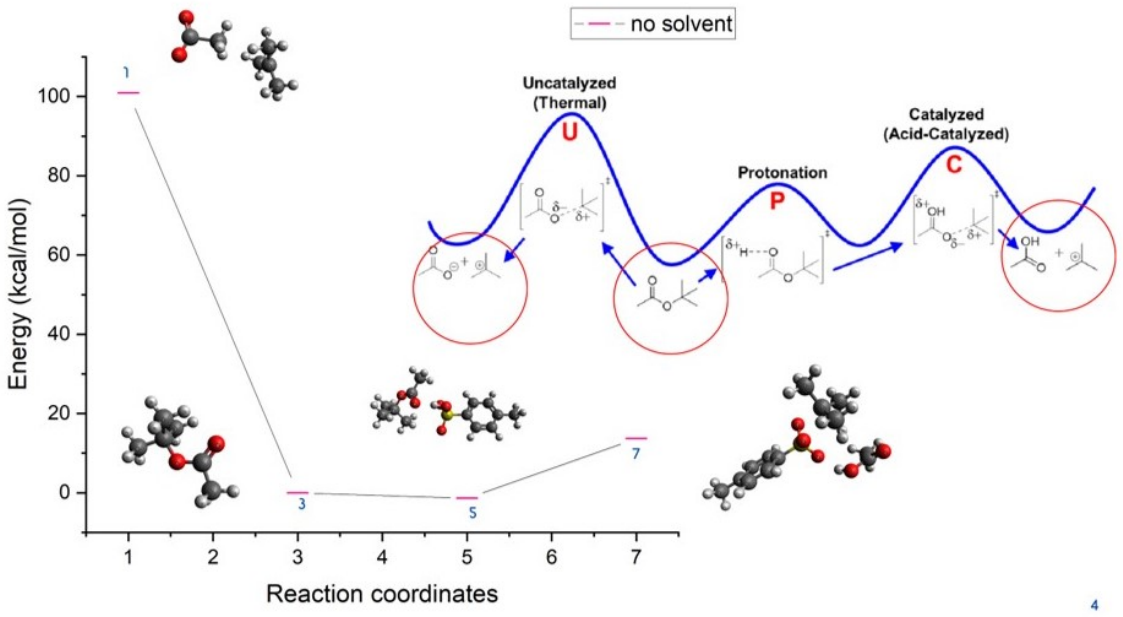

Figure 2: **Mechanism of Acid-Catallyzed reaction modelling obtained using ORCA software.**

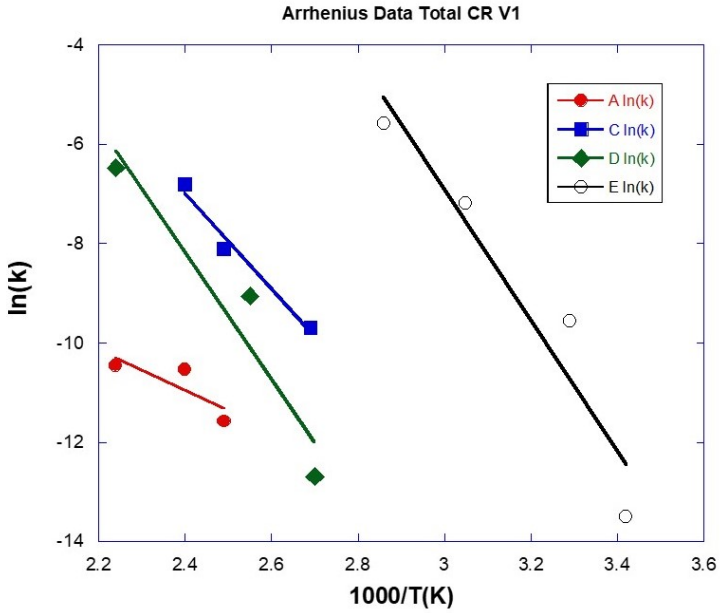

Figure 3: **1H NMR Kinetics: Arrhenius Plot for the four reactions performed.**

References

[1] H. Ito, W. England, M. Ueda, "Chemical Amplification based on acid-catalyzed depolymerization", J. Photopoly. Sci. Tech. vol. 3, 219-233, (1990).

[2] E. Ismailova, R. Tiron, C. Chochos, C. Brochon, P. Bandelier, D. Perret, C. Sourd, C. Brault, C. Serra, G. Schlatter, G. Hadziioannou, "Impact of molecular structure of polymer in 193 nm resist performance", Microelectronic Engineering 86(4-6), 796-799, (2009).

[3] R. Brainard, J. Guevremont, S. Reeves, X. Zhou, T. Nguyen, J. Mackevich, G. Taylor, Gary E. Anderson, "Multiple anion nonvolatile acetal (MANA) resists", J. Photopoly. Sci. Tech., 14(4), 531-542 (2001)

Acta Microscopica Vol. 34, Supp. 2, 2025
Abstract Book NSSY 2024 - Galapagos 19-25 May, 2024

Examining atom positions in bi-layer MoS2/WSe2 heterostructure: A theoretical spectroscopy analysis

Francis G. Villacrés Merchán[1], Duncan J. Mowbray[1]
[1] *Yachay Tech University*
francis.villacres@yachaytech.edu.ec

Abstract

Since 2004, with the first isolation and electrical characterization of the graphene transistor reported by Novoselov and Geim [1], the family of 2D materials has significantly expanded. Among these materials, layered van der Waals (vdW) solids have taken the forefront. For example, theoretical studies have shown that numerous MX2 (where X represents a chalcogen anion, and M is a transition metal) heterostructures (bilayered materials) form type II heterojunctions, facilitating efficient electron-hole separation. Specifically, the MoS2/WSe2 heterostructure has been observed to exhibit a type II band alignment [2]. Additionally, Zhen et al [3]. conducted a study investigating the impact of S vacancies and interlayer interactions on the electronic structure and optical properties of the MoS2/WSe2 heterostructure.

In this context, the present work aims to explore the influence of atomic positions in the interlayer region (stacking configurations) of the MoS2/WSe2 heterostructure on its mechanical, electronic, and optical properties. This work revolves around modelling different spectroscopic techniques, such as Fourier-transform infrared spectroscopy (FTIR), Raman spectroscopy, ultraviolet photoelectron spectroscopy (UPS)/ inverse photoemission spectroscopy (IPS), and optical absorption spectroscopy. Raman and Fourier-transform infrared spectroscopy models are employed to capture differences in vibrational modes. Moreover, To model UPS/IPS, the density of states (DOS) are computed. To complement DOS information, the band structures for each stacking motif are computed. Finally, optical properties are evaluated through optical absorption spectroscopy simulations using a G0W0@BSE approach. These simulations are conducted on top of Density Functional Theory (DFT) calculations, along with dispersion corrections using Density Functional Dispersion Correction (DFTD3), to account for van der Waals interactions between layers. These techniques provide insights into the structural, vibrational, electronic, and optical properties of this vertically-stacked heterostructure. All DFT calculations were performed with plane-waves and the projector augmented wave (PAW)

implementation within the Grid-based Projected Augmented Wave method (GPAW) code.

Four stacking configurations were studied (see Fig. I). These configurations are labeled as AA, AA', AB, and AB'. The considered stacking configurations do not result in unstable systems (they exhibit a positive binding energy, See Table 1). The most stable configuration turns out to be AB'. Vibrational and optical properties vary among different stacking configurations. Regarding vibrational modes, irrespective of the stacking configurations, the Raman and IR active modes for each layer are decoupled: the MoS2 layer moves while the WSe2 does not vibrate, and vice versa (See Fig. 2). Concerning optical properties, a relative shift between the layers leads to a different optical response. For example, compared to the most stable configuration, the absorption spectra for the other configurations are blue-shifted, with the peaks displaced to higher energies. Regarding the electronic structure, the band structures show that the band gap is located around the K-point. Changes in stacking configurations lead to a change in the band gap (See Fig. 3).

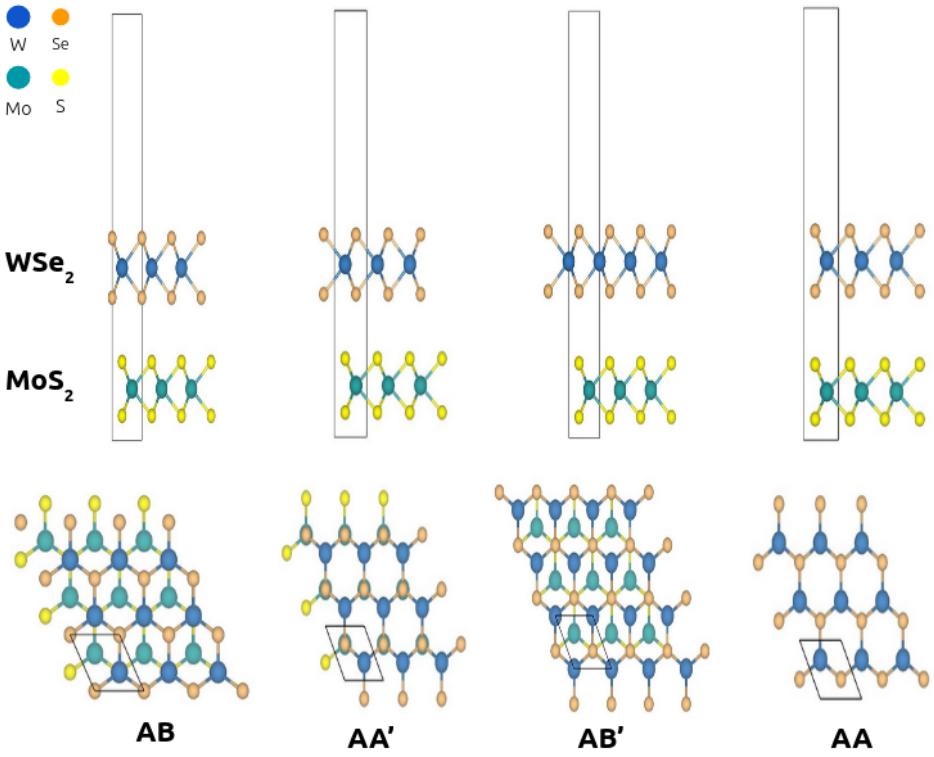

Fig. 1: Stacking configurations considered in this study.

Figure 1: **Stacking configurations considered in this study.**

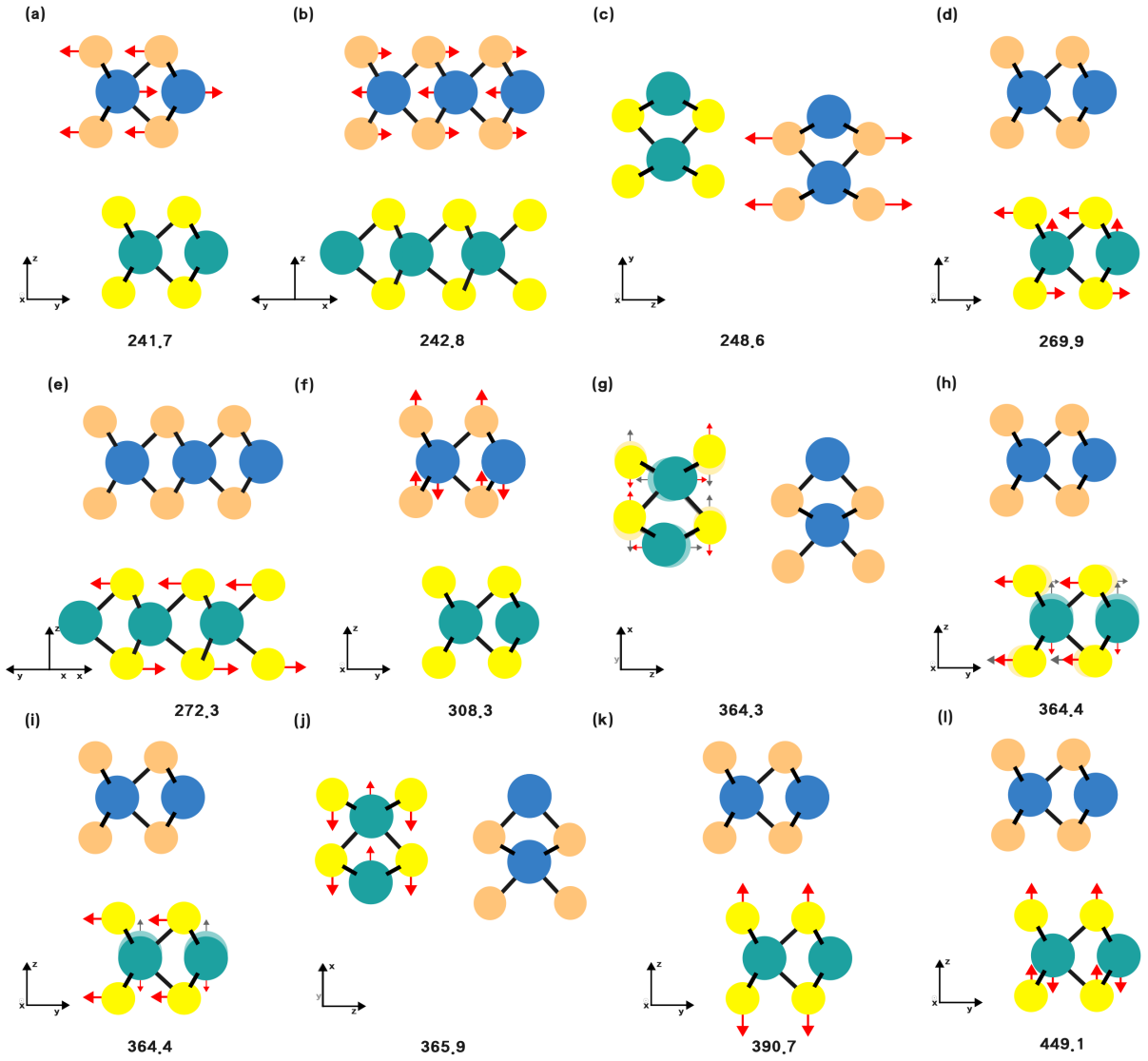

Figure 2: **(Raman-active) Vibrational modes for the most stable configurations.**

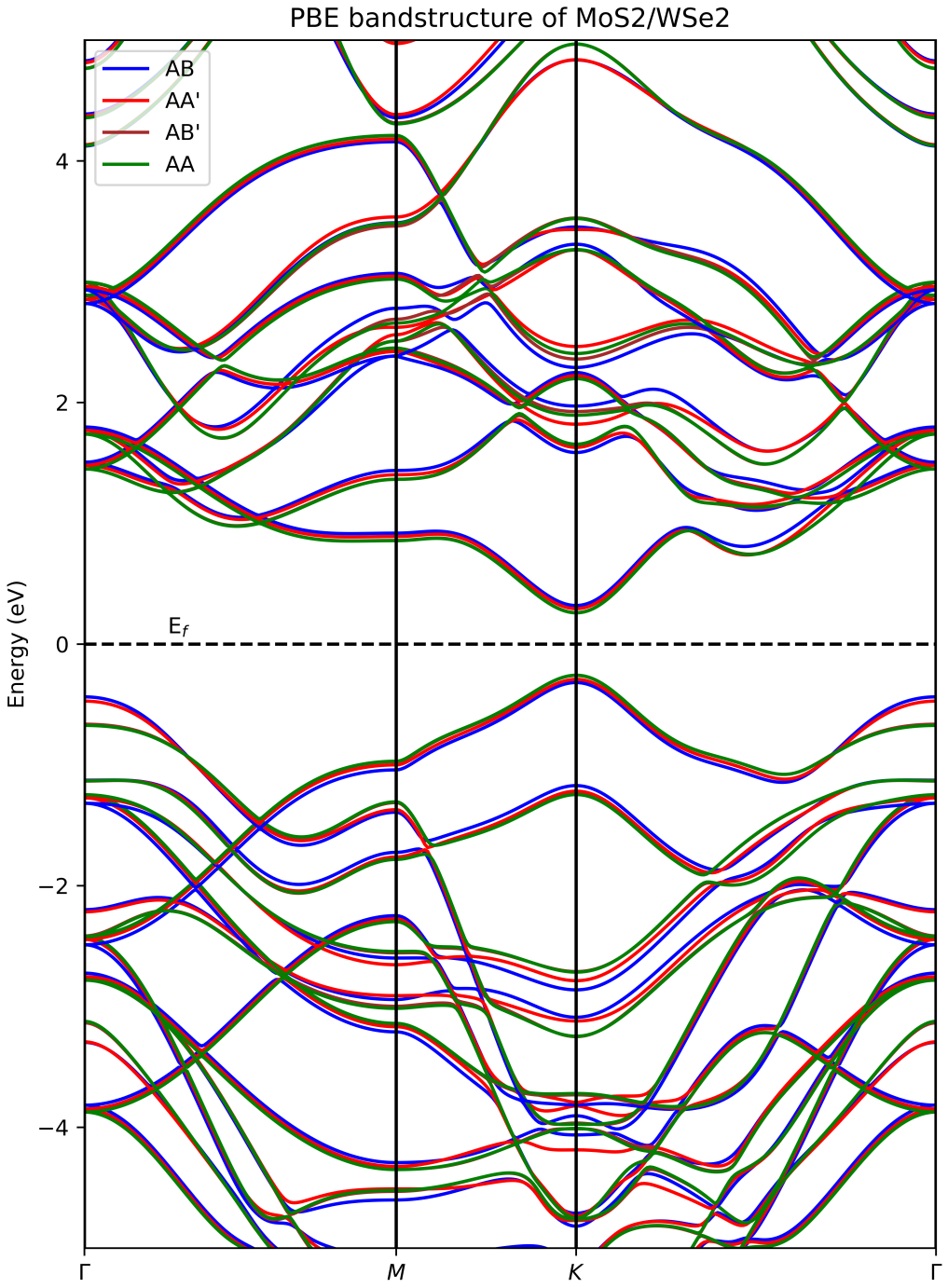

Figure 3: **Band structure for the four different stacking configurations.**

TABLE I: Computed total energies and binding energies of the four different atom positions motifs at MoS_2/WSe_2 and its lattice parameters.

	AB[a]	AA'[b]	AB'[c]	AA[d]
Lattice vectors (Å)	$\boldsymbol{a_1} = [\,3.232\,,\,0.\,,\,0.\,]$ $\boldsymbol{a_2} = [-1.616, 2.799, 0.]$ $\boldsymbol{a_3} = [\,0.\,,\,0.\,,\,24.332\,]$[e]	$\boldsymbol{a_1} = [\,3.231\,,\,0.\,,\,0.\,]$ $\boldsymbol{a_2} = [-1.615, 2.798, 0.]$ $\boldsymbol{a_3} = [\,0.\,,\,0.\,,\,24.332\,]$[e]	$\boldsymbol{a_1} = [\,3.231\,,\,0.\,,\,0.\,]$ $\boldsymbol{a_2} = [-1.615, 2.78, 0.]$ $\boldsymbol{a_3} = [\,0.\,,\,0.\,,\,24.332\,]$[e]	$\boldsymbol{a_1} = [\,3.231\,,\,0.\,,\,0.\,]$ $\boldsymbol{a_2} = [-1.615, 2.798, 0.]$ $\boldsymbol{a_3} = [\,0.\,,\,0.\,,\,24.332\,]$[e]
ΔE (meV/cell)	0.0	0.014	73	76
ΔE (meV/nm^2)	0.0	0.154	808	841
$E_{binding}$(meV/cell)	266	266	193	190

[a] W atop S, and Se atop Mo.
[b] Se atop S.
[c] W atop S.
[d] Se atop S, and W atop Mo.
[e] ∼14Å for vacuum.

Figure 4: **Computed total energies and binding energies of the four different atom positions motifs at MoS2/WSe2 and lattice parameters.**

References

[1] K. S. Novoselov, A. K. Geim, S. V. Morozov, D. Jiang, Y. Zhang, S. V. Dubonos, I. V. Grigorieva, and A. A. Firsov, Electric field effect in atomically thin carbon films, Science 306, 666 (2004), https://www.science.org/doi/pdf/10.1126/science.1102896.

[2] F. Wang, J. Wang, S. Guo, J. Zhang, Z. Hu, and J. Chu, Tuning coupling behavior of stacked heterostructures based on mos2, ws2, and wse2, Scientific reports 7, 1(2017)

[3] X. Zhen, H. Liu, F. Liu, S. Zhang, J. Zhong, and Z. Huang, Effect of s vacancy and interlayer interaction on the electronic and optical properties of mos2/wse2 heterostructure, Journal of Electronic Materials 52, 1186 (2023)

Acta Microscopica Vol. 34, Supp. 2, 2025
Abstract Book NSSY 2024 - Galapagos 19-25 May, 2024

A mini-review on functional multilayered materials

Claudia Alarcón-López[1]

[1] *Instituto Tecnológico y de Estudios Superiores de Monterrey*

claudia.alarconlpz@gmail.com

Abstract

Multilayered materials are ubiquitous in nature offering a wide range of relevant functionalities, going from mechanical performance to complex biosynthesis processes.

In materials engineering, biomimickry or bio-inspiration approaches have been effective strategies to develop complex multifunctional materials [1,2,3]

The rational combination of the properties of different materials in multilayer systems have been capitalized in science and engineering for several practical applications.

In this document, we review literature that present multilayered materials for different applications: mechanically enhanced materials, tissue-engineering, energy and sensing.

The interest in these multifunctional materials comes not only from their properties but also from the great possibilities of extrapolating their usage in seemingly unrelated areas with innovative techniques.

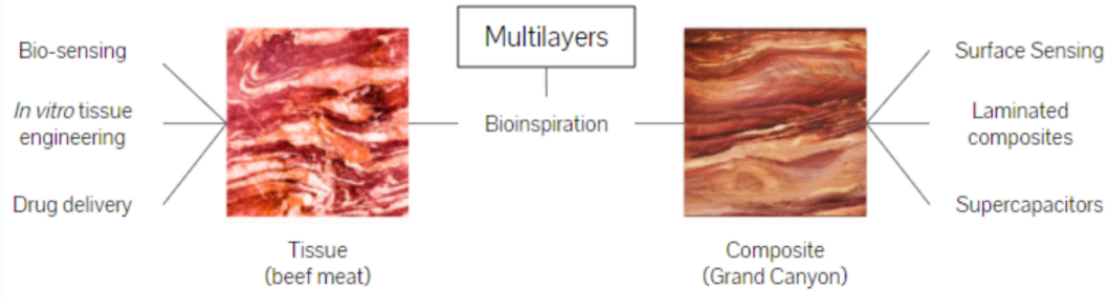

Figure 1: **Visual Abstract.**

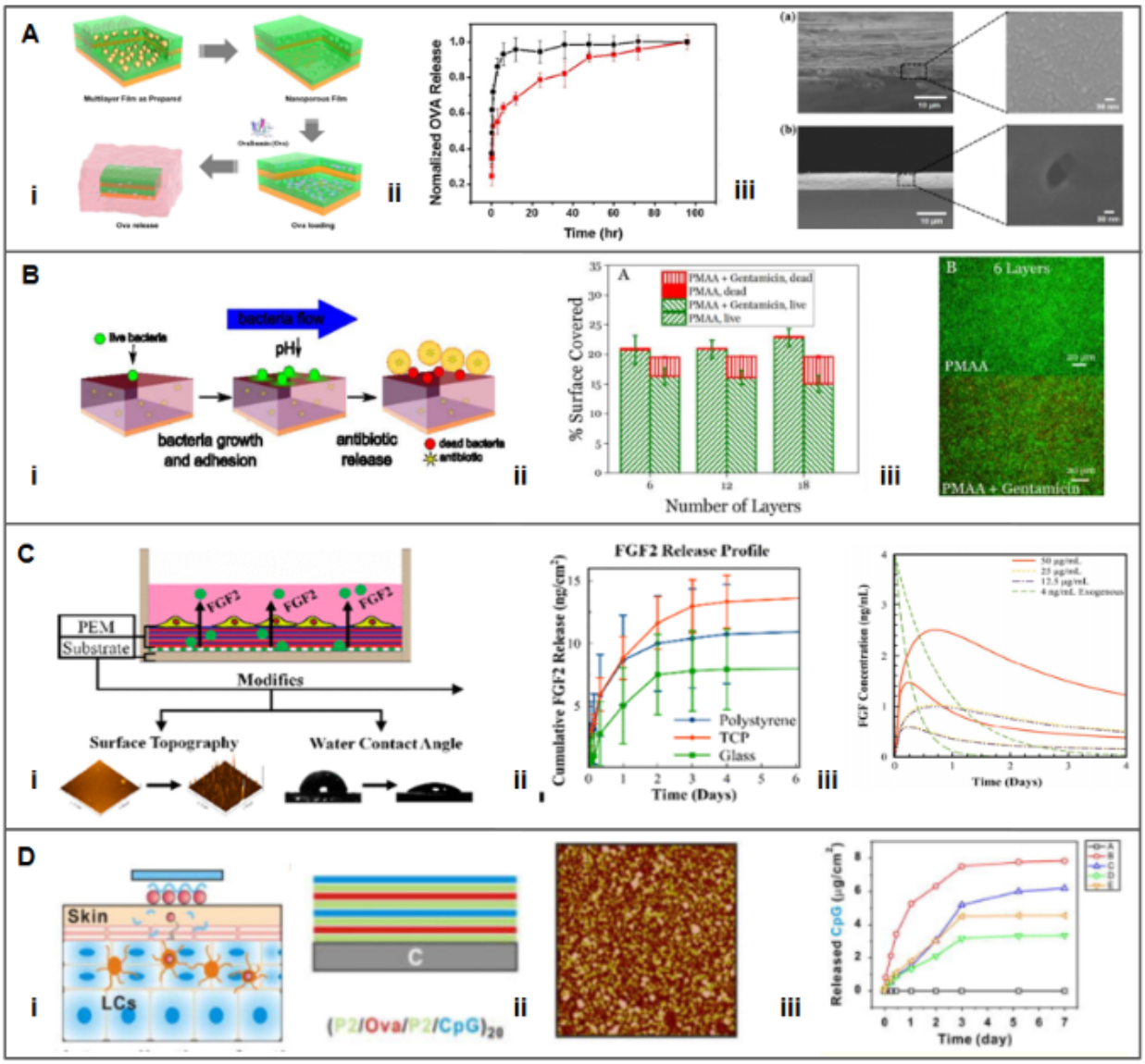

Figure 2: **Multilayers in controlled delivery systems.**

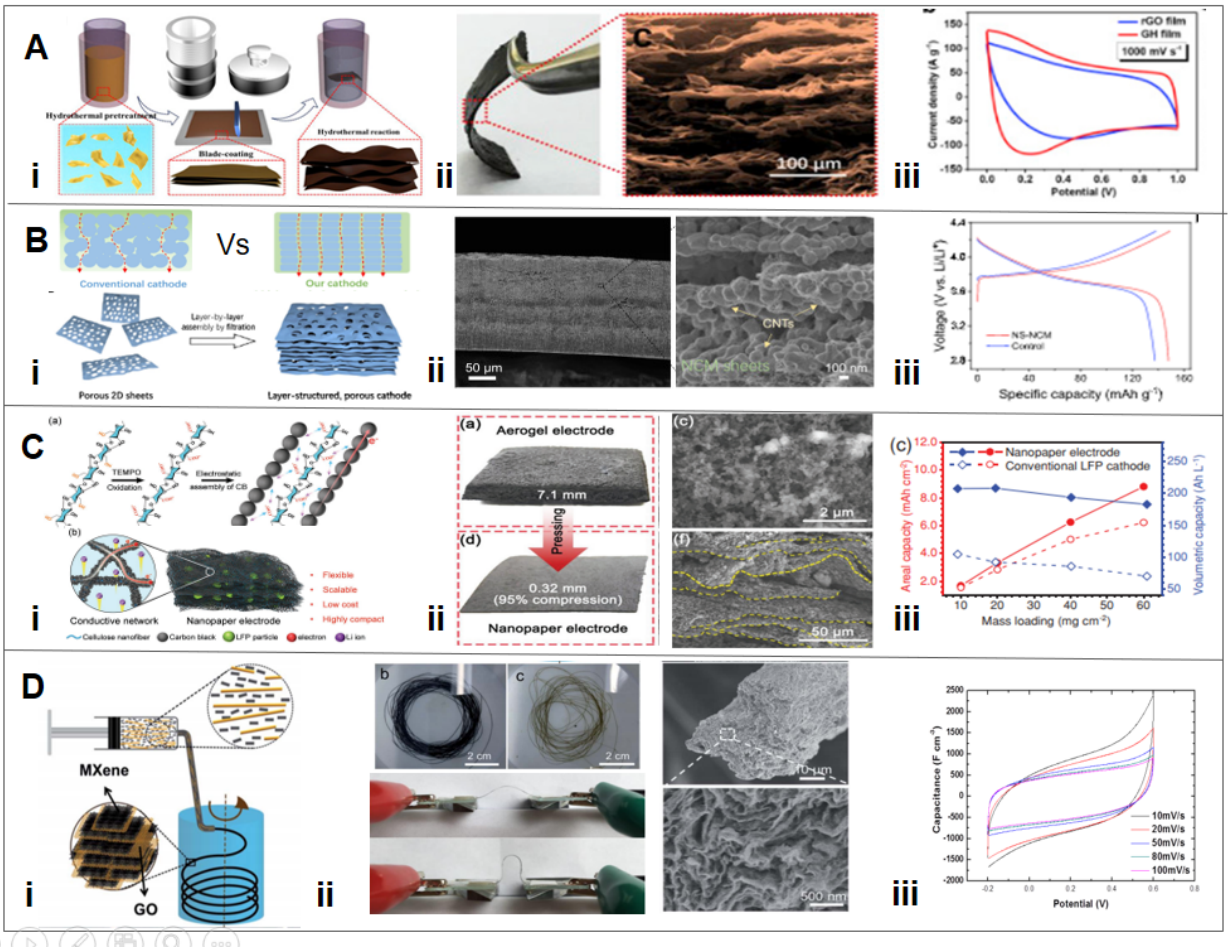

Figure 3: **Electrical properties of multilayer systems.**

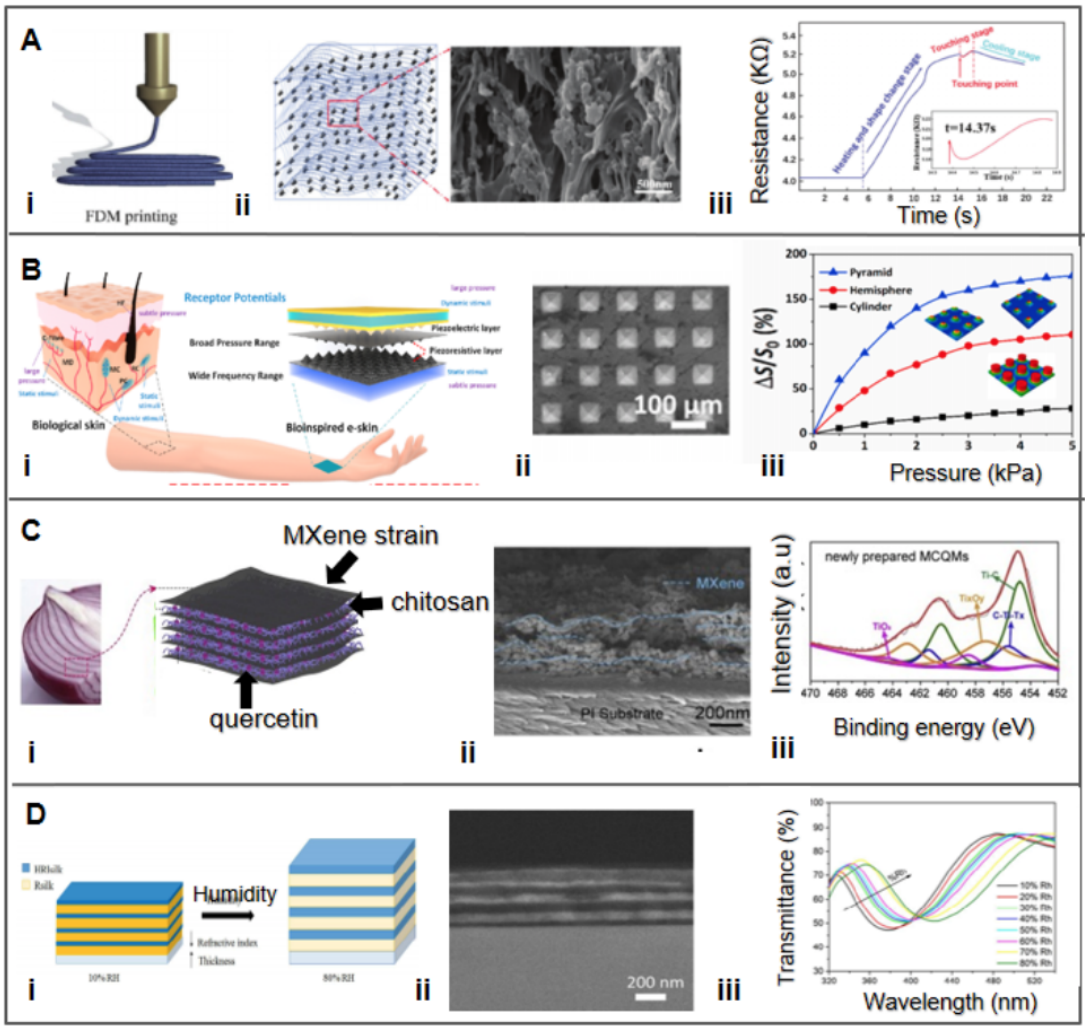

Figure 4: **Multilayer relevance in sensing technologies.**

References

[1] Y. Liu, K. He, G. Chen, W. R. Leow, X. Chen, Nature-inspired struc- tural materials for flexible electronic devices, Chemical reviews 117 (2017) 12893–12941.

[2] A. Bandyopadhyay, K. D. Traxel, S. Bose, Nature-inspired materials and structures using 3d printing, Materials Science and Engineering: R: Reports 145 (2021) 100609.

[3] C. Xu, A. R. Puente-Santiago, D. Rodríguez-Padrón, M. J. Muñoz- Batista, M. A. Ahsan, J. C. Noveron, R. Luque, Nature-inspired hierar- chical materials for sensing and energy storage applications, Chemical Society Reviews (2021).

Acta Microscopica Vol. 34, Supp. 2, 2025
Abstract Book NSSY 2024 - Galapagos 19-25 May, 2024

Surface-Enhanced Raman Scattering Detection of Atrazine in Water using Diatoms doped with Gold Nanoparticles

Melany Aguilar[1], Sarah Briceño[1], Carlos Reinoso[1], Gema Gonzalez[1]
[1] *School of Physical Sciences and Nanotechnology, Yachay Tech University, Urcuqui*
melany.aguilar@yachaytech.edu.ec

Abstract

Surface-enhanced Raman scattering (SERS) has increasingly captured the attention of research groups due to its remarkable capability for sensing and identifying trace substances. By analyzing the vibrational absorption spectrum, it enables the label-free detection of chemical and biological complexes with exceptional sensitivity and specificity [1]. However, conventional SERS substrates often suffer from poor reproducibility and instability, which limits their practical applications. Among the various nanostructured materials developed in research laboratories, porous materials have been extensively investigated [2]. They possess a unique feature compared to their bulk or planar counterparts: a substantial specific surface area available for sensing molecular probe-target interactions. The key to successful SERS analysis lies in carefully selecting the plasmonic material and its preparation. In response, scientists have explored new types of artificial optical structures called "photonic crystals"[3]. In this context, diatoms have emerged as promising plasmonic substrates when combined with metal plasmonic structures. This combination offers an attractive alternative to costly photolithography fabrication methods for SERS substrates. By integrating the photonic-crystal-like structure of Aulacoseira frustules with the plasmonic resonance properties of gold nanoparticles (AuNPs), the localized surface plasmon resonance can be significantly enhanced for the detection of atrazine. In this study, we use gold-doped diatom Aulacoseira genus microalgae-derived biosilica from Guayllabamba – Ecuador frustules as a cost-effective and readily available functional support for Surface-Enhanced Raman Scattering for the detection of atrazine in water. Our results revealed that this AuNPs doped on diatoms shows a SERS effect within the molecule of atrazine as well as the fluorescence that it enhances as a detector of the atrazine. This was confirmed using Raman Spectroscopy Fourier transform infrared spectroscopy (FTIR), and Fluorescence Optical Microscopy. This innovative approach holds great promise for advancing SERS technology and its practical applications in various fields.

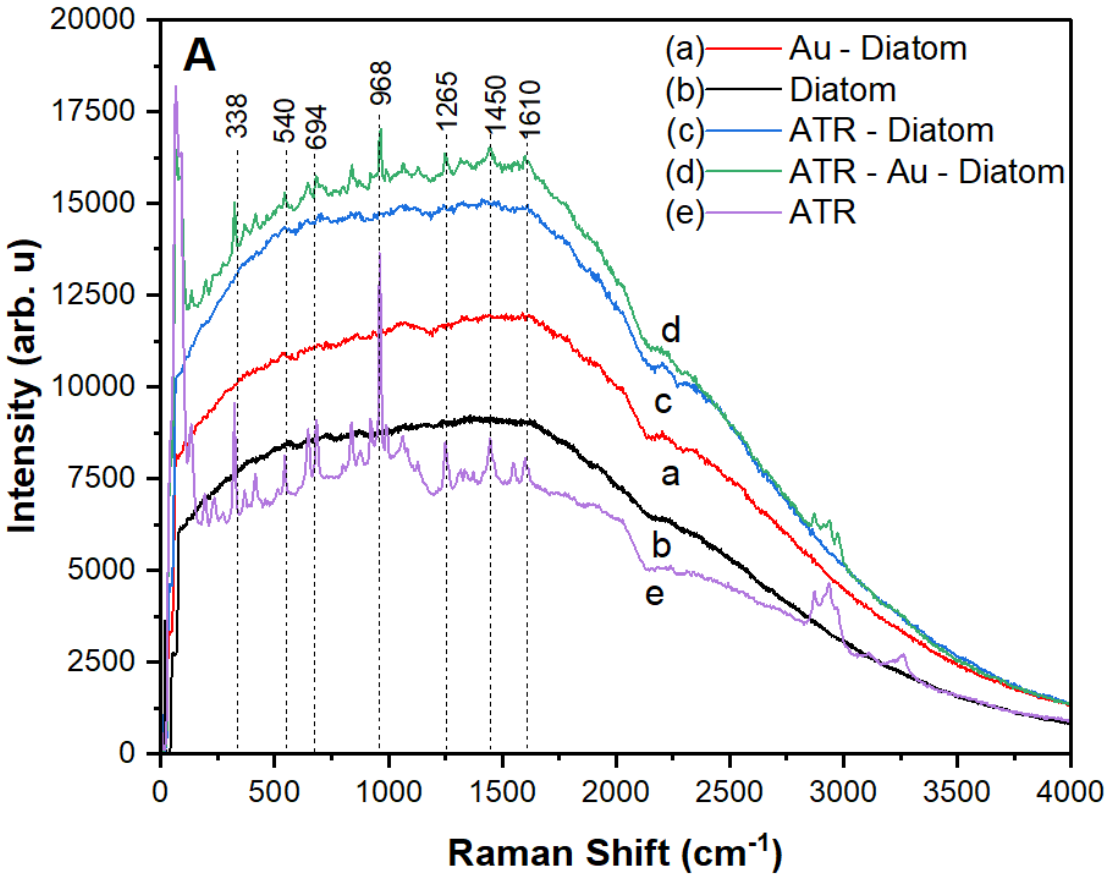

Figure 1: **Raman spectra of: (a) Diatoms loaded with AuNPs (Au-Diatom), (b) Diatom, (c) Diatoms + atrazine (ATR - Diatom), (d) Diatoms + AuNPs + Atrazine (ATR - Au - Diatom), and (e) Atrazine (ATR).**

References

[1] Briceño, S., Chavez-Chico, E. A., & González, G. (2021). Diatoms decorated with gold nanoparticles by In-situ and Ex-situ methods for in vitro gentamicin release. Materials Science and Engineering: C, 123, 112018.

[2] Bapat, G., Labade, C., Chaudhari, A., & Zinjarde, S. (2016). Silica nanoparticle based techniques for extraction, detection, and degradation of pesticides. Advances in colloid and interface science, 237, 1-14.

[3] Rea, I., & De Stefano, L. (2019). Recent advances on diatom-based biosensors. Sensors, 19(23), 5208.

Acta Microscopica Vol. 34, Supp. 2, 2025
Abstract Book NSSY 2024 - Galapagos 19-25 May, 2024

Green synthesis of hard carbon nanostructures

M. Daniela Serrano-Larrea[1], Julio C. Chacón-Torres[1], HJ Ojeda-Galván[2], M Quintana[3]

[1] *School of Physical Sciences and Nanotechnology, Yachay Tech University, 100119 Urcuqui, Ecuador.*

[2] *CIACYT, Facultad de Ciencias, UASLP, San Luis Potosí, México*

[3] *CICSaB, Facultad de Ciencias, UASLP, San Luis Potosí, México*

maria.serrano@yachaytech.edu.ec

Abstract

Nowadays, the green synthesis of nanomaterials and nanostructures is increasing exponentially because these synthesis techniques are economical, efficient, and eco-friendly. In addition, green synthesis promotes a circular economy, as diverse waste products could be used to produce semi-crystalline nanostructures such as "hard carbon", thus avoiding biowaste burning and preventing air pollution and greenhouse gas emissions. [3] For instance, biomass contains a high content of cellulose, starch, and lignin, which are the main components, with a high carbon yield (¿50 wt %). For this reason, biomass waste has become one of the most effective sources of hard carbon nanostructures. [1] [2] In this investigation, we develop "hard carbon" nanostructures by using a laser anneal treatment of endemic coconut-based biomass to obtain carbonaceous semi-crystalline nanostructures composed mostly of amorphous carbon in major percentage, followed by graphite and graphene at lower concentrations.[3] Thermal treatments, such as pyrolysis or laser ablation, are novel methods for green synthesis of carbon-based nanostructures [3] by inducing a heating of the organic biomass. Our "hard carbon" nanostructures were characterized by means of X-ray diffraction (XRD), X-ray photoelectron spectroscopy (XPS), scanning electron microscopy (SEM), transmission electron microscopy (TEM), and Raman spectroscopy to describe its structure, chemical composition, and morphology. The Raman spectra from our hard carbon showed the presence of carbonous materials by revealing a clean spectrum with the D, G, and 2D bands, being those sharp and thin peaks similar to graphite/graphene. In the case of the D and G bands the peaks, showed a good intensity with a clearly different size, being the D band a much shorter than the G band, with a Id/Ig ratio of 0.25, showing that the structure has graphite and amorphous carbon on it, with a I; however, in the case of the 2D band, even though the intensity was lower than G band, but bigger than D band, the 2D peak is sharp, with a FWHM= 81cm2 reveling the presence of a very few layer graphene. The XPS, the analysis of the pristine sample showed the presence of mostly carbon and oxygen matching with the organic composition of the Parajubea Cocoides (starch and cellulose). The laser annealed hard carbon showed a stronger sp2 graphitic carbon structure, as desired. Regarding the

SEM images, the pristine sample showed to have clear amorphous and similar-sized "rocks", which corresponded to the starch, and, notorious fibers that are representative of conventional coconut shell structure, corresponding to lignin and cellulose composition. On the other hand, the hard carbon revealed a porous structure characteristic of the material that according to the XRD analysis showed the presence of some planes (002), that correspond to graphitic structure with well-arranged planes, but with different interplanar distances. The TEM analysis confirmed our findings. The images support the XRD results by showing that the material contains aligned graphitic planes. The overall systematic characterization analyses conducted on our hard carbon material evinces the fact that Parajubea Cocoides conformed of starch and cellulose can be transformed into graphitic hard carbon nanostructures - graphite "blocks" separated by amorphous carbon and vacancies in between with enlarged surface areas. This kind of structures are of high importance for the development of high storage capacity of Li ion battery electrodes made out of endemic biowaste.

References

[1] Xie, L., et al. (2021). Hard Carbon Anodes for Next-Generation Li-Ion Batteries: Review and Perspective. Advanced Energy Materials, 2101650. doi:10.1002/aenm.202101650

[2] Beda, A., Le Meins, J.-M., Taberna, P.-L., Simon, P., & Ghimbeu, C. M. (2020). Impact of biomass inorganic impurities on hard carbon properties and performance in Na-ion batteries. Sustainable Materials and Technologies, e00227. doi:10.1016/j.susmat.2020.e00227

[3] Baldinelli, A., Dou, X., Buchholz, D., Marinaro, M., Passerini, S., & Barelli, L. (2018). Addressing the energy sustainability of biowaste-derived hard carbon materials for battery electrodes. Green Chemistry, 20(7), 1527–1537. doi:10.1039/c8gc00085a

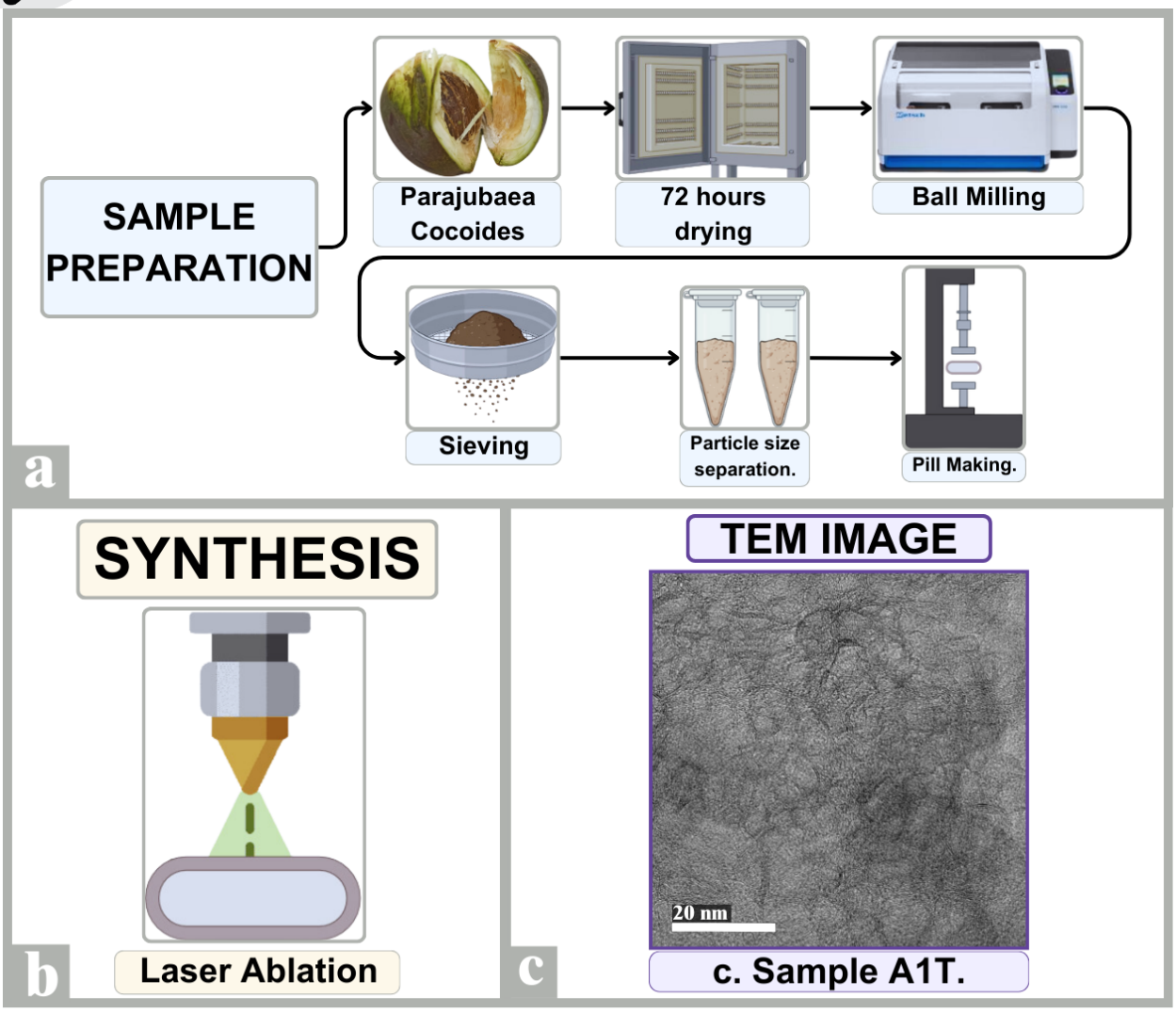

Figure 1: **Methodology. a. Sample preparation steps. b. Synthesis method used. c. TEM image of Hard Carbon, from sample A1T (particle size bigger than 75µm).**

Acta Microscopica Vol. 34, Supp. 2, 2025
Abstract Book NSSY 2024 - Galapagos 19-25 May, 2024

Multi-walled carbon nanotube anodes optimized for a new generation of sodium ion batteries

A Castillo[1], C Reinoso[1], L Corredor[2]

[1] *School of Physical Sciences and Nanotechnology, Yachay Tech University, Urcuquí 100119, Ecuador.*

[2] *School of Chemical Sciences and Engineering, Yachay Tech University, Urcuquí 100119, Ecuador*

antonio.castillo@yachaytech.edu.ec

Abstract

The applicability of carbon nanotubes (CNTs) has revolutionized materials science, increasing properties like conductivity, resistivity, and other benefits that this material offers depending on the way it is used. Carbon-based materials are attracting extensive study for the new generation of sodium ion batteries (SBIs) due to their sustainability, natural abundance, adequate redox potential, efficient sodium ion intercalation capacity, cyclable stability, and low polarization. The variety of carbon forms, such as graphene, hard carbon, nanotubes, etc., allows adaptation to specific design and performance requirements which are suitable for storing and releasing energy efficiently[1]. The objective of this work is to synthesize electrodes with multi-walled carbon nanotubes (MWCNTs) to be used in the fabrication of Sodium batteries to increase and optimize their performance, as well as the efficiency on them. Here, multi-walled carbon nanotubes (MWCNTs) were synthesized by Carbon Vapor Deposition (CVD) with two types of catalysts: one in aqueous medium and the other with iso-propanol, both with a metal composition of 10%. Iron (Fe) and cobalt (Co) deposit in a $CaCO_3$ as a matrix, subsequently a layer of each catalyst was applied in ceramic containers and exposed to acetylene under controlled temperature for the growth of MWCNTs [2]. Characterization by Raman spectroscopy confirmed the presence of carbonaceous material. In order to avoid the pollution in the electrodes by the byproducts from the synthesis and also from the catalyst, a purification of the samples was mandatory. A chemical approach was taken as a purification of the samples, with hydrogen peroxide (H_2O_2), hydrochloric acid (HCl), and a combination of both so that they were rinsed by entering them to a centrifugation, filtration, and drying process. Thanks to this process, the defect index can be deduced, which is the relationship between the D band and the G band of the spectrum, which indicates that the sample of Iso+HCL+H_2O_2 MWCNTs are the least harmful when purifying. Fig1. Regarding the use of carbon structures in batteries since graphite was explored in the 1980s, and its Na^+ insertion capacity was limited. In the 1990s, soft coals such as petroleum coke, carbon black, and pitch were tested, but they also had limited

capabilities. Hard carbons, with their disordered structure and distance between layers, have been used as promising anodes for (SBIs). These advances highlight the continuous evolution in the search for efficient materials for sodium ion batteries, as studies show how sodium batteries are being applied in different projects but the challenge of using Na instead of Li lies in energy density and weight, but it is anticipated that Multi-Walled Carbon Nanotubes (MWCNTs) will optimize energy retention and provide a structure for swift sodium ion movement, enhancing charging and discharging processes. However, one of the applications of these batteries is in electric cars. Since the first-generation sodium ion battery has a slightly lower energy density than the current lithium iron phosphate batteries. However, it stands out for its low-temperature performance and fast charging, especially in high-power applications in wide regions. Nowadays there is a trending effort from many companies to explode the fabrication and market of sodium-ion batteries, with a lower cost than lithium-ion batteries due to the high availability, they are ideal for cost-sensitive applications with moderate energy needs, such as storage or two-wheeled vehicles, thanks to these previous studies and taking into account how profitable this alternative could be, the manufacturing and synthesis process of said electrodes will be discussed, which will be shared in detail during the poster session.

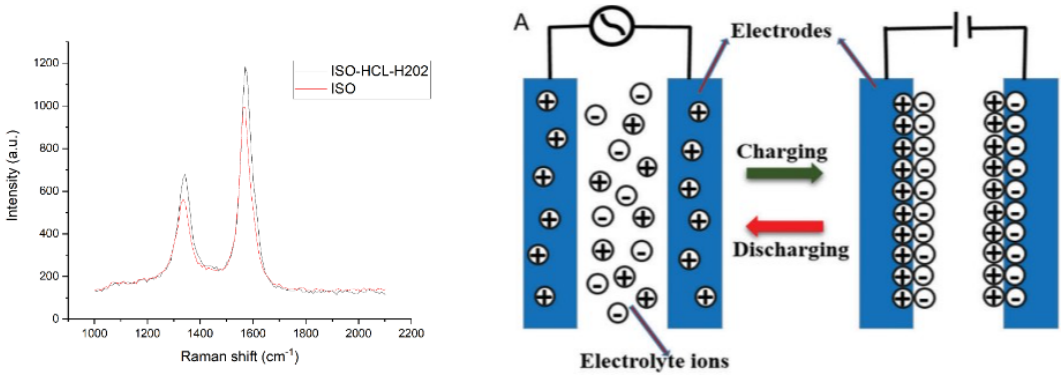

Figure 1: **Figure 1. On the left, we can see the comparison before/after purification with MWCNT-ISO along HCl-H_2O_2 , and on the right, we can see the diagram of a battery taken from (G. Kothandam. et al).**

References

[1] S. Mukherjee. et al. Electrode Materials for High-Performance Sodium-Ion Batteries - Materials. (2019) (12) (1952). doi: 10.3390/ma12121952. PMID: 31212966; PMCID: PMC6630545.

[2] J. Andrade. (2021) Catalyst Dependency for the Growth of Carbon Nanotubes, Urcuquí, Technology Research University Yachay Experimental, pp. 27.

[3] G. Kothandam. et al. Recent Advances in Carbon-Based Electrodes for Energy Storage and Conversion. (2023) (10), (2301045). doi: 10.1002/advs.202301045.

Acta Microscopica Vol. 34, Supp. 2, 2025
Abstract Book NSSY 2024 - Galapagos 19-25 May, 2024

Photoinduced quantum transport: EQE modeling through NEGF formalism applied on PCBM

Duncan J. Mowbray, **Jeyson Patricio Alomoto Catota**,
Daniel Esteban Gonzalez Tamayo, Vito Despoja
[1] *Yachay Tech University*
[2] *University of Zagreb*
jeyson.alomoto@yachaytech.edu.ec

Abstract

Over time and with the harness of current technology, the cost per watt produced by a solar cell went from 96$ in 1970 to 3$ in 2020. Nowadays, the most common material for constructing solar cells worldwide is silicon, which has a maximum theoretical efficiency of 32% and a commercial efficiency of 24%. Cheaper solar devices with higher efficiencies can only be constructed by continue making efforts to develop novel materials that can surpass the efficiency of silicon at a reasonable cost. Then, the photoinduced quantum transport is still an open field to develop high-impact science. Current computational models can be helpful for a large set of physical applications and have become crucial for accelerating any investigation process. The current work proposes a model to calculate external quantum efficiency (EQE) theoretically and the main goal is to provide a simple method for comparing the efficiency of different semiconductor materials. EQE is defined as the fraction of the transmitted electrons to incident photons in the solar cell[**?**], $\eta_{EQE} = \frac{N_e}{N_\omega}$, and can be used to measure the capability of a material to produce charge carriers when it is irradiated with light. The EQE process can also be described as the probability of an electron is initially at energy ε_i, is then exited by an incident photon to intermediate energy $\varepsilon_i + \hbar\omega$, and finally is transmitted out at an energy ε_f. The model is constructed using the non-equilibrium Green's function (NEGF) formalism to describe the quantum transport[**?**]. The model includes an operator $\hat{\mathcal{A}}(\mathbf{r}, t) = \frac{e}{2mc}\hat{\mathbf{A}}.\hat{\mathbf{p}}$ defined as the time-dependent interaction which acts as a coupling between the occupied and unoccupied states via the external electromagnetic field as $\langle\varphi_\mu|\hat{\mathcal{A}}(\mathbf{r}, t)|\varphi_v\rangle$ [**?**]. The methodology used to set up the DFT calculations of the PCBM was to implement a GPAW Python code, together with ASE repositories. The model was applied over an arrangement of 2 PCBM molecules oriented in the z-direction using periodic boundary conditions. It uses LCAO to represent all the matrices used in the NEGF methodology and the Kohn-Sham wavefunctions. Additionally, it was stated a GLLB-SC exchange-correlation functional calculation for the explicit evaluation of the derivative discontinuity cor-

rection. The structure was treated through a FIRE minimization-relaxation process using the PBE-D3 approach to consider the Van der Waals interactions of the molecules. The results suggest an important EQE for photons with energies of 2.8 to 3.6 eV, which corresponds to the near UV range. Moreover, both the occupied and unoccupied density of states present two band gaps. Then, in the energy range from 0 to 4 eV, the transmission goes from 1 to 10% in the three places where the occupied and unoccupied states show strong overlapping. For further research, the model can be used in parallel with artificial intelligence to analyze large sets of databases looking for those materials with high EQE for their design in silico.

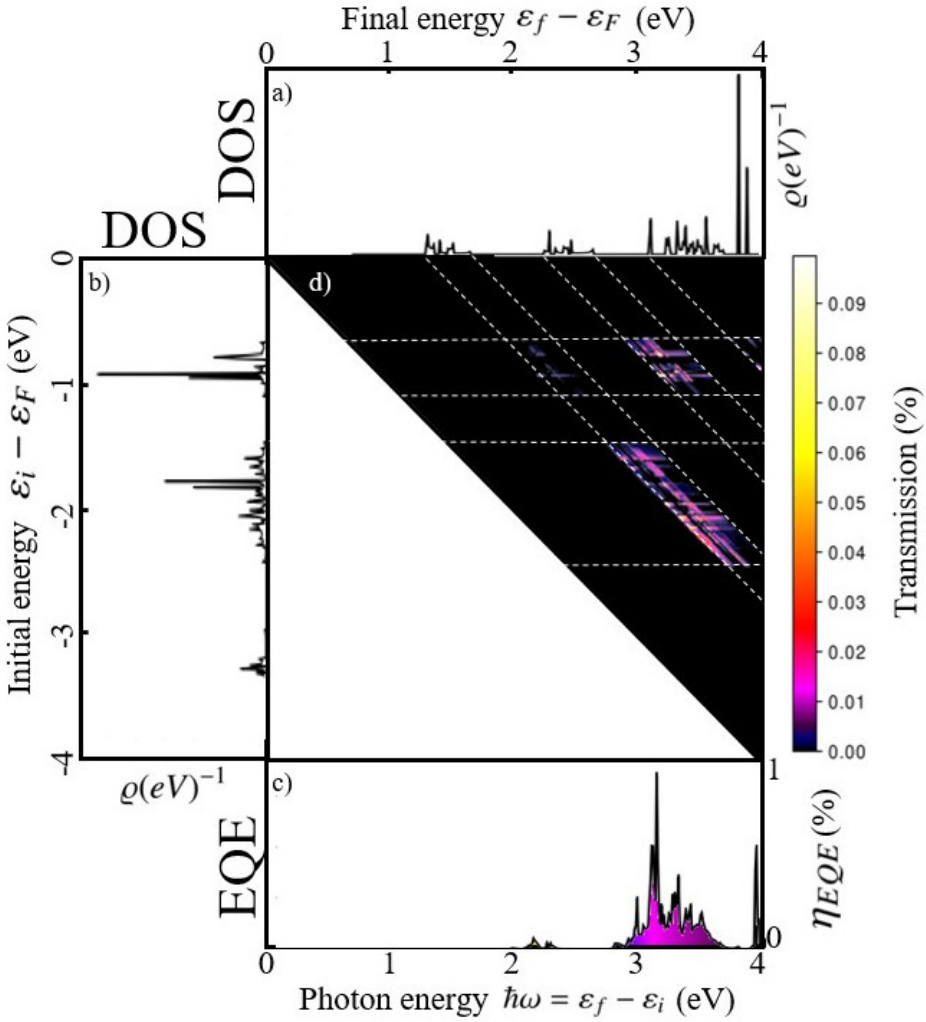

Figure 1: **Schematic results of the EQE model applied on the PCMB molecules. a): Unoccupied DOS vs final energy (eV), b) occupied DOS vs initial energy, c) EQE vs photon exitation energy, d) resultant transmission from the occupied and unoccupied overlapings.**

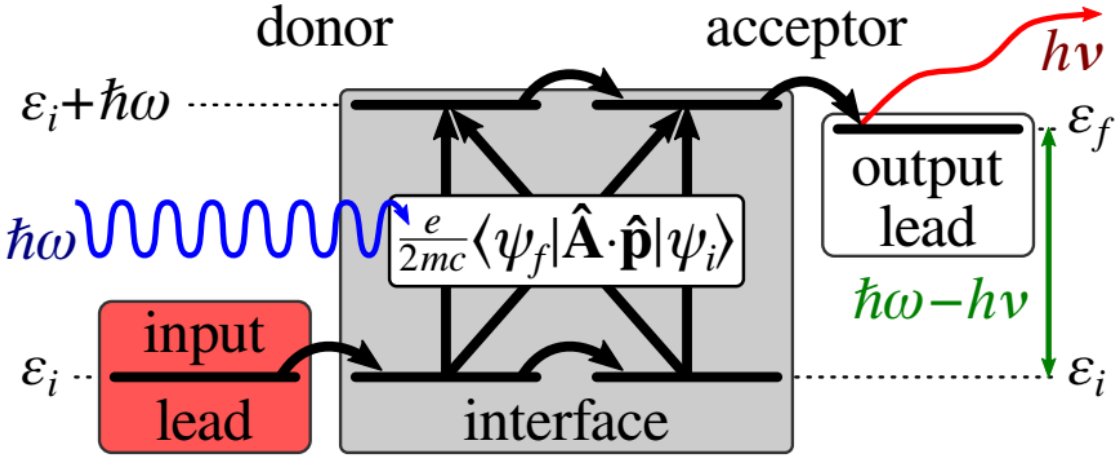

Figure 2: **Schematic of an excitation process across a donor–acceptor interface from an occupied initial state in the input lead to an unoccupied intermediate state, and to final state in the output lead.**

References

[1] Slami, A.; Benramdane, N. Manual method for measuring the external quantum efficiency for solar cells. 2021.

[2] Datta, S. The non-equilibrium Green's function (NEGF) formalism: An elementary introduction. 2002.

[3] Meis, C.; Dahoo, P.-R. Vector potential quantization and the photon wave-particle representation. 2016

Acta Microscopica Vol. 34, Supp. 2, 2025
Abstract Book NSSY 2024 - Galapagos 19-25 May, 2024

Synthesis of Graphene species in a simulated non-terrestrial environmental condition

Angie C. Dávila Porras[1], Helga Dénes[1], Julio Chacón-Torres[1]
[1] *Yachay Tech University, School of Physical Sciences and Nanotechnology, 100119. Urcuqui-Ecuador*
angie.davila@yachaytech.edu.ec

Abstract

Nowadays, graphene has called the attention of many researchers worldwide because of its unique mechanical, electronic, and optical properties, which have been used to develop novel electronic materials such as transparent conductive electrodes, photodetectors and light emitting devices [1]. Unfortunately, it does not grow naturally on Earth, consequently, some methods for its synthesis have been developed. In the extraterrestrial medium, there exist a rich environment of chemical structures and molecules that can not be found naturally on Earth. Carbon is an element exclusively formed in the hot interiors of stars and expelled into the interstellar environment to be part of the stellar dust, from which 80% has been incorporated into gaseous polycyclic aromatic hydrocarbon (PAHs) and other carbon allotropes such as diamond, fullerenes, amorphous carbon, graphite, and carbides (i.e. silicon carbide), among others [2]. Surprisingly, Giri et. al. (2021) reported the presence of nanoscale graphene found embedded in the refractory calcium-aluminum-rich inclusion (CAI) inside the Allende and QUE 94366 CV3-type meteorites [3].

The aim of this project is to prove the viability and required conditions for graphene formation in the outer space, simulating an extraterrestrial controlled environment. Following this purpose, we have searched for the possible sources and star dust components that could have given way to the growth of graphene in this medium. As a result, we simulated a circumstellar envelope of a carbon-rich red giant star system that could be approximated to a chemical vapor deposition (CVD) synthesis method over a non-crystalline substrate of 6H-SiC composed of grains of different grit sizes. We studied three main grain sizes: i) 60/90 (¿160 µm, ¡250 µm), ii) 120/220 (¿58 µm, ¡100 µm), and iii) 500/600 (¿10.7 µm, ¡14 µm). Considering the abundance of hydrogen gas, the presence of methane from some cold carbon-rich stars, and the residuals of inert gasses detected in SiC grains, the samples were exposed to various carrier gasses as hydrogen (H2) and argon (Ar), with carbon precursors as methane (CH4), at different flow rates and at a temperature of 1000 °C. Later, the synthesized samples were characterized via Raman

spectroscopy to disclose the presence of the graphene fingerprint over the 6H-SiC grains.

When working with CH4, H2 and Ar fluxes, it was seen that a poor graphene structures were formed with too many defects (ID/IG= 0.85) derived from the excess of carbon attached to the substrate generated by methane. Later, we exposed the SiC grains just to H2 and Ar fluxes, simulating a standard interstellar environment. A characteristic defect caused by the functionalization of hydrogen with graphene was expected from the line-shape of the D to G line region. Finally, from the tests with Ar we detected the presence of an almost pure one-layer graphene (ID/IG= 0.42) and a single 2D line, as well as we realized that the synthesis was reproducible over the same parameters of time, temperature and flow rate of gas. Furthermore, the Raman mapping over a 6H-SiC grain after synthesis showed that graphene was formed mostly in the edges of the grain in a non-homogeneous way, where 2D, G and D characteristic bands of graphene were detected.

In summary, we have demonstrated that almost pure graphene can be formed in the chaotic environment of the interstellar medium even at temperatures up to 1000 °C, specifically in the CSE of carbon-rich AGB stars. Furthermore, the grain size is not a determining factor for growing graphene, but the gasses flowing around and the time of synthesis become an extremely relevant factor to be considered. In this case, the best suitable extraterrestrial environment for growing graphene in outer space is at the presence of argon gas with no high presence of hydrogen, that is similar to the early-type stars with low reddening and some nebulae system.

References

[1] Chang, H., & Wu, H. Advanced Functional Materials. (2012) 23 (16)

[2] X. H. Chen et al. The Astrophysical Journal (2017) 850 104

[3] Giri, C., Steele, A., & Fries, M. Planetary and Space Science. (2021) (203) (105267).

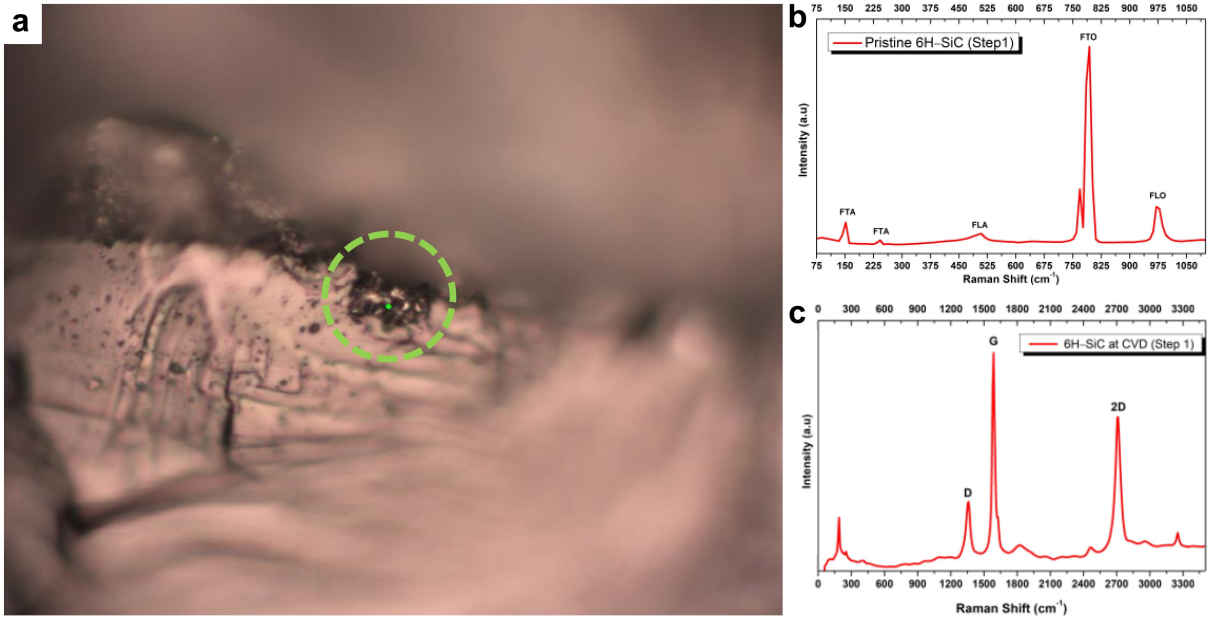

Figure 1: **Figure 1. (a) Optical image of a 6H-SiC grain after synthesis taken with an objective of 50x, showing the region of graphene formation. (b) Raman spectra of pristine 6H-SiC. (c) Raman spectra of one-layer graphene detected at the edge of a 6H-SiC grain.**

Acta Microscopica Vol. 34, Supp. 2, 2025
Abstract Book NSSY 2024 - Galapagos 19-25 May, 2024

Evaluation of coffee grounds as a natural adsorbent for the removal of phosphates in aqueous solutions

Enma D.A. Carrion[1], Diana Guaya[2]
[1] *Universidad Yachay Tech*
[1] *Universidad Tecnica Particular de Loja*
enma.armijos@yachaytech.edu.ec

Abstract

My research focuses on using organic waste, specifically coffee waste, to create a natural adsorbent material to reduce the impact of pollution in wastewater. Since Ecuador is one of the countries with the highest consumption of this beverage, the waste is not utilized for any purpose, thus becoming a significant source of pollution. This research offers multiple advantages associated with low energy requirements, cost reduction, and promotion of wastewater decontamination, combining approaches with new technologies for the treatment and removal of heavy metals in aqueous solutions through physicochemical and electrochemical processes. Additionally, it has a second application, which is to recover the material from the water and return it to the soil full of adsorbed metals, especially phosphates, as a natural fertilizer, thereby addressing two major environmental issues.

References

[1] Andrade, T. S., Vakros, J., Mantzavinos, D., & Lianos, P. (2020). Biochar obtained by carbonization of spent coffee grounds and its application in the construction of an energy storage device. Chemical Engineering Journal Advances, 4. https://doi.org/10.1016/j.ceja.2020.100061

[2] Carvajal-Flórez, E., Fernanda, L., & Giraldo, M. (2020). Coffee Waste used as Biosorbent for Heavy Metals Removal in Wastewater. https://doi.org/10.21500/20275846.44477

[3] Klug, M., Gamboa, N., & Lorber, K. (2015). Fluidized bed pyrolysis with coffee grounds-Overview and first results of the research for generation of renewable energy in Peru. European International Journal of Science and Technology, 4(3), 1–17. www.eijst.org.uk

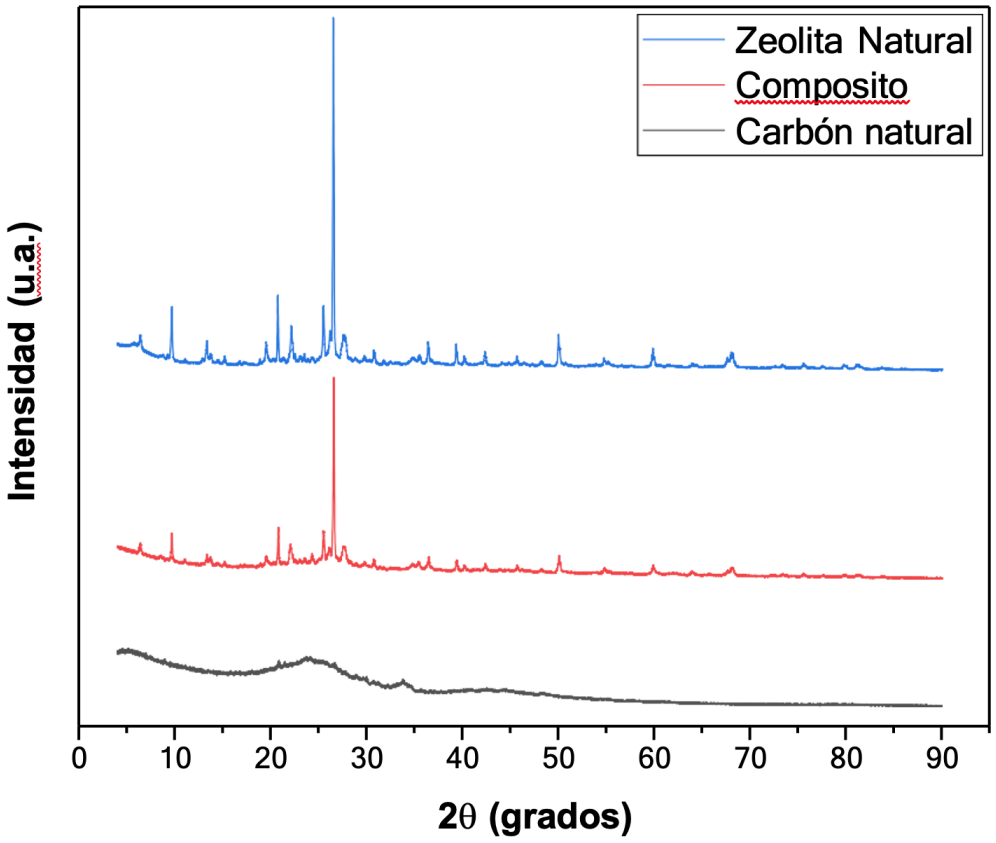

Figure 1: **DRX Carbón Natural, Zeolita Natural y Composito**

Tabla 9

Resultados área superficial BET composito

Parámetros	Resultados BET Single Point (Composito)
Área superficial BET	47,35 m^2/g
Volumen de monocapa	10,878 cm^3/g
Masa de muestra inicial	0.0941g

Figure 2: **Resultados área superficial BET composito**

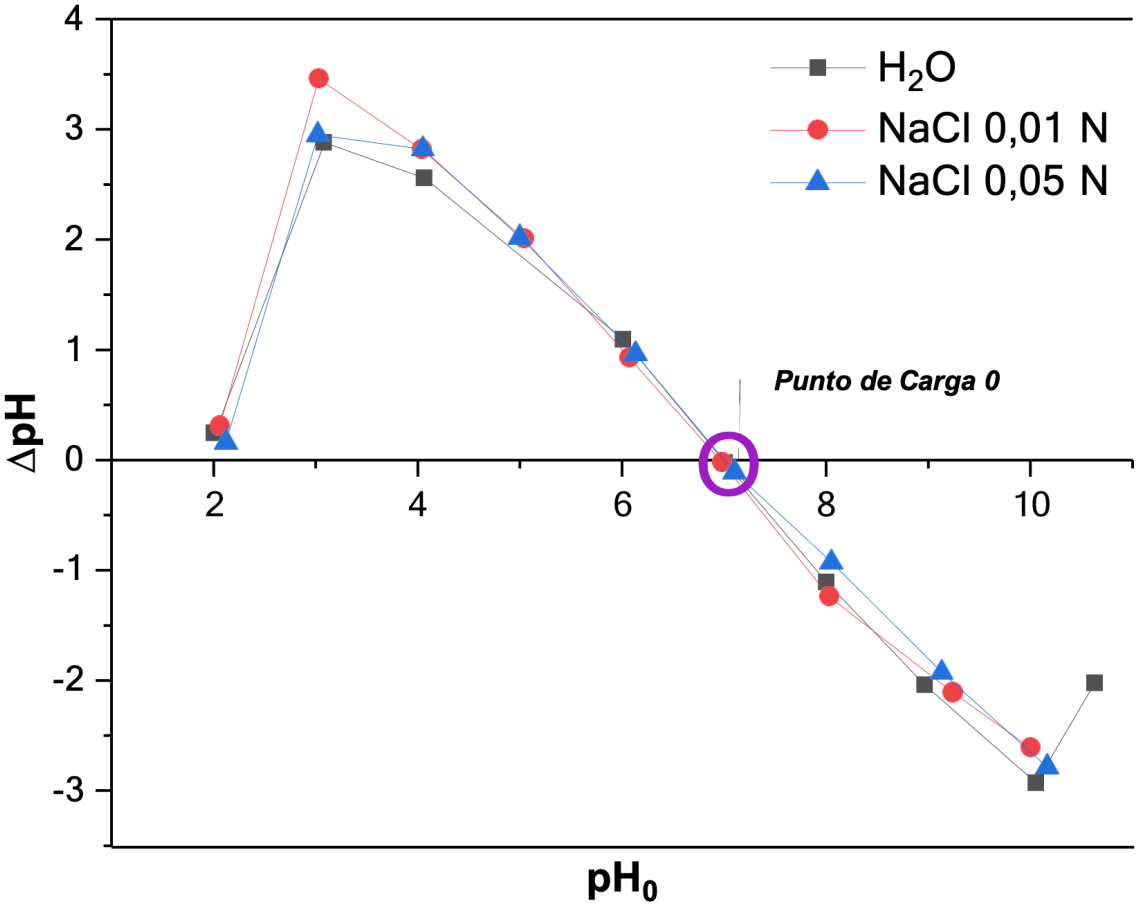

Figure 3: **Punto de carga cero composito**

Acta Microscopica Vol. 34, Supp. 2, 2025
Abstract Book NSSY 2024 - Galapagos 19-25 May, 2024

Level alignment, charge transfer, and optical absorption of organic photovoltaics using LCAO-TDDFT-k-omega code

Yomaira Elizabeth López Revelo[1], Duncan John Mowbray[1]
[1] *School of Physical Science and Nanotechnology, Yachay Tech University, Urcuquí, Ecuador.*
yomaira.lopez@yachaytech.edu.ec

Abstract

The solar radiation in Ecuador ranges between 2.9 kWh/m^2 day and 6.3 kWh/m^2 day. Indeed, the recommended amount of insolation for photovoltaics (PV) is exceeded in 75% of the Ecuadorian territory. Nevertheless, solar energy generation is just around 0.12% of the total energy production per year. The main limitations come from production costs for conventional solar cells. These problems are approached by looking for alternative optically active materials that promise more efficient, ecological, and economical solar cells, as is the case of organic photovoltaics (OPVs)s. Such cells can contain materials from dyes and polymers to carbon-based structures such as graphene, fullerenes, and carbon nanotubes.

This project intends to contribute to the computational design of OPVs and their understanding of the donor-acceptor excitonic process that allows their photoconductivity properties by modeling their optical absorption spectra. We applied a highly efficient linear combination of atomic orbitals (LCAOs) representation of the Kohn–Sham (KS) orbitals within time dependent density functional theory (TDDFT) in the reciprocal space (k) and frequency (ω) domains (LCAO-TDDFT-k-ω code) that, compared with DFT and GW-BSE methods, allows us to know the optical behavior for larger systems via an optimal computational performance. Thus, LCAO-TDDFT-k-ω offers the possibility to accurately describe the optical absorption and level alignment for complex OPV-based systems.

In this research, we considered two types of chlorophyll: a and b (Chl a/b), like the donor system. Its long chain was cut because the main electron-hole interaction is related with the chlorine ring (1), characterized by π-delocalized orbitals that facilitate efficient charge transfer. Likewise, the central magnesium atom functions to maximize the lifetime of the excited state. The effective and secure conversion of this excited state into chemical energy forms the foundation of the photosynthetic process.

Furthermore, their absorption spectra have their maximum of the solar spectrum

photon flux density at the Earth's surface, which corresponds to the visible region. For the acceptor system, single-wall carbon-nanotubes (SWCNTs) are attractive for their distinctive physical attributes, including ballistic conductance, customizable band gaps, photoluminescence, and high optical absorbance. They come in various chiralities, which, depending on the way they are rolled up, change their energy band gaps yielding potentially exploited in photovoltaic applications (2). These two systems can be physisorpted forming an OPV device, perfect to test our LCAO-TDDFT-k-ω code.

The calculations were performed through High Performance Computing (HPC) with the Imbabura Cluster using the GPAW python code based on the projector-augmented wave (PAW) method and the atomic simulation environment (ASE). The structures were firstly relaxed using the BFGS algorithm until a maximum force of less than 0.03 eV/Å was achieved. For the exchange and correlation function, the Perdew-Burke-Ernzerhof (PBE)-D3 was employed, a generalized gradient approximation with a Van-der-Waals correction because of the long-range interaction between the chlorophyll and SWCNT. A linear combinations of atomic orbitals (LCAO) with a double-z-polarized (DZP) basis set were utilized to represent the electron density and the Kohn-Sham wavefunctions, this is the most optimal parameter based on ref. 2 for the convergence of spectra. Later, the absorption spectra for the twelve systems were obtained using the LCAO-TDDFT-k-ω code with the imaginary part of the dielectric function and including the derivative discontinuity correction from GLLB-SC modified functional (See Fig 1).

Consequently, deriving the imaginary part of the dielectric function within the LCAO-TDDFT-k-ω code involves the straightforward multiplication of pre-computed matrices. This provides a significant speed-up compared with other methods, for example, Casida method. Finally, the spectra were analyzed based on its excitonic density and the contribution of the combined system of the peaks that indicates a carrier mobility between the molecules (See Fig 2).

Therefore, by studying the level alignment, charge transfer, and optical absorption of these complex OPV donor/acceptor systems, we aim to provide the means to design and improve the efficiency of these potential materials for solar cell applications.

References

[1] Preciado-Rivas, M. R., Mowbray, D. J., Lyon, K., Larsen, A. H., & Milne, B. F. (2019). Optical excitations of chlorophyll a and b monomers and dimers. The Journal of Chemical Physics, 151(17), 174102.

[2] Preciado-Rivas, M. R., Torres-Sánchez, V. A., & Mowbray, D. J. (2019). Optical absorption and energy loss spectroscopy of single-walled carbon nanotubes. Physical Review B, 100(23), 235429.

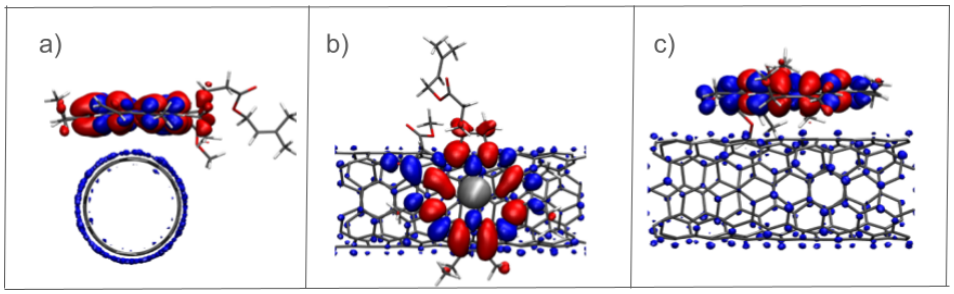

Figure 1: **Comparison among LCAO-TDDFT-k-omega spectra with PBE-sol functional (solid lines), PBE-D3 functional (dashed-lines) and experimental spectra (filled regions) for different CNTs chiralities.**

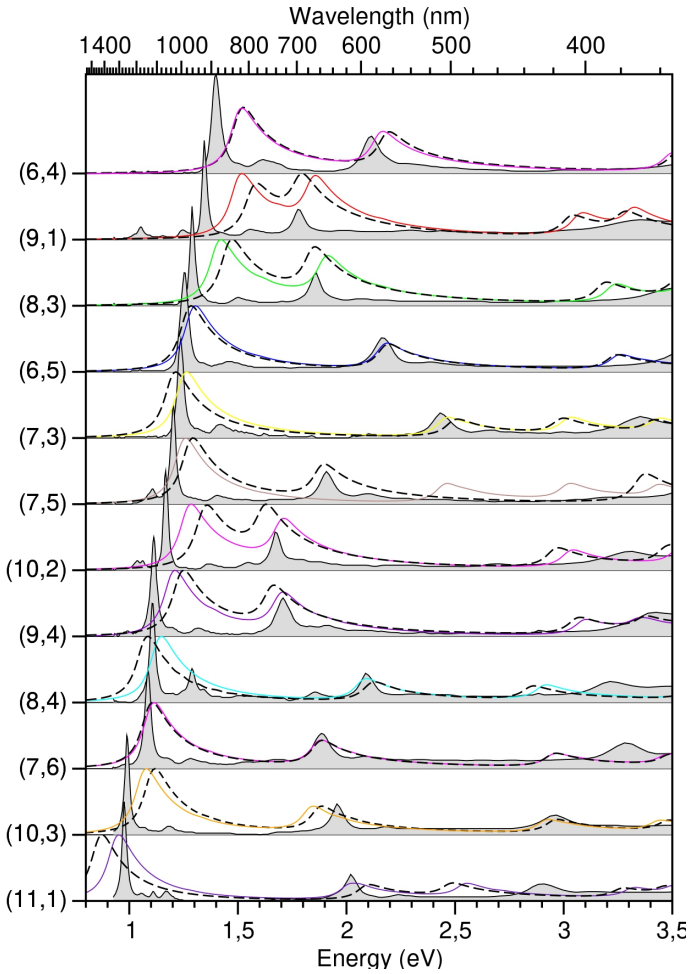

Figure 2: **Exciton density spatial distribution for a combined system of Chlorophyll a and SWCNT (6,4) from the HOMO –> LUMO transition peak at 1.9 eV. Holes density is given by red orbitals and electron density is given by blue orbitals.**

Acta Microscopica Vol. 34, Supp. 2, 2025
Abstract Book NSSY 2024 - Galapagos 19-25 May, 2024

Development and Characterization of nanobiocomposite: PVA/gelatin/GO for biomedical applications

Alisson L. Fajardo-Cabrera[1], Carlos D. Loyo-Dávila[2], María Gabriela Ruiz[1], Julio C. Chacón- Torres[3]

[1] *Yachay Tech University, School of Biological Sciences and Engineering, 100119 Urcuquí, Ecuador*

[2] *Yachay Tech University, School of Chemical Sciences and Engineering, 100119 Urcuquí, Ecuador*

[3] *Yachay Tech University, School of Physical Sciences and Nanotechonology, 100109 Urcuquí, Ecuador*

alisson.fajardo@yachaytech.edu.ec

Abstract

Polyvinyl alcohols (PVA) and gelatin are extensively utilized in various industrial and biomedical applications due to their unique properties. This study investigates the mechanical and thermal properties of films produced from PVA, gelatin, and their blends, including graphene oxide (GO) as a reinforcing agent. Solutions of 4% PVA and 10% gelatin were prepared and mixed in different proportions, with additional treatment involving GO. The films were subjected to mechanical testing, Fourier-transform infrared spectroscopy (FTIR), thermogravimetric analysis (TGA), and X-ray diffraction (XRD). Results indicate distinctive spectral peaks corresponding to functional groups within the materials, with notable shifts observed upon addition of gelatin and GO. TGA reveals enhanced thermal stability with increased gelatin content and the presence of GO. XRD patterns highlight changes in crystalline structure with varying composition. Mechanical testing demonstrates that as gelatin concentration increases, elongation at break decreases, while tensile strength and Young modulus are enhanced, especially with GO incorporation. These findings underscore the potential of PVA-gelatin blends, particularly when augmented with GO, for applications requiring tailored mechanical and thermal properties.

References

[1] Burgalassi, S., Zucchetti, E., Ling, L., Chetoni, P., Tampucci, S., & Monti, D. (2022). Hydrogels as Corneal Stroma Substitutes for In Vitro Evaluation of Drug Ocular Permeation. Pharmaceutics, 14(4). https://doi.org/10.3390/pharmaceutics14040850

[2] Krishna, D. V., & Sankar, M. R. (2024). Functionally graded Gelatine/PVA-based composite hydrogel for repairing the soft tissues of diarthrodial joints. Materials Today Communications, 38. https://doi.org/10.1016/j.mtcomm.2024.108070

[3] Thanganadar Appapalam, S., Paul, B., Arockiasamy, S., & Panchamoorthy, R. (2020). Phytofabricated silver nanoparticles: Discovery of antibacterial targets against diabetic foot ulcer derived resistant bacterial isolates. Materials Science and Engineering C, 117. https://doi.org/10.1016/j.msec.2020.111256

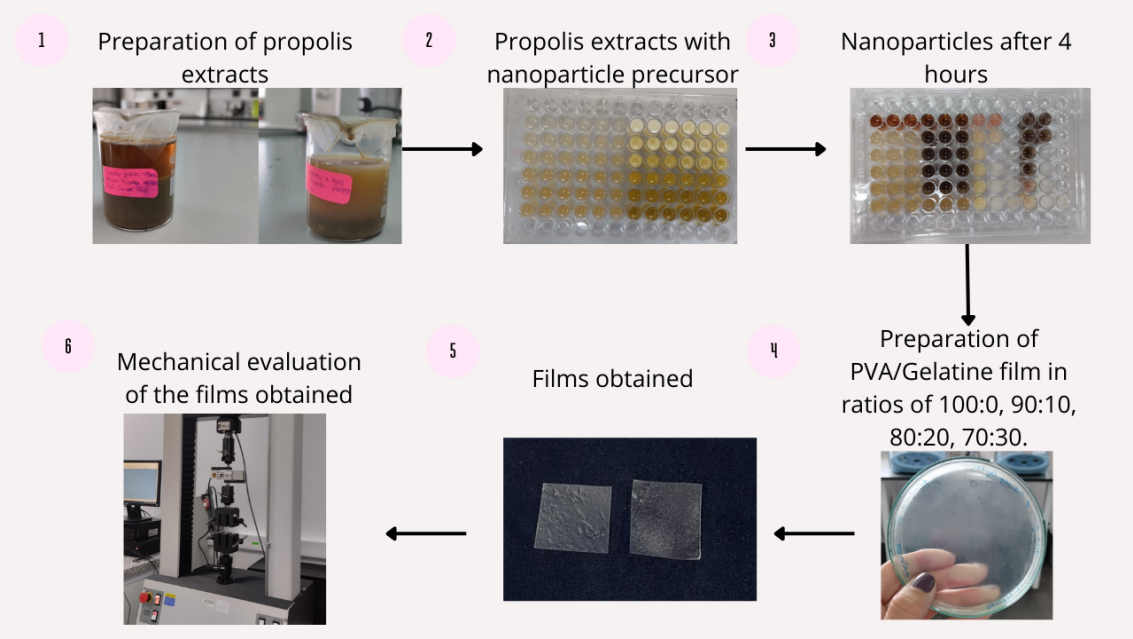

Figure 1: **This figure shows a graphical abstract of the methodology used in this research work.**

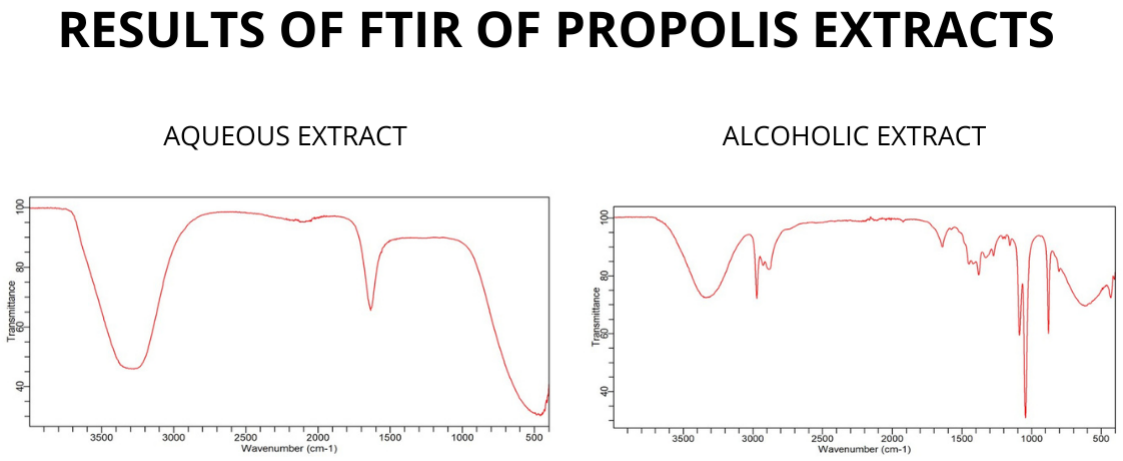

Figure 2: **This figure compares the IR spectrum of the aqueous and alcoholic extract of propolis.**

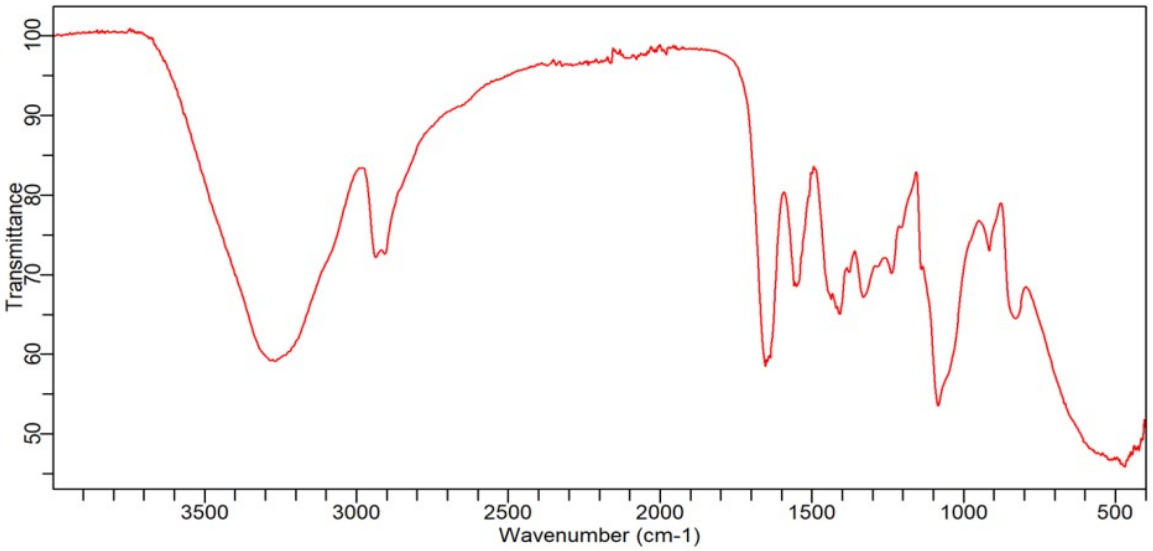

Figure 3: **This image shows the IR spectrum of the PVA/gelatin film, using the transmittance and wavenumber parameters.**

Acta Microscopica Vol. 34, Supp. 2, 2025
Abstract Book NSSY 2024 - Galapagos 19-25 May, 2024

Comparative study of in situ multiwalled carbon nanotubes Synthesis over Metal substrate for harvesting the solar energy to be used at the industry

Jorge Salvador Pico Vela[1] Carlos Reinoso[1]
[1] *Yachay Tech School of physical science and nanotechnology*
jorge.pico99@outlook.com

Abstract

The aim of the investigation is to find an optimal way to harvest solar energy by using copper and aluminum substrates where CNTs are grown using CVD methods. This way we take advantage of the absorptance properties of CNTs and the conductivity of the metal. This investigation will cover the synthesis from a superficial treatment of the metal using mechanical and chemical methods, next the growth in situ of multiwalled carbon nanotubes and lastly the characterization of the material synthetized and a comparative study of absorptance to find the most efficient device.

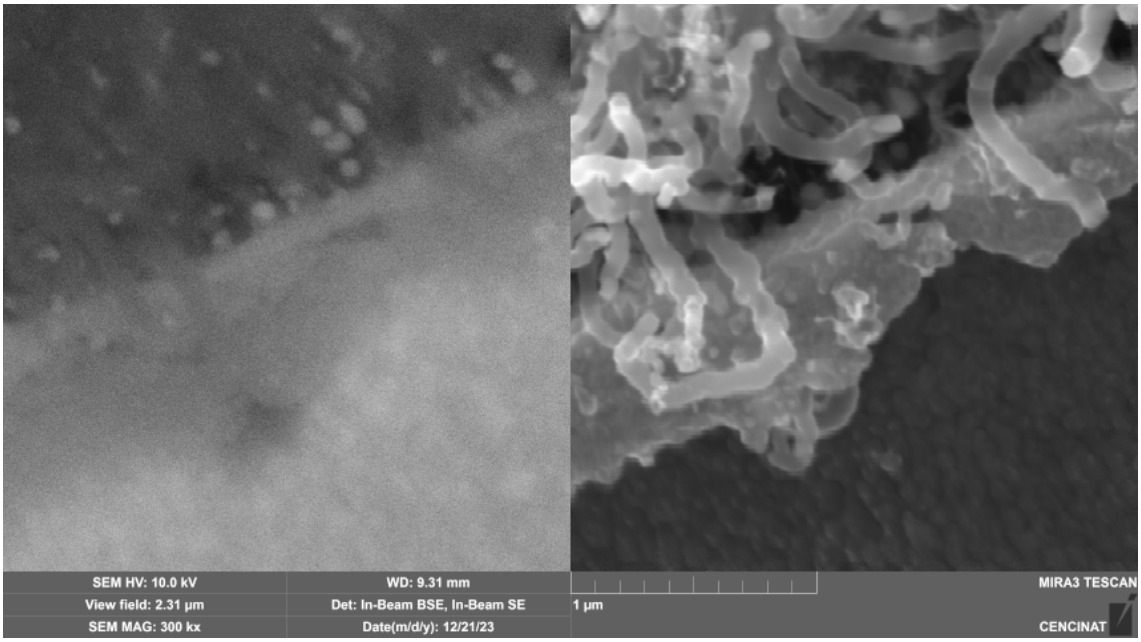

Figure 1: **SEM image of CNT over Al**

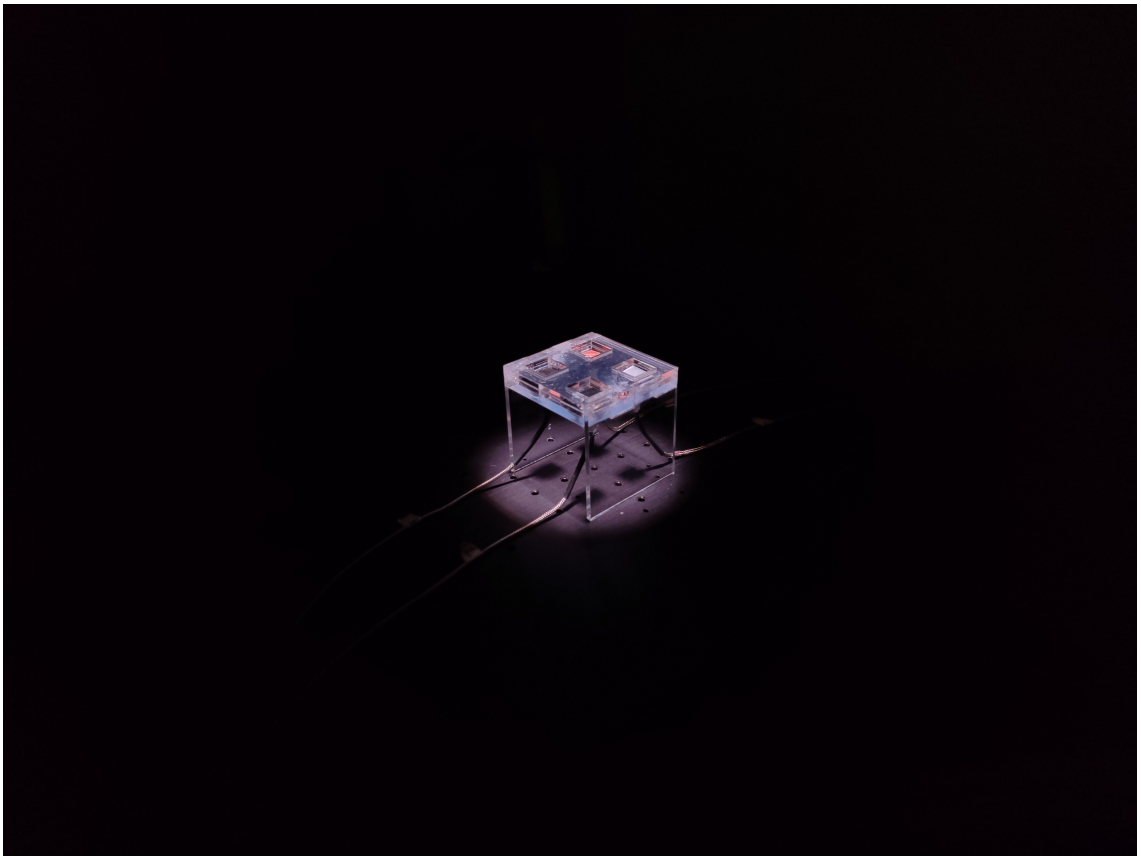

Figure 2: **CNT-Cu and CNT-Al on a solar simulation chamber to test heat capture capabilities.**

References

[1] Kumanek, B.; Janas, D. Thermal conductivity of carbon nanotube networks: A review. Journal of materials science 2019, 54, 7397–7427.

[2] Szabó, A.; Perri, C.; Csató, A.; Giordano, G.; Vuono, D.; Nagy, J. B. Synthesis methods of carbon nanotubes and related materials. Materials 2010, 3, 3092–3140

Acta Microscopica Vol. 34, Supp. 2, 2025
Abstract Book NSSY 2024 - Galapagos 19-25 May, 2024

Synthesis and characterization of a Diatom electrode with magnetic nanoparticles

María Silva[1], Gema González, Ph.D.[1], Sarah Briceño, Ph.D.[1]
[1] *Yachay Tech University, Physical and Nanotechnology Department*
maria.silvaz@yachaytech.edu.ec

Abstract

The advance in the study of materials for use in the manufacture of electrodes has led to take into account diatoms as a very promising material due to its properties and structure. In this project we designed a diatom material with different sources of carbon and magnetic nanoparticles for use as an electrode or biosensor these materials composed of diatoms with lignin, glucose, and active carbon with and without magnetite nanoparticles were synthesized, This design process involved several electrochemical and structural characterization techniques in which the presence of elements characteristic of diatoms and Iron Carbide nanoparticles Figure 2, which is a characteristic compound in the synthesis of magnetic nanoparticles using carbon sources in the CVD, was verified [1]. The presence of the materials in the fabricated composite is also noticeable in the Scanning Electron Microscope, where the morphologies corresponding to diatoms can be observed, in addition to the magnetite present, finally in the structural analysis Raman spectroscopy was performed with which the precense belong to carbon functional groups G and D of the samples was verified by analyzing the peaks present, which were characteristic of black carbon. In the electrochemical characterization that includes the analysis by means of the potentiostat with the Electrochemical Impedance Spectroscopy (EIS), Cyclic Voltammetry and Staircase Galvanostatic techniques, the response of the materials with different frequencies and voltages was studied. Obtaining the difference in the resistance of the material with the presence of magnetite in the pellets of diatomaceous earth composites. The components of the equivalent circuit for each sample were calculated with the EC-Lab software and the capacitance was obtained with galvanostatic charge/discharge tests in which the material showed capacitive behavior, in the Nyquist and Bode analysis it is observed how the resistance of the material is affected in the presence of magnetite, being thus that the samples manufactured with magnetite nanoparticles show lower resistance being more conductive.. This study was based on research on the functionalization of diatom surfaces with magnetic nanoparticles, in particular iron oxide nanoparticles, for various applications, including biomedical and nanotechnology applications as a low-cost fabricated biosensor. The research carried out confirms the potential use

of diatoms in the development of materials for high-per formance electrodes, or supercapacitors, due to its porous surface and charge storage capacity, diatoms can also provide a structure of high strength and hardness, as well as good electrical and thermal conductivity, because of this diatoms remain a study material for the development of devices[2], however, these investigations are still in process due to the analysis of the mechanical properties of these materials.

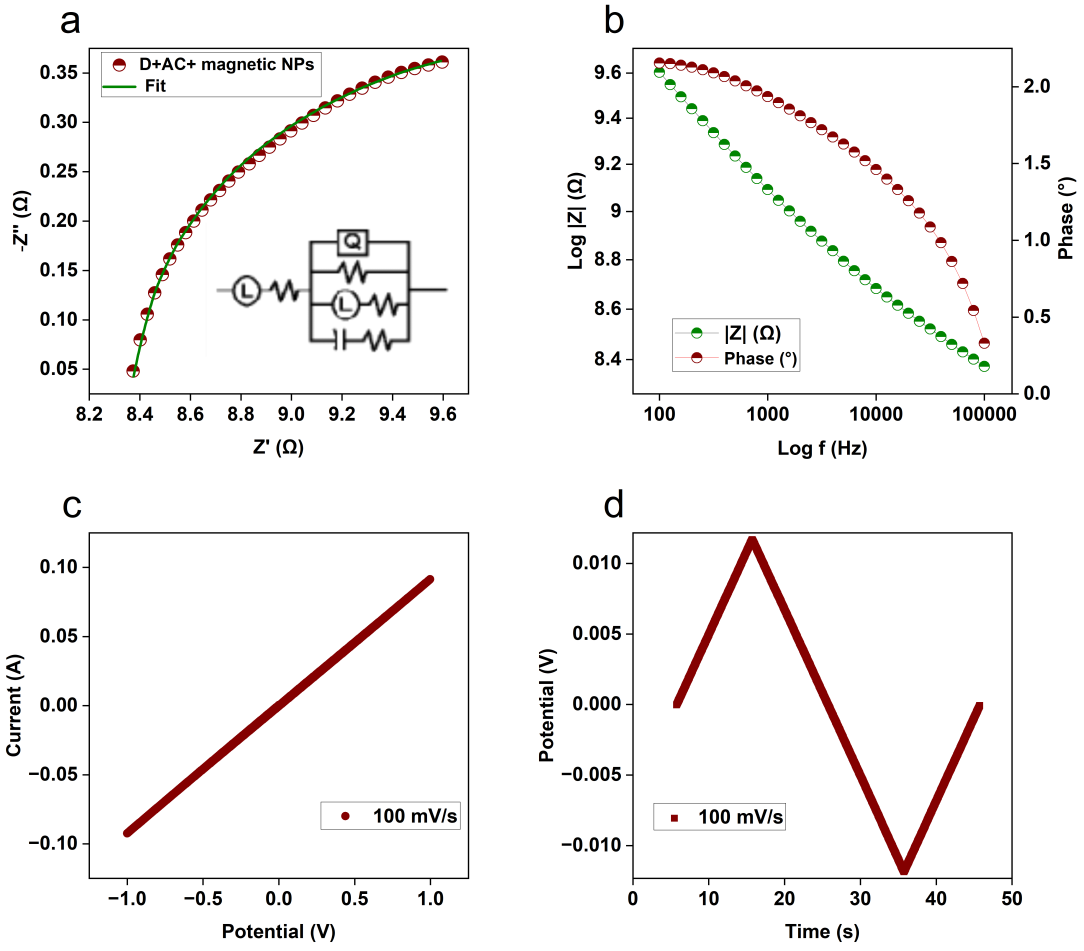

Figure 1: **Diatoms with Activated Carbon (a) Nyquist plot; (b) Bode plot; (c) I-V Curves; d) Galvanostatic charge-discharge curves.**

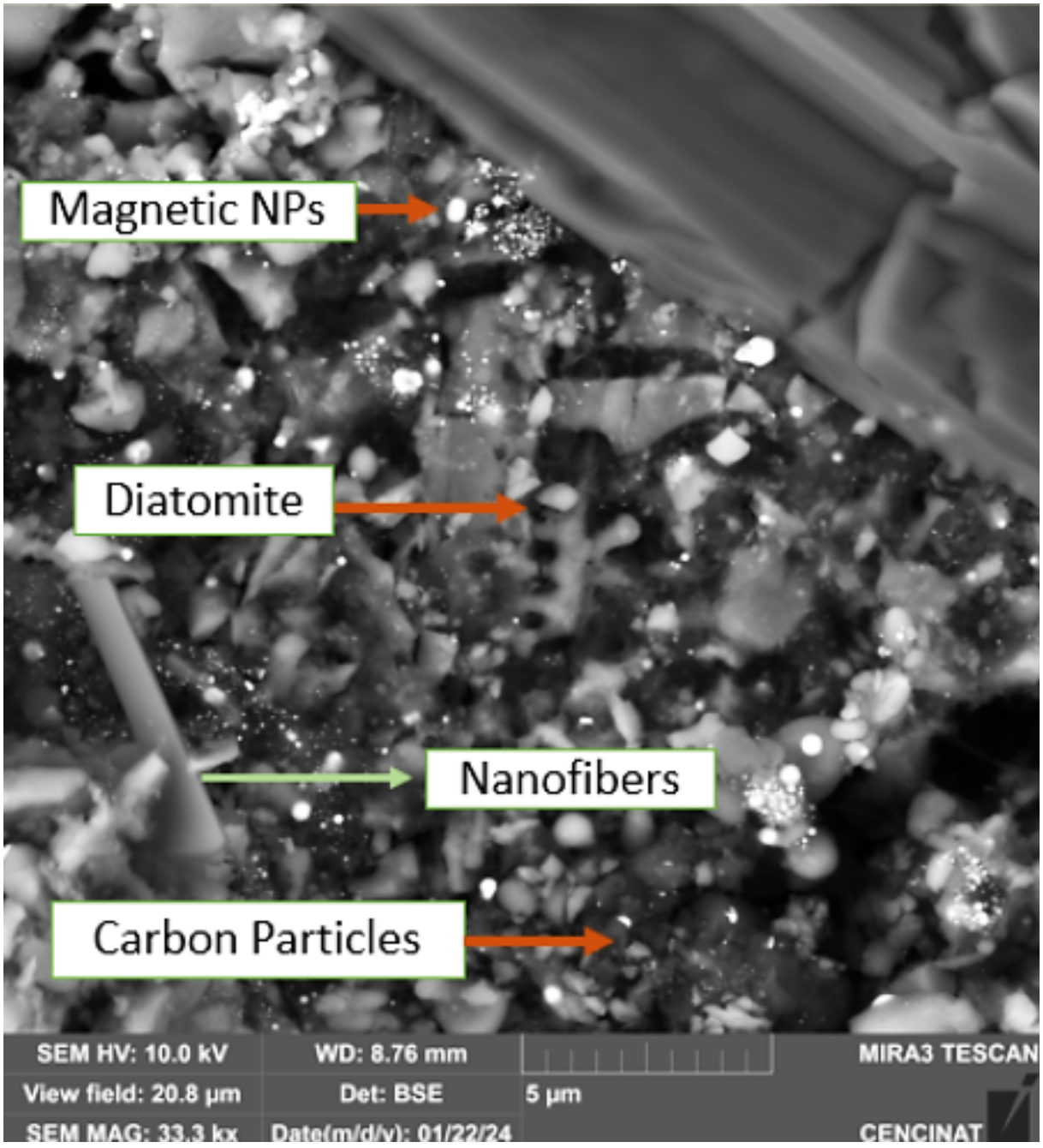

Figure 2: **SEM micrograph of Diatomites with Lignin and Magnetic NPs Composite**

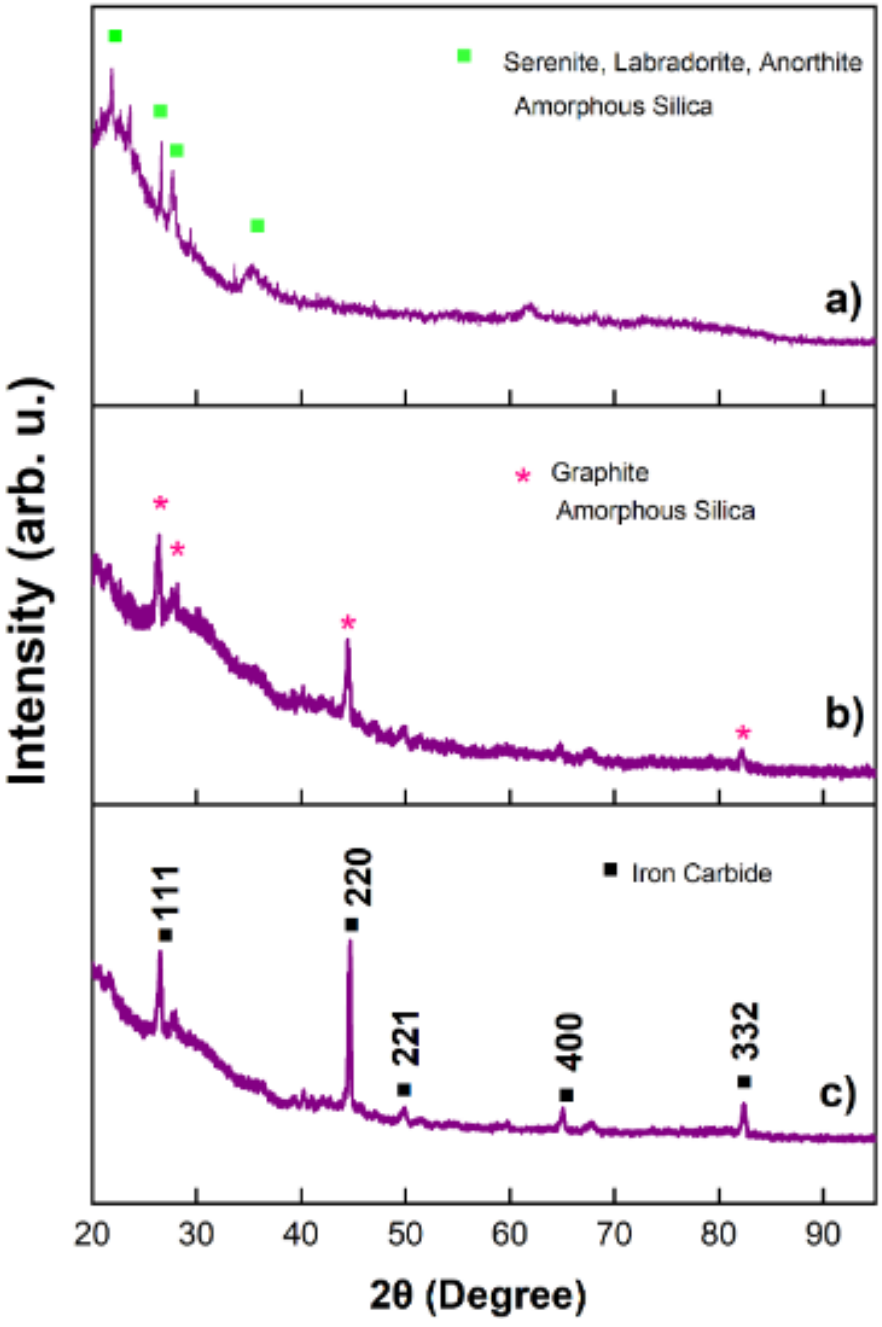

Figure 3: **XRD patterns of a) Diatomites b) Diatomites with Activated Carbon c) Diatomites with Activated Carbon and magnetic NPs.**

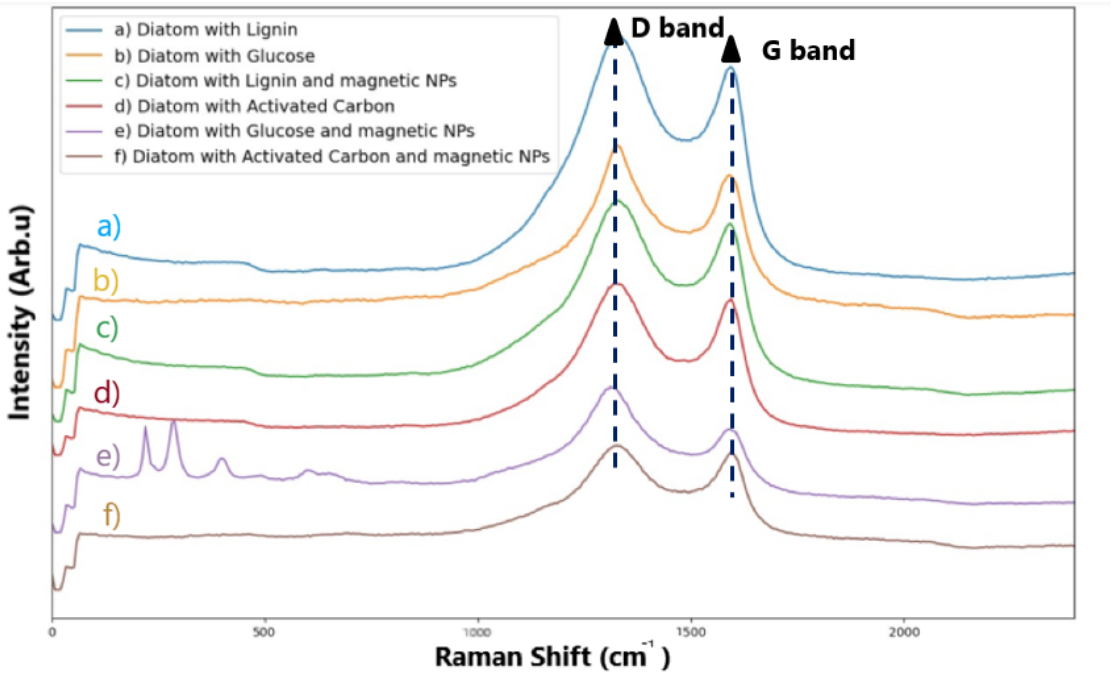

Figure 4: **Raman spectra of Diatomite with carbon sources and Magnetic NPs Composite.**

References

[1] Saadattalab, V., Wang, X., Szego, A. E., & Hedin, N. (2020b). Effects of Metal Ions, Metal, and Metal Oxide Particles on the Synthesis of Hydrochars. ACS Omega, 5(11), 5601-5607. https://doi.org/10.1021/acsomega.9b03926

[2] Medarevic, Djordje & Losic, Dusan & Ibrić, Svetlana. (2015). Diatoms – Nature materials with great potential for bioapplications. Hemijska industrija. 70. 69-69. 10.2298/HEMIND150708069M.

Acta Microscopica Vol. 34, Supp. 2, 2025
Abstract Book NSSY 2024 - Galapagos 19-25 May, 2024

Extracting quantitative data from STM images using Machine Learning Techniques

Leonel A. Cabrera[1], Lauri Kurki[2], Adam S. Foster[2]

[1] *School of Physical Sciences and Nanotechnology, Yachay Tech University, Urcuqui 110119, Ecuador*

[2] *SIN group, Department of Applied Physics, Aalto University, Finland*

leonel.cabrera@yachaytech.edu.ec

Abstract

The Scanning Tunneling Microscope (STM) operates by scanning a conductive probe, or tip, in close proximity to a sample surface. By applying a bias voltage, electrons are induced to tunnel through the gap between the tip and the sample due to the quantum tunneling effect. The resulting STM image, which is a reconstruction based on variations in tunneling current, reveals atomic-scale surface features. Despite advancements such as tip functionalization [1] that have enhanced image resolution, the interpretation and quantitative analysis of STM images remain complex and labor-intensive tasks for researchers.

In this study, we utilized a model architecture previously developed by [2], which incorporates a U-net type Convolutional Neural Network (CNN) with attention gates. This is augmented by a peak finding algorithm that facilitates the extraction of atom positions. Subsequently, a Graph Neural Network (GNN) is employed to construct a graph representing atom classes and edges, by iteratively adding nodes. This method allows for a more structured and efficient approach to analyzing STM data, potentially reducing the complexity and time required for interpretation.

References

[1] Krejčí, O., Hapala, P., Ondráček, M., & Jelínek, P. (2017). Principles and simulations of high-resolution STM imaging with a flexible tip apex. Physical Review B, 95(4), 045407.

[2] Oinonen, N., Kurki, L., Ilin, A. et al. Molecule graph reconstruction from atomic force microscope images with machine learning. MRS Bulletin 47, 895–905 (2022).

[3] Alldritt, B., Hapala, P., Oinonen, N., Urtev, F., Krejci, O., Federici Canova, F., ... & Foster, A. S. (2020). Automated structure discovery in atomic force microscopy. Science advances, 6(9), eaay6913.

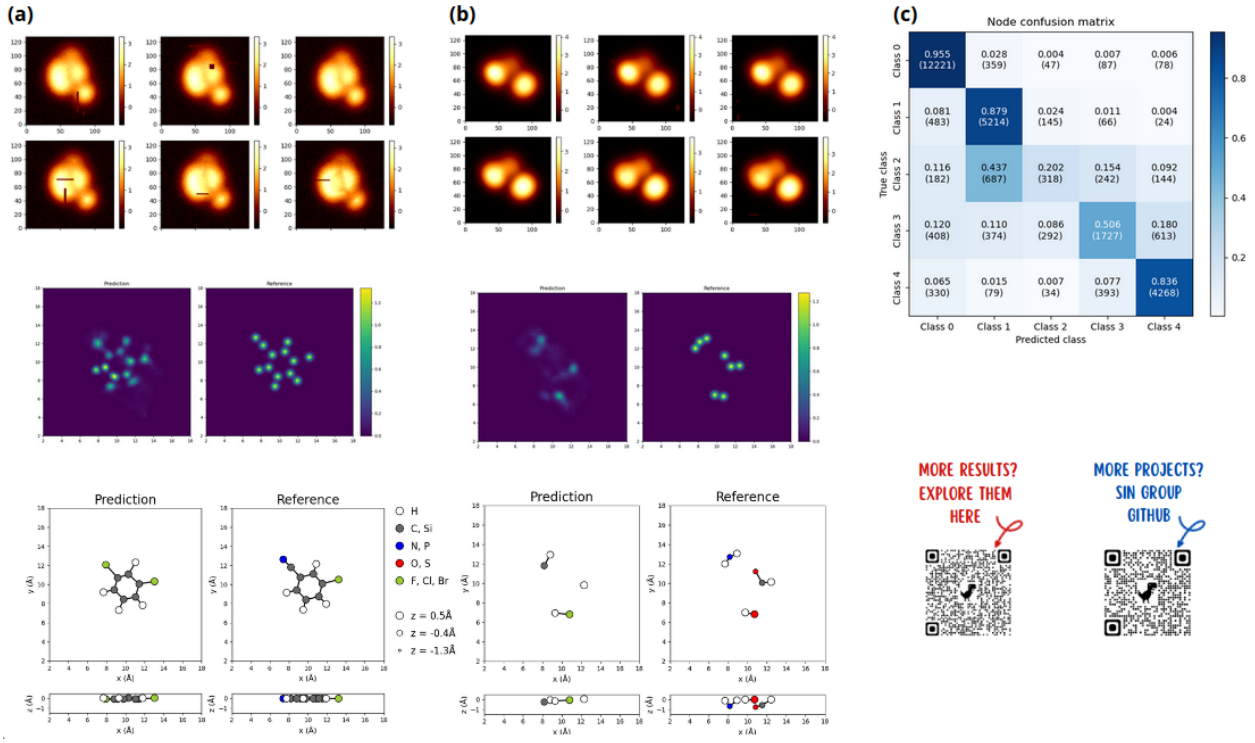

Figure 1: **(a), (b) Graph predictions from simulated STM images. (c) Confusion Matrix of atom classification. The values have been normalized by the total number of true cases of the corresponding class, and the values in parenthesis show the total number of cases with the corresponding true and predicted class.**

Acta Microscopica Vol. 34, Supp. 2, 2025
Abstract Book NSSY 2024 - Galapagos 19-25 May, 2024

Chitosan/collagen based nanofibers for possible skin regeneration dressing applications

Laila Procel, Gema Gonzales, Sarah Briceño
[1] *Physics Science and Nanotechnology school at Yachay Tech University*
[2] *Biology and biomedical sciences school at Yachay Tech University*
email

Abstract

The purpose of this research thesis project is the synthesis of chitosan/collagen polymer nanofibers obtained by electrospinning technique for tissue engineering and regenerative medicine applications. These nanofibers scaffolds mimic the composition and structure of protein fibrils of the Extracellular matrix (ECM) by recreating the native microenvironment of cells promoting the tissue regeneration. Chitosan and collagen possess biocompatible and biodegradable properties, rendering them suitable for use as biomaterials. The formation of a complex between chitosan and collagen results in a synergistic performance with regards to cell growth properties; this complex is enhaced by dopping hydroxyapatite (HA) and PLGA (Poly(lactic-co-glycolic acid)) to promote cicatrization and biocompatible properties to the nanofibers films. All methodology is detailed for each biopolymer complex obtained and their precursors.

The solvent trifluoroacetic acid (TFA) has a lower boiling point than acetic acid, which is reported in most research to obtain chitosan nanofibers, which is why acetic acid was replaced by TFA, since this solvent allows better dissolution of chitosan and its evaporation is faster than acetic acid under the electroospinning process. The present work reveals parameters for obtaining doped fibers, as well as parameters that do not optimize the formation of fibers. Parameters such as concentration, flow rate,taylor cone, distance , collector type , needle size, temperature, voltage , solvent and molecular weight of polymers ; were optimized after several trials to achieve parameters that allow repeatability in obtaining fibers.

The obtained nanofibers were correctly collectet , for the characterization. In this investigation some characterization methods were selected to analyze and nterpret reults. The characterization techniques used are : Raman Spectroscopy , SEM (Scanning Electron Microscope), TEM (Transmission electron microscopy), FTIR (Fourier-transform infrared spectroscopy), TGA (Thermogravimetric analysis) and Optical Microscopy.

The antimicrobial performance is tested and proved, also woound tests were done five times to prove its cicatrization properties in skin as a potential film wound

dressing for burns or wounds by proving in fibroblasts.

The healing applications of chitosan are undoubtedly a new biomaterial for future dressings.

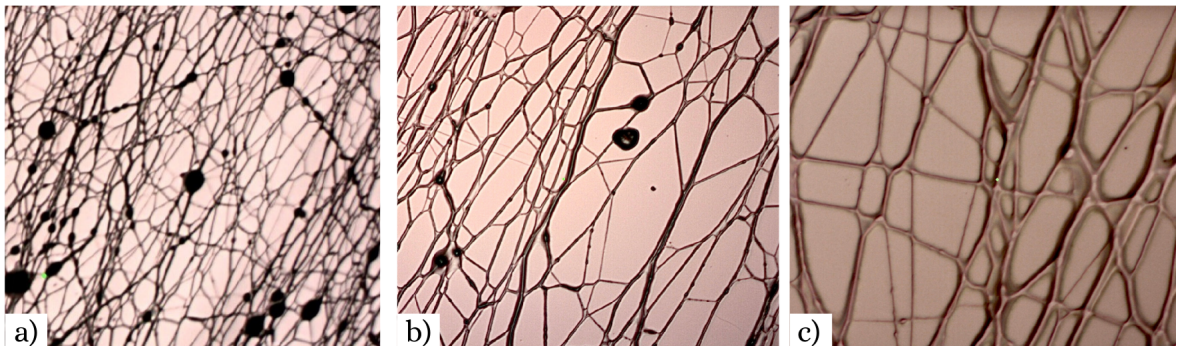

Figure 1: **Chitosan/Collagen nanofibers - Optical Microscopy**

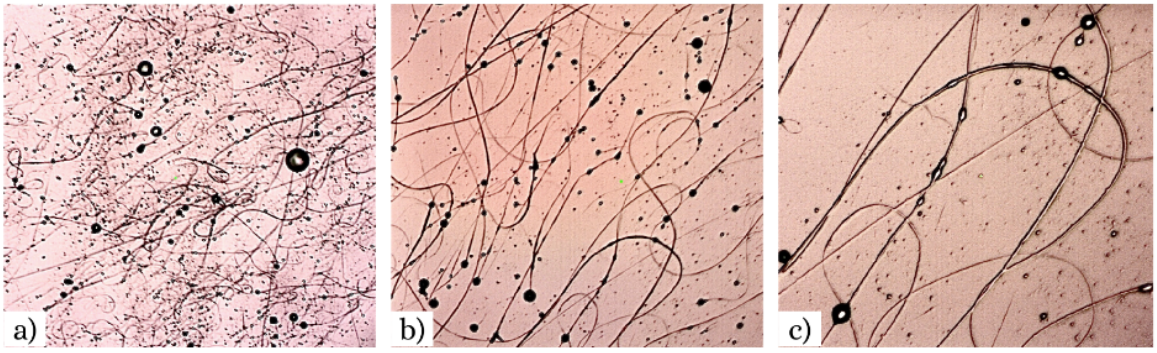

Figure 2: **Hydroxyapatite/Chitosan/Collagen nanofibers- Optical Microscopy**

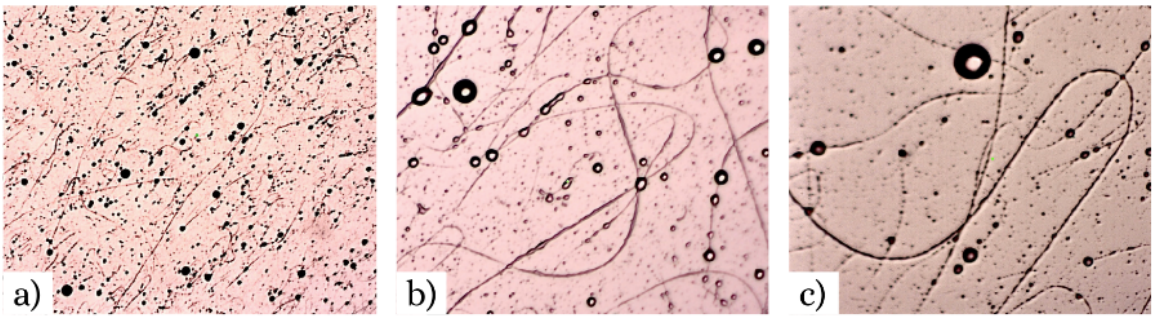

Figure 3: **Hydroxyapatite/PLGA/Chitosan/Collagen nanofibers- Optical Microscopy**

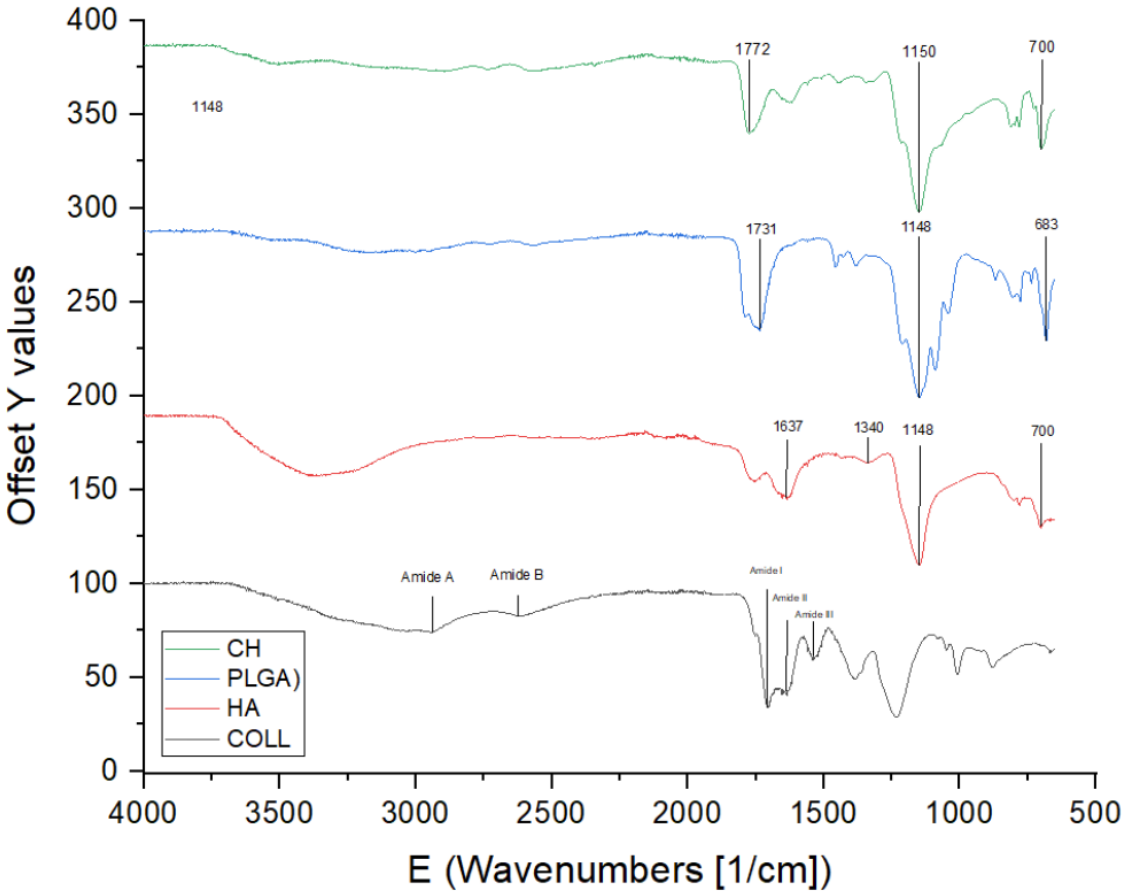

Figure 4: **HA/PLGA/CH/COLL - FTIR**

References

[1] Huang, Z.-M.; Zhang, Y.-Z.; Kotaki, M.; Ramakrishna, S. A review on polymer nanofibers by electrospinning and their applications in nanocomposites. Composites science and technology 2003, 63, 2223–2253.

[2] an, W.; Krishnaraj, R.; Desai, T. A. Evaluation of nanostructured composite collagen–chitosan matrices for tissue engineering. Tissue engineering 2001, 7, 203–210.

[3] Chen, Z.; Wang, P.; Wei, B.; Mo, X.; Cui, F. Electrospun collagen–chitosan nanofiber: A biomimetic extracel-lular matrix for endothelial cell and smooth muscle cell. Acta biomaterialia 2010, 6, 372–382.

Acta Microscopica Vol. 34, Supp. 2, 2025
Abstract Book NSSY 2024 - Galapagos 19-25 May, 2024

Thermal-Response Layer for Bio Roll Up Polymer Synthesis and Formulation

Andrea Valarezo[1], Julia Garrison[2], Anthony Tenace[2] and Robert Brainard[2]
[1] *School of chemistry and Engineering. Yachay Tech University*
[2] *Nanoscale Science, University at Albany, [3]Nanoscale Science, University at Albany*
andrea.valarezo@yachaytech.edu.ec

Abstract

Many efforts have been made in previous years to create artificial human organs and 3-dimensionsal (3D) body tissues [1].However, there are still many obstacles to overcome, especially considering how different types of tissues and organs will need to be artificially produced by different methods. Some organs, such as salivary glands, mammary glands, kidneys, and lungs, are composed of epithelial cells organized in 3D monolayers such as tubes, spheres and intersections (Figure 1). Composing structures artificial 3D-monolayers of cells can be used to study the differentiation of stem cells into 3D-monolayers. This will help with designing treatments for damaged epithelial cells that are organized as 3D-monolayers. Although some researchers have begun to propose the usage of hydrogels (water-based polymers) for salivary gland tissue engineering, further research must be conducted [2].

This work will describe an exploratory project, called Bio Roll-Up (BRU). BRU aims to build multilayer stacks of photo-imageable, biocompatible hydrogels that promote cell growth. These multilayer stacks will self-assemble into functional tube-shaped structures of 3D-monolayers of cells when immersed in pH 7.4 buffer. Self-assembly occurs due to the differential swelling of hydrogel bilayers, which contain different amounts of crosslinker. However, the timing of self-assembly must be controllable for cells to proliferate and form a 3D-monolayer on top of the multilayer stacks. At the time, the stacks self-assembled immediately or not at all. This presentation will describe several approaches for controlling the time of self-assembly, including the use of a release layer made with a thermo-responsive polymer known as PNIPAM, as well as changing the chemical composition of hydrogel bilayers to slow the rate of self-assembly.

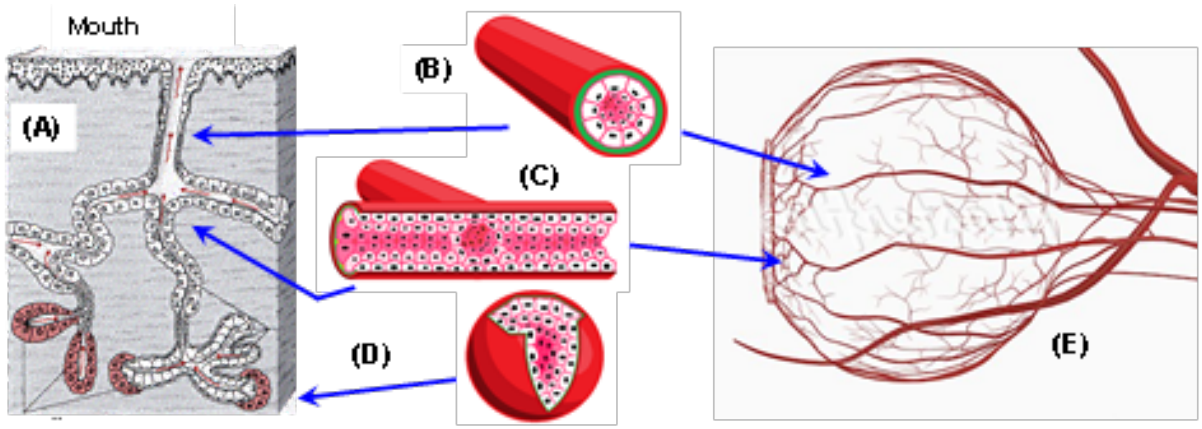

Figure 1. *BRU can be used to build 3D structures for:* ***(A)*** *Salivary gland,* ***(B)*** *Tube.* ***(C)*** *Intersection* ***(D)*** *Sphere,* ***(E)*** *Blood vessels in the eye.*

Figure 1: **BRU can be used to build 3D structures for: (A) salivary gland, (B)Tube, (C)Intersection, (D)Sphere, (E)Blood vessels in the eye.**

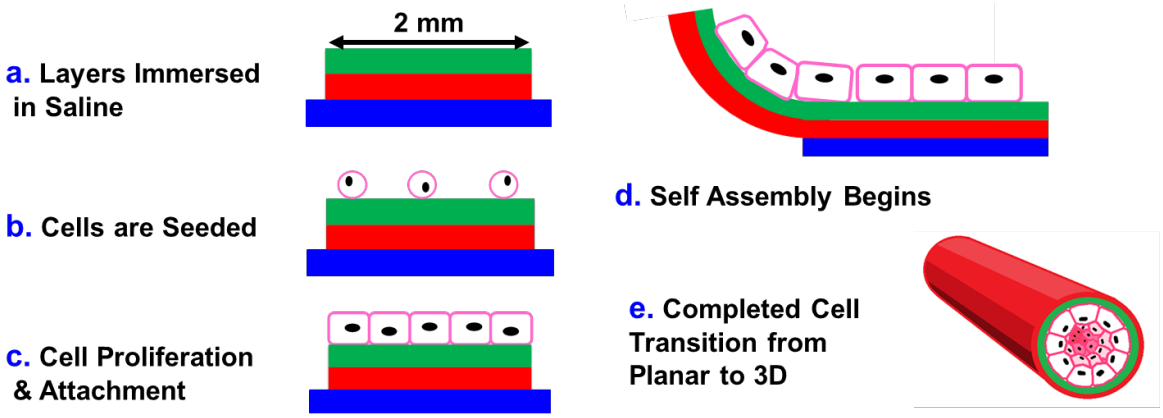

Figure 2: **This diagram describes the major steps of self-assembly in Bio Roll-Up. A trilayer hydrogel stack is (A) fabricated and immersed in saline and (B) seeded with cells, (C) which are later proliferated. (D) The bottom release layer dissolves away in response to thermal trigger as differential swelling in the hydrogel bilayers induces self-assembly into (E) the target structure.**

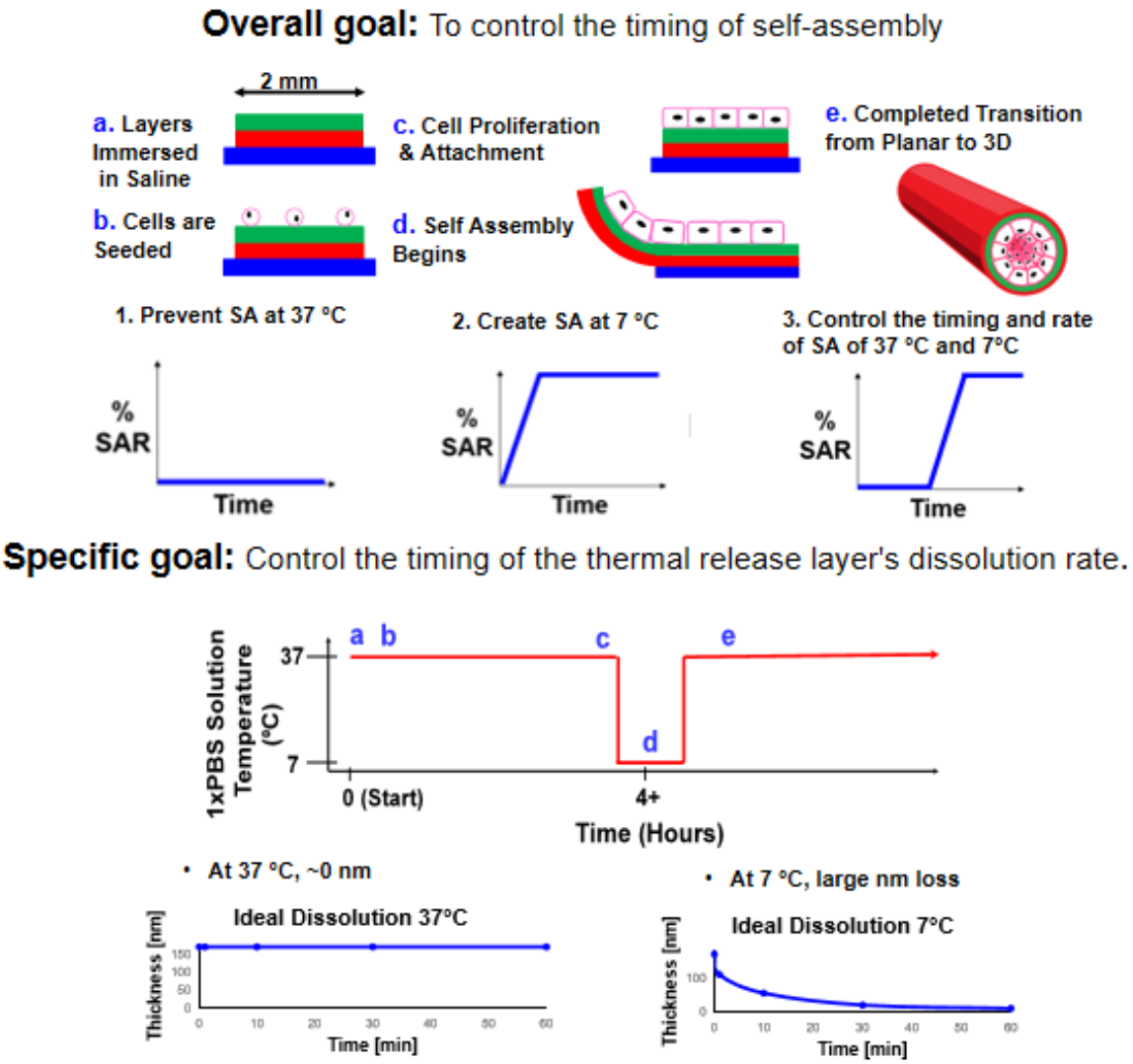

Figure 3: **A)Overall goal: To control the timing of self-assembly. B) Specific goal: Control the timing of the thermal release layer's dissolution rate**

References

[1] Kobayashi, E. Organ Fabrication: Progress and Hurdles to Overcome. Current Transplantation Reports 2022, 9 (4), 297–301.

[2] Pillai, S.; Munguia-Lopez, J. G.; Tran, S. D. Hydrogels for Salivary Gland Tissue Engineering. Gels 2022, 8 (11), 730.